

University of Alberta

Genetic, genomic and molecular studies of signaling pathways controlling
ecdysone biosynthesis in *Drosophila melanogaster*

by

Qiuxiang Ou

A thesis submitted to the Faculty of Graduate Studies and Research
in partial fulfillment of the requirements for the degree of

Doctor of Philosophy

in

Molecular Biology and Genetics

Department of Biological Sciences

©Qiuxiang Ou

Fall 2013

Edmonton, Alberta

Permission is hereby granted to the University of Alberta Libraries to reproduce single copies of this thesis and to lend or sell such copies for private, scholarly or scientific research purposes only. Where the thesis is converted to, or otherwise made available in digital form, the University of Alberta will advise potential users of the thesis of these terms.

The author reserves all other publication and other rights in association with the copyright in the thesis and, except as herein before provided, neither the thesis nor any substantial portion thereof may be printed or otherwise reproduced in any material form whatsoever without the author's prior written permission.

Dedication

I dedicate this thesis to the memory of my late aunt, Xiangyun Ou, and my late uncle, Zhenyuan Chen, who gave me fond memories of my childhood that I will cherish for my whole life.

Abstract

In insects, the prothoracic gland (PG) releases periodic pulses of the molting hormone ecdysone, which control all major developmental transitions of the insect life cycle, such as the molts and metamorphosis. The synthesis and release of ecdysone, a steroid hormone, is under the control of PTTH, a brain-derived neuropeptide. PTTH mRNA levels oscillate with an 8-hour periodicity during the third instar, but it remains unclear how these oscillations are related to the timing of ecdysone pulses. PTTH stimulates the production of ecdysone by activating the Ras/Raf/MAPK signaling pathway through its receptor Torso in PG cells, but little is known about its direct downstream targets. The first part of this thesis demonstrates that nuclear receptor DHR4 is a critical target of the PTTH pathway and has a key role in appropriately timing ecdysone pulses. I show that DHR4 oscillates between the nuclei and cytoplasm of PG cells and that this oscillatory behavior is blocked when PTTH signaling is altered. Increasing *DHR4* levels in the PG blocks molting or metamorphosis, while loss of *DHR4* causes developmental acceleration due to the de-repression of ecdysone production. I also show that DHR4 negatively regulates the expression of *Cyp6t3*, a novel player of ecdysone biosynthesis. Together, I propose that nuclear DHR4 inhibits ecdysone synthesis through repressing *Cyp6t3* and possibly other target genes, and that this repressive function can be overturned by the disappearance of DHR4 from PG nuclei via activating the PTTH pathway.

While we have a relatively good understanding of the enzymatic steps regarding the synthesis of steroid hormones in vertebrates and insects, it is largely unclear which signaling pathways regulate their production. In the second part of this thesis, I present the first comprehensive genomic and genetic analysis of the *Drosophila* ring gland in an attempt to identify novel players acting in ecdysteroidogenesis. Using ring gland-specific microarrays, I identified 233 transcripts with strong enrichment in the ring gland. To examine the roles of these genes, I used RNA interference to disrupt the expression of these genes in a tissue-specific manner. I identified 20 genes that have likely novel roles in ecdysone synthesis, including cytochrome P450 genes, transcription factors, ABC transporters and signaling pathway components. This study establishes the ring gland as a prime model for examining signaling pathways that control the regulation of steroid hormone synthesis and release.

In the last part of this thesis, I describe a novel developmental role of neurotrophin Spätzle5 and NO signaling in governing heme synthesis in PG cells. Heme is a cofactor for ecdysteroidogenic cytochrome P450 enzymes. *spätzle5* represents one of the 233 ring gland-specific transcripts. I show that Spätzle5 is required for NO production possibly through controlling the activity of NOS. RNAi knockdown of *spätzle5* or *NOS* specifically in the PG causes larval arrest and a dramatic upregulation of *ALAS* expression, which is the rate-limiting enzyme of heme synthesis. This phenotype suggests that heme biosynthesis is impaired, and that an unknown heme sensor

upregulates *ALAS* expression when heme concentrations fall below a critical threshold. Using a candidate gene approach, I show that DHR51 is required for the upregulation of *ALAS* in *spätzle5* and *NOS* knockdowns. This study broadens our current perspective of ecdysteroidogenic regulation, and sheds light on a novel pathway, in which Spätzle5 upregulates heme synthesis to increase ecdysone production.

Acknowledgements

Working on my PhD has been a wonderful and unforgettable experience for me. Here, I would like to thank many people who have provided me valuable assistance during my PhD career.

First of all, I am deeply grateful to my supervisor, Kirst King-Jones. To work with you has been a great experience to me. Thank you so much for always being patient and encouraging when you listen to my ideas (unconventional at times) about my research, and for many constructive discussions and great ideas that often helped me to gain key insights into my project. Thank you so much for spending considerable time in teaching me how to make good presentation slides, how to prepare for a good talk, and how to become a better science writer. Thank you a lot for your support in times when I was depressed.

Furthermore, I would like to express my gratitude to my committee members, Dr. Andrew Waskiewicz and Dr. Shelagh Campbell, for your support and suggestions on my projects.

I also want to thank all members of the King-Jones lab (present and past): Mattéa Bujold, Emma Nally, Ran Zhuo, Akila Gopalakrishnan, Jie Zeng, Francesca Di Cara, Morris Kostiuik and Brian Phelps. I want to give special thanks to Mattéa for all your help in qPCR training and correcting my English (I really appreciate it!). Special thanks to Ran, who is like my elder sister, for sharing me skills of doing fly crosses and giving me company in the lab at many freezing nights.

Specifically for the DHR4 project, I want to give my special thanks to Dr. Vincent Henrich and Dr. Sasha Necakov, who gave me great suggestions on how to improve my skills in the dissection of the ring gland. These suggestions helped to make the first ring gland-specific microarray possible. Special thanks to our collaborator, Dr. Michael O'Connor, for sharing me reagents and exchanging ideas. I wish to thank Dr. Pierre Leopold and Dr. Henry Krause for sharing reagents. I also wish to thank Dr. Christen Mirth for your help in making *DHR4* RNAi transgenic flies. Thanks to Geanette Lam with the purification of DHR4 antibodies. Thanks to Anna Hutton for your kind help with microarrays. Thanks

to Scott Hanna for your help with *Drosophila* embryo microinjections. Specifically for the Ring Gland project, I want to thank Dr. Adam Magico for your help with the ring gland RNAi screen.

Specifically for the thesis, I wish to express my thanks to Kirst for your time in revising the thesis and for offering many beautiful figures. Special thanks to Brian for your useful comments and suggestions.

My very sincere gratitude to my whole family far back in Mainland China, mother, father, brother, aunts, uncles, and cousins for your infinite support during the past several years. I am really grateful to my parents for your understanding and continuous support throughout everything during my PhD career. Mom, dad, I love you so very much. I wish I could have spent more time with you.

Finally, I want to thank the Department of Biological Sciences GTA program, which has supported me during my PhD work. NSERC and CIHR research grants have supported my project.

Table of Contents

Chapter 1	1
Introduction.....	1
1.1 Insect metamorphosis and the steroid hormone ecdysone	2
1.2 Downstream of hormone: The ecdysone hierarchy at the onset of metamorphosis	4
1.3 New insight into an old story: The ecdysone hierarchy genes in regulation of ecdysone synthesis.....	10
1.4 Outline of the thesis.....	12
1.5 Figures	14
1.6 Bibliography	16
Chapter 2	21
Nuclear receptor DHR4 controls the timing of steroid hormone pulses during <i>Drosophila</i> development	21
2.1 Introduction	22
2.2 Methods	26
2.3 Results	33
2.4 Discussion.....	53
2.5 Final comments	62
2.6 Tables	63
2.7 Figures	66
2.8 Bibliography	103
Chapter 3	110
Transcriptome and functional analysis of the <i>Drosophila</i> ring gland in controlling ecdysone synthesis.....	110
3.1 Introduction	111
3.2 Methods	118
3.3 Results	125
3.4 Discussion.....	143
3.5 Outlook	149

3.6 Tables	150
3.7 Figures	159
3.8 Bibliography	175
Chapter 4	184
Examining the role of neurotrophin Spätzle5 and NO signaling in the regulation of heme synthesis during <i>Drosophila</i> larval development	184
4.1 Introduction	185
4.2 Methods	194
4.3 Results	198
4.4 Discussion.....	217
4.5 Tables	226
4.6 Figures	229
4.7 Bibliography	277
Chapter 5	284
Summary and future directions.....	284
5.1 The role of nuclear receptor DHR4 in the proper timing of ecdysone pulses during <i>Drosophila</i> development.....	285
5.2 Cyp6t3: a novel player of ecdysone synthesis downstream of DHR4	287
5.3 Transcriptome and functional analysis of the <i>Drosophila</i> ring gland in controlling ecdysone synthesis	288
5.4 Microarrays reveal genes with PTH-dependent expression.....	289
5.5 The role of spätzle5 and NO signaling in governing heme synthesis: a new layer of ecdysteroidogenic regulation	291
5.6 Future directions	292
5.7 Figure.....	295
5.8 Bibliography	297

List of Tables

Table 2.1. Primer pairs for qPCR and *in situ* probe

Table 2.2. Genes affected by *DHR4*-RNAi

Table 3.1. GOstat results for 233 ring gland-specific transcripts

Table 3.2. RNAi lines screened with the *phm22-Gal4* driver

Table 3.3. RNAi lines identified with the ring gland- and fat body-specific *Gal4* drivers

Table 3.4. Primer/probe mix used in the high-throughput qPCR time-course experiment

Table 3.5. Cytochrome P450 genes with moderate to strong transcript enrichment in ring glands from third instar larvae

Table 3.6. Primer pairs for *in situ* probes

Table 3.7. Genes affected by PTTH signaling

Table 4.1. Primer pairs for qPCR analysis

Table 4.2. Genetic interactions

Table 4.3. Ring gland hypertrophy

List of Figures

Figure 1.1. Ashburner model

Figure 1.2. Overview of *Drosophila* ecdysone hierarchy genes at the onset of metamorphosis

Figure 2.1. Ecdysone directs developmental transitions in *Drosophila*

Figure 2.2. A schematic diagram of ecdysone biosynthesis in the *Drosophila* prothoracic gland

Figure 2.3. Disruption of *DHR4* ring gland function affects developmental timing

Figure 2.4. A schematic representation of *DHR4* expression profiles during *Drosophila* larval development

Figure 2.5. *DHR4* expression in the early L3 contributes to the precocious wandering behavior

Figure 2.6. *DHR4*-RNAi affects the timing of ecdysone-mediated responses

Figure 2.7. Time course qPCR analysis of *E74* transcripts levels in larvae heat-treated in late second instar or early third instar

Figure 2.8. Time course analysis of whole-body ecdysteroid titers

Figure 2.9. Overexpression of *DHR4* in the PG blocks molting

Figure 2.10. *DHR4* oscillates between cytoplasm and nucleus in PG cells of L3 larvae

Figure 2.11. Phenotypes of *phm22>Ras^{V12}* larvae

Figure 2.12. Effects on *DHR4* subcellular localization by manipulating PTTH pathway components

Figure 2.13. *DHR4* antibody stains of *Cg>w¹¹¹⁸* and *Cg>Ras^{V12}* fat body cells

Figure 2.14. Epistasis analysis of *DHR4* and *Ras*

Figure 2.15. ERK antibody stains of *w¹¹¹⁸* ring glands during the first 8 hr of the third instar

Figure 2.16. *DHR4*-RNAi ring gland microarray reveals misregulated cytochrome P450 genes

Figure 2.17. *Cyp6t3* expression is highly specific to the prothoracic gland

Figure 2.18. Disrupting *Cyp6t3* function in the PG results in ecdysone deficiency

Figure 2.19. Phenotypic characterization of *Cyp6t3*-RNAi line (VDRC#30896)

Figure 2.20. *Cyp6t3* is a novel component in the “Black Box” of ecdysone synthesis

Figure 2.21. Analysis of *Cyp6t3*^{Mi(CG8858)} allele (Bloomington stock#31021)

Figure 2.22. *Cyp6t3* is epistatic to *DHR4*

Figure 2.23. A model for DHR4 function

Figure 2.24. Prediction of ERK phosphorylation sites of DHR4 protein

Figure 2.25. A predicted nuclear receptor response element that is located upstream of *Cyp6t3*

Figure 3.1. An overview of mechanisms underlying regulation of ecdysone biosynthesis in the *Drosophila* prothoracic gland

Figure 3.2. Experimental design and timeline of *Drosophila* larval ring gland microarrays

Figure 3.3. Experimental design and timeline of ring gland microarrays examining gene expression changes affected by altered PTTH signaling

Figure 3.4. Pie charts show the distribution of 233 ring gland-enriched transcripts representing 208 genes

Figure 3.5. Expression profiles of ring gland-specific transcripts

Figure 3.6. Different categories of PG-specific RNAi phenotypes

Figure 3.7. 20E rescue of PG-specific RNAi phenotypes

Figure 3.8. Gene expression profiles in the brain-ring gland complex (BRRG) of L3 larvae

Figure 3.9. Genes affected by PTTH signaling

Figure 3.10. RNA *in situ* analysis of cytochrome P450 genes

Figure 4.1. Neurotrophin signaling pathways

Figure 4.2. NO signaling regulates ecdysteroidogenesis in the *Drosophila* PG.

Figure 4.3. Role of heme in ecdysone biosynthesis

Figure 4.4. Heme biosynthesis in animals

Figure 4.5. Deficiencies of heme biosynthetic enzymes result in a group of human disorders designated the porphyrias and X-linked sideroblastic anemia

Figure 4.6. Iron metabolism in *Drosophila*

Figure 4.7. Neurotrophin Spätzle5 is developmentally required for *Drosophila* metamorphosis

Figure 4.8. Loss of *spätzle5* specifically in the prothoracic gland impairs ecdysone production

Figure 4.9. The expression of a modified cDNA partially rescues the *PG>spätzle5-RNAi* ring gland phenotype

Figure 4.10. The alignment between *D. melanogaster* and *D. pseudoobscura* for the hairpin of the *spätzle5-RNAi* line (VDRC#102389)

Figure 4.11. Spätzle5 is required for NO production in the PG

Figure 4.12. The expression of *βftz-fl* and *dib* in the brain-ring gland complex of *PG>spätzle5-RNAi* larvae

Figure 4.13. A constitutively active form of NOS or the ectopic expression of *βftz-fl* did not rescue *PG>spätzle5-RNAi* phenotype

Figure 4.14. The ring gland phenotype of PG-specific disruption of *spätzle5* and *NOS* function

Figure 4.15. PG-specific knockdown of *spätzle5* results in the overgrowth of ring gland

Figure 4.16. Ubiquitous knockdown of *spätzle5* and *NOS* gives phenotypes similar to that observed in the *PPOX¹³⁷⁰²* mutant

Figure 4.17. The expression of heme biosynthetic genes in PG-specific *spätzle5* and *NOS* knockdowns

Figure 4.18. Loss of *ALAS* abolishes the autofluorescence of *PG>spätzle5-RNAi* ring glands

Figure 4.19. Loss of *spätzle5* and *NOS* results in an accumulation of heme precursors in the PG

Figure 4.20. Disrupting *spätzle5* and *NOS* results in punctate fluorescence signals in the PG under UV

Figure 4.21. Loss of *DHR51* rescues the larval lethality caused by PG-specific *spätzle5* RNAi

Figure 4.22. DHR51 is required for *ALAS* upregulation caused by PG-specific knockdown of *spätzle5*

Figure 4.23. *DHR51* knockdown rescues *NOS*-RNAi and *PPOX*-RNAi ring gland phenotypes

Figure 4.24. A model of nuclear receptor *DHR51* acting as a heme sensor in the *Drosophila* PG

Figure 4.25. Loss of *DHR51* partially rescues protoporphyrins accumulation in *spätzle5*-RNAi oenocytes

Figure 4.26. Ras contributes to the ring gland phenotype of *PG>spätzle5*-RNAi larvae

Figure 4.27. NO signaling is epistatic to RAS signaling

Figure 4.28. The epistasis of Spätzle5 and NO to RAS signaling

Figure 4.29. PI3K signaling ameliorates the accumulation of protoporphyrins in the PG caused by *spätzle5* RNAi

Figure 4.30. Ectopic expression of wild type *spätzle5* results in pupariation and growth defects

Figure 4.31. A model for the role of Spätzle5 and NO signaling in the regulation of heme synthesis in the *Drosophila* PG

Figure 4.32. Two possible mechanisms underlying Spätzle5 and NO signaling in the regulation of heme synthesis in the *Drosophila* PG.

Figure 4.33. A possible role of NO signaling in modulating cellular iron availability in the PG

Figure 4.34. A proposed experiment of testing the transcriptional activity of *DHR51* under normal and low heme conditions

Figure 5.1. A dual function of *DHR4* in *Drosophila* development

Abbreviations

5 β KD	5 β -ketodiol
7dC	7-dehydrocholesterol
20E	20-hydroxyecdysone
aa	amino acid
ABC	ATP-binding cassette
AED	after egg deposit
<i>act</i>	<i>actin5C</i>
Akh	adipokinetic hormone
ALAS	5'-aminolevulinate synthase
Atet	ABC transporter expressed in trachea
BR-C	broad-complex
BSA	bovine serum albumin
BTB/POZ	Broad Tramtrack Bric-a-brac/poxvirus and zinc finger
C424	Carolina Biological Supply Company medium 4-24
C	cholesterol
CA	<i>Corpus allatum</i>
CC	<i>Corpora cardiaca</i>
cDNA	complementary DNA
CNS	central nervous system
Cyp	cytochrome P450
DAPI	4', 6-diamidino-2-phenylindole
DBD	DNA-binding domain
DHR3	<i>Drosophila</i> Hormone Receptor 3
DHR4	<i>Drosophila</i> Hormone Receptor 4
DHR51	<i>Drosophila</i> Hormone Receptor 51
<i>dib</i>	<i>disembodied</i>
DIG	digoxigenin
DNT	<i>Drosophila</i> neurotrophin
DR	direct repeat

E ecdysone
EcR ecdysone receptor
EDTA ethylenediaminetetraacetic acid
EIA enzyme immunoassay
EMSA electrophoretic mobility shift assay
ERK extracellular-signal-regulated kinase
Fer1HCH ferritin 1 heavy chain homologue
FTZ-F1 fushi tarazu factor 1
GCNF germ-cell nuclear factor
GFP green fluorescent protein
Glu-RIB glutamate receptor IB
GnRH gonadotrophin releasing hormone
Gpb5 glycoprotein hormone beta 5
GPCR G-protein coupled receptor
hr hour
HSP heat shock protein
IIS insulin/ILP signaling
ILP insulin-like peptide
IRE iron responsive element
IRP iron regulatory protein
IVT *in vitro* transcription
Kif3C kinesin family member 3C ortholog
L1 first instar
L2 second instar
L3 third instar
LBD ligand-binding domain
LDL low-density lipoprotein
MAPK mitogen-activated protein kinase
min minute
mld molting defective

meth	methuselah
methl	methuselah-like
NGS	normal goat serum
NIG	National Institute of Genetics (Japan)
NO	nitric oxide
NOS	nitric oxide synthase
Npc1a	Niemann-Pick type C-1a
Nrk	neurospecific receptor kinase
NT	neurotrophin
OE	oenocyte
otk	off-track
PBS	Phosphate buffered saline
PBST/PBT	Phosphate buffered saline + Triton-X
PBTB	Phosphate buffered saline + Triton-X + blocking reagents
PDF	pigment dispersing factor
PG	prothoracic gland
<i>phm</i>	<i>phantom</i>
PLC	phospholipase C
PNR	photoreceptor-specific nuclear receptor
PPF	prior to puparium formation
PPOX	protoporphyrinogen oxidase
Pvf2	PDGF- and VEGF-related factor 2
PTTH	prothoracicotropic hormone
qPCR	quantitative PCR
RG	ring gland
RNAi	RNA interference
ROR	retinoid-related orphan receptor
rPTTH	recombinant PTTH
RT	room temperature
SCNF	SoxNeuro Co-Factor

SDHB succinate dehydrogenase B
sec second
Sgs salivary gland secretion 4
spz5 spätzle5
TNFR tumor necrosis factor receptor
Traf4 TNF-receptor-associated factor 4
Trk tropomyosin-receptor-kinase
TSA tyramide signal amplification
tub tubulin
Ugt37c1 UDP-glycosyltransferase 37c1
USP ultraspiracle
VDRC Vienna *Drosophila* Research Center
vvl ventral veins lacking
w/ with
w/o without
woc without children
Znf zinc finger

Chapter 1
Introduction

1.1 Insect metamorphosis and the steroid hormone ecdysone

Metamorphosis translates into “change in form”. While most organisms display some changes in form during development, one typically uses the term “metamorphosis” in the context of the dramatic remodeling that occurs during the transition from a larval to an adult stage, as seen in holometabolous insects or amphibians. Insect metamorphosis is arguably one of the most striking developmental processes in the animal kingdom, allowing us to witness the transformation of an entire body plan into another. The change in body plans is not just a developmental necessity. In insects, for example, the use of different body plans serves as a remarkable adaptation to different habitats and food sources while undergoing development (Truman and Riddiford, 1999).

Typically, an insect’s life cycle comprises embryonic, larval, pupal and adult stages, where growth occurs exclusively during larval development. The succession of different stages and body plans begs the question as to how these transitions are regulated. Key components responsible for the dramatic reprogramming of body plans are small lipophilic hormones, such as ecdysteroids in insects and thyroid hormones in amphibians (Galton, 1992). In either case these hormones act as ligands for members of the nuclear receptor superfamily that, upon ligand binding, initiate a cascade of gene programs that drive forward the remodeling process. In *Drosophila*, the ligand-bound ecdysteroid receptor activates a small group of early response genes, which mostly encode transcription factors. These early (or primary) regulatory proteins will then coordinate the expression of late (or secondary) response genes that ultimately effectuate the required developmental changes (**Figure 1.1**). These downstream effects of steroid and thyroid hormones are complex events, however, they represent just one side of the coin. Clearly, one may also ask what happens upstream of the hormone to understand how the synthesis and release of these

hormones are controlled in the first place. As it turns out, the release of these developmentally important hormones is strictly controlled, resulting in precisely timed pulses that control the onset of developmental transitions such as hatching, molting, and metamorphosis itself (Thummel, 1995) (see Chapter 2 for a detailed discussion on the regulation of ecdysone pulses).

The identification of ecdysone as the key molting hormone in the 1950s is a milestone in the history of insect endocrinology. In 1954, Peter Karlson and his colleagues purified 25 mg of ecdysone crystals from 500 kg of silk moth pupae, and used the *Calliphora* bioassay (“pupariation test for ecdysone”) to track the activity of the hormone (Butenandt, 1954; Fraenkel and Zdarek, 1970; Rybczynski et al., 2001). In a series of chemical experiments and the analysis of the crystals, ecdysone was later shown to be a steroid hormone (Huber, 1965; Karlson, 1965). The first evidence that ecdysone has a direct role in regulating gene expression was based on the puffing of the salivary gland polytene chromosomes. Puffs are enlargements of specific loci on these giant chromosomes and were interpreted as local transcriptional activity. In particular, it was found that some of these puffs were induced rapidly after the addition of ecdysone to cultured salivary glands of the midge *Chironomus* (Clever, 1960). Curiously, some of the puffs were responding rapidly to the hormone (early puffs), while others were delayed (late puffs). To test whether puffing was a direct consequence of ecdysone activity, a series of elegant studies by Clever (in *Chironomus*) and later by Ashburner (in *Drosophila*) tested whether protein synthesis was a requirement for the induction of puffs by ecdysone. These studies showed that the early puffs were still induced in the presence of protein synthesis inhibitors, while the late puffs were not. Ashburner also found that these early puffs are auto-regulated, because they failed to regress when protein synthesis was inhibited. Ashburner correctly predicted that the early puffs are direct targets of

the ecdysone-bound receptor and that the corresponding early genes encode regulatory proteins that are required for inducing the late puffs (**Figure 1.1**). To this day, this conceptual framework is referred to as the Ashburner model (Ashburner, 1974; Ashburner et al., 1974). The studies performed by Karlson, Clever, Ashburner and colleagues not only offered some of the first insights into how genes may be regulated, but also produced the key ingredients for establishing an elegant and versatile model for how steroid hormones coordinate complex developmental processes.

1.2 Downstream of hormone: The ecdysone hierarchy at the onset of metamorphosis

The Ecdysone hierarchy I: Hormone action at the onset of metamorphosis. In *Drosophila*, all major developmental transitions, including the molts and the onset of metamorphosis, are triggered by major pulses of ecdysone (Riddiford, 1993). Each of these pulses has its own characteristics, such as amplitude and duration, which are largely determined by the rate and duration of hormone synthesis, how efficiently the hormone is converted to its biologically active form and how fast it is degraded. Ecdysone is produced and released from the prothoracic gland (PG) cells, which are part of a composite endocrine organ called the ring gland. Once taken up by its target tissues, ecdysone is converted to the biologically active form 20-hydroxyecdysone (hereafter refer to as 20E) (Gilbert et al., 2002). Like vertebrate steroid hormones, 20E acts by binding to members of the nuclear receptor superfamily. These are ligand-dependent transcription factors that harbor a highly conserved DNA-binding domain (DBD) as well as less conserved ligand-binding domain (LBD) (King-Jones and Thummel, 2005). The identification of the *Drosophila* ecdysone receptor gene (*EcR*) and the discovery of several early ecdysone response genes established the

molecular era of ecdysone biology in the early 1990's (Burtis et al., 1990; DiBello et al., 1991; Koelle et al., 1991; Segraves and Hogness, 1990).

EcR requires heterodimerization with another nuclear receptor, Ultraspiracle (USP) to form a functional ecdysteroid receptor capable of binding to 20E with high affinity (Thomas et al., 1993; Yao et al., 1993). *EcR* encodes three protein isoforms, EcR-A, EcR-B1 and EcR-B2, as a result of two promoters and alternative splicing (Talbot et al., 1993). All three EcR isoforms are able to interact with USP and all can bind to 20E with similar affinity. The crystal structure of the EcR LBD suggested that USP is required for forming a ligand-binding conformation, corroborating the observation that EcR alone cannot transcriptionally activate genes (Billas et al., 2003; Hu et al., 2003). Likewise, structural studies demonstrated that the LBD of dipteran and lepidopteran USP are locked in an inactive conformation, consistent with the idea that ecdysteroids achieve transcriptional activation through binding to EcR (Billas et al., 2001; Clayton et al., 2001).

The EcR/USP heterodimer functions at the top of ecdysone regulatory cascade and triggers the transcription of primary and secondary response genes in ecdysone target tissues that play more direct functions during development (**Figure 1.2**). Mutations affecting the region common to all isoforms of *EcR* are embryonic lethal, consistent with the finding that ecdysone signaling plays a critical role during germ band retraction in the developing *Drosophila* embryo (Bender et al., 1997; Kozlova and Thummel, 2003). *EcR-B1* is predominantly expressed in larval tissues that do not contribute to adult structures, and loss of *EcR-B1* function blocks the ecdysone responses in these tissues, resulting in a failure to complete metamorphosis (Bender et al., 1997; Schubiger et al., 1998). In contrast, the *EcR-A* isoform is expressed in imaginal discs and the ring gland, and animals that are mutant for *EcR-A* arrest development during late stages of pupal

development (Davis et al., 2005; Talbot et al., 1993), indicating that the different EcR isoforms have distinct functions during development.

The EcR dimerization partner USP is the fly homolog of vertebrate RXR (Henrich et al., 1990; Oro et al., 1990). Like EcR, USP is required during embryogenesis and metamorphosis, consistent with the idea that USP acts as a key partner for EcR throughout development (Hall and Thummel, 1998; Oro et al., 1992; Perrimon et al., 1985). USP also dimerizes with the nuclear receptors DHR38 and Seven-up (Baker et al., 2003; Zelhof et al., 1995), and a recent report found that EcR forms functional dimers with DHR38 as well (Van Gelder et al., 1990). In addition, genetic evidence shows that *usp* is not required for the ecdysone-dependent induction of the larval glue genes, raising the possibility that EcR requires a different partner for this response (Costantino et al., 2008). The ability of nuclear receptors to form multiple heterodimers adds another layer of regulatory complexity that will be fascinating to unravel in the future.

The Ecdysone hierarchy II: Early response genes. The molecular characterization of three early ecdysone-inducible genes *BR-C*, *E74*, and *E75* revealed that all of them encode transcription factors, albeit belonging to different DNA-binding protein families (Thummel, 1990). These primary ecdysone response genes are key regulators of the ecdysone genetic hierarchy, which induce the transcription of secondary response genes that in turn execute the appropriate biological effects in response to ecdysone pulse at the onset of metamorphosis (**Figure 1.2**).

Mutations that disrupt all *BR-C* functions (*npr1* alleles) result in larval lethality, indicating that *BR-C* is an essential gene for entry into metamorphosis (Kiss et al., 1988). The *broad* gene (here referred to as *Broad-Complex* or *BR-C*), maps to the 2B5 early puff, and is undoubtedly the most complex of the early genes. FlyBase currently acknowledges 14 transcript isoforms (McQuilton et al.,

2012), and genetically the locus contains up to four complementation groups (DiBello et al., 1991). *BR-C* produces four protein classes, dependent on which zinc finger module, designated Z1 to Z4, is incorporated into a given isoform. The common N-terminal region comprises a BTB/POZ domain, which is a protein-protein interaction domain commonly found in chromatin and transcription factors. The zinc fingers are believed to confer target specificity (DiBello et al., 1991; Zollman et al., 1994). However, high affinity DNA-binding was never established for BR-C proteins, and existing EMSA (Xiang et al., 2010) and footprinting (von Kalm et al., 1994) studies all used uncommonly high BR-C concentrations to achieve DNA binding. Future research will have to address whether BR-C recognizes its target genes via binding to DNA elements or through interactions with other chromatin-bound proteins, in which case the zinc finger domains may have a less direct role in target gene recognition.

Like BR-C, *E74* is directly induced by ecdysone and responsible for the 74EF early puff. Mutations in *E74* confer pupal lethality, indicating that this gene plays essential roles during metamorphosis. *E74* produces two protein isoforms, E74A and E74B, which share a C-terminal ETS DNA-binding domain (Burtis et al., 1990). Both isoforms are precisely controlled by changes in ecdysone titers, and display complementary profiles. *E74A* is induced when hormone concentrations are high, while *E74B* is abundant when ecdysone concentrations have fallen to intermediate or lower levels. Correspondingly, *E74A* transcript levels fall when ecdysone concentrations start to decline, and *E74B* mRNA is repressed by rising hormone titers. This behavioral link between the two isoforms is critical for the proper timing of secondary gene responses (Fletcher et al., 1997; Karim and Thummel, 1991; Urness and Thummel, 1995).

The *E75* early gene maps to the 75B early puff and encodes a member of the nuclear receptor superfamily. *E75* forms at least three protein isoforms

(E75A-C) (Segraves and Hogness, 1990). Like all *Drosophila* nuclear receptor genes, alternative splicing tends to produce protein isoforms that differ in their N-terminal sequences, but share a common ligand-binding domain in the C-terminus. This is not any different for E75, however, the E75B isoform represents an unusual nuclear receptor protein: While E75A and E75C both have a complete DBD and LBD domain, splicing of *E75B* removes a part of the DBD domain, which abolishes its ability to bind to DNA. This splice form appears to be a fairly ancient invention, since its closest fly homolog, *E78*, also generates a protein isoform (E78B) with a truncated DBD domain (Stone and Thummel, 1993). Mutations specific for *E75B* are viable, however, molecular data demonstrated that E75B binds to another nuclear receptor, DHR3, in an inhibitory fashion to delay the induction of a third nuclear receptor, β FTZ-F1 (White et al., 1997). It should be noted that *E75B* null mutants do not display defects in the timing of *β ftz-f1* expression, raising the possibility that E75B and E78B are functionally redundant (Russell et al., 1996; Stone and Thummel, 1993).

In contrast to *E75B*, animals mutant for *E75A* display larval lethality, molting defects, and developmental delays, while *E75C* is required for late pupal development and adult viability (Bialecki et al., 2002). In 2005, the Krause lab published the surprising finding that E75 binds with high affinity to heme (Reinking et al., 2005). This led to the suggestion that the protein either acts as a heme or gas sensor. A recent study from the same lab showed that E75 is a sensor for the signaling molecule nitric oxide, which will be discussed in Chapter 4.

As briefly alluded to above, many components of the ecdysone regulatory hierarchy are – like EcR and USP - members of nuclear receptor superfamily. These include DHR3 (*Drosophila* Hormone Receptor 3), DHR4 (*Drosophila* Hormone Receptor 4), DHR39 (*Drosophila* Hormone Receptor 39), E75, E78, and FTZ-F1 (fushi tarazu factor 1) (King-Jones and Thummel, 2005; Woodard et

al., 1994). Below is a brief review of the roles of DHR3, DHR4, and FTZ-F1 in the context of early metamorphic stages.

The Ecdysone hierarchy III: Early-late response genes and *βftz-f1*.

Early-late genes can be operationally defined as genes that require both the 20E-bound EcR/USP heterodimer and an early gene product for maximal transcriptional induction (**Figure 1.2**). This is typically shown in organ culture assays using protein synthesis inhibitors to block the translation of early gene mRNAs. Two early-late genes with very similar temporal expression profiles are the nuclear receptor genes *DHR3* and *DHR4*. *DHR3* is orthologous to the vertebrate retinoid-related orphan receptor (ROR), while *DHR4* is represented by germ-cell nuclear factor (GCNF) in vertebrates. *DHR3* and *DHR4* expression profiles show a peak at the beginning of prepupal stage, when the expression of early genes such as *BR-C*, *E74A*, and *E75A* is receding, and *βftz-f1* expression is about to be induced. Both *DHR3* and *DHR4* are sufficient to repress the early genes, and are required for maximal *βftz-f1* expression in mid-prepupae (King-Jones et al., 2005; Lam et al., 1997), strongly suggesting that these two factors act in concert to regulate the early genes and *βftz-f1*. Interestingly, *DHR4* mutants display precocious wandering behavior followed by premature onset of metamorphosis, resulting in a small body size due to a shortened feeding period, a phenotype not observed in any other mutants associated with the ecdysone hierarchy (King-Jones et al., 2005). This peculiar phenotype was eventually tracked to a role for *DHR4* in the prothoracic gland, which will be discussed in detail in Chapter 2.

The *Drosophila ftz-f1* gene encodes yet another nuclear receptor acting in the ecdysone cascade, and is orthologous to vertebrate steroidogenic factor 1 (SF-1). Two protein isoforms have been described, α FTZ-F1 and β FTZ-F1 (Lavorgna et al., 1991; Ueda et al., 1990). While α FTZ-F1 is maternally supplied

and has critical roles in embryogenesis, β FTZ-F1 is also expressed in the early stages of puparium formation (Yamada et al., 2000; Yu et al., 1997). Mutations in *βftz-f1* severely perturb the ecdysone signaling pathway at the onset of metamorphosis and consequently result in prepupal lethality. Later it was shown that *βftz-f1* functions as a competence factor during prepupal development, ensuring that the responses to the late larval ecdysone pulse are different from the prepupal pulse 12 hours later (Broadus et al., 1999). Taken together, the interplay between nuclear receptors E75, DHR3, and DHR4 controls the expression of *βftz-f1* during the prepupal stage, thereby safeguarding the appropriate sequence of programs necessary for the progression of pupal development.

1.3 New insights into an old story: The ecdysone hierarchy genes in the regulation of ecdysone biosynthesis

The ecdysone regulatory cascade is best understood at the onset of metamorphosis, and the finding that some components of the hierarchy might also play important roles in regulating ecdysone synthesis is not entirely new. One of the first indicators was that EcR-A is expressed in the *Drosophila* prothoracic gland, but not the other two isoforms encoded by *EcR* (Talbot et al., 1993). Another study reported that USP modulates ecdysone synthesis in the prothoracic gland of tobacco hornworm *Manduca sexta* (Song and Gilbert, 1998). Together, these observations suggested that EcR and USP might have roles in ecdysteroidogenesis, possibly through a negative feedback mechanism in response to rising levels of 20E. In addition, a null mutation in *Drosophila E75A* causes a dramatic decrease of ecdysone levels, indicating that E75A has dual roles as a 20E target during the onset of metamorphosis and a regulator of ecdysone synthesis in the prothoracic gland (Bialecki et al., 2002).

More recently, evidence showed that *broad* serves as a key regulator for

coordinating available cholesterol levels required for ecdysone synthesis in the prothoracic gland of the fruit fly. *Drosophila*, like all other insects, is a cholesterol auxotroph, and must obtain cholesterol or other suitable sterols directly from a dietary source (Carvalho et al., 2010; Clayton, 1964). Therefore, cholesterol uptake by the prothoracic gland and the intracellular trafficking of the sterol represents critical steps for the synthesis of steroid hormones in insects. It was shown that *broad* positively regulates the expression of *Npc1a* in the prothoracic gland, a cholesterol transporter gene. Disrupting *broad* function specifically in the prothoracic gland results in failure to enter metamorphosis because low levels of *Npc1a* cause a shortage of available cholesterol and consequently insufficient ecdysone production (Xiang et al., 2010). Furthermore, a report from Henry Krause's laboratory showed that nitric oxide (NO) plays a key role in the production of ecdysone through regulating the interaction of DHR3 and E75 to control the transcriptional activation of *βftz-f1*, all well characterized players of the ecdysone hierarchy (Caceres et al., 2011). β FTZ-F1 was shown to regulate the expression of at least two ecdysone biosynthetic enzymes, Phantom and Disembodied in prothoracic gland cells (Parvy et al., 2005). Therefore, Caceres et al. (2011) proposed that NO signaling modulates the DHR3/E75-mediated regulation of β FTZ-F1 in *Drosophila* prothoracic gland, which in turn controls ecdysone production (see Chapter 4 for a discussion of a novel role of NO signaling in the prothoracic gland).

Taken together, these findings have shown that some ecdysone hierarchy genes play a dual function, acting both downstream of ecdysone as 20E targets prior to metamorphosis, and also upstream of the hormone in the regulation of ecdysteroidogenesis in the prothoracic gland. Later, I will show that DHR4 appears to be another example of this category of genes.

1.4 Outline of the thesis

Overall, this thesis consists of three major parts. Firstly, I studied the function of *DHR4* during *Drosophila* larval development. As mentioned earlier, nuclear receptor DHR4 represents a component of the ecdysone hierarchy (**Figure 1.2**). *DHR4* mutants display two major phenotypes: the premature onset of wandering behavior and prepupal lethality. A failure to induce the expression of *βftz-f1* due to loss of *DHR4* accounts for the prepupal lethality observed in *DHR4* mutants (King-Jones et al., 2005). However, how DHR4 regulates the timing of the wandering behavior remained unaddressed. DHR4 protein was shown to be abundant in the cytoplasm of prothoracic gland cells (King-Jones et al., 2005), the principal site of larval ecdysone production, but it was unclear how DHR4 expression in this tissue was linked to the precocious wandering behavior observed in *DHR4* mutants. In Chapter 2, I will show that *DHR4* function in the prothoracic gland is critical for the timing of wandering behavior, and that the removal of *DHR4* in this tissue de-represses ecdysone synthesis which consequently elicits the premature onset of wandering behavior. Furthermore, I will demonstrate that DHR4 is a key target of the pathway signaled by a brain-derived peptide called PTTH, which stimulates ecdysone production in the prothoracic gland (McBrayer et al., 2007). DHR4 represents the first transcription factor identified to be under the control of PTTH signaling, and appears to function by counteracting PTTH-induced rises of ecdysone levels by oscillating between the nucleus and cytoplasm of prothoracic gland cells. I will also show that DHR4 negatively regulates the expression of *Cyp6t3*, which is a novel player of the ecdysone biosynthetic pathway. Together, my work shows that DHR4 acts as a readout of the PTTH signaling cascade in controlling ecdysone synthesis.

Over the years, we have gained a relatively good understanding of the enzymatic steps of steroid hormone synthesis in vertebrates and insects, but our

knowledge of the underlying regulatory processes is by comparison insubstantial. As the second task of my PhD research, I wanted to use the *Drosophila* ring gland as a model to study how steroid hormone production and release are regulated in a developmental context. In Chapter 3, I will present the first comprehensive genomic and genetic analysis of the ring gland by employing whole-genome microarray analysis as well as studying gene functions via RNA interference (RNAi). I will report that a total of 20 genes which have likely novel functions in ecdysone synthesis have been identified using this approach. A neurotrophin encoded by *spätzle5* represents one of them. I have been examining the role of Spätzle5 in the regulation of ecdysone production. In Chapter 5, I will show that Spätzle5 is required for the production of NO in the prothoracic gland, and that Spätzle5 and NO signaling may function in the same pathway in governing heme synthesis in prothoracic gland cells. Heme is a cofactor for ecdysteroidogenic enzymes. However, the molecular details of how heme production is controlled and coordinated with ecdysone synthesis in *Drosophila* remain largely unexplored. My research represents the first insight into this aspect of ecdysteroidogenic regulation, which will ultimately advance our understanding of insect metamorphosis and the regulation of steroid hormone synthesis in other organisms.

1.5 Figures

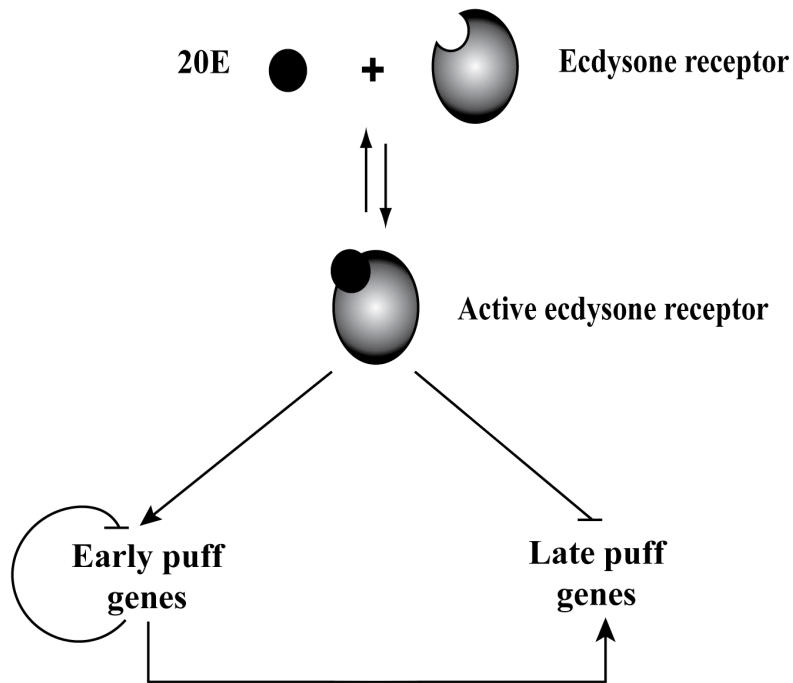


Figure 1.1. Ashburner model.

The hormone-bound and thus active ecdysone receptor directly induces the expression of early puff genes and represses late puff genes. A small set of early puff genes repress their own expression and are required for the induction of a large set of late puff genes.

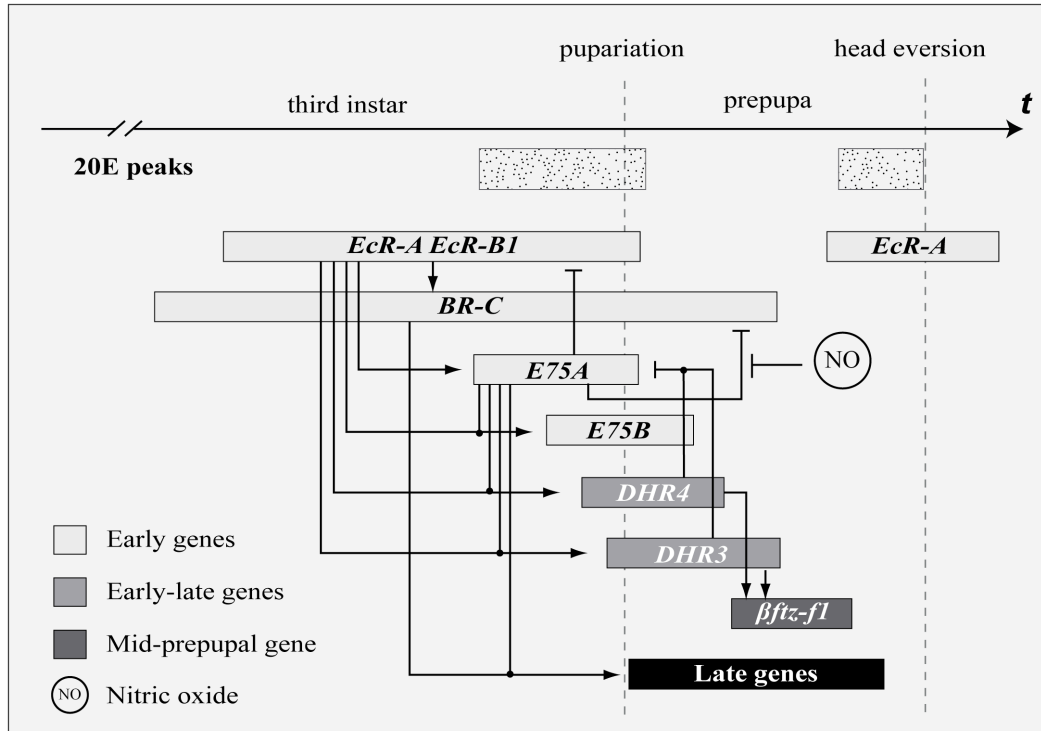


Figure 1.2. Overview of *Drosophila* ecdysone hierarchy genes at the onset of metamorphosis.

The expression of genes is shown in bars with different shades of grey representing different gene categories (see inset), and the length of the bars indicates the approximate duration of their expression. Positive and inhibitory interactions are shown. Ecdysone peaks are shown in dotted boxes at the top, and the approximate timing of puparium formation and head eversion are indicated by dotted lines. Black dots represent the combined effects of regulators. The repressive action of NO on the *E75*-mediated inhibition of *BR-C* during the larval-pupal transition was reported by Johnston et al. (Johnston et al., 2011). 20E, 20-hydroxyecdysone. EcR, ecdysone receptor. BR-C, broad-complex. DHR3, *Drosophila* hormone receptor 3. DHR4, *Drosophila* hormone receptor 4. *βftz-f1*, fushi tarazu factor 1β.

1.6 Bibliography

- Baker, K.D., Shewchuk, L.M., Kozlova, T., Makishima, M., Hassell, A., Wisely, B., Caravella, J.A., Lambert, M.H., Reinking, J.L., Krause, H., *et al.* (2003). The *Drosophila* orphan nuclear receptor DHR38 mediates an atypical ecdysteroid signaling pathway. *Cell* *113*, 731-742.
- Bender, M., Imam, F.B., Talbot, W.S., Ganetzky, B., and Hogness, D.S. (1997). *Drosophila* ecdysone receptor mutations reveal functional differences among receptor isoforms. *Cell* *91*, 777-788.
- Bialecki, M., Shilton, A., Fichtenberg, C., Segraves, W.A., and Thummel, C.S. (2002). Loss of the ecdysteroid-inducible E75A orphan nuclear receptor uncouples molting from metamorphosis in *Drosophila*. *Developmental cell* *3*, 209-220.
- Billas, I.M., Iwema, T., Garnier, J.M., Mitschler, A., Rochel, N., and Moras, D. (2003). Structural adaptability in the ligand-binding pocket of the ecdysone hormone receptor. *Nature* *426*, 91-96.
- Billas, I.M., Moulinier, L., Rochel, N., and Moras, D. (2001). Crystal structure of the ligand-binding domain of the ultraspiracle protein USP, the ortholog of retinoid X receptors in insects. *The Journal of biological chemistry* *276*, 7465-7474.
- Broadus, J., McCabe, J.R., Endrizzi, B., Thummel, C.S., and Woodard, C.T. (1999). The *Drosophila* beta FTZ-F1 orphan nuclear receptor provides competence for stage-specific responses to the steroid hormone ecdysone. *Molecular cell* *3*, 143-149.
- Burtis, K.C., Thummel, C.S., Jones, C.W., Karim, F.D., and Hogness, D.S. (1990). The *Drosophila* 74EF early puff contains E74, a complex ecdysone-inducible gene that encodes two ets-related proteins. *Cell* *61*, 85-99.
- Butenandt, A., Karlson, P. (1954). *Z Naturforsch* *9b*, 389-391.
- Caceres, L., Necakov, A.S., Schwartz, C., Kimber, S., Roberts, I.J., and Krause, H.M. (2011). Nitric oxide coordinates metabolism, growth, and development via the nuclear receptor E75. *Genes & development* *25*, 1476-1485.
- Carvalho, M., Schwudke, D., Sampaio, J.L., Palm, W., Riezman, I., Dey, G., Gupta, G.D., Mayor, S., Riezman, H., Shevchenko, A., *et al.* (2010). Survival strategies of a sterol auxotroph. *Development (Cambridge, England)* *137*, 3675-3685.
- Clayton, G.M., Peak-Chew, S.Y., Evans, R.M., and Schwabe, J.W. (2001). The structure of the ultraspiracle ligand-binding domain reveals a nuclear receptor locked in an inactive conformation. *Proceedings of the National Academy of Sciences of the United States of America* *98*, 1549-1554.
- Clayton, R.B. (1964). The Utilization of Sterols by Insects. *Journal of lipid research* *15*, 3-19.
- Clever, U., and Karlson, P. (1960). *Exp Cell Res* *20*, 623-626.
- Costantino, B.F., Bricker, D.K., Alexandre, K., Shen, K., Merriam, J.R., Antoniewski, C., Callender, J.L., Henrich, V.C., Presente, A., and Andres, A.J. (2008). A novel ecdysone receptor mediates steroid-regulated developmental events during the mid-third instar of *Drosophila*. *PLoS genetics* *4*, e1000102.
- Davis, M.B., Carney, G.E., Robertson, A.E., and Bender, M. (2005). Phenotypic analysis of

- EcR-A mutants suggests that EcR isoforms have unique functions during *Drosophila* development. *Developmental biology* 282, 385-396.
- DiBello, P.R., Withers, D.A., Bayer, C.A., Fristrom, J.W., and Guild, G.M. (1991). The *Drosophila* Broad-Complex encodes a family of related proteins containing zinc fingers. *Genetics* 129, 385-397.
- Fletcher, J.C., D'Avino, P.P., and Thummel, C.S. (1997). A steroid-triggered switch in E74 transcription factor isoforms regulates the timing of secondary-response gene expression. *Proceedings of the National Academy of Sciences of the United States of America* 94, 4582-4586.
- Fraenkel, G., and Zdarek, J. (1970). The evaluation of the "Caliphora test" as an assay for ecdysone. *Biol Bull* 139, 138-150.
- Galton, V.A. (1992). The role of thyroid hormone in amphibian metamorphosis. *Trends in endocrinology and metabolism: TEM* 3, 96-100.
- Gilbert, L.I., Rybczynski, R., and Warren, J.T. (2002). Control and biochemical nature of the ecdysteroidogenic pathway. *Annual review of entomology* 47, 883-916.
- Hall, B.L., and Thummel, C.S. (1998). The RXR homolog ultraspiracle is an essential component of the *Drosophila* ecdysone receptor. *Development (Cambridge, England)* 125, 4709-4717.
- Henrich, V.C., Sliter, T.J., Lubahn, D.B., MacIntyre, A., and Gilbert, L.I. (1990). A steroid/thyroid hormone receptor superfamily member in *Drosophila melanogaster* that shares extensive sequence similarity with a mammalian homologue. *Nucleic acids research* 18, 4143-4148.
- Hu, X., Cherbas, L., and Cherbas, P. (2003). Transcription activation by the ecdysone receptor (EcR/USP): identification of activation functions. *Molecular endocrinology (Baltimore, Md)* 17, 716-731.
- Huber, R., and Hoppe, W. (1965). *Chem Ber* 98, 2403-2424.
- Johnston, D.M., Sedkov, Y., Petruk, S., Riley, K.M., Fujioka, M., Jaynes, J.B., and Mazo, A. (2011). Ecdysone- and NO-Mediated Gene Regulation by Competing EcR/Usp and E75A Nuclear Receptors during *Drosophila* Development. *Molecular cell* 44, 51-61.
- Karim, F.D., and Thummel, C.S. (1991). Ecdysone coordinates the timing and amounts of E74A and E74B transcription in *Drosophila*. *Genes & development* 5, 1067-1079.
- Karlson, P., Hoffmeister, H., Hummel, H., Hocks, P., and Spitteler, G. (1965). *Chem Ber* 98, 2394-2402.
- King-Jones, K., Charles, J.P., Lam, G., and Thummel, C.S. (2005). The ecdysone-induced DHR4 orphan nuclear receptor coordinates growth and maturation in *Drosophila*. *Cell* 121, 773-784.
- King-Jones, K., and Thummel, C.S. (2005). Nuclear receptors--a perspective from *Drosophila*. *Nature reviews* 6, 311-323.
- Kiss, I., Beaton, A.H., Tardiff, J., Fristrom, D., and Fristrom, J.W. (1988). Interactions and developmental effects of mutations in the Broad-Complex of *Drosophila melanogaster*. *Genetics* 118, 247-259.
- Koelle, M.R., Talbot, W.S., Segraves, W.A., Bender, M.T., Cherbas, P., and Hogness, D.S. (1991).

- The *Drosophila* EcR gene encodes an ecdysone receptor, a new member of the steroid receptor superfamily. *Cell* *67*, 59-77.
- Kozlova, T., and Thummel, C.S. (2003). Essential roles for ecdysone signaling during *Drosophila* mid-embryonic development. *Science* (New York, NY *301*, 1911-1914.
- Lam, G.T., Jiang, C., and Thummel, C.S. (1997). Coordination of larval and prepupal gene expression by the DHR3 orphan receptor during *Drosophila* metamorphosis. *Development* (Cambridge, England) *124*, 1757-1769.
- Lavorgna, G., Ueda, H., Clos, J., and Wu, C. (1991). FTZ-F1, a steroid hormone receptor-like protein implicated in the activation of fushi tarazu. *Science* (New York, NY *252*, 848-851.
- McBrayer, Z., Ono, H., Shimell, M., Parvy, J.P., Beckstead, R.B., Warren, J.T., Thummel, C.S., Dauphin-Villemant, C., Gilbert, L.I., and O'Connor, M.B. (2007). Prothoracicotropic hormone regulates developmental timing and body size in *Drosophila*. *Developmental cell* *13*, 857-871.
- McQuilton, P., St Pierre, S.E., and Thurmond, J. (2012). FlyBase 101--the basics of navigating FlyBase. *Nucleic acids research* *40*, D706-714.
- Oro, A.E., McKeown, M., and Evans, R.M. (1990). Relationship between the product of the *Drosophila* ultraspiracle locus and the vertebrate retinoid X receptor. *Nature* *347*, 298-301.
- Oro, A.E., McKeown, M., and Evans, R.M. (1992). The *Drosophila* retinoid X receptor homolog ultraspiracle functions in both female reproduction and eye morphogenesis. *Development* (Cambridge, England) *115*, 449-462.
- Parvy, J.P., Blais, C., Bernard, F., Warren, J.T., Petryk, A., Gilbert, L.I., O'Connor, M.B., and Dauphin-Villemant, C. (2005). A role for betaFTZ-F1 in regulating ecdysteroid titers during post-embryonic development in *Drosophila melanogaster*. *Developmental biology* *282*, 84-94.
- Perrimon, N., Engstrom, L., and Mahowald, A.P. (1985). Developmental genetics of the 2C-D region of the *Drosophila* X chromosome. *Genetics* *111*, 23-41.
- Reinking, J., Lam, M.M., Pardee, K., Sampson, H.M., Liu, S., Yang, P., Williams, S., White, W., Lajoie, G., Edwards, A., *et al.* (2005). The *Drosophila* nuclear receptor e75 contains heme and is gas responsive. *Cell* *122*, 195-207.
- Riddiford, L.M. (1993). Hormone receptors and the regulation of insect metamorphosis. *Receptor* *3*, 203-209.
- Russell, S.R., Heimbeck, G., Goddard, C.M., Carpenter, A.T., and Ashburner, M. (1996). The *Drosophila* Eip78C gene is not vital but has a role in regulating chromosome puffs. *Genetics* *144*, 159-170.
- Rybczynski, R., Bell, S.C., and Gilbert, L.I. (2001). Activation of an extracellular signal-regulated kinase (ERK) by the insect prothoracicotropic hormone. *Molecular and cellular endocrinology* *184*, 1-11.
- Schubiger, M., Wade, A.A., Carney, G.E., Truman, J.W., and Bender, M. (1998). *Drosophila* EcR-B ecdysone receptor isoforms are required for larval molting and for neuron

- remodeling during metamorphosis. *Development (Cambridge, England)* *125*, 2053-2062.
- Segraves, W.A., and Hogness, D.S. (1990). The E75 ecdysone-inducible gene responsible for the 75B early puff in *Drosophila* encodes two new members of the steroid receptor superfamily. *Genes & development* *4*, 204-219.
- Song, Q., and Gilbert, L.I. (1998). Alterations in ultraspiracle (USP) content and phosphorylation state accompany feedback regulation of ecdysone synthesis in the insect prothoracic gland. *Insect biochemistry and molecular biology* *28*, 849-860.
- Stone, B.L., and Thummel, C.S. (1993). The *Drosophila* 78C early late puff contains E78, an ecdysone-inducible gene that encodes a novel member of the nuclear hormone receptor superfamily. *Cell* *75*, 307-320.
- Talbot, W.S., Swyryd, E.A., and Hogness, D.S. (1993). *Drosophila* tissues with different metamorphic responses to ecdysone express different ecdysone receptor isoforms. *Cell* *73*, 1323-1337.
- Thomas, H.E., Stunnenberg, H.G., and Stewart, A.F. (1993). Heterodimerization of the *Drosophila* ecdysone receptor with retinoid X receptor and ultraspiracle. *Nature* *362*, 471-475.
- Thummel, C.S. (1990). Puffs and gene regulation--molecular insights into the *Drosophila* ecdysone regulatory hierarchy. *Bioessays* *12*, 561-568.
- Thummel, C.S. (1995). From embryogenesis to metamorphosis: the regulation and function of *Drosophila* nuclear receptor superfamily members. *Cell* *83*, 871-877.
- Truman, J.W., and Riddiford, L.M. (1999). The origins of insect metamorphosis. *Nature* *401*, 447-452.
- Ueda, H., Sonoda, S., Brown, J.L., Scott, M.P., and Wu, C. (1990). A sequence-specific DNA-binding protein that activates fushi tarazu segmentation gene expression. *Genes & development* *4*, 624-635.
- Urness, L.D., and Thummel, C.S. (1995). Molecular analysis of a steroid-induced regulatory hierarchy: the *Drosophila* E74A protein directly regulates L71-6 transcription. *The EMBO journal* *14*, 6239-6246.
- Van Gelder, R.N., von Zastrow, M.E., Yool, A., Dement, W.C., Barchas, J.D., and Eberwine, J.H. (1990). Amplified RNA synthesized from limited quantities of heterogeneous cDNA. *Proceedings of the National Academy of Sciences of the United States of America* *87*, 1663-1667.
- von Kalm, L., Crossgrove, K., Von Seggern, D., Guild, G.M., and Beckendorf, S.K. (1994). The Broad-Complex directly controls a tissue-specific response to the steroid hormone ecdysone at the onset of *Drosophila* metamorphosis. *The EMBO journal* *13*, 3505-3516.
- White, K.P., Hurban, P., Watanabe, T., and Hogness, D.S. (1997). Coordination of *Drosophila* metamorphosis by two ecdysone-induced nuclear receptors. *Science (New York, NY)* *276*, 114-117.
- Woodard, C.T., Baehrecke, E.H., and Thummel, C.S. (1994). A molecular mechanism for the stage specificity of the *Drosophila* prepupal genetic response to ecdysone. *Cell* *79*, 607-615.
- Xiang, Y., Liu, Z., and Huang, X. (2010). *br* regulates the expression of the ecdysone biosynthesis

- gene *npc1*. *Developmental biology* 344, 800-808.
- Yamada, M., Murata, T., Hirose, S., Lavorgna, G., Suzuki, E., and Ueda, H. (2000). Temporally restricted expression of transcription factor betaFTZ-F1: significance for embryogenesis, molting and metamorphosis in *Drosophila melanogaster*. *Development (Cambridge, England)* 127, 5083-5092.
- Yao, T.P., Forman, B.M., Jiang, Z., Cherbas, L., Chen, J.D., McKeown, M., Cherbas, P., and Evans, R.M. (1993). Functional ecdysone receptor is the product of *EcR* and *Ultraspiracle* genes. *Nature* 366, 476-479.
- Yu, Y., Li, W., Su, K., Yussa, M., Han, W., Perrimon, N., and Pick, L. (1997). The nuclear hormone receptor *Ftz-F1* is a cofactor for the *Drosophila* homeodomain protein *Ftz*. *Nature* 385, 552-555.
- Zelhof, A.C., Yao, T.P., Chen, J.D., Evans, R.M., and McKeown, M. (1995). Seven-up inhibits ultraspiracle-based signaling pathways in vitro and in vivo. *Molecular and cellular biology* 15, 6736-6745.
- Zollman, S., Godt, D., Prive, G.G., Couderc, J.L., and Laski, F.A. (1994). The BTB domain, found primarily in zinc finger proteins, defines an evolutionarily conserved family that includes several developmentally regulated genes in *Drosophila*. *Proceedings of the National Academy of Sciences of the United States of America* 91, 10717-10721.

Chapter 2

Nuclear receptor DHR4 controls the timing of steroid hormone pulses
during *Drosophila* development

A version of this chapter has been published. Ou Q, Magico A, King-Jones K.
(2011) Nuclear receptor DHR4 controls the timing of steroid hormone pulses
during *Drosophila* development. PLoS Biol 9(9): e1001160.
doi:10.1371/journal.pbio.1001160

(Note: Qiuxiang Ou conducted all experiments shown in this chapter.)

2.1 Introduction

2.1.1 *Drosophila* development and ecdysone pulses

In humans, the onset of puberty is triggered by an increase in gonadotropin releasing hormone (GnRH) secretion from a region in the brain called the hypothalamus (Terasawa and Fernandez, 2001). Elevated GnRH levels ultimately cause the ovaries or testes to increase production of steroid hormones, estrogens and testosterone, which coordinate the developmental and behavioral changes associated with reproductive maturation. In insects, maturation is also governed by a steroid hormone, 20-hydroxyecdysone (20E), which is the biologically active form of the insect molting hormone ecdysone (E). It is well known that the prothoracic gland cells (part of the ring gland) are the principal source of ecdysone that is further converted into 20E in target tissues (**Figure 2.1A**). The production, release and degradation of ecdysone are tightly controlled resulting in systemic pulses of defined duration. During *Drosophila* development, as indicated in **Figure 2.1B**, six major ecdysone pulses control embryogenesis, the molts, the onset of metamorphosis and the differentiation of adult tissues (Riddiford, 1993), while the three minor pulses of ecdysone in the last larval instar (Warren et al., 2006) are critical for physiological and behavioral changes prior to metamorphosis, including the commitment of a larva to a pupal fate (critical weight checkpoint), the induction of the glue genes that attach the pupa to a solid substrate, and the transition from feeding to wandering behavior (Davidowitz et al., 2003; Lehmann, 1996; Mirth et al., 2005; Riddiford, 1993; Sokolowski, 2001; Warren et al., 2006). However, the mechanisms that regulate the onset, amplitude and duration of ecdysone pulses remain poorly understood.

The ecdysone biosynthetic genes appear to be the best-known players in our current understanding of the ecdysteroidogenic pathway, which encode enzymes that convert dietary cholesterol to the active hormone 20E (Gilbert, 2004;

Gilbert et al., 2002) (**Figure 2.2**). In particular, *neverland*, encoding a Rieske electron oxygenase, is required for the first step of ecdysone biosynthesis converting cholesterol into 7-dehydro-cholesterol (Yoshiyama et al., 2006). The Halloween genes, including *phantom*, *disembodied*, *shadow* and *shade*, encode the cytochrome P450 hydroxylases that are responsible for the last four steps in the formation of 20E (Chavez et al., 2000; Niwa et al., 2005; Nusslein-Volhard and Wieschaus, 1980; Petryk et al., 2003; Warren et al., 2002; Warren et al., 2004). However, relatively little is known about the enzymatic steps that catalyze the reactions converting 7-dehydro-cholesterol to 5 β -ketodiol, commonly referred to as the ‘Black Box’, which is believed to harbor the rate-limiting step(s) of ecdysone synthesis (Gilbert, 2004). Prior to my work, only two genes have been shown to function in the ‘Black Box’, including *shroud*, which encodes a short-chain dehydrogenase/reductase (Kavanagh et al., 2008; Niwa et al., 2010), and *spookier*, which also encodes a cytochrome P450 enzyme (Ono et al., 2006) (**Figure 2.2**). Despite considerable efforts, it still remains unclear how the expression of these biosynthetic genes are modulated to shape the ecdysone pulses that are switched on and off rapidly throughout development.

2.1.2 PTTH and ecdysone biosynthesis

It has long been known that a small brain-derived peptide, now known as the prothoraciotropic hormone (PTTH), triggers the production and release of ecdysone. Kataoka et al. purified 226 μ g of the silkworm *Bombyx mori* PTTH from 3 million *Bombyx* heads collected from 1.5 tons of moths, which was shown to have activity in stimulating ecdysone production in *Bombyx* prothoracic glands (Kataoka et al., 1991). Previous studies on *Bombyx* and the tobacco hornworm *Manduca sexta* showed that the PTTH prohormone is synthesized in a pair of neurosecretory cells in the brain, released into the hemolymph, where it is

processed into its mature form, whereupon it reaches the prothoracic glands to initiate a signaling cascade that eventually results in an increase in ecdysone production (Kawakami et al., 1990; Westbrook and Bollenbacher, 1990). More recently, McBrayer et al. (2007) identified the gene encoding *Drosophila* PTTH, *ptth*, which is also expressed in a pair of neurons in the embryonic and larval brain. *Drosophila* PTTH-producing neurons directly innervate the prothoracic gland cells and stimulate ecdysone production. Genetic ablation of these neurons gives rise to prolonged larval stages and significantly larger animals compared to wild type. This observation is somewhat surprising because removal of PTTH does not abolish molting altogether, raising the question of whether PTTH is required for developmental events prior to metamorphosis. It is worth noting that PTTH-ablated animals have significantly decreased expression of the Halloween genes, suggesting that these biosynthetic enzymes are modulated at least in part through PTTH (McBrayer et al., 2007). Interestingly, in the same report, it has been demonstrated that PTTH mRNA displays an unusual cyclic pattern with transcript levels peaking every 8-hour during the L3. It remains unknown whether this unusual transcriptional profile reflects corresponding changes of PTTH peptide levels, but it is plausible that these PTTH mRNA oscillations are causally associated with the minor ecdysone pulses that occur during the L3 in *Drosophila* (**Figure 2.1B**).

How does PTTH exert its function on the prothoracic gland? Rewitz et al. (2009) have recently reported that Torso, a receptor tyrosine kinase that regulates embryonic terminal cell fate in *Drosophila* (Klingler et al., 1988; Sprenger et al., 1989), is the receptor for PTTH (Rewitz et al., 2009b). Disruption of *torso* function via RNAi in a PG-specific manner recapitulates the phenotypes displayed by PTTH-ablated animals. It has been demonstrated that, upon binding PTTH, Torso activates a small G-protein (GTPase), Ras, a well-characterized signaling

molecule that transduces extracellular signals. Ras then activates Raf/ERK that triggers a signaling cascade to promote ecdysone synthesis (Li, 2005; Rewitz et al., 2009b). Loss-of-function of these pathway components (*ERK*, *dRaf*, and *Ras1*) via PG-specific RNAi again phenocopies PTTH ablation and *torso* RNAi, resulting in large, delayed animals. Conversely, when a constitutively active form of Ras (Ras^{V12}) was expressed specifically in the PG, larval development was accelerated, resulting in small, precocious pupae (Rewitz et al., 2009b). What are the downstream effectors of PTTH signaling? Previous studies on *Manduca* have suggested that the ribosomal protein S6 serves as a target of PTTH, which is supported by the evidence that S6 was phosphorylated in the vertebrate system when PTTH is present (Song and Gilbert, 1995, 1997). It will be of interest to determine whether S6 is phosphorylated directly by the PTTH/Ras/ERK pathway. However, there is no doubt that the ribosomal protein S6 is not the sole target of PTTH signaling. More recently, a study by Lin and Gu in the *Bombyx* PG revealed that the phosphorylation of another component in addition to ERK, a 120-kDa protein of unknown identity, showed time- and dose-dependent stimulation by PTTH *in vitro*, and ecdysone synthesis is impaired when the phosphorylation is attenuated (Lin and Gu, 2011). This observation suggested a role of this unknown protein in PTTH-stimulated *Bombyx* ecdysteroidogenesis. In the future, identifying new components and mechanisms of controlling ecdysteroidogenesis will help us understand the physiology of the prothoracic gland and also the genetics of animal steroidogenesis in general.

2.1.3 Outline

In this chapter, my findings show that a nuclear receptor DHR4, *Drosophila* Hormone Receptor 4, serves as a critical readout of PTTH signaling in mediating the proper timing of ecdysone pulses in the *Drosophila* prothoracic

gland. As described in Chapter 1, animals mutant for *DHR4* (the *DHR4*¹ mutant) display small body size due to shortened larval stages and a concomitant reduced feeding time (King-Jones et al., 2005), which is strikingly similar to the phenotype observed in animals expressing *Ras*^{V12} specifically in the PG (Rewitz et al., 2009b), suggesting a possible link between DHR4 and PTTH signaling. Previous studies have demonstrated that the accelerated larval development of the *DHR4*¹ mutant results from the premature onset of wandering behavior (King-Jones et al., 2005), which may be caused by an aberrant ecdysone peak due to *DHR4* loss-of-function. This observation suggested a possible role of *DHR4* in controlling larval growth and developmental timing by regulating ecdysone levels. In addition, it was shown that DHR4 is highly enriched in the cytoplasm of PG cells in mid and late L3 larvae with little or no protein detected in the nucleus nor in the neighboring two gland tissues, the *corpus allatum* and the *corpora cardiaca* (King-Jones et al., 2005). This data further suggested that *DHR4* has an important function in larval PG, which will be discussed in detail in this chapter.

2.2 Methods

Drosophila stocks

GAL4 drivers were obtained from labs indicated by the references. Ring gland: *P0206-Gal4*, *UAS-mCD8-GFP* (Janning, 1997). Prothoracic gland: *phm22-Gal4* (Rewitz et al., 2009b); *phmN1-Gal4*, *UAS-mCD8-GFP* (Mirth et al., 2005). *Corpus allatum*: *Aug21-Gal4/CyO*, *act-GFP*. Fat body: *Cg-Gal4* (Asha et al., 2003). PTTH-Gal4 driver and PTTH ablation line: *UAS-Grim/CyO*, *act-GFP*; *ptth-Gal4/Ser*, *act-GFP* (McBrayer et al., 2007). *DHR4*¹/*FM7h* and *hsDHR4-RNAi* (King-Jones et al., 2005). *w*¹¹¹⁸ (#3605) and *UAS-Ras*^{V12} (#4847) were ordered from the Bloomington stock center. RNAi lines were ordered from the Vienna *Drosophila* RNAi Center (Dietzl et al., 2007). Flies were reared on

standard agar-cornmeal medium at 25°C.

Developmental timing analysis

Before embryos were collected on grape juice agar plates, flies were allowed to pre-lay eggs 2x2-hr in order to reduce egg retention. After 2-hr egg collection intervals at 25°C, eggs were transferred to Petri dishes containing fresh yeast paste or food plates and reared at 25°C. Time to pupariation was measured in hours from either egg deposition (only for **Figure 2.3C**) or the L2/L3 molt (for the rest of experiments).

For the late L2 *hsDHR4*-RNAi experiments, larvae were reared on yeast until late L2, at which *w¹¹¹⁸* controls and *hsDHR4*-RNAi L2 larvae were heat shocked for 35 min at 37.5°C. After a 4-hr recovery, newly molted L3 larvae (0 hr-old L3) were transferred to yeast paste supplemented with 0.05% bromophenol blue to monitor their gut clearing status. For the early L3 *hsDHR4*-RNAi experiments, larvae were first carefully staged at the L2/L3 molt. After a 4-hr recovery, both control and *hsDHR4*-RNAi L3 larvae were heat shocked for 35 min at 37.5°C. After heat treatment, larvae were transferred to yeast paste supplemented with 0.05% bromophenol blue to monitor their gut purging status. Time to pupariation was measured in hours relative to the L2/L3 molt as stated.

Transgenic constructs

To generate *pUAST-DHR4* cDNA, a 6.3 kb fragment containing the full-length synthetic cDNA of *DHR4* was cut with EcoRI and XbaI from Litmus 28 and cloned into *pUAST* digested with the same enzymes. For the *UAS-DHR4*-RNAi construct, the same inverted repeat used in the *hsDHR4*-RNAi (King-Jones et al., 2005) was used to clone the fragment into *pUAST* using XbaI for all restriction cuts. Transgenic flies were generated by injecting DNA at a

concentration of 0.5 $\mu\text{g}/\mu\text{l}$ along with 0.1 $\mu\text{g}/\mu\text{l}$ of the helper plasmid P Δ 2–3 into embryos following standard procedures (Rubin and Spradling, 1982; Spradling and Rubin, 1982).

Sample collection, total RNA extraction, RNA integrity control

Whole larvae were collected in distilled water and snap-frozen in liquid nitrogen, while dissected tissue samples (brain-ring gland complex) were prepared in ice-cold PBS, rinsed twice with fresh PBS, transferred to 200 μl TRIzol (Invitrogen), and snap-frozen in liquid nitrogen. Total RNA of whole larvae was isolated following a modified TRIzol protocol, where I substituted sodium acetate with lithium chloride for RNA precipitation. Total RNA from tissue samples was extracted using the RNeasy mini kit (Qiagen) or RNAqueous micro kit (Ambion) following the manufacturer's instructions. RNA concentration was measured by NanoDrop spectrophotometer (Thermo Scientific). RNA integrity was evaluated by Agilent Bioanalyzer 2100 Nano chips.

Quantitative real-time PCR (qPCR)

RNA samples (0.5–2 $\mu\text{g}/\text{reaction}$) were reverse transcribed using ABI High Capacity cDNA Synthesis kit (Cat. No. 4368814). Unused RNA samples were aliquoted and stored at -80°C . The synthesized cDNA was used for qPCR (StepOnePlus, Applied Biosystems) using Power SYBR Green PCR master mix (Applied Biosystems, P/N 4368577) or KAPA Green PCR master mix (Kapa Biosystems, KK4605) with 5 ng of cDNA template with a primer concentration of 200 nM. Samples were normalized to *rp49* based on the $\Delta\Delta\text{Ct}$ method (Livak and Schmittgen, 2001). All primer sequences can be found in **Table 2.1**. The primer design (melting temperature [T_m]=60 \pm 1 $^{\circ}\text{C}$) was based on the Roche online assay design center.

Immunostaining

Tissues were dissected from larvae in PBS, fixed in 4% paraformaldehyde (EMS #15710) in PBST (PBS containing 0.3% Triton-X 100) for 20 min at room temperature (RT), and washed in PBST. Tissues were then blocked for 2 hr at RT or overnight at 4°C in PBST/5% NGS. Primary antibodies were incubated at 4°C overnight, while the secondary antibody was either incubated overnight at 4°C or 4 hr at RT. Nuclei were stained with DAPI (1:5000). After several wash steps, tissues were mounted in Antifade Reagent (Invitrogen). Images were captured on a Nikon C1 Plus confocal microscope. Anti-DHR4 antibody was used at a dilution of 1:500, and anti-ERK (nonphospho-ERK) antibody was used at a dilution of 1:100 (Cell Signaling #4695). Secondary antibodies (anti-rabbit Cy3) were used at a dilution of 1:200 (Rockland #611-104-122).

Ring gland microarrays

For the *DHR4*-RNAi ring gland microarrays, *hsDHR4*-RNAi and *w¹¹¹⁸* populations were heat shocked as late L2 larvae for 35 min at 37.5°C. To carefully stage larvae at the L2/L3 molt, L3 larvae were discarded 4 hr after the heat treatment, and L3 larvae that molted in the following hour were allowed to feed for either 4 hr or 8 hr before their ring glands were dissected in ice-cold PBS. Similarly, 10 ring glands per sample were dissected and washed twice in PBS before being transferred to ice-cold TRIzol reagent. The lysates were then vortexed for 5 sec at RT, flash frozen, and stored at -80°C. Ring gland total RNA was isolated by RNAqueous-Micro Kit (Ambion) or RNeasy Kit (Qiagen). Isolated RNA was quantified by RiboGreen Quanti Kit (Invitrogen) and RNA integrity was analyzed by Agilent Bioanalyzer Pico Chips. Whole larvae RNA was isolated according to the standard TRIzol RNA extraction protocol. RNA was quantified by NanoDrop spectrophotometer (Thermo) and RNA integrity was

analyzed by Agilent Bioanalyzer Nano Chips.

Linear amplification of RNA was based on the Message II RNA Amplification kit (Ambion): First-strand cDNA synthesis was carried out by a T7-(dT) primer and ArrayScript reverse transcriptase using 50 ng RNA of each ring gland sample and whole larvae sample. Second-strand cDNA synthesis was performed according to the provided protocol. Purified cDNA was then fed into the *in vitro* transcription (IVT) reactions. The amplified RNA (aRNA) was column-purified and analyzed by Agilent Bioanalyzer Nanochips. 1 µg of aRNA was used for double-stranded cDNA synthesis (Invitrogen SuperScript One-Cycle cDNA Kit) and 1 µg of the purified cDNA was Cy3-labeled by Roche NimbleGen Cy3-labeled one-color cDNA labeling kit. From this, 4 µg of cDNA was hybridized on a NimbleGen *Drosophila melanogaster* Gene Expression 12X135K Array (Roche Applied Science). Each condition was analyzed by three independent biological samples. Chip hybridization and scanning was performed by the Alberta Transplant Applied Genomics Center. Raw data were normalized with the NimbleScan software (NimbleGen) using the RMA algorithm (Bolstad et al., 2003), and data were analyzed with Arraystar 4.0 (DNASTar) as well as Access (Microsoft).

Sterol rescue experiments

Two types of media were used in the experiment, standard medium and instant food. For 20E-containing standard medium, 33 mg of 20E (Steraloids Inc., USA) was dissolved in 3.3 ml of 100% ethanol, which was added to 100 ml of liquid standard agar-cornmeal media. The control food contains 3.3% ethanol without 20E. 30 or 40 larvae were raised on each food plate in order to avoid overpopulation. For the rescue experiment of *Cyp6t3*-RNAi larvae with ecdysteroid precursors, I used an instant fly medium (“4–24,” Carolina Biological

Supply Company, hereafter referred to as C424), which is naturally low in cholesterol and other sterols. Ecdysteroid precursors were dissolved in 100% ethanol, and added to each vial with 1 g of ground C424 powder. Ethanol was allowed to evaporate completely before the medium was mixed vigorously with 5 ml of distilled water. The final concentrations for the precursors used were: cholesterol: 20 µg/ml, 7-dehydro-cholesterol: 100 µg/ml, 5β-ketodiol: 200 µg/ml, E: 40 µg/ml, 20E: 200 µg/ml. 5β-ketodiol was a kind gift from Dr. Ryusuke Niwa (University of Tsukuba, Japan); all other sterols were purchased from Steraloids Inc. (Newport, USA).

Ecdysone measurements

Larvae were collected in 1.5 ml microfuge tubes and stored at -80°C. Samples were then homogenized in methanol and centrifuged at maximum speed (13.3K rpm), after which the precipitates were re-extracted with ethanol. The extracts were pooled and dried with a SpeedVac centrifuge. The dried extracts were thoroughly dissolved in EIA buffer at 4°C overnight prior to the EIA assay. 20E EIA antiserum (#482202), 20E AChE tracer (#482200), Precoated (Mouse Anti-Rabbit IgG) EIA96-Well Plates (#400007), and Ellman's Reagent (#400050) were all purchased from Cayman Chemical (Ann Arbor, USA), and assays were performed according to the manufacturer's instructions.

RNA Probe synthesis

For *in situ* hybridizations, antisense RNA probes of *Cyp6t3* and *phantom* (positive control) were made by *in vitro* transcription. PCR fragments amplified from genomic DNA were inserted into pBlueScript (SK) cloning vectors. The cloning vectors containing each cDNA were linearized by restriction enzymes, EcoRV and XbaI. The linearized plasmids were purified by the QIAquick spin

columns (Qiagen). DIG-labeled RNA probes were generated by *in vitro* transcription following the manufacturer's instructions (Roche DIG RNA Labeling Mix, #11 277 073 910). The linearized plasmid template (~1 µg), 4 µl of 5X transcription buffer, 2 µl of 10X DIG RNA labeling mix, 2 µl of T7 or T3 RNA polymerase, and RNase-free H₂O were added in a total reaction volume of 20 µl. The reaction was incubated at 37°C for 2 hr. After stopping the reaction by the addition of 1 µl of 0.5 M EDTA (pH 8.0), the probe solution was precipitated with the help of 2 µl of 8 M LiCl and 75 µl of absolute ethanol at -20°C overnight. After a 30 min centrifuge at max speed at 4°C, RNA probes were dissolved in nuclease-free H₂O. RNA was quantified by NanoDrop spectrophotometer (Thermo Scientific) and RNA integrity was analyzed by conventional agarose gel electrophoresis.

***In situ* RNA hybridization**

L3 larvae were dissected in ice-cold PBS and fixed in 4% paraformaldehyde for 20 min at RT. After treatment with 1% H₂O₂, samples were stored in hybridization buffer at -20°C. Samples were prehybridized in hybridization buffer for 3 hr at 58°C and RNA probes were denatured for 3 min at 80°C. Probe hybridization was performed for 16-18 hr (overnight) at 58°C, followed by extensive wash steps at 58°C. After cooling, tissues were blocked with PBTB buffer (2% NGS and 1% BSA) for 1 hr at RT before overnight incubation with mouse Anti-Digoxin antibody (Jackson ImmunoResearch Cat. # 200-062-156, 1:500 dilution) at 4°C. Tissues were then incubated with streptavidin-HRP conjugates (Molecular Probes #S991, 1:400 dilution) in PBTB for 1 hr at RT, followed by six wash steps (1 hr each) in PBTB at RT. Before TSA amplification, tissues were washed in PBTB. Tyramide reagents (PerkinElmer TSA Plus Cyanine 3 Kit, Cat. #NEL744001KT) were diluted 1:1000 in 100 µl of

the amplification buffer provided by the kit. TSA reactions were performed for 40 min at RT and washed six times for 1 hr in PBS at RT. Tissues were mounted in the ProLong Gold antifade reagent (Invitrogen, P36934) and analyzed by confocal microscopy (Nikon AZ-C1 Confocal Microscope System).

***Drosophila* embryo cuticle preparation**

Embryos were dechorinated with 50% bleach (freshly diluted) for 2 min at RT, then transferred to a 15 ml Falcon tube containing a mixture of 2 ml of heptane and 2 ml of methanol, and shaken vigorously for 1 min. After embryos settled to the bottom, the heptane phase (top phase) was removed, followed by adding another 2 ml of methanol and shaking for 30 sec. Methanol was then removed, and embryos were washed twice with distilled water. Embryos were then transferred to a microscope slide bearing a drop of Hoyer's medium mixed 1:1 with pure lactic acid, gently pressured with a cover slip, and placed in a 70°C incubator overnight prior to viewing. Cuticle structures were analyzed by phase-contrast microscopy (Leica, Microsystems Inc.).

2.3 Results

2.3.1 *DHR4*^l mutants display a range of growth defects

It has previously been reported by King-Jones et al. (2005) that animals mutant for *DHR4* (hereafter refer to as the *DHR4*^l mutant) stop feeding and start wandering much earlier than controls, giving rise to small prepupae (King-Jones et al., 2005) (**Figure 2.3A**). Furthermore, loss of *DHR4* function results in 100% prepupal lethality owing to defects in the ecdysone hierarchy during early pupal development, which is in line with the role of *DHR4* as a classic ecdysone hierarchy gene. Interestingly, King-Jones et al. (2005) also observed a unique phenotype inflicted by the *DHR4*^l mutation, namely, around 5% of the mutant

population are remarkably small third instars that never pupariate due to insufficient fat stores (**Figure 2.3B**). This extreme growth defect is likely caused by a very early onset of wandering behavior since these animals do not feed during the early third instar, compared to controls which stop feeding roughly one day later.

It has been shown that *DHR4* is expressed in two major tissues during the larval stages, the fat body, the major larval metabolic tissue that is equivalent to the vertebrate liver and adipose tissues, and the ring gland (King-Jones et al., 2005). In particular, *DHR4* is expressed in the prothoracic gland during larval second and third instars (no data shown for the first instar), and in the fat body prior to the larval molts (**Figure 2.4 & Figure 2.13**). Therefore, a major question I wanted to ask was in which tissue the expression of *DHR4* is critical for regulation of developmental timing.

2.3.2 Loss-of-*DHR4* function in the PG results in developmental timing phenotypes

To determine whether it is the expression of *DHR4* in the fat body or the PG that correlates with the developmental timing defects displayed by the *DHR4^l* mutant, I performed a tissue-specific RNAi knockdown of *DHR4* in either of these tissues using the GAL4/UAS system (Brand and Perrimon, 1993; Duffy, 2002). I found that knocking down *DHR4* in the ring gland by the *P0206-Gal4* driver results in acceleration of developmental timing leading to small prepupae (**Figure 2.3A**). In particular, *P0206>DHR4-RNAi* homozygous animals (hereafter refer to it as *P0206>DHR4-RNAi[x2]*) start wandering and pupariate precociously more than 20 hours earlier than homozygous *P0206-Gal4* drivers do, suggesting that the *DHR4* expression in the PG is essential for correct developmental timing (**Figure 2.3C**). In contrast, loss of *DHR4* function

specifically in the fat body does not affect developmental timing, but results in prepupal lethality in the *Cg>DHR4-RNAi(x2)* population (**Figure 2.3A**), which is consistent with a defect in the ecdysone hierarchy, including the failure to evert anterior spiracles, incomplete head eversion, and incorrect location of the gas bubble. This indicates that the *DHR4* expression in the fat body is critical for prepupal development. The defects observed with fat body and ring gland-specific RNA interference of *DHR4* function recapitulate the phenotypes displayed by the *DHR4¹* mutant, suggesting that *DHR4* function is most critical in these two tissues.

2.3.3 *DHR4* expression in the early L3 contributes to the precocious wandering behavior

Since the critical weight is determined in early L3 larvae (Mirth et al., 2005; Nijhout, 1975), I tested whether *DHR4* function is required during this time to ensure proper timing of wandering behavior. To do this, I used a heat-inducible RNAi line (*hsDHR4-RNAi*) to activate *DHR4-RNAi* either in the late second instar or in the early third instar (**Figure 2.5A**). To test whether either of these heat shock treatments affected timing of wandering behavior, I examined the percentage of clear-gut larvae at different times during the L3 stage by incorporating a blue dye called bromophenol blue into fly food. Generally, animals gradually purge their gut contents after they start wandering, and complete gut clearing a few hours prior to puparium formation (Andres and Thummel, 1994; Maroni, 1983) (**Figure 2.5A**). Therefore, the blue food serves as a valid tool to approximately stage larval development. Using this approach, I observed that when *hsDHR4-RNAi* larvae were heat-shocked in the late L2, they displayed premature wandering behavior, since they underwent gut clearing much earlier than controls. ~70% of the *hsDHR4-RNAi* population already initiated

wandering before 30 hr after the L2/L3 molt, compared to only 10% of the control population (**Figure 2.5B**). However, when larvae were heat-treated 8 hours later, in the early L3, *hsDHR4*-RNAi larvae behaved similarly as controls with no premature wandering behavior observed (**Figure 2.5B**), suggesting that *DHR4* function around the L2/L3 molt is critical for triggering the wandering behavior. In addition, I observed that disrupting *DHR4* function via RNAi during the late L2 could phenocopy the dwarf larva phenotype seen in *DHR4^l* mutants (in nearly 5-10% of the late L2 *hsDHR4*-RNAi population), while heat shock treatment applied in the early L3 could not. Lastly, I have also noticed that *hsDHR4*-RNAi larvae that were heat-treated in the late L2 displayed premature onset of autophagy in the fat body, an important cellular response that occurs during wandering (**Figure 2.5D**), but not for larvae heat-shocked in the early L3. Taken together, these data strongly support the idea that *DHR4* function during the molt from a second to a third instar is essential for the proper timing of wandering behavior. Remarkably, the L2/L3 molt corresponds to the time window when critical weight is determined, suggesting that *DHR4* is required for proper execution of this checkpoint. However, neither the late L2 *DHR4*-RNAi nor the early L3 *DHR4*-RNAi could induce premature metamorphosis, instead, *DHR4*-RNAi animals heat-treated in either L2 or L3 were slightly delayed (**Figure 2.5C**). This is possibly because that the effectiveness of a single RNAi treatment has been greatly diminished by the time larvae prepare for puparium formation.

2.3.4 *DHR4* RNAi stimulates premature ecdysone signaling in L3 larvae

As mentioned above, it is generally believed that the wandering behavior at mid-third instar is triggered by a minor ecdysone peak. Therefore, I asked whether early wandering in *P0206>DHR4*-RNAi(x2) larvae is caused by

precocious ecdysone signaling. To answer this question, I examined the expression levels of the glue gene *Sgs-4* via quantitative real-time PCR (qPCR). *Sgs-4* is an ecdysone-inducible gene and, therefore, it serves as an internal marker of ecdysone signaling (Hansson and Lambertsson, 1983; Hansson and Lambertsson, 1989; Hansson et al., 1981). Previous studies have shown that *Sgs-4* is induced in salivary glands by a minor ecdysone pulse around mid-L3, and is expressed at high levels until puparium formation when it is abruptly turned off (Andres et al., 1993; Lehmann, 1996). As shown in **Figure 2.6A**, *Sgs-4* expression was drastically higher in the 16-hr L3 and 24-hr L3 RNAi populations compared to controls, suggesting that *P0206>DHR4-RNAi(x2)* animals have premature ecdysone signaling that stimulates *Sgs-4* expression. I also observed a roughly 2fold increase of *Sgs-4* expression in the wandering cohort compared to the feeding cohort of the RNAi population at the 24-hr L3 time point, indicating that the wandering cohort has received the 20E signal that induces *Sgs-4* earlier than the feeding cohort (**Figure 2.6A**).

I also examined whether heat-induced *DHR4-RNAi* in late L2 would result in precocious *Sgs-4* induction, since this treatment triggers premature wandering behavior (**Figure 2.5B**). I observed that *hsDHR4-RNAi* larvae that were heat-shocked in late L2 had 3fold higher *Sgs-4* transcript levels than controls at 20 hours L3 (**Figure 2.6B**). However, when I examined *Sgs-4* levels four and eight hours later, at 24 hr L3 and 28 hr L3, I found higher expression of the gene in controls, suggesting that *Sgs-4* induction is precocious but later submaximal in *hsDHR4-RNAi* larvae. In contrast to the late L2 heat treatment, I did not observe differences in *Sgs-4* expression between *hsDHR4-RNAi* and wild type larvae when heat shock was conducted in early L3 (**Figure 2.6C**), which is consistent with our observation that only a heat treatment in late L2 triggers early wandering behavior (**Figure 2.5B**).

To corroborate that *DHR4*-RNAi causes premature ecdysone signaling, I analyzed the expression profiles of two isoforms of the *E74* gene (Burtis et al., 1990) (see Chapter 1), *E74A* and *E74B*, by qPCR. *E74A* and *E74B* are direct targets of ecdysone signaling, but respond differentially to the ecdysone titers and can, therefore, be used to indirectly measure relative ecdysone levels (Caldwell et al., 2005; Karim and Thummel, 1991). *E74B* is abundant at low to intermediate ecdysone concentrations, however, *E74A* is only present at high ecdysone levels (**Figure 2.7A**). Therefore, by measuring both isoforms, I can tell whether ecdysone concentrations have fallen or risen. I observed that when animals were heat-treated as late second instars, *E74B* expression levels dropped around 28 hour L3 with a corresponding rise in *E74A* transcript levels (**Figure 2.7B**), suggesting that an aberrant ecdysone pulse caused by *DHR4*-RNAi in late second instar triggers the premature wandering behavior during the mid-L3 in the *hsDHR4*-RNAi population. However, when animals were heat-shocked in the early third instar, I observed no significant differences in *E74A* and *E74B* transcript levels between *hsDHR4*-RNAi animals and controls (**Figure 2.7C**), in line with the observation that *DHR4*-RNAi in early L3 fails to stimulate premature wandering behavior. In summary, these data suggest a preceding rise in ecdysone concentrations, consistent with the precocious induction of *Sgs-4* discussed above.

To test whether these premature ecdysone response events could be triggered by a precocious ecdysone pulse in *DHR4*-RNAi larvae, I measured ecdysone titers during the first 24 hours of the L3 using a 20E EIA immunoassay (Cayman Chemical, Ann Arbor, USA). The antibody recognizes both 20E and its immediate precursor E (Naoki Yamanaka, personal communication), and therefore hormone titers likely reflect a combination of both ecdysteroids. I found that knocking down *DHR4* in the ring gland overall results in significantly higher ecdysteroids levels at all time points examined (**Figure 2.8**). And remarkably,

while I can detect two minor ecdysteroids peaks in the control during the first 24 hours of the L3, I observe no recession of the first L3 pulse in *P0206>DHR4-RNAi(x2)* larvae. Rather, the first and the second L3 ecdysone pulse appear to be fused in RNAi animals, indicating that the first pulse was not properly repressed. These data strongly suggest that DHR4 functions in the ring gland to repress ecdysone synthesis. It is likely that the combination of higher hormone levels and the inability to repress the first pulse causes the premature effects observed for *Sgs-4* and *E74* transcripts, as well as the acceleration of wandering behavior and pupariation in *P0206>DHR4-RNAi(x2)* populations.

2.3.5 Overexpressing *DHR4* in the PG blocks molting by suppressing ecdysone pulses

The failure to repress ecdysone pulses and the concomitant premature ecdysone signaling inflicted by *DHR4-RNAi* suggest that the wild type function of *DHR4* is to inhibit ecdysone synthesis and/or release. To test this idea, I wanted to see whether increasing *DHR4* expression specifically in the PG or the RG using *phmN1-Gal4* and *P0206-Gal4*, respectively, was able to prevent ecdysone pulses from occurring and show low systemic ecdysone levels. As expected, I found that DHR4 blocks molting when it is overexpressed in the PG or the RG, however, the penetrance of this phenotype is dependent on the driver/responder combination being used, as well as the chromosomal location of the transgene, suggesting that this effect is dose-dependent. The data suggest that the more DHR4 protein that is present in the PG or RG, the higher the percentage of larvae that arrest in early developmental stages. As shown in **Figure 2.9A**, *phmN1>DHR4-cDNA* results in 100% larval lethality during L1, however, when *DHR4* cDNA was expressed by a weaker *Gal4* driver (*P0206-Gal4*), animals reached but could not progress beyond the second instar (**Figure 2.9B**).

To examine whether the block in molting caused by *DHR4* overexpression could be rescued by ecdysone, I supplemented the fly medium with 20E and determined the percentage of animals that progressed to later stages. Interestingly, I observed significant rescue: in the presence of the hormone, around 80% of the *phmNI>DHR4*-cDNA animals now developed to the L2 stage, with another 20% reaching the L3 (**Figure 2.9A**). Similarly, most of the *P0206>DHR4*-cDNA animals now progressed to the L3 on the 20E-supplemented diet, and nearly 4% of the population pupariated (**Figure 2.9B**). These data demonstrate that the failure to molt caused by *DHR4* overexpression in the PG or the RG is due to reduced levels of ecdysone. I further asked whether the ability of *DHR4* to block molting was specific to the PG because the *phmNI-Gal4* driver shows some expression in the fat body. To clarify this, I expressed *DHR4* specifically in the fat body using the *Cg-Gal4* driver. Similar to the results obtained with the PG and the RG driver, I observed a developmental arrest in the L1 and L2 stages (**Figure 2.9C**). In contrast to overexpressing *DHR4* in the PG or the RG, however, the developmental arrest caused by *Cg>DHR4*-cDNA cannot be rescued with 20E (**Figure 2.9C**), demonstrating that the function of *DHR4* in blocking molts is specific to the PG or the RG, which further corroborates that *DHR4* plays a crucial role in repression of ecdysone production and/or release.

Furthermore, I have also noticed that *phmNI>DHR4*-cDNA animals survived and continued to grow for up to 10 days as first instars. These L1 larvae continue to grow into very large larvae and accumulate lipids in their fat bodies (**Figure 2.9D**), and have larger organs than controls due to continued proliferation (**Figure 2.9E**). This observation demonstrates that expression of *DHR4* in the PG specifically blocks molting and does not trigger immediate lethality. Rather, it appears that these animals simply lack the ecdysone pulse to molt to the next stage and that all other aspects of larval life function normally.

2.3.6 DHR4 protein oscillates between nucleus and cytoplasm in the PG

My data demonstrated that the DHR4 protein is nuclear in fat body cells of late L2 and late L3 larvae, consistent with its role as a transcription factor in the ecdysone hierarchy. However, it is worth noting that DHR4 was initially found to be highly enriched in the cytoplasm of PG cells (King-Jones et al., 2005), raising the question as to whether DHR4 could enter the PG nucleus at all and, if so, how this translocation is regulated. To determine whether DHR4 can be nuclear at certain times during larval development, I stained ring glands isolated from carefully staged L3 larvae (within 30 min relative to the L2/L3 molt) ranging from 0 to 36 hours after the L2/L3 molt with affinity-purified DHR4 antibodies. Interestingly, I found that the subcellular localization of DHR4 changes periodically in PG cells during the third instar. As shown in **Figure 2.10A**, DHR4 appears to be entirely nuclear at 0, 8, 24, and 36 hr, completely cytoplasmic at 4, 12, and 20 hr, and present in both compartments at 16, 28, and 32 hr after the L2/L3 molt. Therefore, during the first 36 hours of the L3, DHR4 oscillation in PG cells undergoes at least three complete cycles: It oscillates from the nucleus to the cytoplasm and back during the first 8 hours after the molt, while the next two cycles take 16 and 12 hours, respectively (**Figure 2.10B**). Notably, these three oscillations reflect an intriguing correlation with the occurrence of the three minor 20E pulses during the L3, which have been mapped to 8, 20, and 28 hr after the molt (Warren et al., 2006) (**Figure 2.10B**). It should be noted that 20E represents the final and active form of the molting hormone, and that the production of its immediate precursor, ecdysone, would therefore have to take place prior to the depicted 20E pulses. Considering this, it appears that DHR4 is cytoplasmic during a minor pulse, but nuclear between these peaks, consistent with the idea that DHR4 regulates the timing of these pulses possibly by repressing ecdysone synthesis.

2.3.7 DHR4 oscillations are dependent on PTTH signaling

I have provided evidence that DHR4 oscillates between the nucleus and cytoplasm of PG cells (**Figure 2.10A**). Interestingly, *PTTH* mRNA was shown to cycle with an 8-hr periodicity in staged L3 larvae (McBrayer et al., 2007). These observations support the idea that there is a causal link between the cyclic behaviors of *PTTH* expression and DHR4 localization. As mentioned above, PTTH acts through Ras signaling, and animals that express a constitutively active form of Ras (Ras^{V12}) in the prothoracic gland (*phm22>Ras^{V12}*) display shortened larval stages and small pupae, which is strikingly similar to *DHR4* loss-of-function phenotypes (**Figure 2.11**). Therefore, I asked whether DHR4 acts in the PTTH signaling pathway. To examine the impact of altered PTTH activity on the subcellular distribution of DHR4, I decided to analyze the location of the DHR4 protein in ring glands isolated from 0 to 8 hr old L3 larvae after the molt. There are two major reasons why I chose this time window: Firstly, as shown in the **Figure 2.10A**, the first 8 hours into the L3 represents a complete oscillatory cycle of DHR4. Secondly, animals can be more precisely staged during this period compared to later time points.

To test the effects of genetically removing *PTTH* function, I ablated PTTH-producing neurons in *ptth>UAS-Grim* transgenic animals. In *PTTH*-abolished larvae, DHR4 accumulated in the PG nucleus, with some residual protein residing in the cytoplasm (**Figure 2.12**), suggesting that nuclear export and/or degradation of DHR4 is compromised when PTTH activity is reduced. To complement this finding, I further tested the effects of *torso* RNAi, which targets the PTTH receptor. Similar to what was observed in *PTTH*-ablated animals, the DHR4 protein was enriched in PG nuclei and failed to oscillate between these two compartments in *phm22>torso*-RNAi animals(**Figure 2.12**).

Based on these findings, I surmised that hyperactivating PTTH signaling

via constitutively active Ras^{V12} should retain DHR4 in the cytoplasm. To test this idea, I again performed DHR4 antibody staining on ring glands isolated from *phm22>Ras^{V12}* animals. As expected, I observed strong cytoplasmic accumulation of the DHR4 protein in PG cells when *Ras^{V12}* was expressed during the first 8 hours after the L2/L3 molt (**Figure 2.12**), indicating that Ras is a critical determinant for DHR4 nuclear localization. It should be noted that *Ras^{V12}* expression results in ring gland overgrowth, explaining the large and malformed glands observed (**Figure 2.12**).

Taken together, my data strongly suggest that PTTH regulates DHR4 activity by controlling its subcellular distribution in prothoracic gland cells, thereby permitting or preventing access of DHR4 to its target genes.

2.3.8 Ras^{V12} prevents DHR4 nuclear localization in the fat body

I have provided evidence that Ras activity controls DHR4 subcellular localization in the PG. To further examine the ability of Ras^{V12} to prevent DHR4 from entering the nucleus, I wanted to test whether Ras^{V12} could disrupt DHR4 nuclear localization in larval fat body cells, where DHR4 is not believed to shuttle between nucleus and cytoplasm, since at all stages that were examined (L2 and L3 larvae), DHR4 was found to exclusively nuclear (**Figure 2.4, 2.13**). When *Ras^{V12}* is specifically expressed in fat body cells in *Cg>Ras^{V12}* animals, I found DHR4 to be virtually absent from the nuclei and to be significantly abundant in the cytoplasm instead (**Figure 2.13**). This is indicating that constitutively active Ras is sufficient to trigger cytoplasmic retention of DHR4, even in a tissue that is not known to respond to PTTH. This finding provides strong support for the observation in the PG that nucleocytoplasmic distribution of DHR4 is dependent on PTTH signaling pathway.

2.3.9 *DHR4* overexpression in the PG rescues *Ras^{V12}* phenotypes

As described, *Ras^{V12}* represents the other known genetic alteration, apart from the *DHR4^l* mutation, that results in shortened larval stages and small animals. Furthermore, the dwarf larva phenotype seen in *DHR4^l* mutants was also observed in *PG>Ras^{V12}* populations. These observations are in line with the finding that *Ras^{V12}* prevents DHR4 from entering the nucleus of PG cells, thus abolishing its nuclear functions, similar to the *DHR4^l* mutant or *DHR4*-RNAi animals. Therefore, I wanted to ask whether increasing the level of DHR4 in the nucleus could counteract some of the effects of *Ras^{V12}* in the PG cells, more specifically, if I could rescue *Ras^{V12}*-induced phenotypes by co-expressing *DHR4* specifically in the PG.

For this, I first examined the average time to reach pupariation of animals when *Ras^{V12}* or *DHR4*, or both together, are expressed in the ring gland using the *P0206-Gal4* driver. Consistent with previous reports by others (Caldwell et al., 2005; Rewitz et al., 2009b), *P0206>Ras^{V12}* animals develop much faster than controls, which initiated pupariation around 20 hours ahead of controls (**Figure 2.14A**). A second *UAS-DHR4*-cDNA line (*DHR4/2*) was used in this experiment in order to make a homozygous stock that contains both *Ras^{V12}* and *DHR4*. Only 5%-10% of *P0206>DHR4/2* population reached pupariation, and they were more than 20 hours delayed compared to controls (**Figure 2.14A**). However, when *Ras^{V12}* and *DHR4* were co-expressed in the PG, I observed normal timing of pupariation relative to controls, and a partial rescue of the *DHR4*-induced L3 larval lethality (**Figure 2.14A**).

Secondly, closer examinations on the ring gland phenotypes revealed that the *Ras^{V12}*-induced ring gland overgrowth phenotype could also be rescued by overexpressing *DHR4*. Specifically, *P0206>Ras^{V12}* results in strongly overgrown ring glands (**Figure 2.14B**). However, when *DHR4* was co-expressed in the PG,

hypertrophy of the ring gland appeared to be suppressed (**Figure 2.14B**), strongly suggesting that increasing the levels of DHR4 in the PG blocks Ras activity.

2.3.10 Nuclear localization of ERK and DHR4 are inversely correlated

As described earlier, PTTH stimulates ecdysone production in the PG through Ras signaling by ultimately activating ERK, a mitogen-activated protein kinase (MAPK), via phosphorylation (Rewitz et al., 2009b). Activated ERK enters the nucleus and phosphorylates its target proteins such as transcription factors or other kinases in the nucleus (Yoon and Seger, 2006). Since DHR4 counteracts PTTH signaling by repressing ecdysone synthesis, I speculated that PTTH activity could remove nuclear DHR4 by activated ERK shuttling to the nucleus. To test this idea, I stained ring glands isolated from 0-hr-old to 8-hr-old L3 with ERK antibodies to examine the subcellular localization of this protein. The ERK antibodies (Cell Signaling #4695) used detect bulk ERK, defined as both phosphorylated ERK and non-phosphorylated ERK. I found that at 0 hr and 8 hr L3, ERK is evenly distributed between nucleus and cytoplasm of the PG, however, at 4 hr L3, ERK is strongly enriched in the nucleus (**Figure 2.15**). This finding demonstrates that ERK and DHR4 nuclear distribution are inversely correlated at least during the first 8 hours after the L2/L3 molt, namely, ERK is enriched in the nucleus when DHR4 is cytoplasmic, however, DHR4 accumulates in the nucleus when ERK is evenly distributed in both compartments. This observation is consistent with the idea that ERK plays a role in displacing DHR4 from the PG nuclei upon PTTH activation, and further corroborates the finding that the PTTH/Ras/ERK signaling pathway modulates the subcellular localization of DHR4. However, it remains unclear whether nuclear DHR4 disappears from the PG nuclei via direct phosphorylation by ERK (see Discussion 2.4.1).

2.3.11 *DHR4*-RNAi ring gland microarrays reveal misregulation of cytochrome P450 genes

A key question I then asked was what genes act downstream of *DHR4*, which functions as a repressor of ecdysone synthesis in the PG. To identify possible target genes of *DHR4*, I induced *DHR4*-RNAi in late L2 via a heat-inducible *DHR4*-RNAi transgene, isolated RNA from ring glands collected from carefully staged larvae at 4 hr and 8 hr after the L2/L3 molt, and carried out microarrays. I analyzed these two time points in an attempt to select for genes that show significant expression changes at both time points. Using a stringent filtering approach, I identified 54 genes whose transcript levels showed a greater than 4-fold difference between controls and *DHR4*-RNAi animals at both time points (**Table 2.2**, **Figure 2.16A**). Selected genes are shown in **Figure 2.16B**. Intriguingly, among these 54 genes are four cytochrome P450 genes, an enrichment that is highly unlikely to occur by chance (P value = $2.4E-11$ based on Chi-square test). Two of the P450 genes, *Cyp6a17* and *Cyp9c1*, are downregulated in the ring gland from *DHR4*-RNAi larvae, while the other two, *Cyp6t3* and *Cyp6w1*, are upregulated in the ring gland when *DHR4* is silenced. The effects are very similar between the two time points (**Figure 2.16C**). I also found a short-chain dehydrogenase/reductase (encoded by *CG2065*) among the affected genes, which belongs to the same enzyme family as the Halloween gene *shroud* (Niwa et al., 2010). Finally, *CG16957*, which encodes a protein with a cytochrome *b5* domain (Lederer, 1994), is also affected by *DHR4*-RNAi. This protein family is functionally related to cytochrome P450 enzymes because both enzyme classes act as oxidoreductases and carry heme groups. Perhaps surprisingly, I did not observe any substantial changes in the expression of the Halloween genes due to *DHR4*-RNAi at the time points examined (**Figure 2.16C**), suggesting that the Halloween genes are not transcriptional targets of *DHR4*.

To validate these observations, I examined the expression via qPCR of all four affected cytochrome P450 genes along with several control genes, including *phm*, *dib*, and *sad*, in brain-ring gland complexes isolated from *hsDHR4*-RNAi animals as well as *DHR4*¹ mutants of 4 hr-old L3. As expected, I observed the same patterns of expression changes for all four genes in *hsDHR4*-RNAi samples in the qPCR validation experiments (**Figure 2.16D**). When I analyzed the samples taken from *DHR4*¹ mutants, I confirmed that the expression of *Cyp6t3* and *Cyp6w1* were both enhanced when *DHR4* function was lost (**Figure 2.16E**). However, in contrast to the data obtained from *hsDHR4*-RNAi samples, I found that *Cyp9c1* expression was upregulated instead of being downregulated in *DHR4*¹ mutants (**Figure 2.16E**). Furthermore, I was not able to detect *Cyp6a17* expression in *DHR4*¹ mutant brain-ring gland complexes or in the corresponding parental line *P427* (**Figure 2.16E**), suggesting that *Cyp6a17* and *Cyp9c1* expression both vary substantially between different genetic backgrounds. Additionally, qPCR analysis did not detect any substantial effects on the tested Halloween genes (**Figure 2.16D, E**), confirming my microarray results.

Together, my ring gland-specific microarrays revealed two cytochrome P450 genes, *Cyp6t3* and *Cyp6w1*, which were upregulated when *DHR4* function was disrupted either by heat-inducible RNAi or in the *DHR4*¹ mutant, indicating that *DHR4* normally represses the transcription of these two genes.

2.3.12 *Cyp6t3*: a novel player of the ecdysone biosynthetic pathway

My ring gland microarrays have revealed that two cytochrome P450 genes, *Cyp6t3* and *Cyp6w1*, display significantly higher expression levels in the ring gland when *DHR4* function was lost. I chose to analyze *Cyp6t3* in more detail for three major reasons: firstly, at the point of writing, no RNAi lines or mutants were available for *Cyp6w1* for further analysis. Secondly, transcripts of *Cyp6t3*, but not

Cyp6w1, are more than 20fold enriched in the ring gland compared to whole body in the early third instar based on qPCR analysis (**Figure 2.17A**), suggesting an important role for *Cyp6t3* in the ring gland. This result is consistent with the *in situ* hybridization data demonstrating that *Cyp6t3* is specifically expressed in the prothoracic gland and the *corpus allatum* (**Figure 2.17B**). Thirdly, I determined the expression profiles of a few selected genes during the first 12 hours of the L3, and intriguingly, I found that the expression levels of *Cyp6t3*, but not of *Cyp6w1*, oscillate during this time window (**Figure 2.17C**). More specifically, *Cyp6t3* is expressed at higher levels when DHR4 is cytoplasmic at 4 hr and 12 hr L3 (**Figure 2.10A**), in line with the idea that DHR4 represses this gene.

Based on these observations, I decided to examine whether loss of *Cyp6t3* function in the PG via RNAi results in any developmental defects. I found that *PG>Cyp6t3*-RNAi (VDRC#109703) larvae display similar phenotypes as those defective in genes of the ecdysone synthetic pathway. For instance, I observed giant L3 pupae, double mouth hooks, and L2 prepupae (**Figure 2.18A**). The latter phenotype is quite rare, in which case larvae directly undergo metamorphosis from the second instar without progressing to the third instar. The L2 prepupa phenotype has only been observed in the animals mutant for *E75* (Bialecki et al., 2002), *itpr* (Venkatesh and Hasan, 1997), and *dre4* (Sliter and Gilbert, 1992), all of which have severely reduced ecdysone titers, suggesting that disrupting *Cyp6t3* may cause defects in the ecdysone synthetic pathway. I have also tested a second *Cyp6t3* RNAi line (VDRC#30896) that targets to a smaller region of *Cyp6t3* mRNA. In this RNAi line, I also observed large pupae formed after a longer feeding period during L3, however, no L2 pupae were identified (**Figure 2.19**). In later experiments, I focused on the VDRC #109703 line since this line gives stronger phenotypes. Importantly, no phenotypes were observed when *Cyp6t3* is silenced in the fat body, indicating that the phenotypes induced by

phm22>Cyp6t3-RNAi are specific to the PG. Furthermore, the potential function of *Cyp6t3* in the *corpus allatum* has also been investigated using the *corpus allatum*-specific *Gal4* driver, *Aug21-Gal4*. However, no phenotypes were observed in *Aug21>Cyp6t3*-RNAi animals, raising the possibility that either *Cyp6t3* does not have a critical role in this tissue or RNA interference was not efficient enough to elicit any mutant phenotypes.

The next question I asked was whether *Cyp6t3*-RNAi animals have reduced ecdysone titers. To answer this, I measured ecdysteroid levels in *phm22>Cyp6t3*-RNAi animals at different developmental stages, including embryos, first instars, and second instars. I found that *Cyp6t3*-RNAi results in significantly lower ecdysteroids concentrations compared to controls at all times that were examined except in embryos (**Figure 2.18B**). In particular, I compared ecdysteroid titers at multiple time points between L3 control larvae and delayed *phm22>Cyp6t3*-RNAi L2 larvae of the same absolute age. As expected, *phm22>Cyp6t3*-RNAi larvae display drastically reduced hormone levels relative to controls, but generated a small ecdysone pulse prior to L2 prepupae formation (**Figure 2.18C**). These findings demonstrate that disrupting *Cyp6t3* function in the PG impairs ecdysone production. In line with this, I predicted that feeding ecdysone to *phm22>Cyp6t3*-RNAi larvae should rescue some of the phenotypes, and indeed I found that the L2 prepupa phenotype was completely lost when animals were reared on the 20E-supplemented medium (**Figure 2.20A**), further corroborating that *phm22>Cyp6t3*-RNAi results in defects in ecdysone synthesis.

To further investigate which step in the ecdysone biosynthetic pathway is mediated by *Cyp6t3*, I examined which 20E precursors might also result in a rescue. This approach has been commonly used in the previous studies. For instance, larval lethality caused by RG-specific knockdown of *neverland* is completely rescued by 7-dehydrocholesterol (7dC) but not by cholesterol,

suggesting a role for *nvd* upstream of 7dC synthesis (Yoshiyama et al., 2006). Furthermore, larval lethality of RG-specific *shroud*-RNAi larvae was remedied by 5 β -ketodiol but not 7dC, indicating that *shroud* functions upstream of 5 β -ketodiol production in the “Black Box” (**Figure 2.2**) (Niwa et al., 2010). In the sterol rescue experiments of *PG>Cyp6t3*-RNAi larvae, I used an instant fly medium called C424, which is naturally low in cholesterol and other sterols. There are two reasons why I chose C424 in this rescue experiment: Firstly, C424 can easily be supplemented with different kinds of sterols, and has been used by us for sterol rescue studies before (Bujold et al., 2009). More importantly, *Cyp6t3*-RNAi phenotype was more pronounced on this medium (**Figure 2.20**), possibly because C424 contains less cholesterol than standard fly food as the precursor of ecdysone. Thus, I assumed that the rescue by the supplementation of different ecdysone precursors was also more dramatic on C424 than on standard medium. On C424, *phm22>Cyp6t3*-RNAi animals very rarely progressed beyond the L2/L3 molt (less than 0.5%), either dying as L2 larvae or L2 prepupae (**Figure 2.20B**). When I supplemented C424 with solvent only (ethanol), cholesterol, or 7-dehydrocholesterol (7dC), I did not see any rescue, defined by larvae developing to third instars or later stages. In contrast, adding E or 20E to C424 medium resulted in more than 60% rescue, while supplementation with 5 β -ketodiol rescued more than 15% of the *phm22>Cyp6t3* RNAi population past the L2/L3 molt (**Figure 2.20B**). These data suggest that *Cyp6t3* plays a role in the “Black Box” (**Figure 2.2**), since mutations affecting enzymes acting downstream cannot be rescued with 5 β -ketodiol. However, the lower percentage of rescued animals with 5 β -ketodiol may reflect the fact that this compound has to enter the PG, while E and 20E can act directly on the target tissues. However, higher concentrations of 5 β -ketodiol could be encouraged in future studies to test whether that could result in higher rescue rates.

In addition to RNA interference of *Cyp6t3* function, I also analyzed a potential mutation of *Cyp6t3*, *Cyp6t3*^{Mi(CG8858)}, to further investigate the role of *Cyp6t3*. This mutation was generated by a transposon Minos-mediated integration cassette (MiMIC) (Venken et al., 2011) that is located downstream of two divergently transcribed genes, *Cyp6t3* and *CG8858*. The *Cyp6t3*^{Mi(CG8858)} mutation is mainly L1 larval lethal, and I swapped the balancer chromosome with *CyO*, *act-GFP* to identify homozygous larvae for phenotypic analysis and qPCR analysis. As the first step, I asked whether *Cyp6t3* and *CG8858* transcripts are affected in the *Cyp6t3*^{Mi(CG8858)} mutant. Using qPCR, I found that *Cyp6t3* mRNA levels are drastically reduced in homozygotes (~6% of wild type levels), while *CG8858* transcripts levels are moderately affected (~65% of wild type levels) (**Figure 2.21A**). In the *Cyp6t3*^{Mi(CG8858)}/*CyO*, *act-GFP* population, I observed that *Cyp6t3* transcript levels were significantly reduced (~40% of wild type levels), however, *CG8858* remains unaffected (**Figure 2.21A**). Interestingly, I found that this mutation is haploinsufficient. In the *Cyp6t3*^{Mi(CG8858)}/*CyO*, *act-GFP* population, I observed lethality during larval development, and overall, only half of the heterozygous population could survive to pupariation (**Figure 2.21B**). Next, I tested whether this larval lethality could be rescued by adding ecdysone to the medium. This is indeed the case, as shown in **Figure 2.21B**, I observed substantial rescue of larval lethality in all three stages, and furthermore, ecdysone significantly increased the pupariation rate of the heterozygotes (**Figure 2.21C**). In addition, I noticed molting defects in 20~30% of *Cyp6t3*^{Mi(CG8858)}/*CyO*, *act-GFP* second instar larvae (data not shown), in which case larvae were unable to shed their cuticle. However, these molting defects disappeared when ecdysone was added to the medium. Importantly, in the heterozygous population, I observed a low percentage (~1%) of the L2 prepupae phenotype (**Figure 2.21D**), very similar to what I observed in PG-specific *Cyp6t3*-RNAi animals. This suggests

that the RNAi phenotype is not caused by off-target, and also supportive of the idea that *Cyp6t3* is a novel player in ecdysone synthesis.

However, it should be stressed that *Cyp6t3*^{Mi(CG8858)} homozygotes die as first instar larvae, and cannot be rescued by ecdysone feeding. *Cyp6t3*^{Mi(CG8858)} L1 larvae live up to 5 days, but remain very small and do not appear to grow. I carried out a cuticle preparation to examine whether homozygous *Cyp6t3*^{Mi(CG8858)} embryos exhibit a Halloween phenotype. Interestingly, *Cyp6t3*^{Mi(CG8858)} homozygotes do not display a classical Halloween phenotype, instead, I observed that the homozygous embryos display defects in the anterior region, including mouth hook morphology and head structures (**Figure 2.21E**). This observation might explain why *Cyp6t3*^{Mi(CG8858)} homozygotes can not be rescued by ecdysone supplementation, since it is likely that these mutants are impaired in their ability to ingest food. Taken together, my data have strongly demonstrated that *Cyp6t3* is a novel component in ecdysone biosynthesis.

2.3.13 *Cyp6t3* is epistatic to *DHR4*

So far, I have demonstrated that *Cyp6t3* has a novel role in the biosynthesis of ecdysone. *Cyp6t3* appears to be a component in the “Black Box”, which has generally been believed to contain the rate-limiting step(s) of ecdysone biosynthesis. To test whether *Cyp6t3* mediates a rate-limiting step of ecdysone synthesis, I overexpressed *Cyp6t3* cDNA specifically in the PG to examine whether high levels of *Cyp6t3* could result in developmental acceleration. However, I did not observe any obvious phenotypes with respect to timing or overall morphology when *Cyp6t3* was overexpressed in the prothoracic gland (data not shown), suggesting that there might be more than one rate-limiting factor in controlling ecdysone production if *Cyp6t3* represents one such.

Since *Cyp6t3* expression is significantly enhanced in the ring gland of both

DHR4^l mutants and *DHR4*-RNAi animals, I next asked whether the expression of *Cyp6t3* contributes to the precocious pupariation phenotype observed for the *DHR4^l* mutant. To test this, I examined the average time to reach pupariation of animals with the *DHR4^l* mutation, or *Cyp6t3*-RNAi, or both. As shown in **Figure 2.22**, *DHR4^l; phm22>Cyp6t3*-RNAi larvae are delayed in development, in contrast to the accelerated development observed for the *DHR4^l* mutant. This data indicates that the increased expression of *Cyp6t3* in the *DHR4^l* mutant is required for advancing developmental timing. Taken together, I conclude that *Cyp6t3* is necessary but not sufficient for accelerating development.

2.4 Discussion

2.4.1 DHR4 as a readout of PTTH signaling for proper timing of edysone pulses

The identification of Torso as the PTTH receptor as well as Ras/Raf/ERK signaling as the major downstream effector of PTTH, not only in *Drosophila* but also in other insect species, has greatly advanced our understanding in PTTH-mediated stimulation of ecdysone production (Lin and Gu, 2007, 2011; Rewitz et al., 2009a; Rybczynski et al., 2001). My work has shown that DHR4, a nuclear receptor, serves as a critical readout of the PTTH pathway in mediating proper timing of ecdysone pulses. Based on these findings, I propose that DHR4 acts as a repressor of ecdysone pulses by counteracting the PTTH-stimulated rise of ecdysone levels. As illustrated in **Figure 2.23**, when the PTTH pathway is inactive, DHR4 is in the nucleus, where it represses the expression of at least one gene *Cyp6t3* that is required for ecdysone synthesis. However, upon PTTH activation, DHR4 is withdrawn from the nucleus, thereby allowing ecdysone synthesis to occur through de-repression of the ecdysone biosynthetic gene(s) (**Figure 2.23**). Animals lacking DHR4 function, either *DHR4^l* mutants or

PG-specific *DHR4* knockdowns, are small due to the accelerated development. Interestingly, very similar phenotypes were observed when constitutively active *Ras* is expressed in the ring gland (*P0206>Ras^{V12}*). Closer examinations of DHR4 localization in *P0206>Ras^{V12}* animals revealed that *Ras^{V12}* expression results in DHR4 accumulation in the cytoplasm in PG cells. These findings strongly suggest that *P0206>Ras^{V12}* larvae are accelerated in development precisely because DHR4 protein is prevented from entering the nucleus, thereby mimicking the loss-of-function phenotypes observed in *DHR4*-RNAi or mutant animals. Consistently, DHR4 was found to be nuclear in PG cells of PTTH-mutant larvae that display substantial developmental delays prior to metamorphosis. This finding reinforces the model (**Figure 2.23**) that when the PTTH pathway is inactive, DHR4 is in the PG nuclei, where it represses ecdysone pulses, thereby giving rise to large animals that are opposite to loss-of-*DHR4* phenotypes. Lastly, it is of interest to note that PTTH-ablated animals eventually pupariate and develop into viable adults, indicating that PTTH regulates developmental timing but is not essential for viability at least in laboratory fly cultures.

I have demonstrated that the PTTH pathway controls the subcellular localization of DHR4 in the PG. Inactive PTTH signaling results in DHR4 retention in the nucleus, while constitutively activating this pathway leads to cytoplasmic accumulation of the protein. It will be of interest to determine whether the DHR4 oscillations represent shuttling of a stable protein or involve cycles of DHR4 degradation and synthesis. Current data appear to be more in favor of the latter possibility because firstly I have demonstrated that *hsDHR4*-RNAi in late L2 was able to trigger precocious wandering behavior. If the DHR4 oscillations are dependent on a stable protein that moves in and out of the nucleus, this shuttling protein would be immune to RNA interference of gene function induced by heat treatments. Therefore, sufficient turnover of the DHR4

protein must occur, at least around the L2/L3 molt. A second possibility would be *DHR4* mRNA levels oscillate. My ring gland microarrays have revealed that *DHR4* transcripts are constantly expressed at very low levels (Ou et al, manuscript in preparation, see Chapter 3), at least at the time points I examined, which does not support the idea that *DHR4* transcripts levels are oscillating, unless the approach was not sensitive enough to detect any *DHR4* mRNA oscillations. Taken together, I hypothesize that *DHR4* mRNA is highly stable in PG cells and translated when required in L3 larvae.

I have shown that ERK changes its nucleo-cytoplasmic distribution in early L3 larvae, in an apparent inverse relationship to DHR4 localization. This finding is suggestive of the idea that ERK phosphorylates DHR4 to trigger its disappearance from the nucleus when PTTH signaling is active, and this is in keeping with the notion that DHR4 constitutes a downstream target of the PTTH/ERK pathway. However, this has not been demonstrated directly, although indeed, DHR4 is predicted to have several clusters of ERK target sites according to GPS 2.0, a tool to predict kinase-specific phosphorylation sites of proteins (Xue et al., 2008) (**Figure 2.24**). Future studies such as mutational analysis of putative ERK phosphorylation sites of DHR4 will have to be carried out in order to determine whether these sites affect the subcellular localization of the protein. In addition, it remains unclear whether the disappearance of DHR4 from nucleus under the active PTTH signaling is attributed to the translocation of DHR4 out of nucleus, or the degradation of DHR4 in the nucleus, or both (**Figure 2.23**).

I have shown that DHR4 displays an 8-hour, 16-hour, and 12-hour oscillation cycle time for the first 36 hours of the L3 stage. Intriguingly, PTTH mRNA was shown to cycle with an 8-hour periodicity during the L3 (McBrayer et al., 2007), although it remains unknown whether PTTH peptides are released in a corresponding 8-hour cycle during the L3 stage. These findings raise the question

as to how these ultradian periods are established. What could account for the difference in these cycle times? There might be a few possibilities. Simply, I may have not detected all DHR4 cycles. It appears that during some time points, such as 16 hr, 28 hr, and 32 hr after the L2/L3 molt, DHR4 is detected in both compartments, which possibly reflects a transition phase that was overlooked. Future studies could attempt a time course with a 2-hr step size instead of the present 4-hr, in combination with a *Sgs3*-GFP reporter line to re-stage animals in the mid L3 (Biyasheva et al., 2001), in order to reduce the asynchrony that exists in developing *Drosophila* larvae. Alternatively, the difference in cycle duration between DHR4 and PTTH may be indicative of more than one cyclic process that contributes to nucleo-cytoplasmic oscillations of DHR4. An appealing possibility is that circadian rhythms directly and/or indirectly exert influence on the DHR4 oscillations. It was previously shown that animals mutant for *pdf*, which encodes the neuropeptide pigment dispersing factor (PDF) in the central circadian pacemaker cells in the *Drosophila* brain (Renn et al., 1999), altered the periodicity of *PTTH* mRNA expression levels (McBrayer et al., 2007), suggesting that circadian rhythms are superimposed on the PTTH oscillation to indirectly affect DHR4 cycle times. Previous studies also suggested that the gland itself contains an independent clock because cultured prothoracic glands are able to properly time the release of ecdysone, which adds another layer of regulation underlying DHR4 oscillation (Ampleford and Steel, 1985; Vafopoulou and Steel, 1996a, b). In the future, it will be interesting to explore whether PDF or components of the PG-specific circadian clock could affect oscillatory behavior of DHR4 in PG cells.

2.4.2 PTTH and the transcriptional control of ecdysone biosynthetic genes

The mechanism by which PTTH regulates ecdysone biosynthesis has been

a main focus of ecdysone research for many years. Only recently, however, it has emerged that PTTH activates the Ras/Raf/ERK cascade resulting in upregulation of ecdysone production. To achieve this, PTTH triggers a range of events, which, among others, results in the transcriptional upregulation of genes required for ecdysone biosynthesis, at least for the late larval ecdysone peak that trigger puparium formation. The ability of PTTH in stimulating the expression of the Halloween genes was initially demonstrated in cultured *Bombyx* prothoracic glands, where the *Bombyx disembodied* gene is upregulated when PTTH is applied (Niwa et al., 2005). In contrast to *disembodied*, the upregulation of *Bombyx phantom* and *spook* appears to be more moderate, and *shadow* transcription appears not to be induced under these conditions (Niwa et al., 2005; Yamanaka et al., 2007). Currently, no studies have reported successfully generating the recombinant *Drosophila* PTTH, therefore, it remains unclear whether *Drosophila* PTTH is able to stimulate ecdysone production by enhancing the expression of the Halloween genes in cultured *Drosophila* glands. However, loss-of-function analysis of *Drosophila* PTTH by ablating PTTH-producing neurons has confirmed a role for PTTH in the transcriptional regulation of ecdysteroidogenic genes. Specifically, elimination of PTTH-producing neurons results in a drastic reduction of *Drosophila disembodied* (~10fold down) and had a more moderate effect on *phantom*, *shadow*, and *spookier* (4~5fold down) (McBrayer et al., 2007). Similar effects were observed when the PTTH receptor Torso function is disrupted, although it has been shown in an indirect manner. Specifically, when *dSmad2*—the primary transcriptional transducer of *Drosophila* Activin signaling (Brummel et al., 1999)—was knocked down in the PG, *torso* transcripts levels were severely reduced (Gibbens et al., 2011). Concomitantly, *spookier* and *disembodied* are strongly downregulated in PG-specific *dSmad2* knockdowns, but no effect was seen for *phantom* and *shadow* transcripts levels. In

summary, these findings suggest that the increased expression of *disembodied*, after the application of PTTH on *Bombyx* glands *ex vivo* or prior to the major ecdysone pulse in *Drosophila in vivo*, relies more on PTTH signaling, however, *phantom* and *shadow* appear to be less PTTH-dependent.

Another interesting observation made by MacBrayer et al. (2007) is that loss-of-PTTH function hardly results in delays of the first and second instars, although an efficient ablation of the PTTH-producing neurons at these stages was observed (MacBrayer et al., 2007). This finding indicates that ecdysone production occurs efficiently enough during the first and second instars, even without PTTH stimulation. This observation raises the question as to whether PTTH is required for the larval-larval molts. It is possible that the function of PTTH during the early stages can be substituted by that of another stimulating factor, such as Bombyxin, the first “prothoracicotropic hormone” purified from *Bombyx* brain (Ishizaki and Suzuki, 1994; Nagasawa et al., 1986), which belongs to the insulin-like peptide (ILP) family. Insulin/ILP signaling (IIS) has been demonstrated to be a key regulator of tissue growth in *Drosophila* (Garofalo, 2002; Hietakangas and Cohen, 2009; Oldham and Hafen, 2003). Previous studies have shown that Bombyxin is capable of stimulating ecdysone production within hours (Kiriishi et al., 1992), and constitutively activating the components of the IIS pathway in the PG results in moderate upregulation of *disembodied* and *phantom* (Colombani et al., 2005), implying that ILPs, such as Bombyxin, may substitute for PTTH in triggering larval-larval molts and the ultimate pupariation after a prolonged L3 stage of the PTTH-ablated animals. This possibility then gives rise to the idea that PTTH governs the timing of pupariation by acting as a booster of the expression of the Halloween genes towards the end of the third instar when ecdysone titers rise dramatically.

Intriguingly, I found that the Halloween transcripts are expressed at high

levels, comparable to that of ribosomal genes, in L3 larvae long before PTTH stimulates the major ecdysone pulse at the end of the L3 (Ou et al., manuscript in preparation, discussed in Chapter 3). However, it remains untested whether these transcripts are translated. This finding suggests that regulation of the three minor ecdysone peaks via transcriptional downregulation of the highly expressed ecdysteroidogenic genes like *disembodied* or *phantom* seems unlikely, which is in line with our finding that loss-of-*DHR4* function in the ring gland has no effects on these genes. Rather, DHR4 appears to function as a repressor negatively regulating *Cyp6t3* and other uncharacterized genes that play critical roles in ecdysone synthesis. This is in parallel with the function of its vertebrate ortholog Germ Cell Nuclear Factor (GCNF), which has been shown to act as an active transcriptional repressor that is required for germ cell differentiation in human testis (Rajkovic et al., 2004). However, it remains unknown whether DHR4 can be a transcriptional activator in some cases, or the genes that are downregulated in the *hsDHR4*-RNAi microarrays just represent indirect targets of DHR4.

Together, my work has shown that DHR4 acts upstream of ecdysone in the PG, and DHR4 appears to be the first transcription factor that has been reported to repress ecdysteroidogenesis and directly linked to the PTTH pathway.

2.4.3 *Cyp6t3* is a downstream target of DHR4

The ring gland microarrays and qPCR data revealed that *Cyp6t3* mRNA levels are significantly increased in *hsDHR4*-RNAi animals and *DHR4*¹ mutants. I also observed that *Cyp6t3* expression levels oscillates during the first 12 hours after the L2/L3 molt, with lower levels of *Cyp6t3* expression when DHR4 is in the PG nuclei. Based on these observations, it is plausible to hypothesize that *Cyp6t3* is a direct transcriptional target of DHR4. However, no direct evidence such as DNA recognition sites have been identified for DHR4. Nuclear receptor

(subfamily 1, 2, 4-6) dimers bind to DNA sequences composed of two half-sites that are separated by variable spacing and can occur in different orientations (King-Jones and Thummel, 2005; Mangelsdorf et al., 1995; Rastinejad et al., 1995). By using NHR Scan (Sandelin and Wasserman, 2005), a DNA sequence termed DR0 half-sites element (repeats of the sequence AGGTCA without spacing) (Rastinejad et al., 1995) has been detected in the regulatory region of *Cyp6t3* (**Figure 2.25**). It remains unclear whether the predicted DR0 site represents a DHR4 binding site, however, it finds support in previous studies demonstrating that GCNF, the vertebrate homolog of DHR4, binds to DNA sequences with half-sites of the DR0 model (Chen et al., 1994; Hentschke et al., 2006; Yan et al., 1997). With the help of Dr. Adam Magico, transgenic flies that have the entire 5' intergenic region of *Cyp6t3* with or without the predicted DR0 site fused with a reporter gene, *LacZ*, were generated. In the future, I will examine whether the expression of *LacZ* is affected when the putative DHR4 DR0 binding site is ablated.

According to the *DHR4*-RNAi microarray data, the expression of *Cyp6t3* in the PG is relatively low, probably by two orders of magnitude lower than the Halloween mRNAs for *phantom*, *disembodied*, *spookier*, and *shadow* in PG cells. This might explain why *Cyp6t3* was previously neither detected by *in situ* hybridization in any larval tissue, nor amplifiable from larval cDNA (Chung et al., 2009). However, using *in situ* hybridization coupled with the tyramide signal amplification, I confirmed the ring gland-specific expression of *Cyp6t3*. Despite that *Cyp6t3* is expressed at low levels in the ring gland, its transcripts are highly enriched (>9fold relative to the whole-larva level) in this tissue according to my wild type ring gland microarrays (further discussed in Chapter 3). This observation further supports the idea that *Cyp6t3* has an important role in ecdysteroid biosynthesis in the ring gland. In addition, the preliminary analysis on

the putative *Cyp6t3* mutant allele, *Cyp6t3*^{Mi(CG8858)}, corroborates the finding that *Cyp6t3* is a critical player in ecdysone biosynthesis. The heterozygotes *Cyp6t3*^{Mi(CG8858)}/*CyO*, *act-GFP* display lethality throughout larval stages, which is greatly rescued when ecdysone is administered to fly medium. In addition, the L2 prepupa phenotype was also observed in the *Cyp6t3*^{Mi(CG8858)}/*CyO*, *act-GFP* population, which completely disappears in the presence of ecdysone. These findings reinforce that *Cyp6t3* is a pivotal component in the ecdysone biosynthetic pathway.

The fact that *Cyp6t3* is expressed at very low levels underscores that the *Cyp6t3* enzyme might be rate-limiting with regard to ecdysone production. I further observed that 5 β -ketodiol was able to rescue *phm22*>*Cyp6t3*-RNAi animals to later stages, suggesting that *Cyp6t3* is a component in the “Black Box” of the ecdysone biosynthetic pathway, which is generally believed to harbor the rate-limiting step(s) of ecdysone production. These findings raise the question as to whether increased levels of *Cyp6t3* could result in faster accumulation of ecdysone, thereby accelerating developmental timing. However, no such phenotype was observed when I overexpressed a *Cyp6t3* cDNA (Daborn et al., 2007) specifically in the PG, indicating that changing transcript levels of *Cyp6t3* alone is not sufficient to trigger acceleration in development. By contrast, I was able to show that *Cyp6t3* is necessary for the accelerated developmental phenotype exhibited by *DHR4*^l mutants, strongly supporting the notion that *Cyp6t3* is a key target of DHR4-mediated repression of ecdysone pulses.

The amount of DHR4 in the PG nuclei might directly affect the degree by which *Cyp6t3* is repressed. This notion finds support in the evidence that overexpression of *DHR4* cDNA in the PG results in varying degrees of larval arrest, depending on the strength of the *Gal4* driver being used. This suggests that the strength of the phenotype depends on how much DHR4 can enter the nucleus.

Therefore, it is conceivable that the nuclear functions of DHR4 are dose-sensitive, giving rise to the idea that the oscillations of this nuclear receptor do not necessarily represent an all or nothing response, but may in fact fine-tune the expression levels of target genes instead.

2.5 Final comments

My findings have shown that DHR4 acts as a readout of the PTTH/Ras/ERK cascade by repressing ecdysone production in the *Drosophila* PG during larval development. However, it remains unclear whether DHR4 is directly phosphorylated by ERK. Secondly, DHR4 negatively regulates the expression of a cytochrome P450 gene, *Cyp6t3*, which has been demonstrated as a novel player of the ecdysone biosynthetic pathway and suggested to play a role in the “Black Box”. However, it remains to be shown whether *Cyp6t3* represents a direct transcriptional target of DHR4. Lastly, PTTH signaling triggers a wide spectrum of events in the PG to promote ecdysone synthesis, but its downstream targets remain largely unknown. Identifying genes whose expression are dependent on PTTH signaling will gain us insight into mechanisms governed by PTTH. To pursue this goal, a systemic analysis of ring gland transcriptomes in the presence or absence of PTTH signaling using microarrays represents a feasible approach, which will be discussed in detail in the next chapter (Chapter 3, Results 3.3.5).

2.6 Table

Gene	Primer Sequence
<i>rp49</i>	Forward 5' ttcttgacgtgccaaaact Reverse 5' aatgatctataacaaaatcccctga
<i>E74A</i>	Forward 5' ccctttatcgacgatgcact Reverse 5' acctccaacaagacgacat
<i>E74B</i>	Forward 5' cgcgagttcaaagtgtctta Reverse 5' ggagggagagtgggtgtgt
<i>Sgs4</i>	Forward 5' aggcaagaagaacaccacca Reverse 5' ttgctgttttagcaaccacctt
<i>Cyp6t3</i>	Forward 5' ggtgtgtttggaggcactg Reverse 5' ggtgcactctctgttgacga
<i>Cyp6t3 (in situ)</i>	Forward 5' accatcactggaaggagagtccgc Reverse 5' gaggaggtttcaaaccggccagc
<i>Cyp6w1</i>	Forward 5' aaaaacctcttctttgcacga Reverse 5' tgcctgcaagttcttcca
<i>Cyp6a17-1</i>	Forward 5' ggagcaggttgatggaa Reverse 5' tccctggcaatgaagtatctt
<i>Cyp6a17-2</i>	Forward 5' cacctacgagggaatcaagg Reverse 5' tactttcgacgcgttcca
<i>Cyp9c1</i>	Forward 5' tgggtaaagagtcgtacataaaaca Reverse 5' tgaagactccatagaccttgtgc
<i>phantom</i>	Forward 5' ggcatcatgggtggattt Reverse 5' caaggcctttagccaatcg
<i>disembodied</i>	Forward 5' gtgaccaaggagttcattagatttc Reverse 5' ccaaaggtaagcaaacaggttaat
<i>shadow</i>	Forward 5' caagcggatattttagacttgg Reverse 5' aaaaagcccactgactgct
<i>spookier</i>	Forward 5' cggatgatcgaacaactcac Reverse 5' cgagctaaatttctccgcttt

Table 2.1. Primer pairs for qPCR analysis and *in situ* probe.

Gene Symbol	FC 4hr L3	ttest 4h L3	FC 8hr L3	ttest 8hr L3	ANOVA
Downregulated					
Cyp6a17	-114.3	8.66E-05	-130.40	2.40E-05	4.27E-08
CG8858	-5.9	1.14E-04	-6.95	1.12E-02	2.84E-04
CG18278	-14.7	3.41E-04	-14.05	1.36E-05	2.75E-07
Os-C	-6.1	7.64E-04	-8.47	3.28E-05	8.04E-07
ana	-4.4	7.89E-04	-4.13	2.85E-03	3.05E-05
CG5381	-33.5	1.61E-03	-35.31	2.49E-04	9.93E-06
CG14107	-7.5	1.63E-03	-6.18	2.01E-02	9.49E-04
Cyp9c1	-7.3	1.95E-03	-6.98	8.32E-04	2.80E-05
CG40908 (withdrawn)	-9.4	2.10E-03	-11.14	7.27E-03	3.14E-04
CG32212	-6.6	2.36E-03	-6.70	1.03E-03	4.13E-05
CG34439	-4.2	4.04E-03	-5.85	3.86E-03	2.34E-04
CG34278	-49.5	4.40E-03	-54.70	9.02E-03	6.55E-04
CG17134	-9.0	5.92E-03	-9.29	2.21E-03	2.31E-04
dpr6	-7.6	7.56E-03	-5.79	2.43E-06	1.17E-04
CG15818	-7.5	7.65E-03	-16.68	1.83E-04	4.27E-05
CG7046	-9.0	7.71E-03	-9.08	2.52E-02	3.37E-03
CG41124 (withdrawn)	-8.1	9.52E-03	-13.82	6.15E-06	5.17E-05
CG33509	-4.9	1.09E-02	-6.53	6.95E-03	8.87E-04
ImpE1	-4.7	1.63E-02	-4.52	1.47E-02	3.16E-03
ppk13	-7.8	1.90E-02	-13.67	5.84E-05	2.14E-04
npf	-4.7	3.36E-02	-5.31	2.07E-02	8.48E-03
CG14259	-18.2	3.40E-02	-15.03	2.70E-05	2.05E-03
CR32207	-4.4	4.18E-02	-8.58	3.20E-03	2.24E-03
Upregulated					
p24-2	23.6	1.56E-05	31.47	1.82E-07	3.00E-10
Ir76a	13.4	6.96E-05	28.56	1.57E-07	2.17E-09
CG7900	12.8	9.08E-05	11.20	8.81E-05	1.38E-07
Ir76a	16.7	2.19E-04	49.70	6.81E-06	3.56E-08
CG41430 (withdrawn)	9.4	2.44E-04	8.90	7.69E-04	3.65E-06
Ir76a	13.1	3.38E-04	26.75	1.11E-06	5.84E-08
CG6293	6.0	3.96E-04	9.65	6.75E-04	5.25E-06
CG16957	9.8	4.20E-04	11.98	2.03E-05	3.04E-07
CG11741	10.3	4.67E-04	7.64	3.48E-03	3.38E-05
nimC1	9.8	4.97E-04	6.76	4.22E-03	4.12E-05
CG8160	9.4	8.62E-04	16.29	1.18E-02	5.39E-04

Table 2.2, continued					
CG4398	20.5	9.13E-04	21.79	1.83E-03	2.96E-05
CG12460	4.5	1.12E-03	8.54	4.36E-03	1.41E-04
CG41087	4.9	1.38E-03	14.51	3.37E-04	4.92E-06
CG40392 (withdrawn)	7.2	3.35E-03	6.39	1.14E-02	6.71E-04
CG16713	58.9	3.84E-03	55.77	4.39E-03	2.37E-04
CG32440	9.1	3.89E-03	6.71	1.89E-02	1.11E-03
Cyp6t3	4.8	5.93E-03	5.78	1.79E-02	2.08E-03
Cyp6w1	11.4	9.30E-03	10.47	4.34E-02	6.92E-03
CG31226	16.6	9.77E-03	9.35	9.64E-04	4.46E-04
CG13186	8.5	1.12E-02	7.15	2.70E-04	2.55E-04
CG12971	11.5	1.24E-02	37.04	1.71E-04	6.73E-05
CG32437	6.1	1.26E-02	12.79	1.70E-03	3.04E-04
Sop2	5.4	1.35E-02	4.43	5.88E-04	5.18E-04
CG41343	7.6	1.41E-02	8.53	8.61E-03	1.77E-03
CG12831	5.0	1.80E-02	10.59	2.12E-03	4.77E-04
CG2065	5.9	1.86E-02	4.11	2.62E-03	1.66E-03
CG6357	4.7	2.25E-02	5.85	8.51E-03	2.67E-03
LysS	4.9	2.76E-02	4.22	4.83E-03	3.20E-03
CG40467	7.0	2.90E-02	9.24	2.86E-03	1.84E-03
CG6934	5.0	3.64E-02	9.79	4.37E-03	2.06E-03

Table 2.2. Genes affected by *DHR4*-RNAi.

Listed are the 54 genes that were either downregulated or upregulated more than 4fold at both time points in *hsDHR4*-RNAi ring glands. Filtering criteria: Student's *t*-test with a *P* value of <0.05 for both time points, and an ANOVA *P* value of <0.01, sorted by the 4-hour *P* value. # indicates three different probe sets were detected for *Ir76a*. Selected genes are also shown in **Figure 2.16**.

2.7 Figures

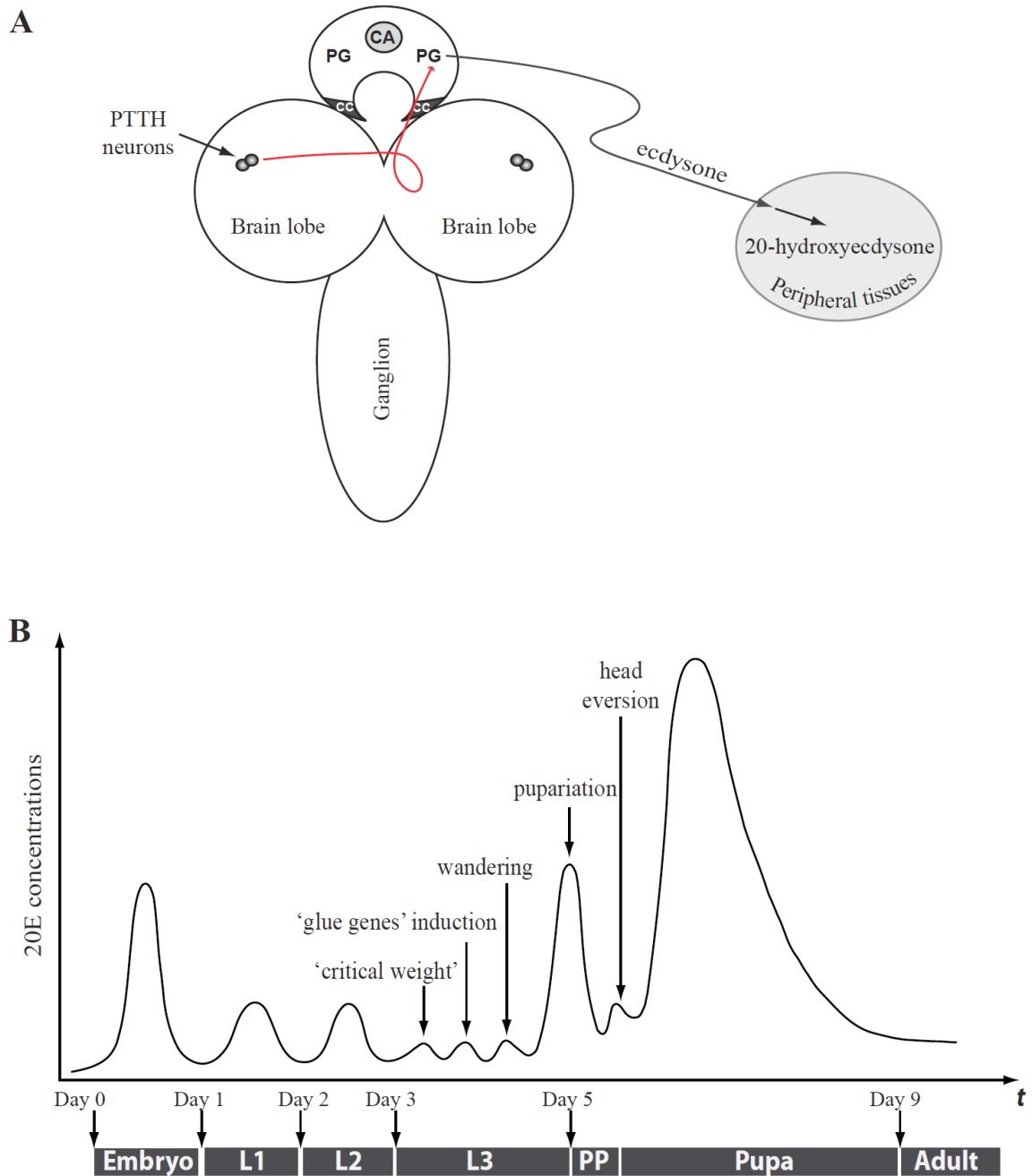


Figure 2.1. Ecdysone directs developmental transitions in *Drosophila*.

(A) Ecdysteroids are produced in prothoracic gland cells of the ring gland, which is attached to the anterior side of the brain. Hormones are then released into the hemolymph and subsequently converted to the biologically active form

20-hydroxyecdysone (20E) in peripheral tissues. (B) Schematic representation of whole-body concentrations of 20E during *Drosophila* development. Three minor ecdysone pulses occur during the third instar and have been suggested to trigger the physiological and behavioral changes indicated by the arrows. PG, prothoracic gland. CA, corpus allatum. CC, corpora cardiaca. L1/L2/L3, first/second/third instar. PP, prepupa.

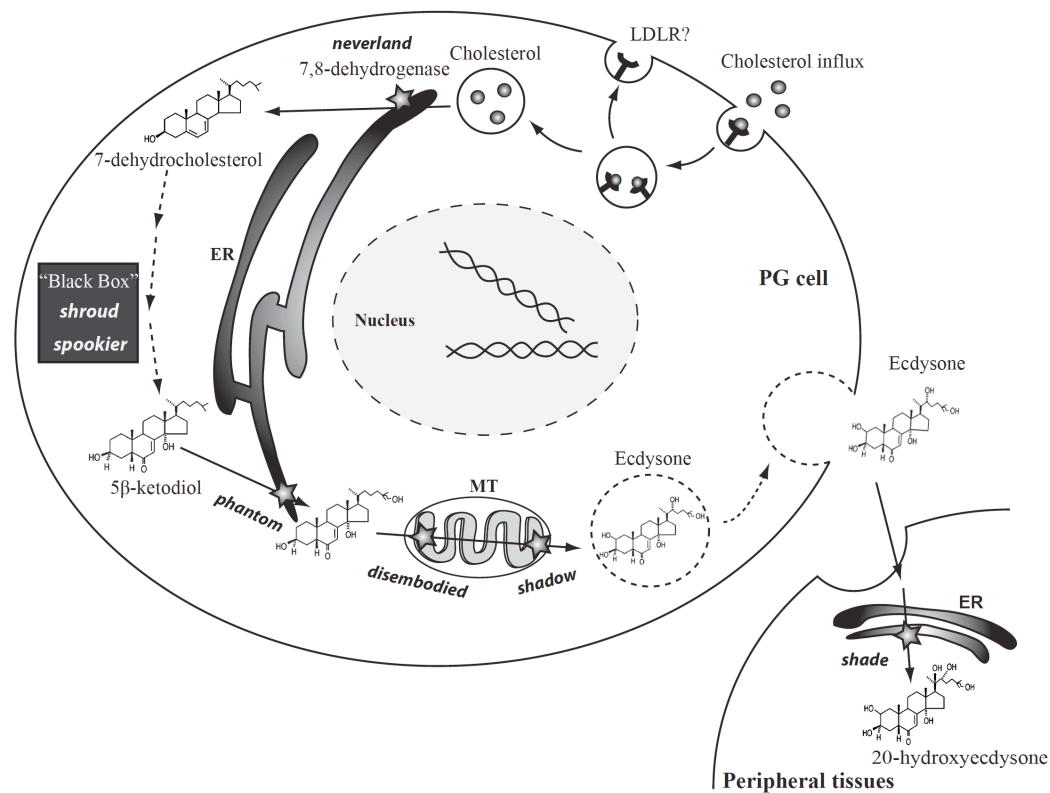


Figure 2.2. A schematic diagram of ecdysone biosynthesis in the *Drosophila* prothoracic gland. Cholesterol is converted into the prohormone ecdysone via a series of reactions (represented by stars) that occur in ER, cytosol (suggested for other arthropod species) (Blais et al., 1996), and mitochondria, and exported possibly by secretory vesicles into hemolymph (O'Connor, 2011). LDLR, low-density lipoprotein receptor. MT, mitochondria. ER, endoplasmic reticulum. N, nucleus. PG, prothoracic gland.

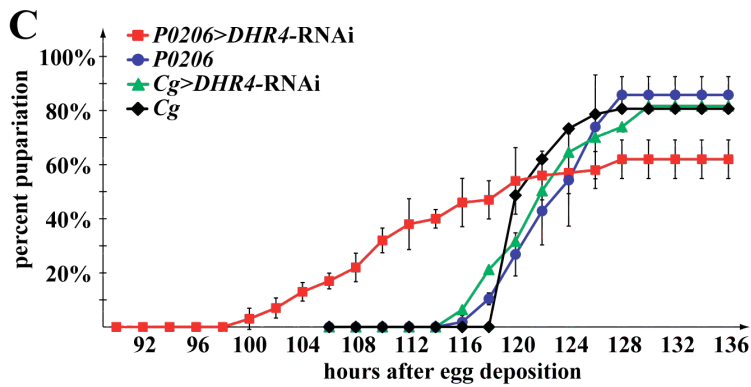
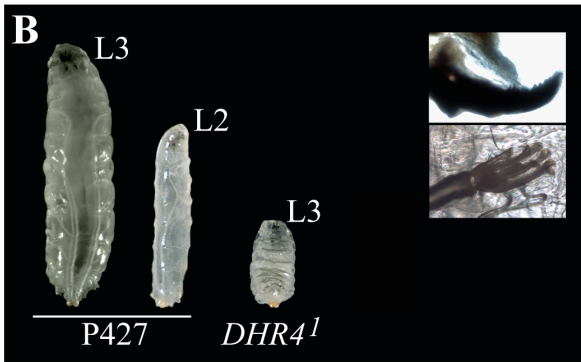
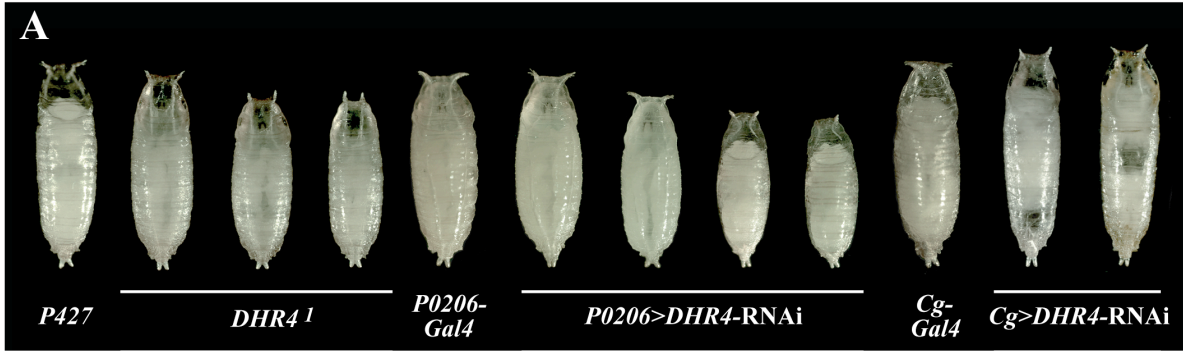


Figure 2.3. Disruption of *DHR4* ring gland function affects developmental timing.

(A) Pupal and prepupal phenotypes include size defects and malformations. From left to right: *P427* parental control line for *DHR4*¹ mutants, *DHR4*¹, *P0206-Gal4* (x2), *P0206>DHR4-RNAi* (x2) prepupae of various sizes, *Cg-Gal4* (x2) pupa, *Cg>DHR4-RNAi* (x2). *P0206-Gal4* is a ring gland *Gal4* driver. *Cg-Gal4* is a fat body *Gal4* driver. (B) Dwarf larvae. *P427* L3 and L2 are controls. A severe

growth defect is observed in populations of *DHR4^l* mutants. The two insets show the morphology of mouth hooks and anterior spiracles of a *DHR4^l* L3 dwarf larva at high magnification. (C) Expression of *DHR4*-RNAi in the RG causes premature pupariation. Percentages of embryos (staged within a 2-hr interval) that reached pupariation, hours are after egg deposition (AED). Unpaired Student's *t*-test between *P0206>DHR4*-RNAi (x2) (red, N=386) and *P0206-Gal4* (x2) (blue, N=143) for time points 104 to 118 are all $P<0.0001$ (not indicated in the graph). *Cg-Gal4* (x2) (black, N=150) and *Cg>DHR4*-RNAi (x2) (green, N=251) examine whether timing differences exist when *DHR4*-RNAi is induced specifically in the fat body.

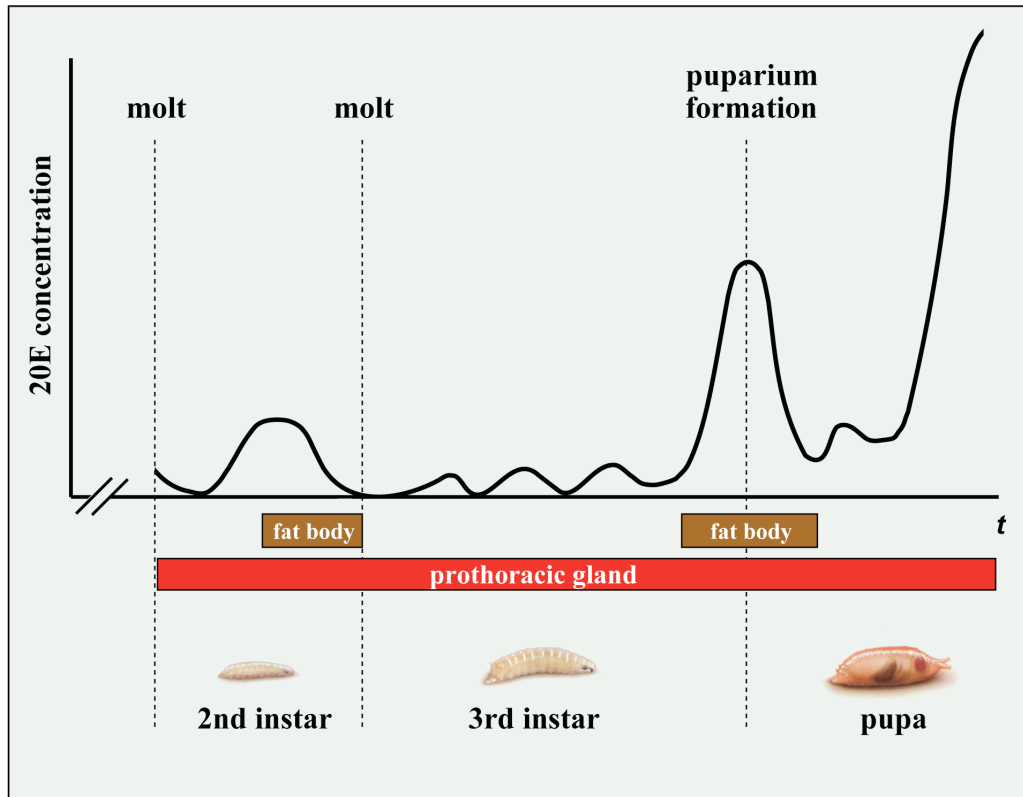


Figure 2.4. Schematic representation of *DHR4* expression profiles during *Drosophila* larval development. *DHR4* is expressed in the prothoracic gland (red) throughout larval development, but fat body expression of *DHR4* (brown) only occurs prior to molts and during puparium formation. y -axis represents relative 20E titers. The tissue-specific expression of *DHR4* represents data from Ou et al. 2011 and King-Jones et al. 2005.

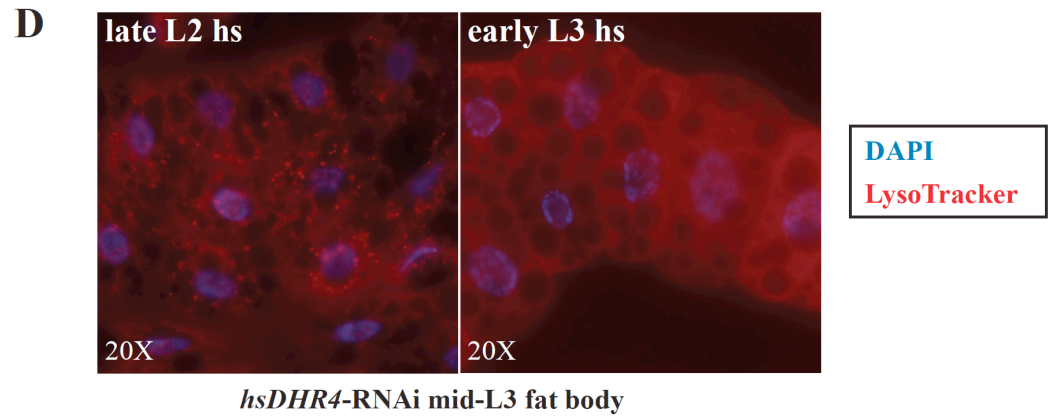
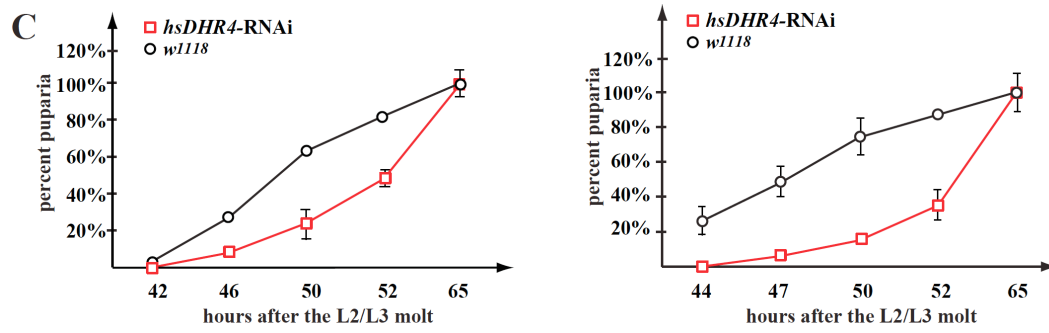
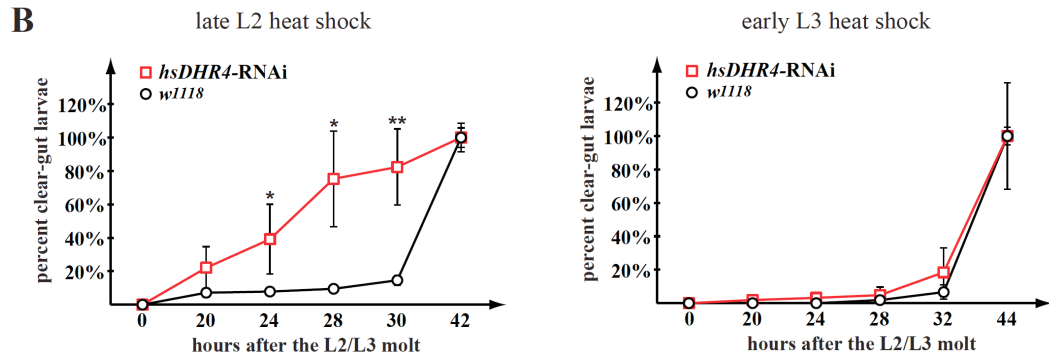
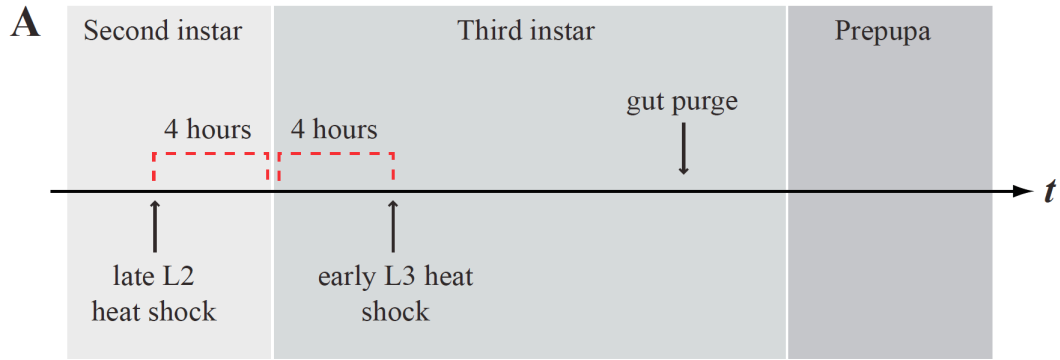


Figure 2.5. *DHR4* expression in the early L3 contributes to the precocious wandering behavior.

(A) The activation of *DHR4*-RNAi by a single heat shock done in either late L2 (~4 hr prior to the L2/L3 molt) or early L3 (~4 hr after the L2/L3 molt). Both controls and *hsDHR4*-RNAi larvae were examined for the color of their gut by using bromophenol blue during mid-L3. (B, C) Time course shows percentage of clear gut larvae (B) as a means to measure wandering behavior, and percentage of puparia (C) as a means to measure pupariation. Red: *DHR4*-RNAi (N=122 for late L2 heat shock, N=133 for early L3 heat shock). Black: *w¹¹¹⁸* controls (N=157 for late L2 heat shock, 115 for early L3 heat shock). *P* values (* $P < 0.05$, ** $P < 0.01$) are based on Student's *t*-test and compare *hsDHR4*-RNAi and *w¹¹¹⁸* at the same time point. Error bars reflect standard deviation from three to six replicates. (D) LysoTracker Red staining. Fat body of *hsDHR4*-RNAi larvae, which were heat shocked in late L2 or early L3, were isolated during mid-L3 and stained with LysoTracker Red as a means to measure autophagy. A DAPI stain is included for nuclei. Images are at 20X magnification.

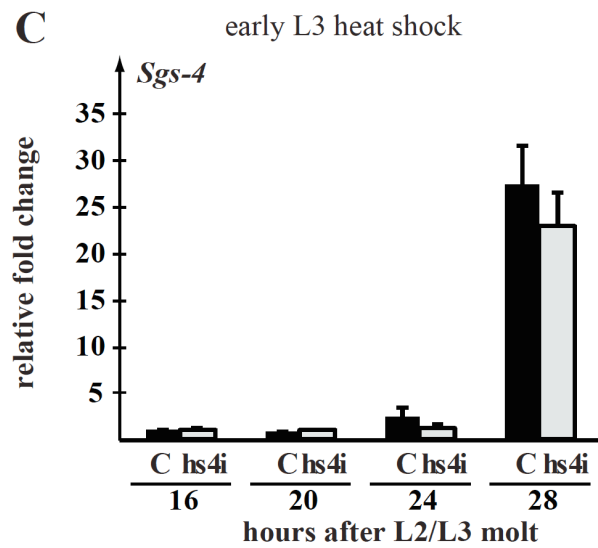
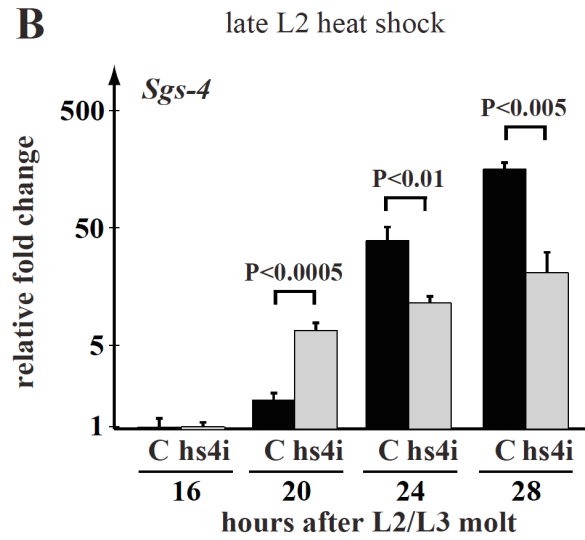
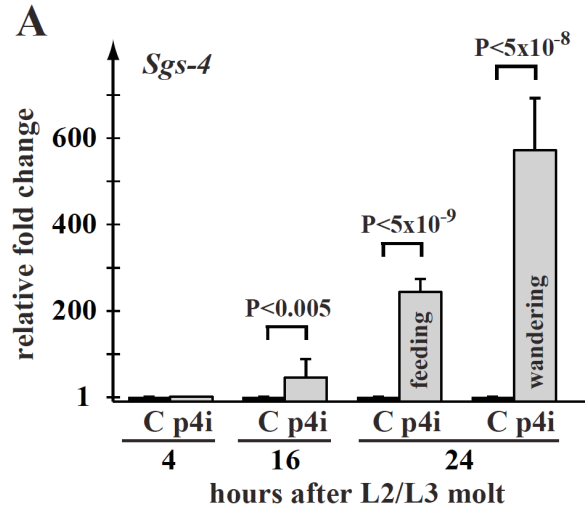
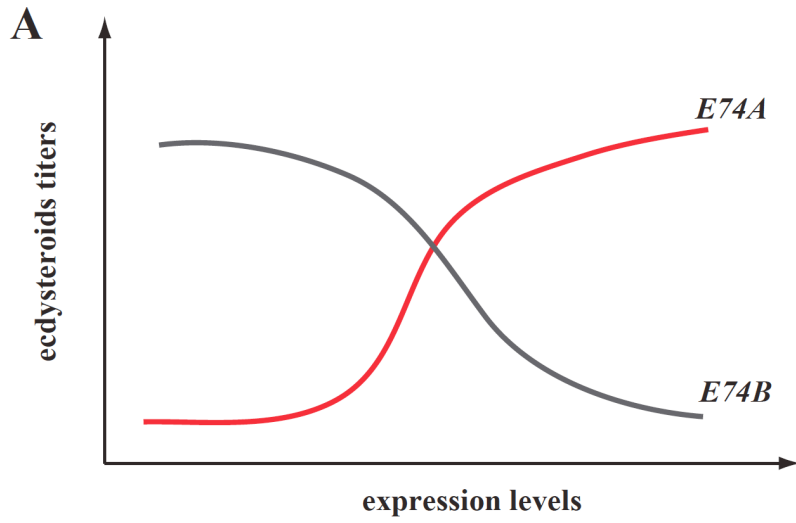
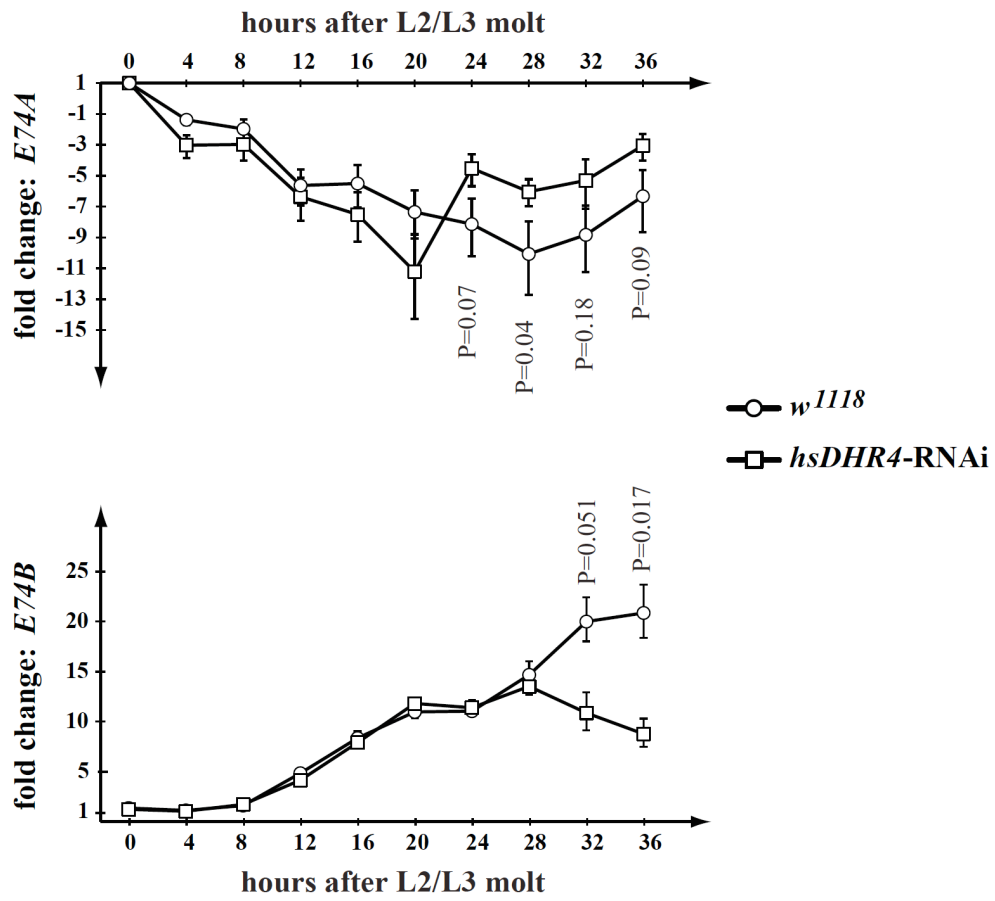


Figure 2.6. *DHR4*-RNAi affects the timing of ecdysone-mediated responses.

qPCR analysis of *Sgs-4* transcript levels in *P0206>DHR4*-RNAi (A) and *hsDHR4*-RNAi animals which were heat-shocked in late L2 (B) or early L3 (C), hours are relative to the L2/L3 molt, and fold changes are relative to the control of 4-hr (A) or 16-hr (B, C) time points. Controls are shown in black, p4i represents *P0206>DHR4*-RNAi, hs4i: *hsDHR4*-RNAi. Error bars represent 95% confidence intervals. *P* values were calculated with the unpaired Student's *t*-test, and data are considered to be insignificant if *P* values are not shown.



B HS: Late second instar



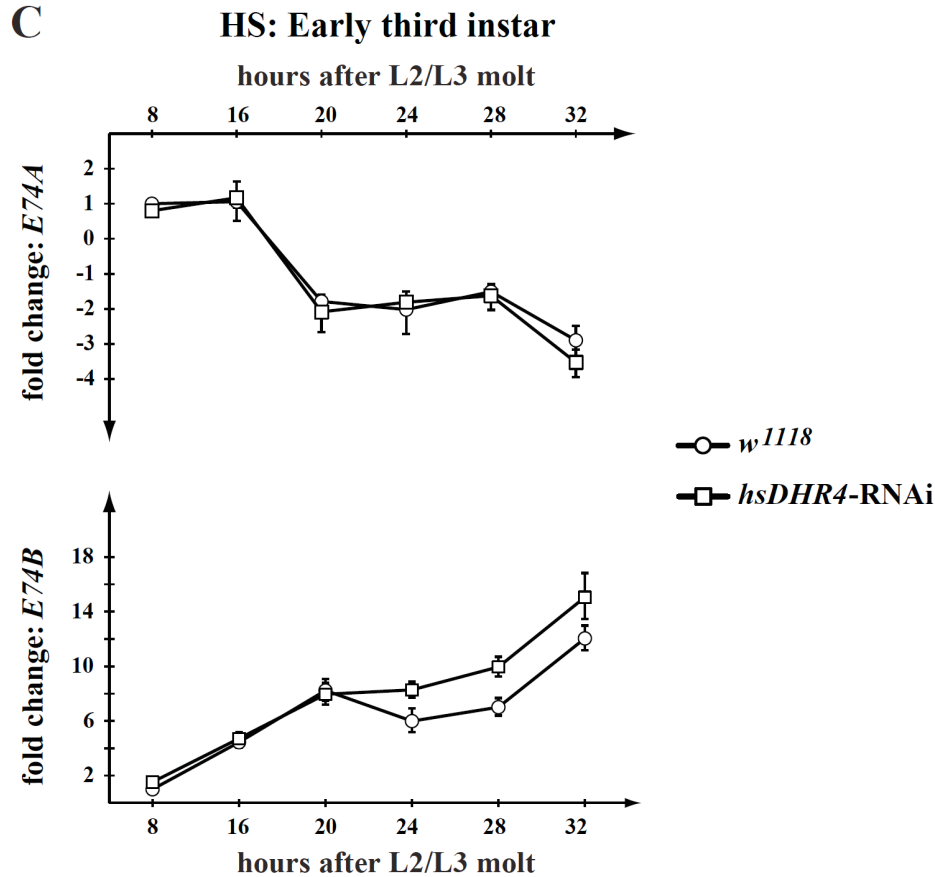


Figure 2.7. Time course qPCR analysis of *E74* transcripts levels in larvae heat-treated in late second instar or early third instar.

(A) A schematic diagram of the expression of *E74* isoforms, *E74A* and *E74B*, as a response to different ecdysone levels. *E74B* is abundant at low to intermediate ecdysone concentrations. *E74A* is only present at high ecdysone levels (Karim and Thummel, 1991). (B, C) *E74A* (upper panels) and *E74B* (bottom panels) transcripts levels were plotted as hours relative to the L2/L3 molt, and all fold changes were calibrated to either the control 0-hr time point (B) or the 8-hr time point (C). Circles represent controls (*w¹¹¹⁸*) and squares stand for *hsDHR4-RNAi* larvae. (B): L2 larvae received heat treatment during late L2 about 4 hr prior to the L2/L3 molt. (C): L3 larvae received heat-shock at early L3 around 4 hr after the molt. Error bars represent 95% confidence intervals. *P* values are based on Student's *t*-test.

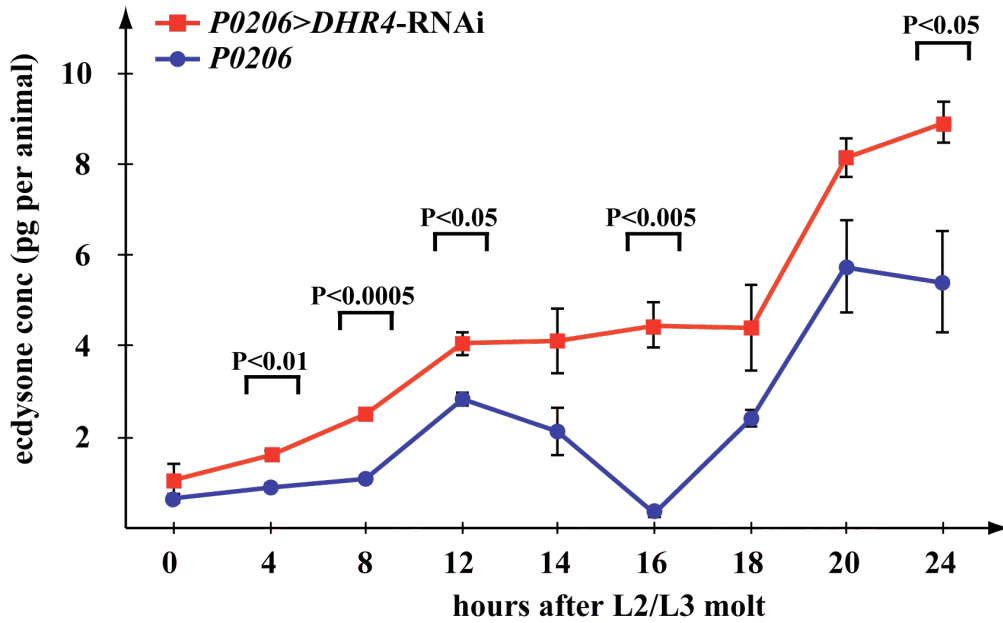


Figure 2.8. Time course analysis of whole-body ecdysteroid titers. Ecdysteroid measurements during the first 24 hours of the third instar. Larvae homozygous either for *P0206>DHR4-RNAi* (red) or *P0206-Gal4* (blue) were compared. At least three samples were tested per time point, and each sample was tested in triplicate. Error bars represent standard error and *P* values are based on Student's *t*-test.

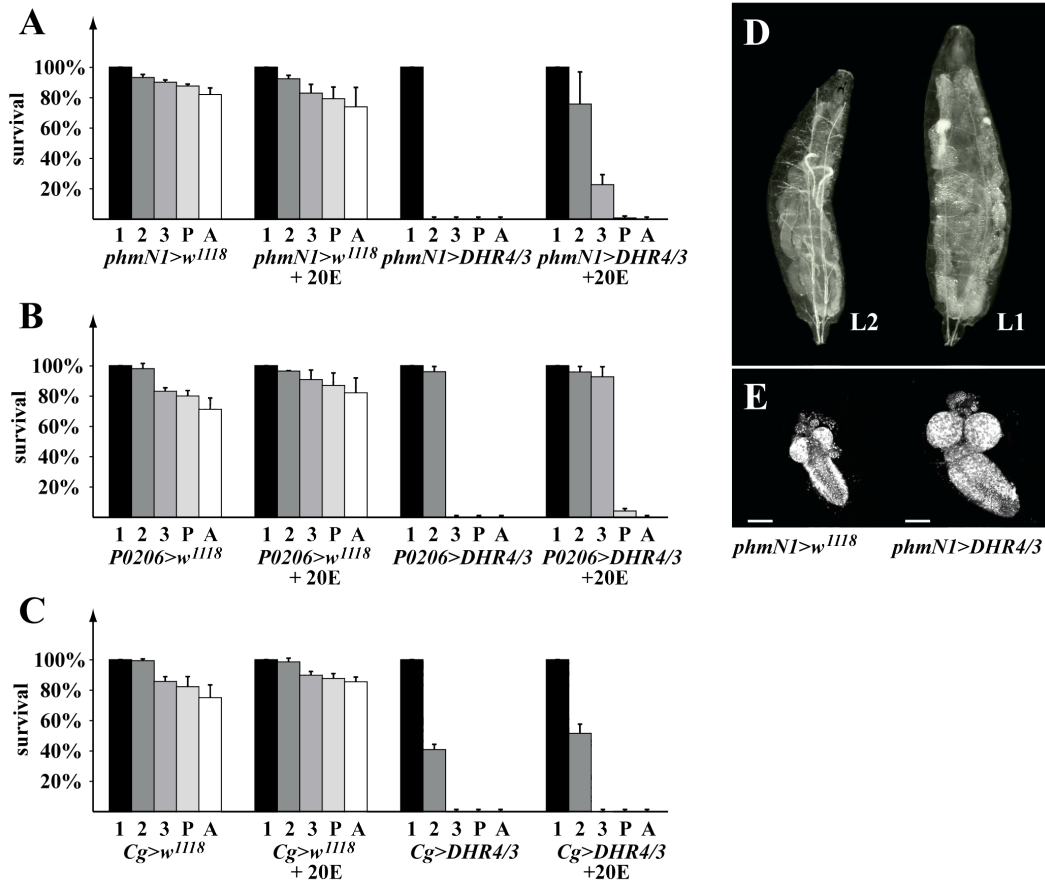


Figure 2.9. Overexpressing *DHR4* in the PG blocks molting.

(A-C) Percent of larvae reaching indicated stage. 1: L1, 2: L2, 3: L3, P: pupae, A: adults. A starter population of 100 L1 larvae was used for all conditions, each tested in triplicate. *phmNI*, *P0206*, *Cg*: Gal4 transgenes driving expression in the PG, ring gland and fat body, respectively. 20E: 20-hydroxyecdysone supplemented in the medium. Error bars represent standard deviation. (D) *phmNI>DHR4/3* cDNA in the PG gives rise to very large L1 larvae (right) when compared to newly molted L2 *phmNI>w¹¹¹⁸* control larva (left). (E) Central nervous systems (CNS) were isolated from larvae equivalent to those pictured in “D”, and stained with DAPI. The scale bars represent 25 μ m. (A-E) *DHR4/3*: *UAS-DHR4* cDNA inserted into the 3rd chromosome.

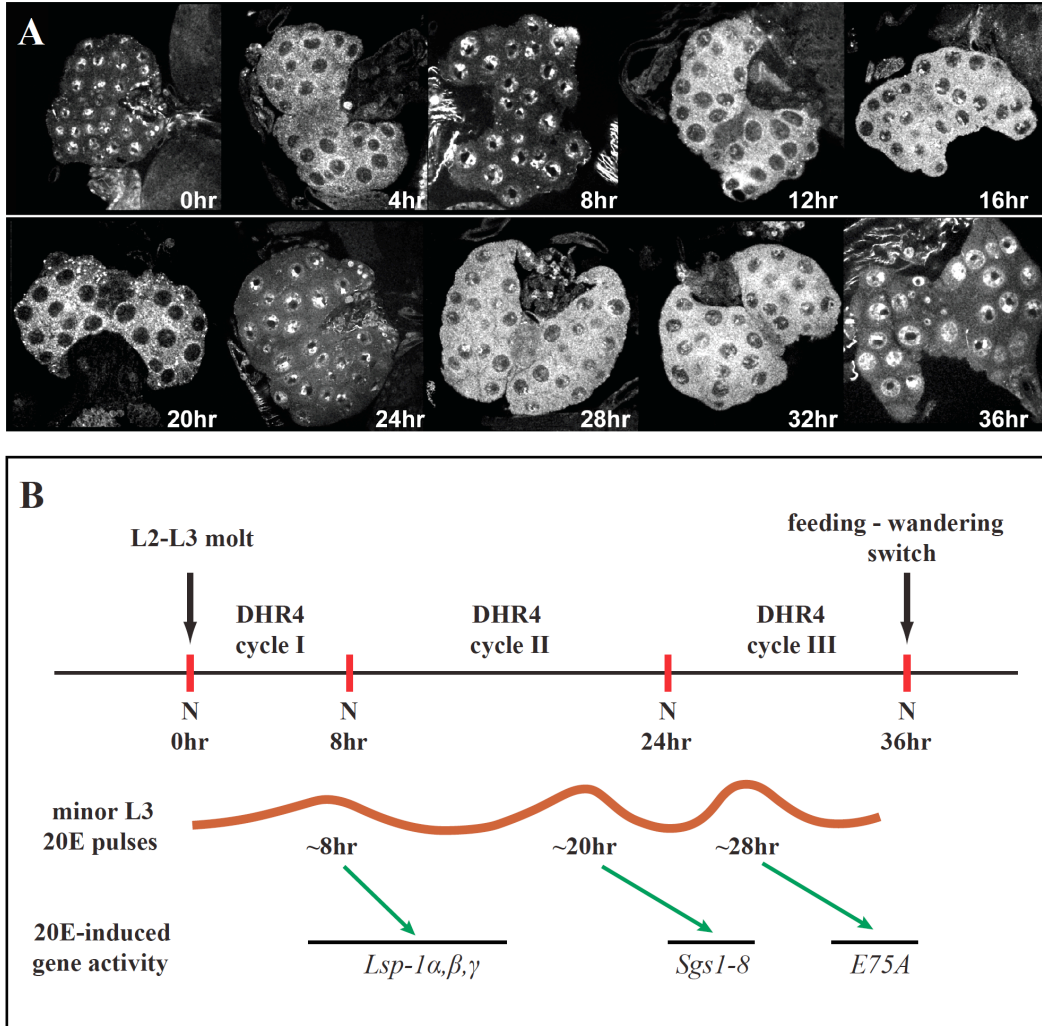


Figure 2.10. DHR4 oscillates between cytoplasm and nucleus in PG cells of L3 larvae.

(A) Confocal images of ring glands isolated from carefully staged w^{1118} L3 larvae at different times relative to the L2/L3 molt. Ring glands were stained with affinity-purified DHR4 antibody. 15-20 ring glands were tested per time point. (B) Schematic representation of DHR4 oscillations. The three cycles observed in (A) correlate with the appearance of the three minor 20E pulses that are documented for the L3 (Warren et al., 2006). These pulses likely induce the *Lsp1*, *Sgs* genes and *E75A* (Andres et al., 1993). N: nucleus.

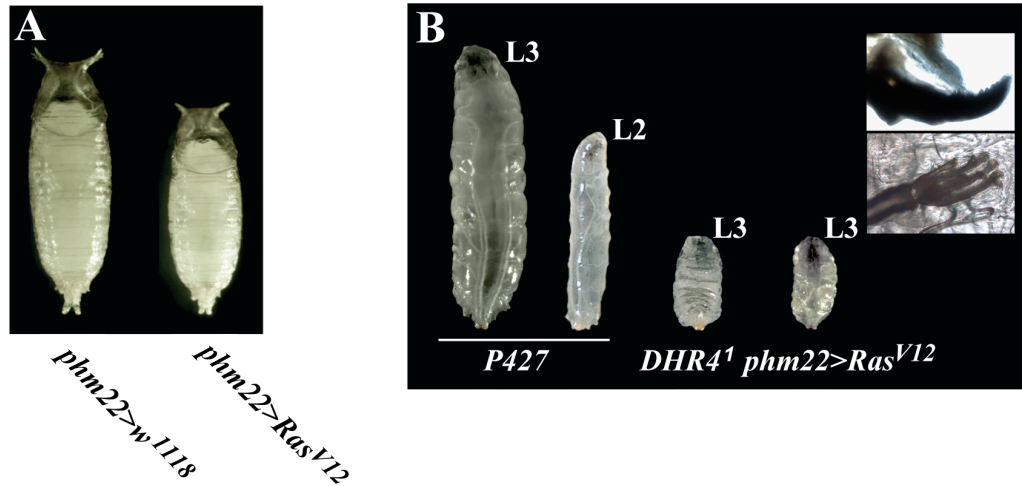


Figure 2.11. Phenotypes of *phm22>Ras^{V12}* larvae.

(A) Small pupae. Expressing a constitutively active form of Ras (*Ras^{V12}*) specifically in the PG results in developmental acceleration, giving rise to small prepupae, strikingly similar to animals with *DHR4* loss-of-function. (B) Dwarf larvae. The dwarf larvae phenotype that was first described as a severe growth defect displayed by *DHR4^l* mutants was also observed in *phm22>Ras^{V12}* larvae. The inset shows the morphology of mouth hooks and anterior spiracles of a dwarf larvae at high magnification.

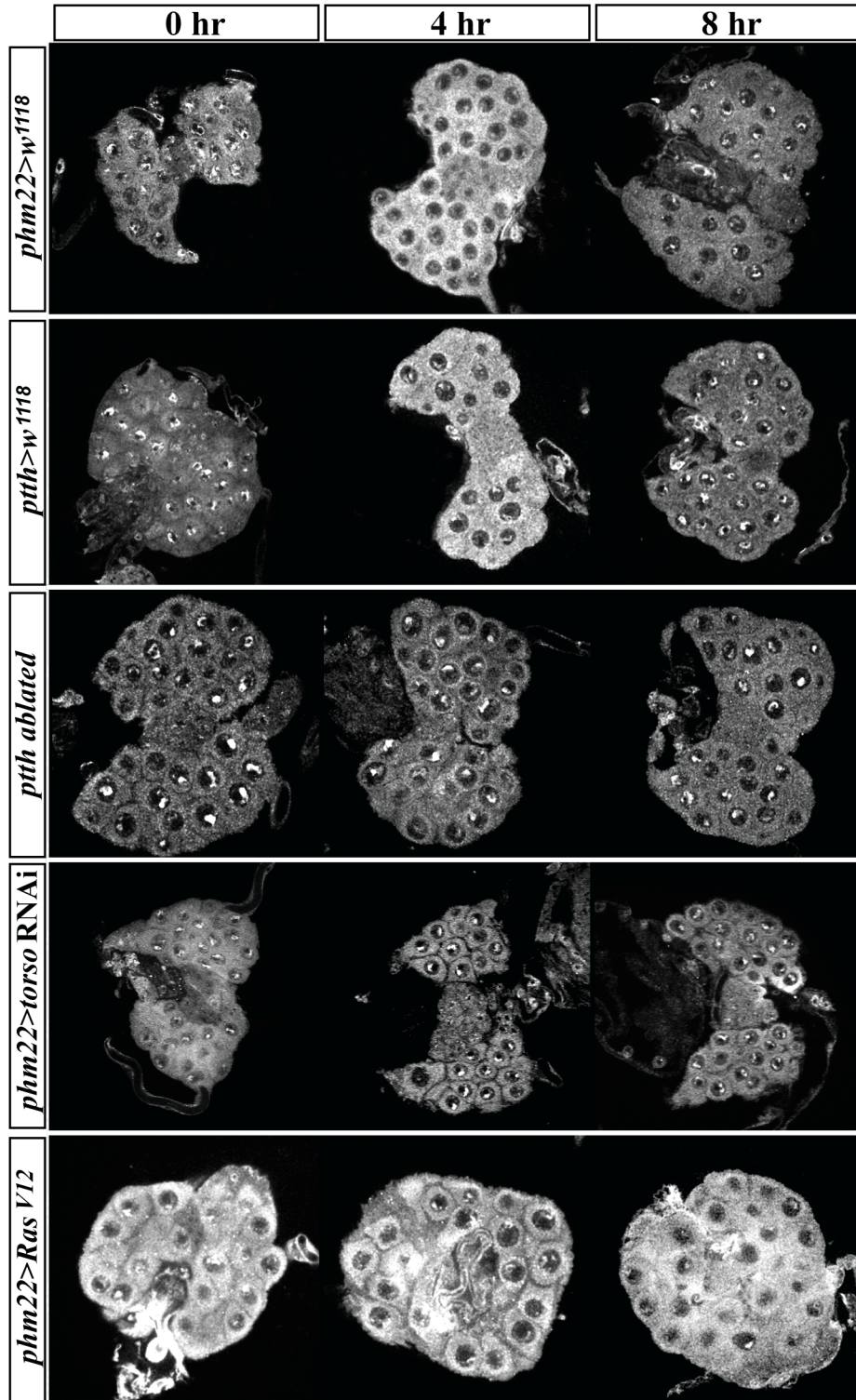


Figure 2.12. Effects on DHR4 subcellular localization by manipulating PTTH pathway components. DHR4 antibody stains. *phm22>w¹¹¹⁸* and *ptth>w¹¹¹⁸* ring glands serve as controls. The *ptth>Grim* and *phm22>torso*-RNAi lines disrupt

PTTH signaling. *phm22>Ras^{V12}* constitutively activates the PTTH pathway. Hours indicate time after the L2/L3 molt. 10-15 ring glands were tested per condition.

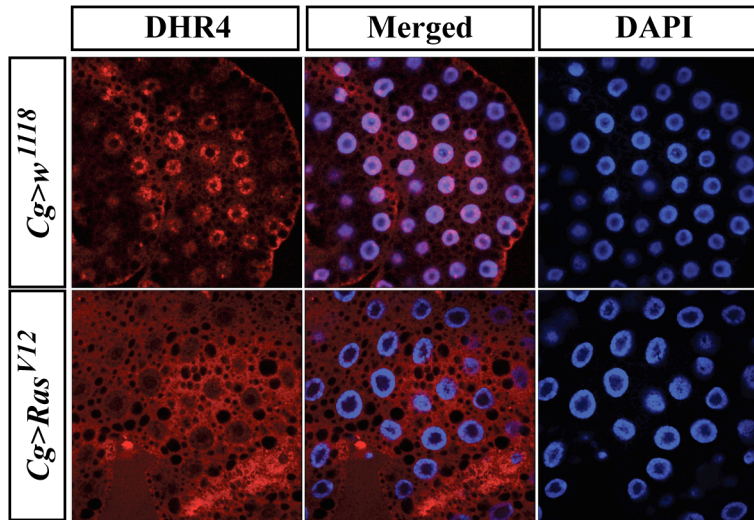


Figure 2.13. DHR4 antibody stains (red) of *Cg>w¹¹¹⁸* and *Cg>Ras^{V12}* late L2 fat body cells. A DAPI stain is included for nuclei.

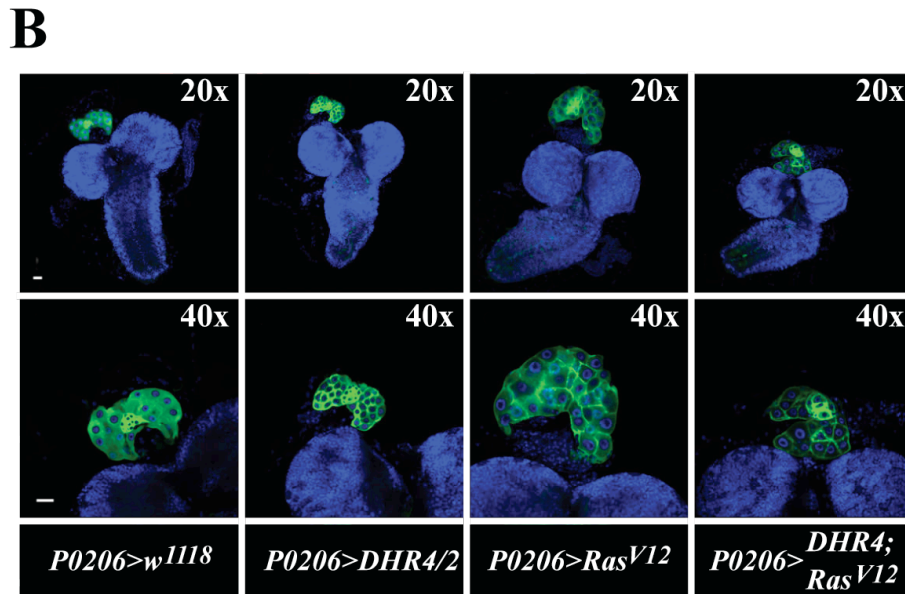
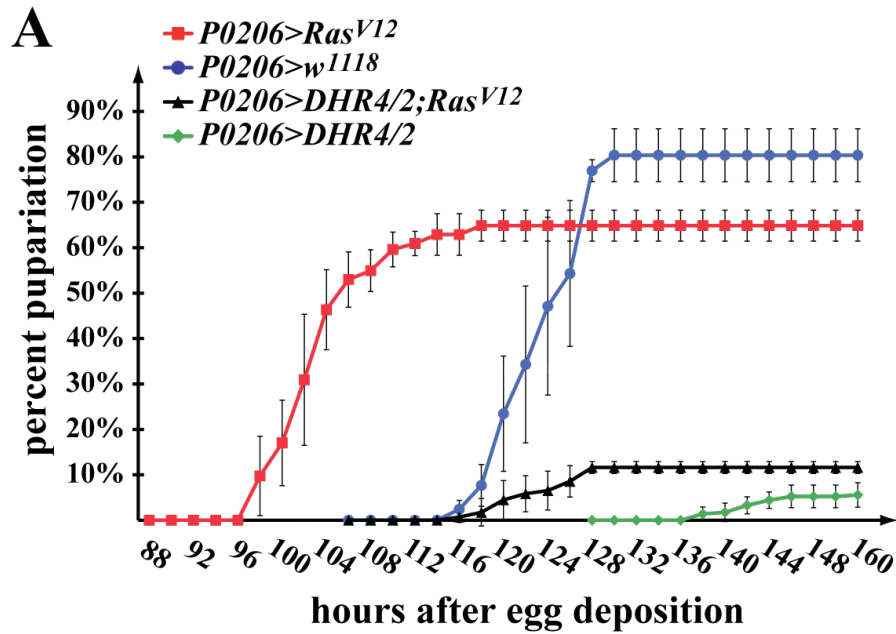


Figure 2.14. Epistasis analysis of *DHR4* and *Ras*.

(A) Genetic epistasis analysis examining the timing of pupariation for transgenic lines expressing *DHR4* cDNA, *Ras^{V12}* or both. Percentages indicate the fraction of embryos that developed into prepupae at a given time point. All populations were tested in triplicate, total N in brackets. Genotypes: *P0206>Ras^{V12}* (red, N=151),

P0206>w¹¹¹⁸ (blue, N=223), *P0206>DHR4/2; Ras^{V12}* (black, N=293), and *P0206>DHR4/2* (green, N=265). Error bars represent standard deviation. (B) *DHR4* overexpression inhibits Ras^{V12}-induced ring gland overgrowth. Brain-ring gland complexes isolated from early L3 larvae, pictures show same sample at 20X and 40X magnification. Blue: DAPI. Green: UASmCD8-GFP is recombined to the same chromosome as *P0206-Gal4*, and therefore reflects the expression pattern of the *P0206* driver. Genotypes are listed below the figure. The scale bars represent 25 μ m. DHR4/2 denotes *UAS-DHR4* cDNA inserted in the 2nd chromosome.

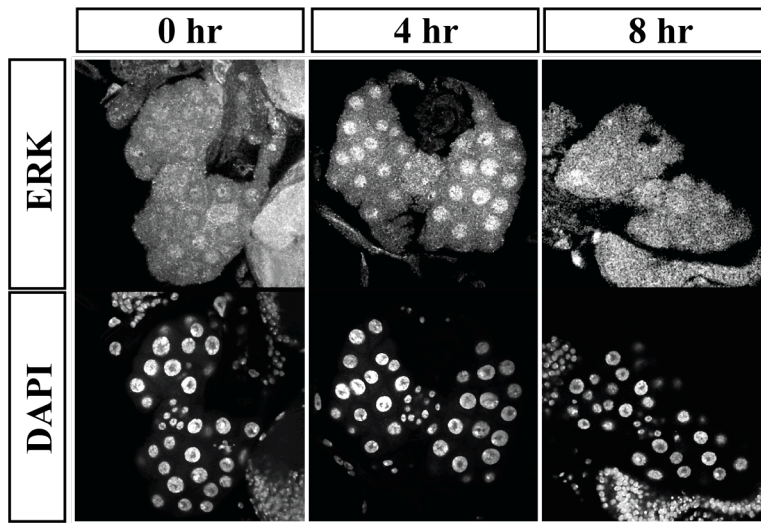
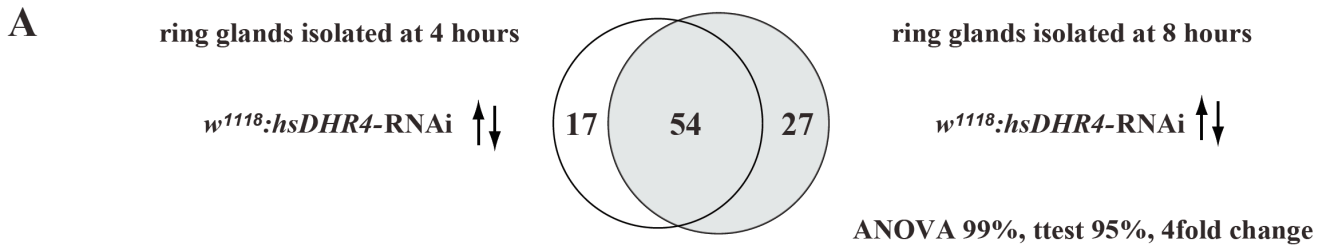


Figure 2.15. ERK antibody stains (upper panel) of w^{118} ring glands during the first 8 hours of the third instar. A DAPI stain (bottom panel) is included for nuclei. 10-15 ring glands were stained per condition.



B DOWNREGULATED

Gene Symbol	Map	Interpro	FC 4hr	ttest 4hr	FC 8hr	ttest 8hr	ANOVA Rank
<i>Cyp6a17</i>	51D1	Cytochrome P450	-114.3	8.7E-05	-130.4	2.4E-05	4.3E-08 1
<i>CG8858</i>	48E8	Armadillo-type fold	-5.9	1.1E-04	-7.0	1.1E-02	2.8E-04 2
<i>CG18278</i>	50A5	N-acetylglucosamine-6-sulfatase	-14.7	3.4E-04	-14.0	1.4E-05	2.8E-07 3
<i>anachronism</i>	45A1	Transforming growth factor beta	-4.4	7.9E-04	-4.1	2.9E-03	3.1E-05 5
<i>Cyp9c1</i>	60D10	Cytochrome P450	-7.3	2.0E-03	-7.0	8.3E-04	2.8E-05 8
<i>CG17134</i>	32B1	Peptidase aspartic	-9.0	5.9E-03	-9.3	2.2E-03	2.3E-04 13
<i>dpr6</i>	67D2	Immunoglobulin subtype 2	-7.6	7.6E-03	-5.8	2.4E-06	1.2E-04 14
<i>CG15818</i>	27F3	C-type lectin	-7.5	7.7E-03	-16.7	1.8E-04	4.3E-05 15
<i>CG7046</i>	94B1	High mobility group	-9.0	7.7E-03	-9.1	2.5E-02	3.4E-03 16
<i>ImpE1</i>	66C8/10	Low density lipoprotein-receptor	-4.7	1.6E-02	-4.5	1.5E-02	3.2E-03 19
<i>ppk13</i>	39A1	Na ⁺ channel, amiloride-sensitive	-7.8	1.9E-02	-13.7	5.8E-05	2.1E-04 20
<i>npf</i>	89D5	Pancreatic hormone-like	-4.7	3.4E-02	-5.3	2.1E-02	8.5E-03 21
<i>CG14259</i>	97E2	Haemolymph juvenile hormone binding	-18.2	3.4E-02	-15.0	2.7E-05	2.1E-03 22

C UPREGULATED

Gene Symbol	Map	Interpro	FC 4hr	ttest 4hr	FC 8hr	ttest 8hr	ANOVA Rank
<i>p24-2</i>	85E4	emp24/gp25L/p24	23.6	1.6E-05	31.5	1.8E-07	3.0E-10 1
<i>Ir76a</i>	76C6	Ionotropic Glutamate Receptor	13.4	7.0E-05	28.6	1.6E-07	2.2E-09 2/4/6#
<i>CG7900</i>	84E11/12	Amidase	12.8	9.1E-05	11.2	8.8E-05	1.4E-07 3
<i>CG6293</i>	86A7	Xanthine/uracil permease	6.0	4.0E-04	9.7	6.8E-04	5.3E-06 7
<i>CG16957</i>	34B10	Cytochrome b5 domain	9.8	4.2E-04	12.0	2.0E-05	3.0E-07 8
<i>nimrodC1</i>	34E5	EGF-like growth factor receptor	9.8	5.0E-04	6.8	4.2E-03	4.1E-05 10
<i>CG4398</i>	53C4	Insect allergen related	20.5	9.1E-04	21.8	1.8E-03	3.0E-05 12
<i>CG12460</i>	no map	RNA recognition motif, RNP-1	4.5	1.1E-03	8.5	4.4E-03	1.4E-04 13
<i>CG16713</i>	24B2/3	Proteinase inhibitor I2, Kunitz	58.9	3.8E-03	55.8	4.4E-03	2.4E-04 16
<i>Cyp6t3</i>	48E7/8	Cytochrome P450	4.8	5.9E-03	5.8	1.8E-02	2.1E-03 18
<i>Cyp6w1</i>	42A12	Cytochrome P450	11.4	9.3E-03	10.5	4.3E-02	6.9E-03 19
<i>CG2065</i>	43E8/9	Short-chain dehydrogenase/reductase	5.9	1.9E-02	4.1	2.6E-03	1.7E-03 27
<i>CG6934</i>	88E1/2	Ras-association, FERM domain	5.0	3.6E-02	9.8	4.4E-03	2.1E-03 31

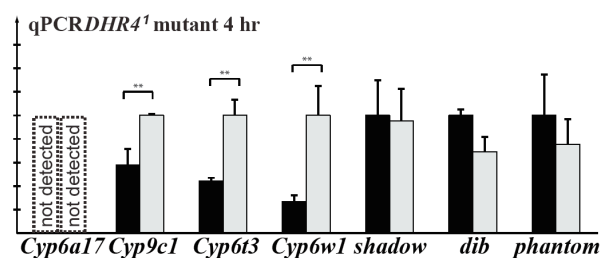
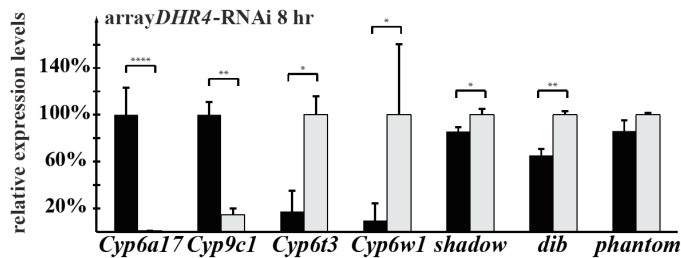
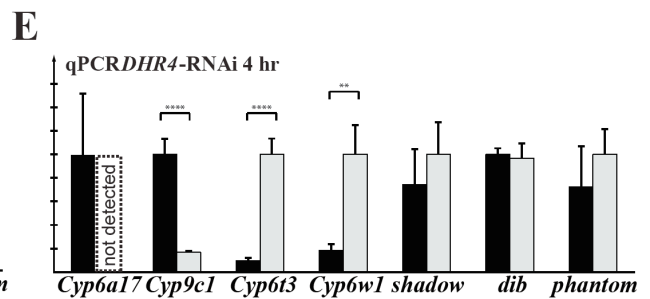
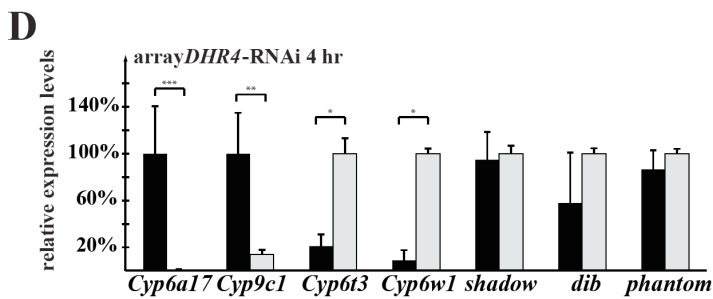


Figure 2.16. *DHR4*-RNAi ring gland microarray reveals misregulated cytochrome P450 genes.

(A) Comparison of microarray data sets representing 71 genes upregulated or downregulated more than 4fold in 4-hr L3, and 81 genes in 8-hr L3 *hsDHR4*-RNAi ring glands. Filtering criteria: >4fold change, Student's *t*-test with a *P* value of <0.05 for both time points, and an ANOVA *P* value of <0.01. (B, C) Selected genes either downregulated (B) or upregulated (C), sorted by the 4-hr *P* value. Genes with possible roles in ecdysone biosynthesis are in bold. # indicates three different probe sets were detected for *Ir76a*. (D) Selected microarray results and qPCR validation in *hsDHR4*-RNAi animals and *DHR4^l* mutants (grey bars). Controls are shown in black, *w¹¹¹⁸* for *hsDHR4*-RNAi and *P427* for *DHR4^l* mutant. *shadow*, *disembodied* and *phantom* failed ANOVA testing at the 95% level, but were included for validation purposes. RNA from brain-ring gland complexes of animals staged at 4-hr L3 was used for qPCR validation. Error bars for the array data represent standard deviation, and error bars for qPCR data show 95% confidence intervals. Asterisks indicate significant differences between groups (**P*<0.05, ***P*< 0.005, ****P*<0.0005, *****P*<0.00005 by Student's *t*-test).

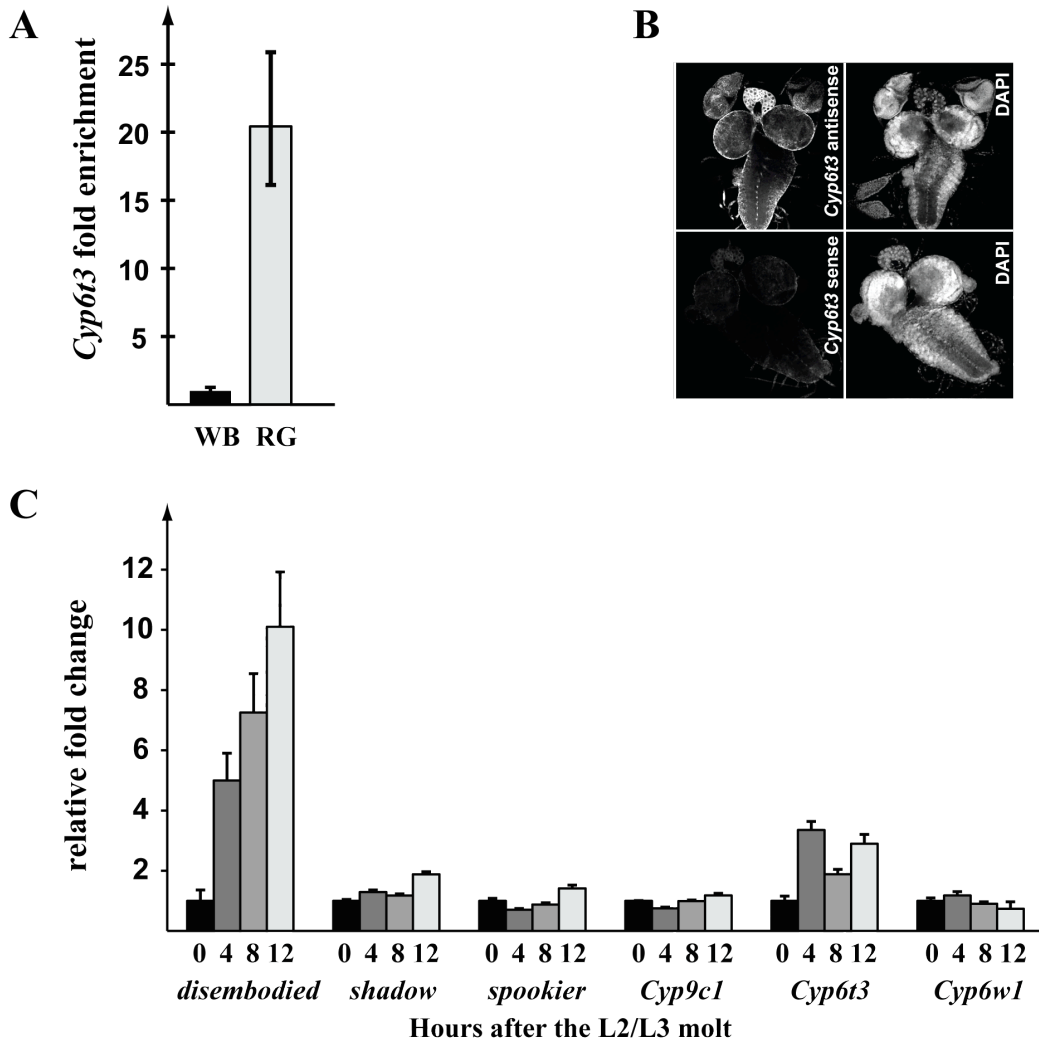


Figure 2.17. *Cyp6t3* expression is highly specific to the prothoracic gland.

(A) qPCR analysis of *Cyp6t3* mRNA levels in ring gland (RG, grey bar) vs. whole body (WB, black bar) isolated at 4 hr after the L2/L3 molt. RNA from *w¹¹¹⁸* ring glands and total larvae were linearly amplified before qPCR analysis. Error bars represent 95% confidence intervals. (B) *In situ* hybridization of *Cyp6t3* antisense and sense probes. Early third-instar larval brain-ring gland complexes with eye-antenna imaginal discs were examined by 20X magnification. A DAPI stain of the nuclei is included. (C) *Cyp6t3* mRNA oscillates during the first 12 hours of the L3 stage. Brain-ring gland complexes were isolated from carefully staged animals, and qPCR was carried out to measure relative mRNA levels of

selected cytochrome P450 genes in *w¹¹⁸* at 0, 4, 8, and 12 hr after the L2/L3 molt. All fold changes were normalized to the 0-hr L3 time point. Error bars represent 95% confidence intervals.

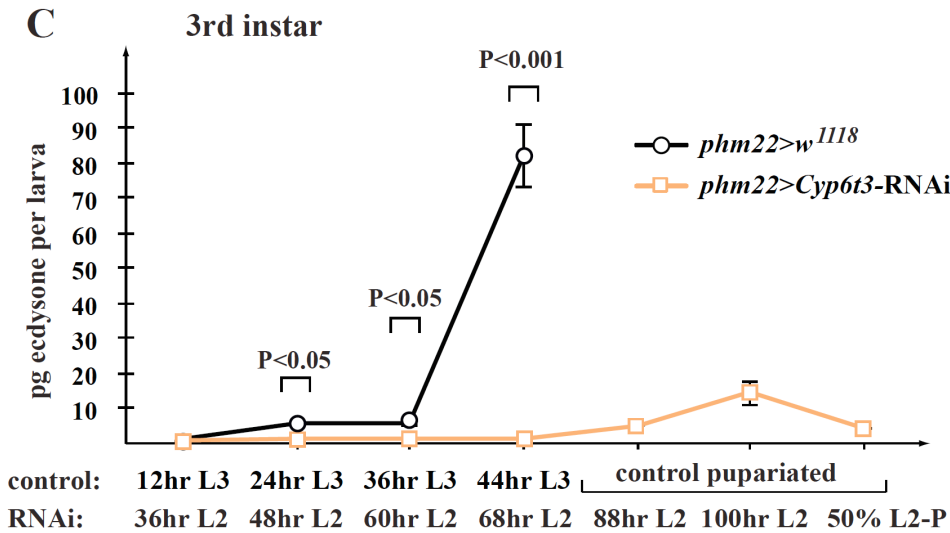
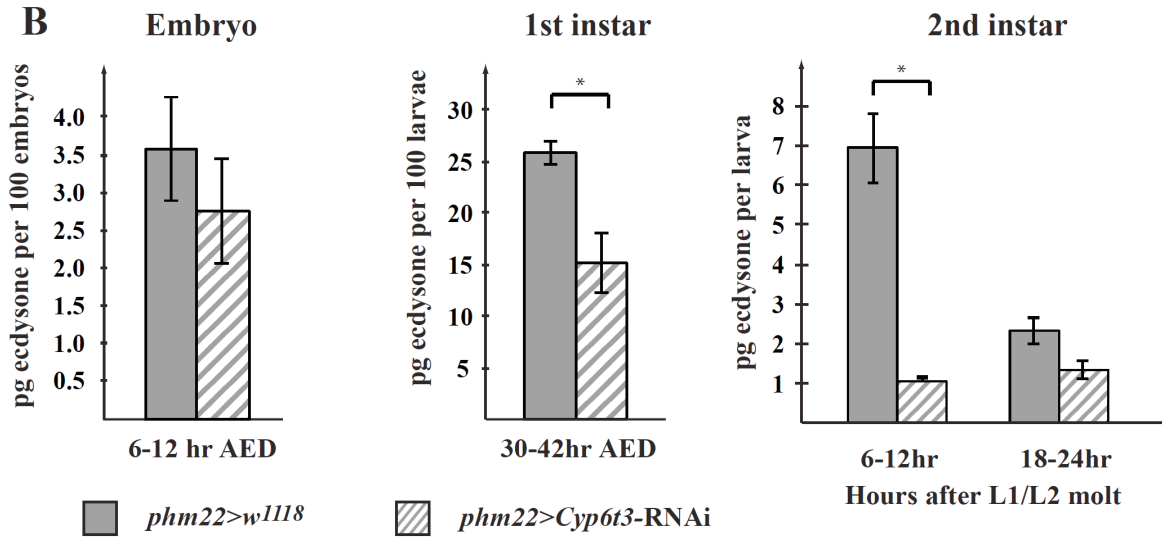
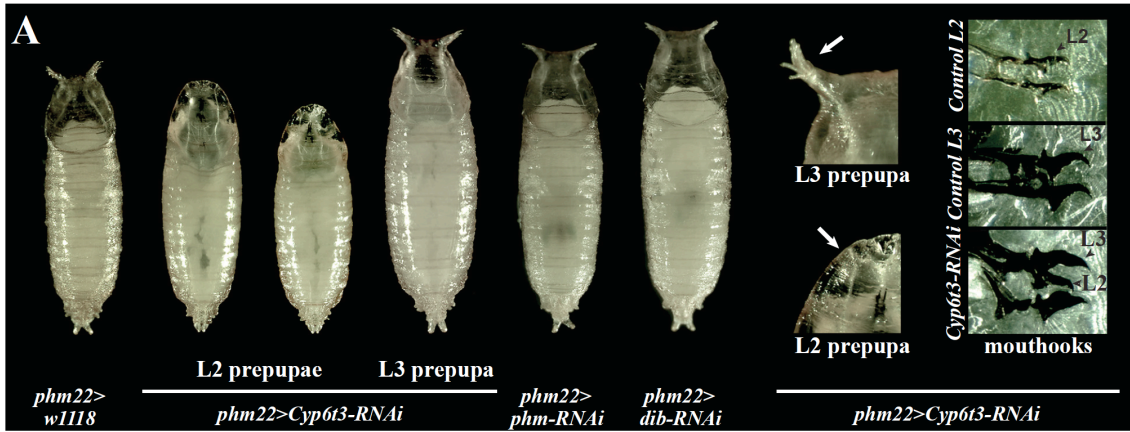


Figure 2.18. Disrupting *Cyp6t3* function in the PG results in ecdysone deficiency. (A) PG-specific *Cyp6t3*-RNAi phenotypes (VDRC#109703), compared to *phm22>w¹¹¹⁸* control (left). Insets show the morphology of anterior spiracles and double mouth hooks of *phm22>Cyp6t3*-RNAi animals compared to controls. (B) Whole-body ecdysteroid titers for *Cyp6t3*-RNAi embryos, L1, and L2 larvae. Control is in grey, *phm22>Cyp6t3*-RNAi is represented by striped bars. Left: embryos (in pg/100 embryos). Middle: L1 larvae (in pg/100 larvae). Right: L2 larvae (in pg/larva) at different time points as indicated. Error bars indicate standard error. *P* values are based on Student's *t*-test. * *P* <0.01. (C) Whole-body ecdysteroid titer measurements comparing equivalent L2 and L3 stages between *phm22>Cyp6t3*-RNAi animals (orange) and *phm22>w¹¹¹⁸* controls (black). Time points indicate hours after the L2/L3 molt (control) or after the L1/L2 molt (*phm22>Cyp6t3*-RNAi). For each condition, 3~4 samples (N=30~45 larvae) were each tested in triplicate. Error bars indicate standard error.

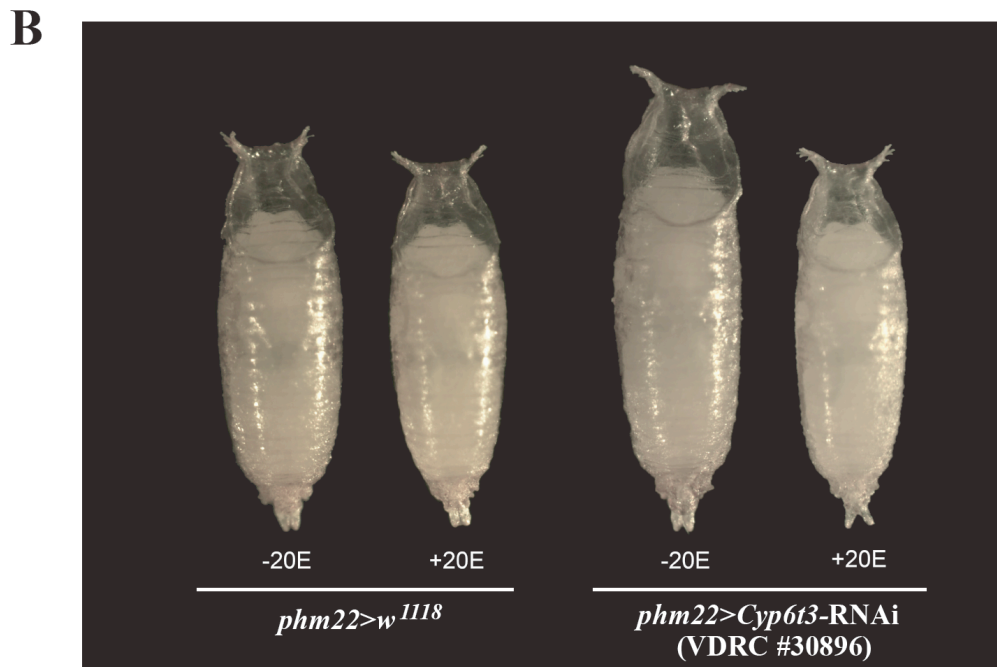
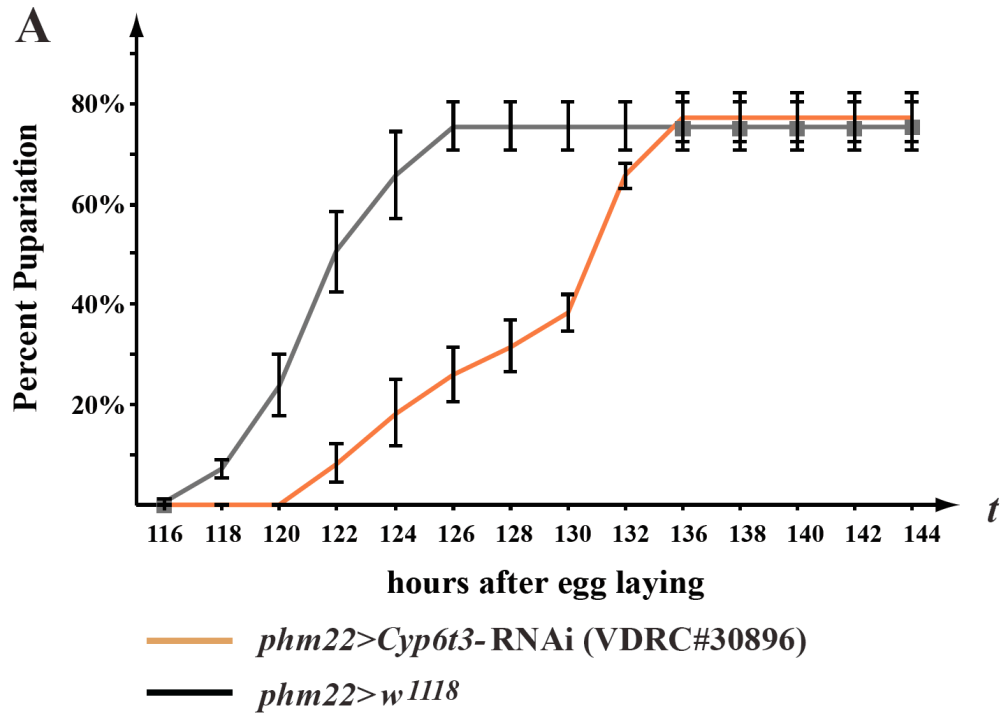


Figure 2.19. Phenotypic characterization of *Cyp6t3*-RNAi line (VDR#30896). (A) Time course of puparium formation in *phm22>Cyp6t3*-RNAi animals (orange) and *phm22>w¹¹¹⁸* controls (black). Error bars represent standard deviation, which

are based on three replicates. (B) 20E rescues large pupal phenotype. The developmental delay shown in (A) results in larger *phm22>Cyp6t3*-RNAi animals (3rd pupa from left), while *phm22>w¹¹¹⁸* controls are of normal size (left pupa). The supplementation of 20E to the fly media restores a normal body size for *phm22>Cyp6t3*-RNAi larvae.

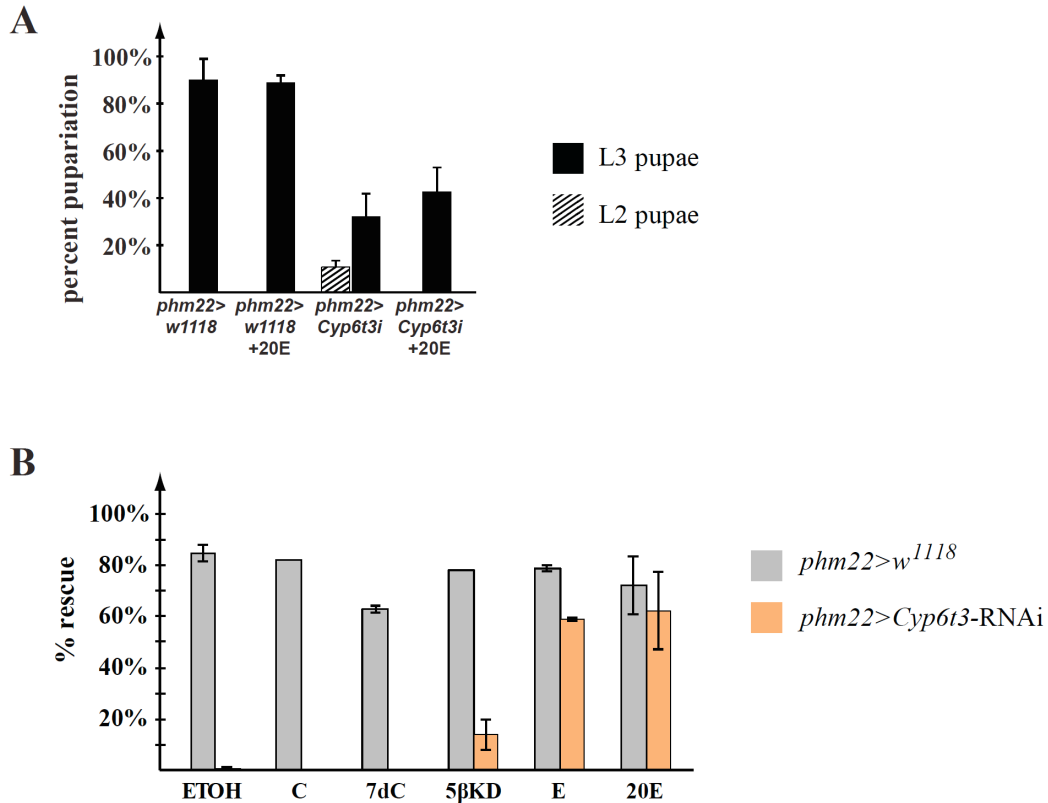


Figure 2.20. Cyp6t3 is a novel component in the “Black Box” of ecdysone synthesis.

(A) Percentages of L2 pupae (striped) and L3 pupae (black) of *phm22>w¹¹¹⁸* and *phm22>Cyp6t3-RNAi* in populations fed a standard medium with or without 20E. Error bars indicate standard deviation, N=150~200 for each condition. (B) Feeding 5β-ketodiol to *phm22>Cyp6t3-RNAi* larvae rescues larvae beyond the L2 stage. C424 instant fly medium was supplemented with different ecdysteroid precursors or the solvent alone (ethanol). Percentages show fraction of embryos reaching the third instar. *phm22>w¹¹¹⁸* is in grey and *phm22>Cyp6t3-RNAi* is in orange. Error bars indicate standard deviation, N=150~200 for each condition. ETOH, ethanol; C, cholesterol; 7dC, 7-dehydrocholesterol; 5βKD, 5β-ketodiol; E, ecdysone; 20E, 20-hydroxyecdysone.

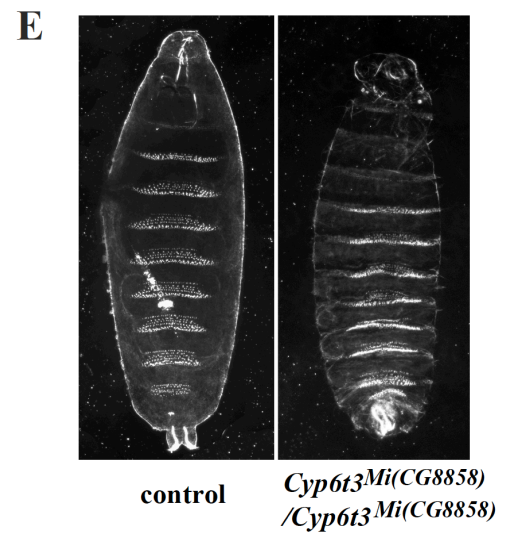
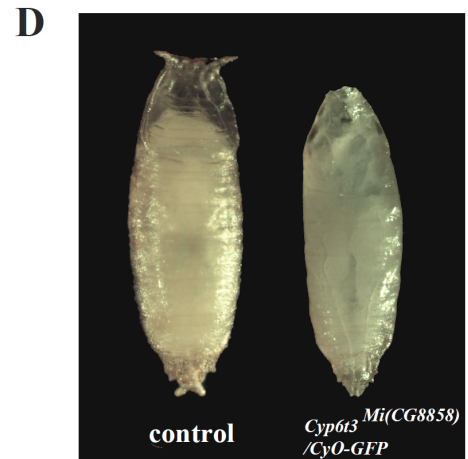
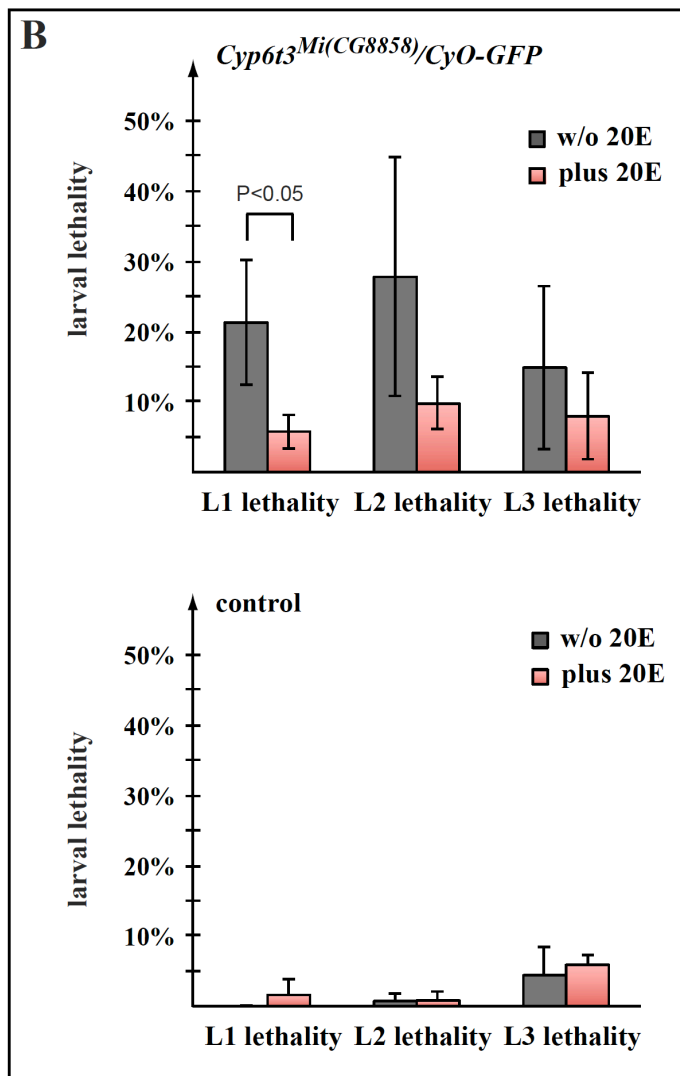
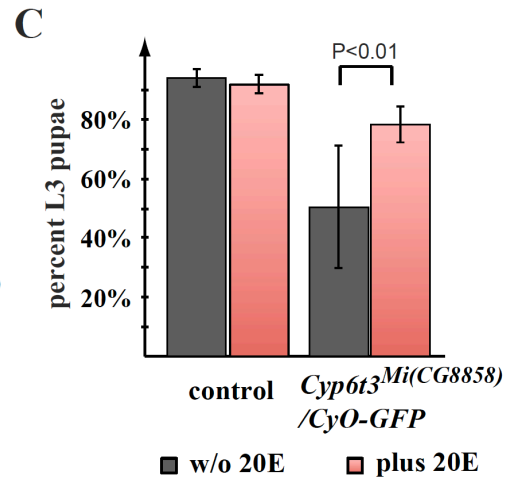
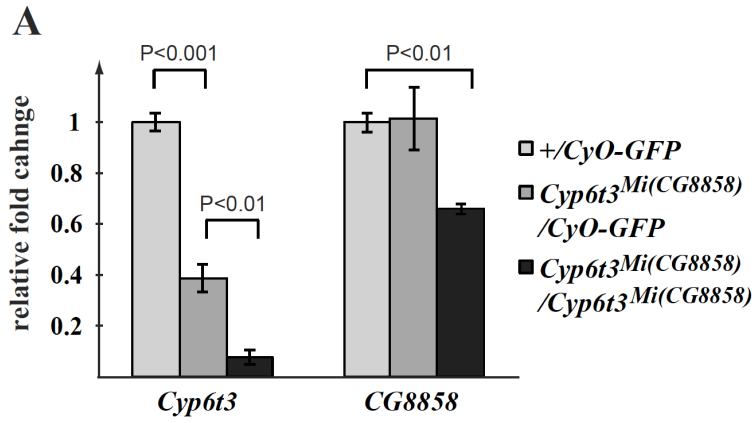


Figure 2.21. Analysis of *Cyp6t3*^{Mi(CG8858)} allele (Bloomington stock #31021).

(A) qPCR analysis of *Cyp6t3* and *CG8858* transcripts levels in controls (+/*CyO-act-GFP*), heterozygotes [*Mi(CG8858)/CyO-act-GFP*] and homozygotes [*Mi(CG8858)/Mi(CG8858)*]. Error bars represent 95% confidence intervals, *P* value based on Student's *t*-test. Each data point represents 3~4 biological samples, each tested in triplicate. (B) Analysis of larval lethality displayed by *Mi(CG8858)/CyO-act-GFP* heterozygotes (upper panel, N=250~300 per stage) and control +/*CyO-act-GFP* animals (bottom panel, N=100~150 per stage), which were fed on yeast paste without (dark grey) or with (red) 0.33 mg/ml 20E. (C) Rescue of L1 larvae to pupariation with ecdysone. Percentages are given for L3 that form pupae in the control group (left, +/*CyO-act-GFP*) and heterozygous animals (right, *Mi(CG8858)/CyO-act-GFP*), fed on yeast paste without (dark grey) or with (red) 20E. Error bars in (B, C) indicate standard deviation, *P* value based on Student's *t*-test. (D) L2 prepupae were observed in heterozygous [*Mi(CG8858)/CyO-act-GFP*] populations. (E) Images of embryonic cuticle preparations. Left: control (22 hr AED). Right: homozygotes *Mi(CG8858)/Mi(CG8858)* (30 hr AED).

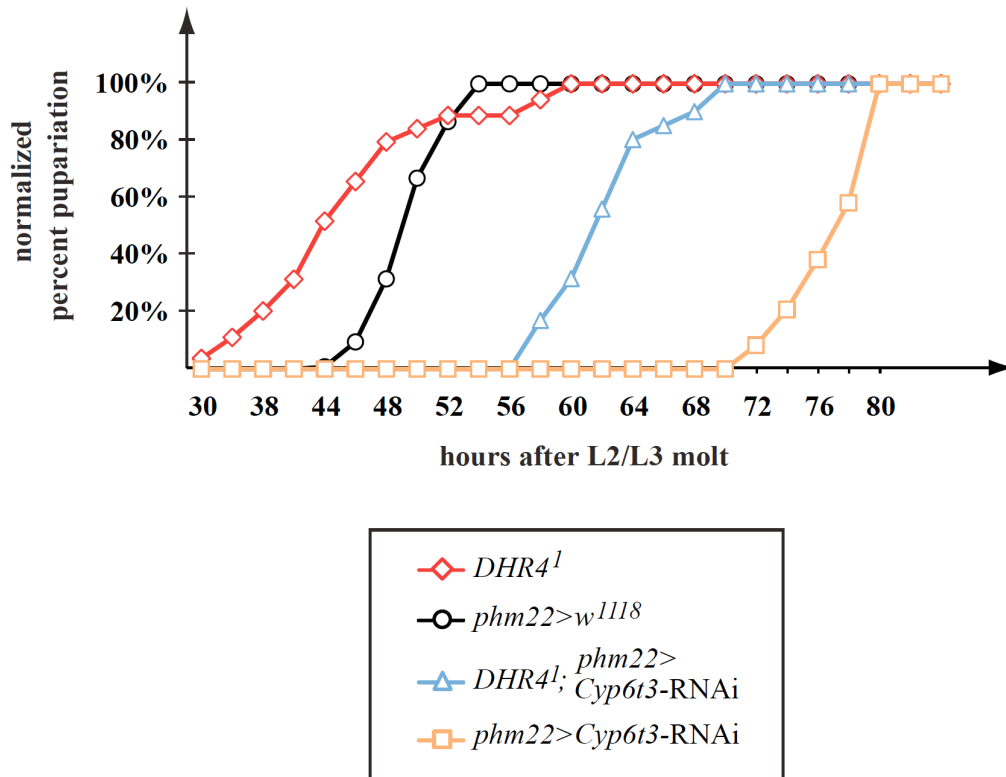


Figure 2.22. *Cyp6t3* is required for the developmental acceleration of *DHR4*¹ mutants.

Genetic epistasis analysis examining the timing of pupariation in animals carrying a *DHR4*¹ mutation, *phm22>Cyp6t3-RNAi* transgenes, or both. Percentages were normalized to the final number of pupae for each genotype, and represent the fraction of larvae that formed pupae at a given time point. *DHR4*¹ mutant (red, N=54), *phm22>w*¹¹¹⁸ (black, N=180), *phm22>Cyp6t3-RNAi* (orange, N=600), and *DHR4*¹; *phm22>Cyp6t3-RNAi* (blue, N=107).

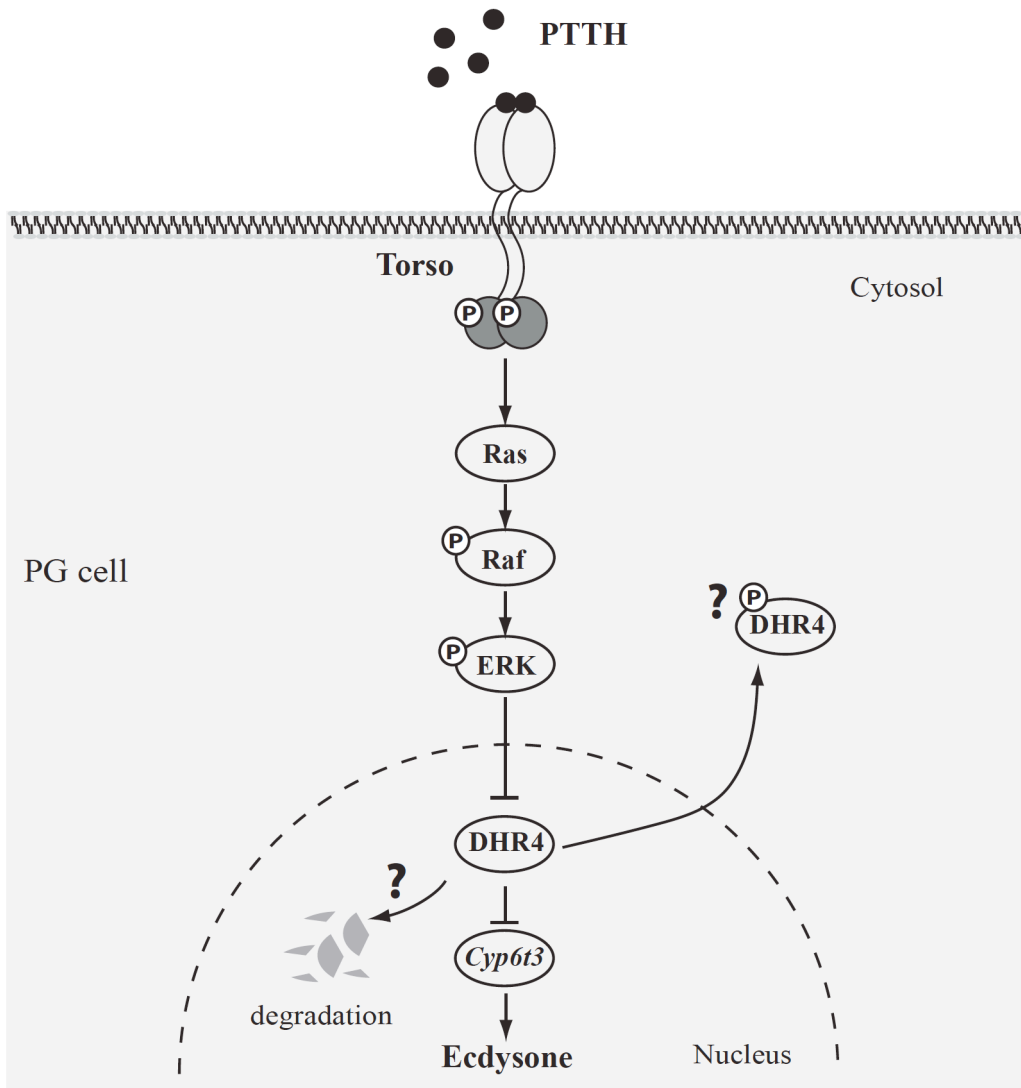


Figure 2.23. A model for DHR4 function.

DHR4 represses ecdysone pulses dependent on whether PTTH signaling is active or inactive. In the presence of PTTH signaling, DHR4 is removed from the PG nuclei either by shuttling to the cytoplasm or by protein degradation, which allows ecdysone biosynthesis to occur. When the PTTH pathway is inactive, DHR4 remains in the nucleus and represses *Cyp6t3* expression and possibly other uncharacterized genes with roles in ecdysone production, thereby lowering ecdysone titers.

DHR4 protein

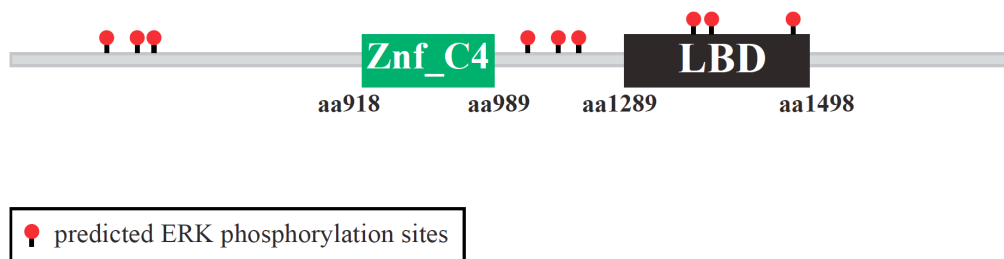


Figure 2.24. Prediction of ERK phosphorylation sites of DHR4 protein. DHR4 protein sequence was run through the NCBI program Simple Modular Architecture Research Tool (SMART) for the identification of the Znf-C4 region and LBD (Letunic et al., 2006). GPS 2.0 (Xue et al., 2008) was used to detect putative ERK phosphorylation sites of DHR4. Znf-C4, zinc finger C4-type. LBD, ligand binding domain. ERK, extracellular-signal-regulated kinase.

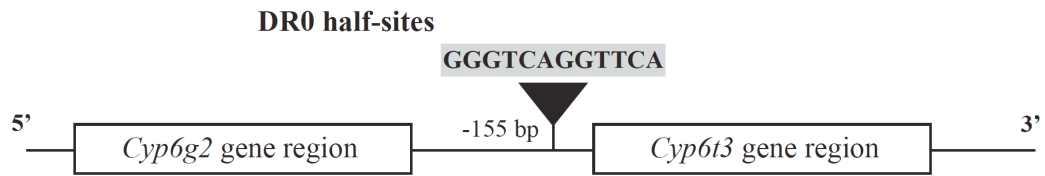


Figure 2.25. A predicted nuclear receptor response element that is located upstream of *Cyp6t3*. The program NHR Scan (Sandelin and Wasserman, 2005) was used to identify half-sites of the DR0 model that is present upstream of the *Cyp6t3* gene region.

2.8 Bibliography

- Ampleford, E.J., and Steel, C.G. (1985). Circadian control of a daily rhythm in hemolymph ecdysteroid titer in the insect *Rhodnius prolixus* (Hemiptera). *General and comparative endocrinology* *59*, 453-459.
- Andres, A.J., Fletcher, J.C., Karim, F.D., and Thummel, C.S. (1993). Molecular analysis of the initiation of insect metamorphosis: a comparative study of *Drosophila* ecdysteroid-regulated transcription. *Developmental biology* *160*, 388-404.
- Andres, A.J., and Thummel, C.S. (1994). Methods for quantitative analysis of transcription in larvae and prepupae. *Methods Cell Biol* *44*, 565-573.
- Asha, H., Nagy, I., Kovacs, G., Stetson, D., Ando, I., and Dearolf, C.R. (2003). Analysis of Ras-induced overproliferation in *Drosophila* hemocytes. *Genetics* *163*, 203-215.
- Bialecki, M., Shilton, A., Fichtenberg, C., Seagraves, W.A., and Thummel, C.S. (2002). Loss of the ecdysteroid-inducible E75A orphan nuclear receptor uncouples molting from metamorphosis in *Drosophila*. *Developmental cell* *3*, 209-220.
- Biyasheva, A., Do, T.V., Lu, Y., Vaskova, M., and Andres, A.J. (2001). Glue secretion in the *Drosophila* salivary gland: a model for steroid-regulated exocytosis. *Developmental biology* *231*, 234-251.
- Blais, C., Dauphin-Villemant, C., Kovganko, N., Girault, J.P., Descoins, C., Jr., and Lafont, R. (1996). Evidence for the involvement of 3-oxo-delta 4 intermediates in ecdysteroid biosynthesis. *The Biochemical journal* *320 (Pt 2)*, 413-419.
- Bolstad, B.M., Irizarry, R.A., Astrand, M., and Speed, T.P. (2003). A comparison of normalization methods for high density oligonucleotide array data based on variance and bias. *Bioinformatics* *19*, 185-193.
- Brand, A.H., and Perrimon, N. (1993). Targeted gene expression as a means of altering cell fates and generating dominant phenotypes. *Development (Cambridge, England)* *118*, 401-415.
- Brummel, T., Abdollah, S., Haerry, T.E., Shimell, M.J., Merriam, J., Raftery, L., Wrana, J.L., and O'Connor, M.B. (1999). The *Drosophila* activin receptor baboon signals through dSmad2 and controls cell proliferation but not patterning during larval development. *Genes & development* *13*, 98-111.
- Bujold, M., Gopalakrishnan, A., Nally, E., and King-Jones, K. (2009). Nuclear receptor DHR96 acts as a sentinel for low cholesterol concentrations in *Drosophila melanogaster*. *Molecular and cellular biology* *30*, 793-805.
- Burtis, K.C., Thummel, C.S., Jones, C.W., Karim, F.D., and Hogness, D.S. (1990). The *Drosophila* 74EF early puff contains E74, a complex ecdysone-inducible gene that encodes two ets-related proteins. *Cell* *61*, 85-99.
- Caldwell, P.E., Walkiewicz, M., and Stern, M. (2005). Ras activity in the *Drosophila* prothoracic gland regulates body size and developmental rate via ecdysone release. *Curr Biol* *15*, 1785-1795.
- Chavez, V.M., Marques, G., Delbecque, J.P., Kobayashi, K., Hollingsworth, M., Burr, J., Natzle, J.E., and O'Connor, M.B. (2000). The *Drosophila* disembodied gene controls late embryonic morphogenesis and codes for a cytochrome P450 enzyme that regulates

- embryonic ecdysone levels. *Development (Cambridge, England)* *127*, 4115-4126.
- Chen, F., Cooney, A.J., Wang, Y., Law, S.W., and O'Malley, B.W. (1994). Cloning of a novel orphan receptor (GCNF) expressed during germ cell development. *Molecular endocrinology (Baltimore, Md)* *8*, 1434-1444.
- Chung, H., Sztal, T., Pasricha, S., Sridhar, M., Batterham, P., and Daborn, P.J. (2009). Characterization of *Drosophila melanogaster* cytochrome P450 genes. *Proceedings of the National Academy of Sciences of the United States of America* *106*, 5731-5736.
- Colombani, J., Bianchini, L., Layalle, S., Pondeville, E., Dauphin-Villemant, C., Antoniewski, C., Carre, C., Noselli, S., and Leopold, P. (2005). Antagonistic actions of ecdysone and insulins determine final size in *Drosophila*. *Science (New York, NY)* *310*, 667-670.
- Daborn, P.J., Lumb, C., Boey, A., Wong, W., Ffrench-Constant, R.H., and Batterham, P. (2007). Evaluating the insecticide resistance potential of eight *Drosophila melanogaster* cytochrome P450 genes by transgenic over-expression. *Insect biochemistry and molecular biology* *37*, 512-519.
- Davidowitz, G., D'Amico, L.J., and Nijhout, H.F. (2003). Critical weight in the development of insect body size. *Evolution & development* *5*, 188-197.
- Dietzl, G., Chen, D., Schnorrer, F., Su, K.C., Barinova, Y., Fellner, M., Gasser, B., Kinsey, K., Oppel, S., Scheiblauer, S., *et al.* (2007). A genome-wide transgenic RNAi library for conditional gene inactivation in *Drosophila*. *Nature* *448*, 151-156.
- Duffy, J.B. (2002). GAL4 system in *Drosophila*: a fly geneticist's Swiss army knife. *Genesis* *34*, 1-15.
- Garofalo, R.S. (2002). Genetic analysis of insulin signaling in *Drosophila*. *Trends in endocrinology and metabolism: TEM* *13*, 156-162.
- Gibbens, Y.Y., Warren, J.T., Gilbert, L.I., and O'Connor, M.B. (2011). Neuroendocrine regulation of *Drosophila* metamorphosis requires TGFbeta/Activin signaling. *Development (Cambridge, England)* *138*, 2693-2703.
- Gilbert, L.I. (2004). Halloween genes encode P450 enzymes that mediate steroid hormone biosynthesis in *Drosophila melanogaster*. *Molecular and cellular endocrinology* *215*, 1-10.
- Gilbert, L.I., Rybczynski, R., and Warren, J.T. (2002). Control and biochemical nature of the ecdysteroidogenic pathway. *Annual review of entomology* *47*, 883-916.
- Hansson, L., and Lambertsson, A. (1983). The role of su (f) gene function and ecdysterone in transcription of glue polypeptide mRNAs in *Drosophila melanogaster*. *Molecular and General Genetics MGG* *192*, 395-401.
- Hansson, L., and Lambertsson, A. (1989). Steroid regulation of glue protein genes in *Drosophila melanogaster*. *Hereditas* *110*, 61-67.
- Hansson, L., Lineruth, K., and Lambertsson, A. (1981). Effect of the l (1) su (f) ts67g mutation of *Drosophila melanogaster* on glue protein synthesis. *Roux's Archives of Developmental Biology* *190*, 308-312.
- Hentschke, M., Kurth, I., Borgmeyer, U., and Hubner, C.A. (2006). Germ cell nuclear factor is a repressor of CRIPTO-1 and CRIPTO-3. *The Journal of biological chemistry* *281*,

33497-33504.

- Hietakangas, V., and Cohen, S.M. (2009). Regulation of tissue growth through nutrient sensing. *Annu Rev Genet* 43, 389-410.
- Ishizaki, H., and Suzuki, A. (1994). The brain secretory peptides that control moulting and metamorphosis of the silkworm, *Bombyx mori*. *The International journal of developmental biology* 38, 301-310.
- Janning, W. (1997). FlyView, a *Drosophila* image database, and other *Drosophila* databases. *Seminars in cell & developmental biology* 8, 469-475.
- Karim, F.D., and Thummel, C.S. (1991). Ecdysone coordinates the timing and amounts of E74A and E74B transcription in *Drosophila*. *Genes & development* 5, 1067-1079.
- Kataoka, H., Nagasawa, H., Isogai, A., Ishizaki, H., and Suzuki, A. (1991). Prothoracicotropic hormone of the silkworm, *Bombyx mori*: amino acid sequence and dimeric structure. *Agricultural and biological chemistry* 55, 73-86.
- Kavanagh, K.L., Jornvall, H., Persson, B., and Oppermann, U. (2008). Medium- and short-chain dehydrogenase/reductase gene and protein families : the SDR superfamily: functional and structural diversity within a family of metabolic and regulatory enzymes. *Cell Mol Life Sci* 65, 3895-3906.
- Kawakami, A., Kataoka, H., Oka, T., Mizoguchi, A., Kimura-Kawakami, M., Adachi, T., Iwami, M., Nagasawa, H., Suzuki, A., and Ishizaki, H. (1990). Molecular cloning of the *Bombyx mori* prothoracicotropic hormone. *Science (New York, NY)* 247, 1333-1335.
- King-Jones, K., Charles, J.P., Lam, G., and Thummel, C.S. (2005). The ecdysone-induced DHR4 orphan nuclear receptor coordinates growth and maturation in *Drosophila*. *Cell* 121, 773-784.
- King-Jones, K., and Thummel, C.S. (2005). Nuclear receptors--a perspective from *Drosophila*. *Nature reviews* 6, 311-323.
- Kiriishi, S., Nagasawa, H., Kataoka, H., Suzuki, A., and Sakurai, S. (1992). Comparison of the in vivo and in vitro effects of bombyxin and prothoracicotropic hormone on prothoracic glands of the silkworm, *Bombyx mori*. *Zool Sci* 9, 149-155.
- Klingler, M., Erdelyi, M., Szabad, J., and Nusslein-Volhard, C. (1988). Function of torso in determining the terminal anlagen of the *Drosophila* embryo. *Nature* 335, 275-277.
- Lederer, F. (1994). The cytochrome b5-fold: an adaptable module. *Biochimie* 76, 674-692.
- Lehmann, M. (1996). *Drosophila* Sgs genes: stage and tissue specificity of hormone responsiveness. *Bioessays* 18, 47-54.
- Letunic, I., Copley, R.R., Pils, B., Pinkert, S., Schultz, J., and Bork, P. (2006). SMART 5: domains in the context of genomes and networks. *Nucleic acids research* 34, D257-260.
- Li, W.X. (2005). Functions and mechanisms of receptor tyrosine kinase Torso signaling: lessons from *Drosophila* embryonic terminal development. *Dev Dyn* 232, 656-672.
- Lin, J.L., and Gu, S.H. (2007). In vitro and in vivo stimulation of extracellular signal-regulated kinase (ERK) by the prothoracicotropic hormone in prothoracic gland cells and its developmental regulation in the silkworm, *Bombyx mori*. *Journal of insect physiology* 53, 622-631.

- Lin, J.L., and Gu, S.H. (2011). Prothoracicotrophic hormone induces tyrosine phosphorylation in prothoracic glands of the silkworm, *Bombyx mori*. *Archives of insect biochemistry and physiology* 76, 144-155.
- Livak, K.J., and Schmittgen, T.D. (2001). Analysis of relative gene expression data using real-time quantitative PCR and the 2(-Delta Delta C(T)) Method. *Methods* 25, 402-408.
- Mangelsdorf, D.J., Thummel, C., Beato, M., Herrlich, P., Schutz, G., Umesono, K., Blumberg, B., Kastner, P., Mark, M., Chambon, P., *et al.* (1995). The nuclear receptor superfamily: the second decade. *Cell* 83, 835-839.
- Maroni, G.a.S., C (1983). Use of blue food to select synchronous late third instar larvae. *Drosophila Information Service* 59, 142-143.
- McBrayer, Z., Ono, H., Shimell, M., Parvy, J.P., Beckstead, R.B., Warren, J.T., Thummel, C.S., Dauphin-Villemant, C., Gilbert, L.I., and O'Connor, M.B. (2007). Prothoracicotrophic hormone regulates developmental timing and body size in *Drosophila*. *Developmental cell* 13, 857-871.
- Mirth, C., Truman, J.W., and Riddiford, L.M. (2005). The role of the prothoracic gland in determining critical weight for metamorphosis in *Drosophila melanogaster*. *Curr Biol* 15, 1796-1807.
- Nagasawa, H., Kataoka, H., Isogai, A., Tamura, S., Suzuki, A., Mizoguchi, A., Fujiwara, Y., Takahashi, S.Y., and Ishizaki, H. (1986). Amino acid sequence of a prothoracicotrophic hormone of the silkworm *Bombyx mori*. *Proceedings of the National Academy of Sciences of the United States of America* 83, 5840-5843.
- Nijhout, H.F. (1975). A threshold size for metamorphosis in the tobacco hornworm, *Manduca sexta* (L.). *Biol Bull* 149, 214-225.
- Niwa, R., Namiki, T., Ito, K., Shimada-Niwa, Y., Kiuchi, M., Kawaoka, S., Kayukawa, T., Banno, Y., Fujimoto, Y., Shigenobu, S., *et al.* (2010). Non-molting glossy/shroud encodes a short-chain dehydrogenase/reductase that functions in the 'Black Box' of the ecdysteroid biosynthesis pathway. *Development (Cambridge, England)* 137, 1991-1999.
- Niwa, R., Sakudoh, T., Namiki, T., Saida, K., Fujimoto, Y., and Kataoka, H. (2005). The ecdysteroidogenic P450 Cyp302a1/disembodied from the silkworm, *Bombyx mori*, is transcriptionally regulated by prothoracicotrophic hormone. *Insect molecular biology* 14, 563-571.
- Nusslein-Volhard, C., and Wieschaus, E. (1980). Mutations affecting segment number and polarity in *Drosophila*. *Nature* 287, 795-801.
- O'Connor, M. (2011). Abstract: Vesicle mediated secretion of ecdysone from the *Drosophila* prothoracic gland. In *NASCE 2011: The inaugural meeting of the North American Society for Comparative Endocrinology*.
- Oldham, S., and Hafén, E. (2003). Insulin/IGF and target of rapamycin signaling: a TOR de force in growth control. *Trends in cell biology* 13, 79-85.
- Ono, H., Rewitz, K.F., Shinoda, T., Itoyama, K., Petryk, A., Rybczynski, R., Jarcho, M., Warren, J.T., Marques, G., Shimell, M.J., *et al.* (2006). Spook and Spookier code for stage-specific components of the ecdysone biosynthetic pathway in Diptera.

- Developmental biology 298, 555-570.
- Petryk, A., Warren, J.T., Marques, G., Jarcho, M.P., Gilbert, L.I., Kahler, J., Parvy, J.P., Li, Y., Dauphin-Villemant, C., and O'Connor, M.B. (2003). Shade is the *Drosophila* P450 enzyme that mediates the hydroxylation of ecdysone to the steroid insect molting hormone 20-hydroxyecdysone. *Proceedings of the National Academy of Sciences of the United States of America* 100, 13773-13778.
- Rajkovic, M., Middendorff, R., Wetzel, M.G., Frkovic, D., Damerow, S., Seitz, H.J., and Weitzel, J.M. (2004). Germ cell nuclear factor relieves cAMP-response element modulator tau-mediated activation of the testis-specific promoter of human mitochondrial glycerol-3-phosphate dehydrogenase. *The Journal of biological chemistry* 279, 52493-52499.
- Rastinejad, F., Perlmann, T., Evans, R.M., and Sigler, P.B. (1995). Structural determinants of nuclear receptor assembly on DNA direct repeats. *Nature* 375, 203-211.
- Renn, S.C., Park, J.H., Rosbash, M., Hall, J.C., and Taghert, P.H. (1999). A pdf neuropeptide gene mutation and ablation of PDF neurons each cause severe abnormalities of behavioral circadian rhythms in *Drosophila*. *Cell* 99, 791-802.
- Rewitz, K.F., Larsen, M.R., Lobner-Olesen, A., Rybczynski, R., O'Connor, M.B., and Gilbert, L.I. (2009a). A phosphoproteomics approach to elucidate neuropeptide signal transduction controlling insect metamorphosis. *Insect biochemistry and molecular biology* 39, 475-483.
- Rewitz, K.F., Yamanaka, N., Gilbert, L.I., and O'Connor, M.B. (2009b). The insect neuropeptide PTHH activates receptor tyrosine kinase torso to initiate metamorphosis. *Science (New York, NY)* 326, 1403-1405.
- Riddiford, L.M. (1993). Hormone receptors and the regulation of insect metamorphosis. *Receptor* 3, 203-209.
- Rubin, G.M., and Spradling, A.C. (1982). Genetic transformation of *Drosophila* with transposable element vectors. *Science (New York, NY)* 218, 348-353.
- Rybczynski, R., Bell, S.C., and Gilbert, L.I. (2001). Activation of an extracellular signal-regulated kinase (ERK) by the insect prothoracicotropic hormone. *Molecular and cellular endocrinology* 184, 1-11.
- Sandelin, A., and Wasserman, W.W. (2005). Prediction of nuclear hormone receptor response elements. *Molecular endocrinology (Baltimore, Md)* 19, 595-606.
- Sliter, T.J., and Gilbert, L.I. (1992). Developmental arrest and ecdysteroid deficiency resulting from mutations at the *dre4* locus of *Drosophila*. *Genetics* 130, 555-568.
- Sokolowski, M.B. (2001). *Drosophila*: genetics meets behaviour. *Nature reviews* 2, 879-890.
- Song, Q., and Gilbert, L.I. (1995). Multiple phosphorylation of ribosomal protein S6 and specific protein synthesis are required for prothoracicotropic hormone-stimulated ecdysteroid biosynthesis in the prothoracic glands of *Manduca sexta*. *Insect biochemistry and molecular biology* 25, 591-602.
- Song, Q., and Gilbert, L.I. (1997). Molecular cloning, developmental expression, and phosphorylation of ribosomal protein S6 in the endocrine gland responsible for insect

- molting. *The Journal of biological chemistry* 272, 4429-4435.
- Spradling, A.C., and Rubin, G.M. (1982). Transposition of cloned P elements into *Drosophila* germ line chromosomes. *Science (New York, NY)* 218, 341-347.
- Sprenger, F., Stevens, L.M., and Nusslein-Volhard, C. (1989). The *Drosophila* gene torso encodes a putative receptor tyrosine kinase. *Nature* 338, 478-483.
- Strecker, T.R., Yip, M.L., and Lipshitz, H.D. (1991). Zygotic genes that mediate torso receptor tyrosine kinase functions in the *Drosophila melanogaster* embryo. *Proceedings of the National Academy of Sciences of the United States of America* 88, 5824-5828.
- Terasawa, E., and Fernandez, D.L. (2001). Neurobiological mechanisms of the onset of puberty in primates. *Endocrine reviews* 22, 111-151.
- Vafopoulou, X., and Steel, C.G. (1996a). Circadian regulation of a daily rhythm of release of prothoracicotropic hormone from the brain retrocerebral complex of *Rhodnius prolixus* (hemiptera) during larval-adult development. *General and comparative endocrinology* 102, 123-129.
- Vafopoulou, X., and Steel, C.G. (1996b). The insect neuropeptide prothoracicotropic hormone is released with a daily rhythm: re-evaluation of its role in development. *Proceedings of the National Academy of Sciences of the United States of America* 93, 3368-3372.
- Venkatesh, K., and Hasan, G. (1997). Disruption of the IP3 receptor gene of *Drosophila* affects larval metamorphosis and ecdysone release. *Curr Biol* 7, 500-509.
- Venken, K.J., Schulze, K.L., Haelterman, N.A., Pan, H., He, Y., Evans-Holm, M., Carlson, J.W., Levis, R.W., Spradling, A.C., Hoskins, R.A., *et al.* (2011). MiMIC: a highly versatile transposon insertion resource for engineering *Drosophila melanogaster* genes. *Nat Methods* 8, 737-743.
- Warren, J.T., Petryk, A., Marques, G., Jarcho, M., Parvy, J.P., Dauphin-Villemant, C., O'Connor, M.B., and Gilbert, L.I. (2002). Molecular and biochemical characterization of two P450 enzymes in the ecdysteroidogenic pathway of *Drosophila melanogaster*. *Proceedings of the National Academy of Sciences of the United States of America* 99, 11043-11048.
- Warren, J.T., Petryk, A., Marques, G., Parvy, J.P., Shinoda, T., Itoyama, K., Kobayashi, J., Jarcho, M., Li, Y., O'Connor, M.B., *et al.* (2004). Phantom encodes the 25-hydroxylase of *Drosophila melanogaster* and *Bombyx mori*: a P450 enzyme critical in ecdysone biosynthesis. *Insect biochemistry and molecular biology* 34, 991-1010.
- Warren, J.T., Yerushalmi, Y., Shimell, M.J., O'Connor, M.B., Restifo, L.L., and Gilbert, L.I. (2006). Discrete pulses of molting hormone, 20-hydroxyecdysone, during late larval development of *Drosophila melanogaster*: correlations with changes in gene activity. *Dev Dyn* 235, 315-326.
- Westbrook, A.L., and Bollenbacher, W.E. (1990). The development of identified neurosecretory cells in the tobacco hornworm, *Manduca sexta*. *Developmental biology* 140, 291-299.
- Xue, Y., Ren, J., Gao, X., Jin, C., Wen, L., and Yao, X. (2008). GPS 2.0, a tool to predict kinase-specific phosphorylation sites in hierarchy. *Mol Cell Proteomics* 7, 1598-1608.
- Yamanaka, N., Honda, N., Osato, N., Niwa, R., Mizoguchi, A., and Kataoka, H. (2007). Differential regulation of ecdysteroidogenic P450 gene expression in the silkworm,

- Bombyx mori*. *Bioscience, biotechnology, and biochemistry* 71, 2808-2814.
- Yan, Z.H., Medvedev, A., Hirose, T., Gotoh, H., and Jetten, A.M. (1997). Characterization of the response element and DNA binding properties of the nuclear orphan receptor germ cell nuclear factor/retinoid receptor-related testis-associated receptor. *The Journal of biological chemistry* 272, 10565-10572.
- Yoon, S., and Seger, R. (2006). The extracellular signal-regulated kinase: multiple substrates regulate diverse cellular functions. *Growth Factors* 24, 21-44.
- Yoshiyama, T., Namiki, T., Mita, K., Kataoka, H., and Niwa, R. (2006). Neverland is an evolutionally conserved Rieske-domain protein that is essential for ecdysone synthesis and insect growth. *Development (Cambridge, England)* 133, 2565-2574.

Chapter 3

Transcriptome and functional analysis of the *Drosophila* ring gland in
controlling steroid hormone synthesis

3.1 Introduction

3.1.1 Signaling pathways underlying the regulation of ecdysteroidogenesis in the *Drosophila* ring gland

The *Drosophila* ring gland is an emerging model for studying how steroid hormone production and release are regulated by developmental and environmental inputs. During *Drosophila* development, the prothoracic gland (part of the ring gland) produces periodic pulses of the steroid hormone ecdysone, which controls all major developmental transitions, such as the molts and metamorphosis (see **Figure 2.1B**) (Riddiford, 1993). The molecular actions of 20E through its cognate receptor, a dimer of the nuclear receptors EcR and Usp, have been studied in great detail (Koelle et al., 1991; Thomas et al., 1993; Yao et al., 1993) (see **Figure 1.2**). These studies have established *Drosophila* as a model for analyzing steroid hormone action in a developmental context, however, comparatively few studies have investigated how steroid hormone pulses are regulated themselves. Over recent decades, some essential mechanisms and pathways have been uncovered in regulation of ecdysteroidogenesis in the *Drosophila* ring gland, but a comprehensive understanding of the endocrine functions of this critical tissue is still lacking.

Our current understanding of ecdysteroidogenesis is based on two cornerstones: The PTTH signaling pathway and the enzymes involved in ecdysone biosynthesis. The ecdysone biosynthetic genes appear to be the best-known players in the ecdysteroidogenic pathway, which encode enzymes that convert dietary cholesterol to the active hormone 20E (Gilbert, 2004; Gilbert et al., 2002) (see **Figure 2.2**). In particular, *neverland*, encoding a Rieske electron oxygenase-like protein, is required for the first step of ecdysone biosynthesis converting cholesterol into 7-dehydrocholesterol (Yoshiyama et al., 2006). The Halloween genes, including *phantom*, *disembodied*, *shadow* and *shade*, encode

the cytochrome P450 hydroxylases that are responsible for the last four steps in the formation of 20E (Chavez et al., 2000; Niwa et al., 2005; Nusslein-Volhard and Wieschaus, 1980; Petryk et al., 2003; Warren et al., 2002; Warren et al., 2004). However, the intermediate steps that convert 7-dehydrocholesterol to 5 β -ketodiol, which are commonly referred to as the ‘Black Box’ (Gilbert, 2004), and the enzymes involved remain poorly understood. A few genes have been shown to function in the ‘Black Box’, including *shroud*, which encodes a short-chain dehydrogenase/reductase (SDR) (Kavanagh et al., 2008; Niwa et al., 2010), *spookier* (Ono et al., 2006) and *Cyp6t3* (Ou et al., 2011), which both encode cytochrome P450 enzymes.

It has long been known that a small brain-derived peptide, PTTH, stimulates the production and release of ecdysone. Recent studies have demonstrated that PTTH triggers ecdysone synthesis by signaling through a MAPK pathway via binding to its receptor Torso (Rewitz et al., 2009) (**Figure 3.1**). Specifically, upon PTTH binding, Torso activates a small GTPase, Ras, which in turn triggers Raf/MAPK phosphorylation, and ultimately, impinging on ecdysone production by upregulating ecdysone biosynthetic enzymes, such as Disembodied and Spookier. Furthermore, my work has shown that the nuclear receptor DHR4 serves as a readout of the PTTH pathway in repressing ecdysone synthesis (Ou et al., 2011) (see Chapter 2). These studies have greatly advanced our understanding on PTTH-stimulated ecdysone production, but relatively little is known about other downstream targets of the PTTH signaling pathway.

In addition to the PTTH pathway, insulin/insulin-like growth factor (IGF) signaling (IIS), a well studied regulator of tissue growth in *Drosophila*, has also been demonstrated to be important for PG function (Colombani et al., 2005; Garofalo, 2002; Hietakangas and Cohen, 2009; Oldham and Hafen, 2003) (**Figure 3.1**). It was shown that suppressing PG growth by attenuating PI3K activity

produced large larvae and adults with substantial developmental delays (Mirth et al., 2005). The same report also proposed that IIS provides the competence of the PG to respond to other developmental cues like PTTH when sufficient nutrients have been obtained. This finding supports the notion that PG cells have to integrate multiple signals including IIS to launch pupariation on time. More interestingly, insulin was shown to be capable of triggering ecdysone production, although not as dramatically as PTTH does (Kiriishi et al., 1992). This observation is reminiscent of the historical fact that the first “prothoracicotropic hormone” isolated from a lepidopteran species is an insulin-related peptide (Ishizaki and Suzuki, 1994; Nagasawa et al., 1986), and is at least partly explained by potential crosstalk with the MAPK signaling cascade (Kim et al., 2004; Kwon et al., 2002). It will be of interest to examine how the IIS and PTTH signaling pathways regulate each other in the *Drosophila* prothoracic gland.

More recently, several new pathways and components have been discovered to be participating in regulating ecdysteroidogenesis. For instance, Gibbens et al. (2011) demonstrated that TGF β /Activin signaling regulates developmental transitions through modulating ecdysone production in the *Drosophila* prothoracic gland (Gibbens et al., 2011; Schmierer and Hill, 2007) (**Figure 3.1**). Specifically, knocking down *dSmad2*, the core downstream mediator of TGF β /Activin signaling (Brummel et al., 1999), specifically in the prothoracic gland via RNAi results in developmental arrest during the third instar, and this defect can be rescued by 20E feeding. Knocking down other key components of the TGF β /Activin pathway gave rise to the same non-pupariating phenotype, suggesting that the TGF β /Activin signaling is required for appropriately timing the onset of metamorphosis. In the same report, it was shown that transcripts levels of *Torso* and *InR* are dramatically reduced when *dSmad2* is silenced (Gibbens et al., 2011). Moreover, two ecdysone biosynthetic genes,

disembodied and *spookier*, are both severely downregulated in the *dSmad2*-RNAi ring gland. However, it remains unclear whether *disembodied* and *spookier* are direct transcriptional targets of dSmad2. Together, these results suggest that the TGF β /Activin pathway plays a critical role in ecdysteroidogenesis through controlling the competence of the prothoracic gland to respond to metamorphic factors, PTHH and insulin-like peptides.

Furthermore, a recent report by Caceres et al. (2011) showed that nitric oxide (NO) plays a key role in the production of ecdysone, which comes undoubtedly as a surprise (Caceres et al., 2011). In brief, it was shown that NO signaling is required for ecdysone synthesis by regulating the interaction of DHR3 and E75 to control the transcriptional activation of *β ftz-f1* (King-Jones and Thummel, 2005) (**Figure 3.1**, also see **Figure 1.2**). β FTZ-F1 was previously demonstrated to be a key regulator of ecdysone biosynthesis via controlling the expression of the ecdysteroidogenic enzymes, Disembodied and Phantom (Parvy et al., 2005). However, it remains unclear whether the knockdown of *NOS*, which encodes the *Drosophila* nitric oxide synthase, ultimately abolishes the expression of *disembodied* and *phantom*. Together, these findings have given us some important insight into the dynamic network governing ecdysteroidogenesis in the *Drosophila* prothoracic gland, but other aspects of ecdysteroidogenic control and their mediators remain to be elucidated.

3.1.2 Previous attempts at the identification of novel components of ecdysteroidogenesis

Over the years, researchers have attempted different means to explore the molecular basis underlying the regulation of ecdysone synthesis and the endocrine functions of the ring gland. Among these approaches, identifying genes with key functions in this tissue appears to be a major strategy. For instance, Harvie et al.

(1998) identified 76 genes that are expressed in the *Drosophila* ring gland during development by using an enhancer-trap approach (Bellen et al., 1989; Grossniklaus et al., 1989; Harvie et al., 1998; O'Kane and Gehring, 1987; Wilson et al., 1989). In brief, 510 different lethal $P\{PZ\}$ element insertions were screened to detect those with a reporter gene expressed in part or the entirety of the ring gland (Adams and Sekelsky, 2002; Mlodzik and Hiromi, 1992). Further analysis revealed 9 out of these 76 genes as strong candidates for playing an important role in endocrine functions controlling development. These candidate genes were suggested to encode signaling components downstream of the PTTH pathway, such as protein kinase A and calmodulin (Gilbert et al., 1988; Lane and Kalderon, 1993), the translational elongation factor EF-1 α F₁ (Hovemann et al., 1988), *couch potato*, which encodes an RNA-binding protein (Bellen et al., 1992), *tramtrack* which encodes a transcription factor (Giesen et al., 1997), *expanded* which is important for the control of cell proliferation in imaginal discs (Boedigheimer et al., 1993; Boedigheimer and Laughon, 1993), the C subunit of vacuolar ATPase (V-ATPase) which is important for synaptic vesicle formation and neurosecretion (van Hille et al., 1993), and two other less well characterized genes. This report not only showed that the enhancer trap approach can be a useful strategy to explore tissue-specific genetic functions in *Drosophila*, but also broadened our knowledge on genes involved in the signaling or biosynthetic pathways required for the development of the ring gland. While none of these 9 genes was recovered in this study, which has identified 233 ring gland-specific transcripts (>10fold enrichment) using microarrays, one major reason is that these genes may have housekeeping functions and have limited specificity to the ring gland. In addition, a notable problem with this enhancer trap-based approach is that the reporter construct may detect only a subset of the regulatory elements controlling nearby genes, indicating that this set of 76 genes only reflects a small fraction of genes

expressed in the ring gland.

More recently, the Kataoka research group used cDNA microarrays to examine the expression of 86 predicted *Drosophila melanogaster* cytochrome P450 genes in the ring gland in comparison with that in the brain-ventral nerve cord designated as the central nervous system (CNS) isolated from wandering third instar larvae (Niwa et al., 2011). This report revealed 7 cDNAs showing a >2fold increase in expression in the ring gland compared to that in the CNS. These seven cDNAs include *phantom*, *disembodied*, *shadow*, and *Cyp6g2*, which were previously known to be predominantly expressed in the ring gland (Chavez et al., 2000; Chung et al., 2009; Warren et al., 2004), and 3 other previously uncharacterized cytochrome P450 genes, *Cyp4g1*, *Cyp12e1*, and *Cyp310a1*. More importantly, it was also shown in the report that the expression of the silkworm *Bombyx mori* homolog of *Cyp4g1* is rapidly and drastically induced in cultured prothoracic glands when treated with *Bombyx* recombinant PTTH (rPTTH), implying that *Cyp4g1* may serve as a downstream target of the PTTH pathway (Ishibashi et al., 1994; Niwa et al., 2011). In addition, the *Drosophila Cyp4g1* mutant exhibits a pupal lethal phenotype (Gutierrez et al., 2007), but it remains unclear whether this is owing to a defect of ecdysone biosynthesis caused by loss of *Cyp4g1* in the PG. These data demonstrated that microarray analysis of differential gene expression in the ring gland and other tissues represents a valuable means to identify novel components required for the development of the ring gland. However, the information here is quite limiting due to a limited focus only on the *Drosophila* cytochrome P450 genes during the wandering stage of the third instar.

3.1.3 Outline

Aiming to systemically identify new components of the ecdysteroidogenic

pathway and key players of other aspects of the endocrine function of the ring gland, I utilized whole-genome microarrays to determine the difference of gene expression between the ring gland and the whole larva in wild type at four time points during the last larval stage of *Drosophila* development (**Figure 3.2**). This approach first enables one to identify ring gland-enriched transcripts at each time point. Furthermore, it presents me with general temporal trends of gene expression pattern in the ring gland of L3 larvae, which would gain insight into when genes-of-interest come into play in the ring gland. In addition to the wild type microarrays, I also performed a series of microarrays on the ring gland isolated from animals expressing a constitutively active Ras (Ras^{V12}) or those expressing *Torso*-RNAi at two developmental times, a low-PTTH phase and a high-PTTH phase, respectively (McBrayer et al., 2007; Rewitz et al., 2009) (**Figure 3.3**). This approach enabled me to identify genes with expression dependent on PTTH signaling. For instance, one could first identify a set of genes whose expression changes from a low-PTTH phase to a high-PTTH phase in the control background. This would imply that the expression of these genes relies on PTTH signaling. I can further test to see if their expression profiles are affected when PTTH signaling is altered in *Torso*-RNAi and Ras^{V12} animals. Thus, it would serve as a means to identify the downstream targets of the PTTH signaling cascade.

Ultimately, I also performed high-throughput qPCR to examine the expression profiles of 25 selected genes, this including transcription factors, cytochrome P450 genes and other known players of the regulation of ecdysone synthesis, in the brain-ring gland complex (BRRG) from carefully staged animals in a 4-hr interval throughout the larval third instar. This data allowed me to detect any oscillatory behaviors regarding the expression of these 25 transcripts during the L3. Taking advantage of this, I can further examine gene transcription

underlying the regulation of low-titer ecdysone peaks. Together, by combining genomic approaches and functional characterization, I have aimed to identify novel players in the regulation of ecdysteroidogenesis in *Drosophila*, and key components of other aspects of the ring gland function during larval development as well.

3.2 Methods

***Drosophila* stocks and maintenance**

GAL4 drivers were obtained from labs indicated by the references. The prothoracic gland: *phm22-Gal4* and *UAS-Dicer2; phm22-Gal4*. The *corpus allatum*: *Aug21-Gal4/CyO*, *act-GFP*. The *corpora cardiaca*: *AKH-Gal4*. Fat body: *Cg-Gal4*. Ubiquitous GAL4 driver: *actin5C-Gal4/CyO*, *act-GFP*. *w¹¹¹⁸* (#3605) and *Sgs3-GFP* (#5884) were ordered from the Bloomington stock center. RNAi lines used in the PG-specific RNAi screen were obtained from the Vienna *Drosophila* Research Center. Flies were reared on standard agar-cornmeal medium at 25°C.

Ring-gland and whole-larva microarrays

Sample collection: For the **wild type ring gland** microarrays, *w¹¹¹⁸* populations were raised at 25°C until they were carefully staged at the L2/L3 molt. Ten ring glands of different developmental times as stated were dissected in ice-cold PBS, rinsed twice with fresh PBS, and immediately transferred to TRIzol reagent (Invitrogen) for RNA extraction later. The lysate was then vortexed for 5 sec at RT, flash-frozen, and stored immediately at -80°C. Similarly, for the **wild type whole larva** microarrays, *w¹¹¹⁸* populations were carefully staged at the L2/L3 molt, and larvae of different developmental ages as indicated were rinsed in distilled H₂O and flash-frozen in liquid nitrogen for RNA isolation later. For

the *UAS-Dicer; phm22>Ras^{V12}* and *UAS-Dicer; phm22>Torso-RNAi* microarrays, animals of all genotypes (including *UAS-Dicer; phm22>w¹¹¹⁸* controls) were first carefully staged at the L2/L3 molt, and reared on standard medium supplemented with 0.05% bromophenol blue to monitor the gut purging status for further development (Andres and Thummel, 1994; Maroni, 1983) (see Results 3.3.5). For the control *UAS-Dicer; phm22>w¹¹¹⁸*, larvae of 30-hr old after the molt (“blue gut”) and larvae of 40-hr old after the molt (“partial blue”) were dissected for the ring gland, designated -18 hr prior to puparium formation (hereafter refer to it as PPF) and -8 hr PPF, respectively (Andres and Thummel, 1994; Maroni, 1983). With respect to *UAS-Dicer; phm22>Torso-RNAi*, samples of 30-hr L3 (“blue gut”) are relative to the L2/L3 molt, designated -18 hr PPF. For *UAS-Dicer; phm22>Torso-RNAi* “partial blue” samples, individual larvae were removed from plates and checked for their gut purging status on day 4 and day 5 after the molt, larvae of partial blue gut were dissected for the ring gland, designated -8 hr PPF. With respect to *UAS-Dicer; phm22>Ras^{V12}*, larvae of 25-26-hr L3 (“blue gut”) and larvae of 33-36-hr L3 (“partial blue”) were dissected for the ring gland, designated -18 hr PPF and -8 hr PPF, respectively. 10 ring glands per sample were isolated and immediately transferred to TRIzol reagent for RNA extraction later.

Total RNA isolation: Total RNA from ring glands was isolated by the Ambion RNAqueous-Micro kit or the Qiagen RNeasy kit. RNA was then quantified by the RiboGreen Quanti Kit (Invitrogen), and RNA integrity was analyzed by Agilent Bioanalyzer Pico Chips. Total RNA of whole-larvae samples was extracted according to the standard TRIzol RNA extraction protocol (Invitrogen). RNA was then quantified by the NanoDrop spectrophotometer (Thermo), and RNA integrity was analyzed by Agilent Bioanalyzer Pico Chips.

RNA amplification and microarrays: Linear RNA amplification was based on the MessageAmpTM II RNA Amplification kit (Ambion): First-strand cDNA

synthesis was carried out by a T7-(dT) primer and ArrayScript reverse transcriptase using 50 ng RNA of each ring-gland sample and whole-larvae sample. Second-strand cDNA synthesis was performed according to the provided protocol (Ambion). Purified cDNA was then fed into the IVT reactions. The amplified RNA (aRNA) was column-purified and analyzed using Agilent RNA 6000 Nano Kit (Cat. No. 5067-1511) on an Agilent 2100 Bioanalyzer. 1 µg of aRNA was used for double-stranded cDNA synthesis (Invitrogen SuperScript One-Cycle cDNA Kit) and 1 µg of the purified cDNA was Cy3-labeled by Roche NimbleGen Cy3-labeled one-color cDNA labeling kit. From this, 4 µg of cDNA was hybridized on a NimbleGen *Drosophila melanogaster* Gene Expression 12X135K Array (Roche Applied Science). Each condition was analyzed by three independent biological samples. Chip hybridization and scanning was performed by the Alberta Transplant Applied Genomics Center. Raw data were normalized with the NimbleScan software (NimbleGen) using the RMA algorithm (Bolstad et al., 2003), and data were analyzed with Arraystar 4.0 (DNASTar) as well as Access (Microsoft).

Prothoracic gland-specific gene disruption via RNAi

A total of 120 RNAi lines for 108 ring gland-enriched transcripts were obtained from the Vienna *Drosophila* Research Center (**Table 3.2**). The *phm22-Gal4* driver was used in the prothoracic gland-specific RNAi screen (me and Dr. Adam Magico contributed equally to this screen). Eight homozygous *phm22-Gal4* virgin females were crossed to 5 or 6 males of a given RNAi stock. Three samples were tipped from the same cross, and reared at 25°C until scoring. Phenotypes were scored at several points during development, namely the L2/L3 molt (on day 3 after egg deposit [AED]), the onset of pupariation (on day 5 AED), and when eclosion would occur in controls (on day 10 AED), respectively.

phm22>w¹¹¹⁸ was used as a negative control, *phm22>ras^{V12}* and *phm22>Torso-RNAi* were used as positive controls. All crosses were maintained on standard agar-cornmeal medium at 25°C.

20E rescue experiments

20E (Cat. No. 7980-000) was purchased from Steraloids Inc. (Newport, USA). 20E stock of 10 mg/ml in absolute ethanol was stored at -20°C. Standard cornmeal-agar medium was supplemented with 0.33 mg/ml of the hormone, or an equivalent amount of ethanol (solvent). Specifically, 33 mg of 20E was dissolved in 3.3 ml of 100% ethanol, which was added to 100 ml of liquid standard agar-cornmeal media. The control food contains 3.3% ethanol without 20E. For the rescue experiment, embryos of different genotypes were collected in 2-hr intervals and reared on the 20E-supplemented medium or the control medium afterwards. *phm22>w¹¹¹⁸* was used as a control.

Time course analysis of gene expression by high-throughput qPCR (BioMark™ HD system, Fluidigm)

Fly entrainment and sample collection: *Sgs3-GFP* flies were first entrained under a 12hr light/dark cycle under 70% of relative air humidity at 25°C for 3 days (BINDER BD720, Germany). Embryos were collected in 2-hr intervals and immediately transferred to food during light cycle, and raised under the same condition until they were carefully staged at the L2/L3 molt. For time points later than 24-hr after the L2/L3 molt, staged *Sgs3-GFP* populations were re-synchronized at 24-hr L3 (absolute time relative to the L2/L3 molt). For this, individual animals were removed from the food and examined for the presence of salivary gland GFP by fluorescence stereomicroscopy. Larvae with 1/4 to 1/3 of salivary glands full of GFP were either collected for the 24-hr L3 time point or

transferred to food for further development until they were collected at time points as indicated (Biyasheva et al., 2001). This method was previously employed to precisely stage animals during the second half of the L3 for measuring ecdysteroid titers (Warren et al., 2006). The time of the formation of white prepupa was designated as the 48-hr L3 time point after the L2/L3 molt. 10 brain-ring glands were isolated per sample in ice-cold PBS, rinsed twice with fresh PBS, and immediately snap-frozen with 100 μ l of TRIzol in liquid nitrogen. Four samples were prepared per time point.

RNA isolation, cDNA synthesis and cDNA preamplification: Total RNA was isolated using the RNeasy mini kit (Qiagen) following the manufacturer's instructions. RNA concentration was measured by the NanoDrop 1000 spectrophotometer (Thermo Scientific), and RNA integrity was evaluated using Agilent RNA 6000 Nano Kit (Cat. No. 5067-1511) on an Agilent 2100 Bioanalyzer. Subsequently, cDNA synthesis (from 2 μ g of total RNA) was performed by the ABI High Capacity cDNA Synthesis kit (Cat. No. 4368814). For high-throughput qPCR (BioMark, Fluidigm), pre-amplification of cDNA was further carried out. For this, an equivalent of 5 ng of total RNA was used to amplify each cDNA sample with the TaqMan Pre-Amp 2X Master Mix (Applied Biosystems, Part No. 4384266) following the procedures suggested by Fluidigm.

Fluidigm BioMark high-throughput qPCR: High-throughput qPCR (9,216 reactions per run) was performed on preamplified cDNA samples and analyzed on 96.96 dynamic arrays (BioMark, Fluidigm). Sample mixtures were prepared according to the manufacturer's instructions using Fluidigm DA Sample Reagent, TaqMan Universal PCR Master Mix, and preamplified cDNA samples. Assay mixtures were prepared following the manufacturer's instructions using Fluidigm DA Assay Reagent in combination with Roche UPL probes and oligonucleotides (IDT). All primers along with corresponding probes are listed in **Table 3.4**.

Primer/probe mix selection was based on the Roche Universal ProbeLibrary Assay Design (Roche Applied Science) and pre-validated by conventional qPCR. The validation of each primer/probe mix follows: 0.125 μ l of cDNA (synthesized from 12.5 ng of *w¹¹¹⁸* L3 larval total RNA), 5 μ l of TaqMan Universal PCR Master Mix (Applied Biosystems, Part No. 4324018), 0.5 μ l of each primer/probe mix, and 4.375 μ l of nuclease-free H₂O (in a total of 10 μ l reaction). The high-throughput qPCR was run according to thermal-cycling parameters recommended by Applied Biosystems for the TaqMan Universal PCR Master Mix. Four samples were tested for each experimental condition, and each sample was tested in duplicate. Five housekeeping control genes were included per run: *CG7939* (ribosomal protein 49), *CG1913* (α Tubulin 84B), *CG3180* (RNA polymerase II 140-kDa subunit), *CG9282* (ribosomal protein L24), and *CG4898* (Tropomyosin 1). $\Delta\Delta C_T$ values were calculated individually for each control gene, and differential expression of a given gene was determined as the geometric mean of all 80 $\Delta\Delta C_T$ values (4 biological samples/given gene x 4 biological samples/control gene x 5 control genes=80 measurements).

RNA Probe synthesis

For *in situ* hybridization, antisense and sense RNA probes for genes of interest were made by *in vitro* transcription. PCR fragments amplified from genomic DNA were inserted into pBlueScript (SK+) cloning vectors. The cloning vectors containing each cDNA were linearized by restriction enzymes, EcoRV and XbaI. The linearized plasmids were purified by QIAquick spin column (Qiagen). DIG-labeled RNA probes were generated by *in vitro* transcription following the manufacturer's instructions (Roche DIG RNA Labeling Mix, #11 277 073 910). The linearized plasmid template (~1 μ g), 4 μ l of 5X transcription buffer, 2 μ l of 10X DIG RNA labeling mix, 2 μ l of T7 or T3 RNA polymerase,

and nuclease-free H₂O were added in a total reaction volume of 20 µl. The reaction was incubated at 37°C for 2 hr. After stopping the reaction by the addition of 1 µl of 0.5 M EDTA (pH8.0), the probe solution was precipitated with the help of 2 µl of 8M LiCl and 75 µl of absolute ethanol at -20°C overnight. After a 30 min centrifugation at max speed at 4°C, RNA probes were dissolved in nuclease-free H₂O. RNA was quantified by NanoDrop 1000 spectrophotometer (Thermo Scientific) and RNA integrity was analyzed by conventional agarose gel electrophoresis. Primers used to PCR-amplify genes of interest are listed in **Table 3.6**.

***in situ* RNA hybridization**

DIG-labeled RNA probes were generated by *in vitro* transcription following the manufacturer's instructions (Roche DIG RNA Labeling Mix, #11 277 073 910). L3 larval ring glands were dissected in ice-cold PBS and fixed in 4% paraformaldehyde for 20 min at RT. After treatment with 1% H₂O₂, samples were stored in hybridization buffer at -20°C. Samples were prehybridized in hybridization buffer for 3 hr at 58°C and RNA probes were denatured for 3 min at 80°C. Probe hybridization was performed for 16-18 hr (overnight) at 58°C, followed by extensive wash steps at 58°C. After cooling, tissues were blocked with PBTB buffer (2% NGS and 1% BSA) for 1 hr at RT before overnight incubation with mouse anti-Digoxin antibody (Jackson ImmunoResearch #200-062-156, 1:500 dilution) at 4°C. Tissues were then incubated with streptavidin-HRP conjugates (Molecular Probes #S991, 1:400 dilution) in PBTB for 1 hr at RT, followed by six wash steps (1 hr each) in PBTB at RT. Before TSA amplification, tissues were thoroughly washed in PBS. Tyramide reagents (PerkinElmer TSA Plus Cyanine 3 Kit, #NEL744001KT) were diluted 1:1000 in 100 µl of the amplification buffer provided by the kit. TSA reactions were

performed for 40 min at RT and washed 6 times for 1 hr in PBS at RT. Tissues were then mounted in the ProLong Gold antifade reagent (P36934, Invitrogen) and analyzed by confocal microscopy (Nikon AZ-C1 Confocal Microscope System).

3.3 Results

3.3.1 Gene expression profiling uncovers new genes with specific expression in the ring gland

An established procedure for identifying tissue-specific transcripts is to compare the expression of a gene in a given tissue to its average expression in the whole organism. This method has successfully been used by the “*Drosophila* gene expression ATLAS” project to detect genes with specific expression in a broad spectrum of larval and adult tissues, including midgut, CNS, salivary glands, and trachea (Chintapalli et al., 2007). However, the ring gland has not been analyzed in this manner, which is not only because it is technically challenging to dissect this very small tissue (44~48 cells), but also the low RNA yields from this tissue pose a problem for microarrays and RNA-Seq. Identifying genes that are specifically expressed in the ring gland enables us to define a set of candidate genes with potentially critical functions in this tissue, which will open the door for us to further dissect and better understand the role of the ring gland in *Drosophila* larval development.

Therefore, I analyzed four time points from L3 larvae, 4-hr, 8-hr, 24-hr and 36-hr after the L2/L3 molt (**Figure 3.2**). There are several reasons for this strategy: firstly, ring glands are bigger in L3 compared to earlier stages, which makes dissection much easier. Secondly, the L3 stage has three low-titer ecdysone peaks, while no such pulses have been reported for earlier stages, which allows us to correlate gene expression profiles to these peaks. Thirdly, L3 larvae can be

easily and precisely staged at the L2/L3 molt, allowing stringent synchronization of the population. As shown in **Figure 3.2A**, the four time points chosen for this analysis were 4-hr, 8-hr, 24-hr, and 36-hr after the L2/L3 molt, respectively. The first two time points are prior to the critical weight (around 12 hr L3), a checkpoint when the larva determines whether it has stored sufficient nutrients to survive metamorphosis (Davidowitz et al., 2003). The 24-hr L3 time point represents a feeding stage shortly after the second minor ecdysone peak (around 20 hr after the L2/L3 molt), and the 36-hr time point depicts the onset of wandering behavior that is likely stimulated by the third minor ecdysone peak (around 28 hr after the L2/L3 molt). To determine whether a gene was specifically expressed in the ring gland, I compared gene expression of the ring gland to that of the whole larva during each time point (**Figure 3.2B**). More specifically, I isolated RNA from both sources and carried out linear RNA amplification, which overcomes the limiting amount of RNA yields from the ring gland, followed by microarray analysis. I determined the signal ratio between ring gland and whole larva transcripts for each time point, and identified 233 transcripts representing 208 genes based on an enrichment of >10fold for at least one of the four time points ($P<0.01$) (**Figure 3.4**). 16 of the 208 genes were previously reported to have specific expression in the ring gland (**Figure 3.4A**, red type), demonstrating that our experimental approach is successful in identifying known players in the ring gland. For example, all known ecdysteroidogenic cytochrome P450 genes, *phantom*, *disembodied*, *shadow*, *spookier*, and *shroud*, are on this list (Chavez et al., 2000; Niwa et al., 2010; Ono et al., 2006; Warren et al., 2002; Warren et al., 2004). Other well-characterized genes with known expression in the ring gland, such as *Torso* (Rewitz et al., 2009), *nocturnin* (Gronke et al., 2009), *molting defective* (Neubueser et al., 2005), *NPC1a* (Huang et al., 2005), *Cyp6g2* (Chung et al., 2009), and *Akh* (Lee and Park, 2004) all display >10fold transcript enrichment.

A 10fold transcript enrichment represents a fairly stringent cutoff, as I find some genes with known specific expression in the ring gland to be excluded by this strategy. For instance, *Cyp6t3*, another known ecdysone biosynthetic gene (Ou et al., 2011) (**Table 3.5**), and *start1*, a putative sterol transporter (Roth et al., 2004), both missed the cutoff narrowly, as they are 9fold and 6fold enriched in the ring gland, respectively.

To test the 233 ring gland-enriched transcripts for statistically overrepresented categories such as “biological process”, “molecular function” and “InterPro” domains (Hunter et al., 2012), a program called Gostat (Beissbarth and Speed, 2004). As illustrated in **Table 3.1**, significant GO terms identified by Gostat are listed (the lower the *P*-value is, the more significant the term applies to a given category). As expected, the terms “oxidoreductases”, “hormone biosynthetic process”, and “sterol metabolic process” are highly significant, which is consistent with the observation that many known ecdysteroidogenic genes are specifically expressed in the ring gland. However, other terms were somewhat unexpected. In particular, the GO terms “signaling transduction” and “Receptor activity” are significantly overrepresented (**Table 3.1**), indicating that a wide range of signaling molecules and regulatory components participate in coordinating multiple biological processes in the ring gland. Interestingly, the “GO” term “Tube morphogenesis” shows moderate enrichment (**Table 3.1**), raising the possibility that genes with roles in making and shaping biological tubes, such as the trachea and heart, have uncharacterized functions in the ring gland. Ultimately, Gostat identifies “heat response” and “GPCR signaling pathway” as overrepresented because of an enrichment of genes from the HSP70 and GPCR families, respectively.

To further characterize the 233 ring gland-enriched transcripts, I manually grouped them into two major categories based on protein function. The first

category is represented by genes with **executive** functions, this includes all enzymes with metabolic roles, chaperones, and transport proteins. The other category is enriched with genes having **regulatory** roles, including transcription factors, hormone/growth factors, kinases, receptors, and other signaling components, which comprises 66 of the 233 transcripts with >10fold enrichment in the ring gland. These data corroborate the GOstat findings, suggesting that one can mine the data to identify novel signaling pathways that coordinate steroidogenic processes in the fly ring gland.

Closer examination of the “regulatory” category have revealed a subgroup which has a total of 13 transcripts encoding DNA-binding proteins, most of which are presumed to act as transcription factors. Among these, *molting defective (mld)* and *timeless (tim)* were already shown to have strong expression in the ring gland (Myers et al., 2003; Neubueser et al., 2005), and a third gene in this clan, *tinman*, has been linked to the embryonic development of the *corpora cardiaca* (Park et al., 2011), but no expression of *tinman* has been reported in the larval ring gland. For *snail*, a well-studied C₂H₂ transcription factor necessary for embryonic development, is indirectly linked to the ring gland (Leptin, 1991). It was previously reported that the P-element insertion *P[Gal4]P0206*, which is commonly used to drive *Gal4* expression specifically in the ring gland, is localized to the upstream region of the *snail* gene (Janning, 1997; Suster and Bate, 2002; Zhou et al., 2004). Snail and Escargot, another C₂H₂ protein on this list, have redundant functions in wing imaginal discs. A previous study demonstrated that *snail* and *escargot* are co-expressed in embryonic and wing disc tissue and interact genetically (Fuse et al., 1996). It is therefore of interest that both *snail* and *escargot* appear on this list, raising the possibility that they play redundant roles in the ring gland as well. In addition, the DNA-binding protein with the highest transcript enrichment in the ring gland is a C₂H₂ zinc finger protein encoded by

CG11762 (Chung et al., 2002), exhibiting 40-70fold enrichment compared to the whole-larva signal. The function of *CG11762* remains poorly understood, while tissue-specific RNAi analysis of this gene has suggested an important role of *CG11762* in the ring gland (**Table 3.3**, also see Results 3.3.3). Similarly, *hand*, which encodes a helix-loop-helix protein, shows quite high transcript specificity of 24-62fold in the ring gland. Previous data showed that *hand* is highly expressed in the heart of the adult fly, and appears to act together with *tinman* to form the embryonic heart tube (Han and Olson, 2005). This finding raises an interesting question as to whether *hand* and *tinman* again work together in the ring gland. Finally, another transcription factor involved in tube formation on this list is ventral veinless (*vvl*), a POU/homeodomain protein. *vvl* was previously shown to have multiple functions in regulating the development of tracheal, central and peripheral nervous system (CNS and PNS) in *Drosophila* (Inbal et al., 2003; Llimargas and Casanova, 1997; Meier et al., 2006).

In the “Hormones and growth factors” subgroup, a total of 8 genes were identified. Among them, only *Akh*, a glucagon-like neuropeptide, was previously reported to be ring gland-specific. Specifically, *Akh* was shown to express exclusively in the *copora cardiaca* from late embryo to adult stages (Lee and Park, 2004). Interestingly, one of the peptide hormones, *Ryamide*, appears to act in an autocrine or paracrine manner, because its receptor, *NepYr*, is one of the 11 G protein-coupled receptors (GPCRs) with ring gland-specific expression (Ida et al., 2011). *ana* (*anachronism*) encodes a secreted glycoprotein that controls the timing of postembryonic neurogenesis (Ebens et al., 1993), and its expression was found to be under circadian control (Cirelli et al., 2005). The identification of *timeless* and *anachronism* as ring gland-enriched transcripts raises the question as to whether the ring gland harbors its own circadian clock in coordinating diverse processes. Finally, I also identified *spätzle5* as a ring gland-specific transcript

(discussed in detail in Chapter 4). Some members of the Spätzle peptide family, including *spätzle5*, are nerve growth factors collectively designated neurotrophins that promote neuronal survival, targeting, and synaptic plasticity in *Drosophila* embryogenesis (Zhu et al., 2008).

In the “Cell signaling” category, *Plc21C* (phospholipase C at 21C) stands out as a ring gland-specific transcript. PLC21C belongs to the PLC- β subfamily, a crucial enzyme that catalyzes the cleavage of phospholipids to generate second messengers diacylglycerol (DAG) and 1,4,5-triphosphate (IP3) that further signals through the activation of protein kinase C (PKC) and intracellular Ca^{2+} release. Previous studies have shown that PLC- β is activated through G-protein coupled receptors (Bunney and Katan, 2011), suggesting that PLC21C represents a key component in mediating extracellular signals in the ring gland. However, pathways in which PLC21C participates in the ring gland remain unknown. In addition, I also noticed *Rgk1* to be highly expressed in the ring gland. *Rgk1* encodes a member of the *Drosophila* RGK protein family of small GTPase (Smibert and Saint, 2003). Previous studies showed that in various mammalian tissues, RGK family proteins function as potent inhibitors of voltage-dependent Ca^{2+} channels (VDCCs) and regulators of actin cytoskeletal dynamics. VDCCs mediate Ca^{2+} influx resulting in increased intracellular Ca^{2+} levels that are critical for a wide panel of processes including neurotransmitter release, hormone secretion, and excitation-contraction coupling in muscle systems (Correll et al., 2008). For instance, opening of the VDCCs and resultant Ca^{2+} influx represents a common step in insulin secretion induced by glucose in pancreatic β -cells (Hsu et al., 1991). In *Drosophila*, it was demonstrated that the elevation of intracellular Ca^{2+} levels is required for the ecdysone-driven secretion of glue granules from the salivary gland (Biyasheva et al., 2001). While the mechanistic detail of ecdysone secretion in *Drosophila* remains poorly understood, ring gland-enrichment of

RGK1 and the previous observation that binding of PTTH to its receptor increases intracellular Ca^{2+} levels in the PG (Henrich, 1995) suggest a potential role of RGK1 and VDCCs in mediating ecdysone release from the ring gland.

In the “executive” group, an enrichment of genes encoding oxidoreductases was observed. In particular, 6 of the 16 transcripts that were classified as oxidoreductases encode known ecdysteroidogenic enzymes. A seventh gene, *Cyp6g2*, was shown to be expressed in the *corpus allatum*, but not in the prothoracic glands (Chung et al., 2009). In addition, I observed three other cytochrome P450 genes with >10fold enrichment in the ring gland, *Cyp28c1*, *Cyp303a1*, and *Cyp6a13*, but their functions in this tissue are poorly understood. Interestingly, *Cyp4g1*, which was shown to be predominantly expressed in the prothoracic gland of L3 wandering larvae (Niwa et al., 2011), has not been identified as ring gland-enriched transcript by the current approach (further see Discussion 3.4.1). Another gene with a potential role in the ecdysteroidogenic pathway is *CG1319*, which encodes a protein with homology to vertebrate adrenodoxin. In vertebrate steroidogenic tissues, adrenodoxin represents an essential component of the steroid hormone biosynthetic machinery, which initiates the electron-transport chain serving mitochondrial cytochrome P450s (Jefcoate et al., 1986). This implies that *CG1319* may act as a soluble electron carrier between adrenodoxin reductase (encoded by the *dare* gene in *Drosophila*) and downstream cytochrome P450 enzymes (Freeman et al., 1999). Ultimately, *CG40485*, which encodes a short-chain dehydrogenase, may possibly participate in the synthesis of ecdysone, based on the fact that *CG40485* and *shroud* are from the same protein family (Niwa et al., 2010).

3.3.2 Genes with temporally dynamic expression profiles

The next question to ask was which genes are temporally regulated during

the L3. While the four time points examined are not sufficient to resolve the three minor ecdysone pulses, it should provide a general trend between early and late L3 stages, suggesting whether or not a given gene is up- or down-regulated relative to the major ecdysone peak prior to pupariation. I analyzed the 233 transcripts that show high specificity of expression in the ring gland, and filtered for a 3fold change in expression between early (either 4-hr or 8-hr) and late (either 24-hr or 36-hr) time points. This strategy has revealed that 21 transcripts are downregulated and 37 upregulated during the first 36-hr of the third instar (**Figure 3.5A, C**).

Four of the 13 transcription factors (**Figure 3.4A**) that I identified are downregulated using this filtering criteria, *CG33557*, *snail*, *timeless*, and *SCNF* (**Figure 3.5B**). A fifth gene, *escargot*, is ~2fold reduced in expression from early time points to the 36-hr L3 time point. In contrast, none of the transcription factors listed here showed significant upregulation towards the end of the third instar, rather 8 out of the 13 genes in this category display relatively constant expression levels. It therefore would be of interest to identify a set of transcription factors that increase in expression.

Intriguingly, two genes in the “oxidoreductase” category, *Cyp28c1* and *CG40485*, exhibit a decreasing expression profile (**Figure 3.5B**), which differs from the expression profile of the Halloween genes such as *phantom* and *shadow* in the same category (**Figure 3.5E**). This implies that *Cyp28c1* and *CG40485* have different functions that are not required during late L3.

Closer inspection of the genes that are upregulated in the first 36 hours of the L3 have revealed an enrichment of genes in the categories of the “Hormones and growth factors” (**Figure 3.5C, D**), including *spätzle5*, *Gpb5*, *pvf2*, and *RYamide*, the “Cell signaling”, *Glu-RIB*, *Traf4*, and *MstProx*, and the “GPCRs”, *mthl12* and *star1*. These findings imply that a range of growth factors and

signaling pathways come into play in the ring gland at the end of the third instar, but they may only have minor roles prior to this particular stage. In the “Transport” group, *ImpE1*, which belongs to the low-density lipoprotein (LDL) receptor protein family (Ikonen, 2008), is significantly upregulated (**Figure 3.5D**). This finding raises the interesting possibility that *ImpE1* may function as a ring gland-specific cholesterol receptor in mediating cholesterol influx. This idea agrees with the observation that an increase of *ImpE1* transcript levels at the end of the L3 corresponds to the presumed increase of cholesterol input at this stage in order to make the major ecdysone peak. In addition, *Atet* and *CG4822*, which both encode ABC transporter proteins, and *Syt7*, which mediates vesicle exocytosis (Lloyd et al., 2000), are also upregulated more than 3fold towards the end of the L3 (**Figure 3.5D**). It is therefore possible that they are involved in the transport and secretion of the endocrine products of the ring gland into the hemolymph.

3.3.3 A *UAS*-RNAi Screen in the prothoracic gland

To identify which of the ring gland-specific transcripts encode functionally relevant genes, a set of 108 genes was selected and screened via RNAi using three ring gland Gal4 drivers, thus interfering with gene function in either the prothoracic gland (*phm22-Gal4*) (contributed equally by Qiuxiang Ou and Dr. Adam Magico), the *corpus allatum* (*Aug21-Gal4*) (by Jie Zeng), and the *corpora cardiaca* (*Akh-Gal4*) (by Dr. Adam Magico). A control cross with a strong ubiquitous Gal4 driver, *actin-Gal4*, was also carried out to assess whether the tested line would yield any phenotype at all (by Jie Zeng).

The ring gland *UAS*-RNAi screen revealed a total of 26 hits, of which a vast majority was identified for the prothoracic gland (25 out of 26) (by myself and Dr. Adam Magico). Specifically, two lines exhibited major embryonic lethality (*Ugt37c1* and *Cyp317a1*), three lines died as large first instar larvae

(*NPC1a*, *shroud*, and *vvl*) (**Figure 3.6A**), and two lines arrested development as large second instar larvae (*Hsp70Ba* and *Rgk1*) (**Figure 3.6B**). Notably, the most common phenotype was a large body phenotype, which was observed in 16 of the remaining 19 lines. The large body phenotype arises from prolonged feeding times when the molt to a pupa is either delayed (**Figure 3.6D**) or blocked (**Figure 3.6E**), which is typically caused by insufficient rates of ecdysone production, resulting in no or delayed ecdysone pulses. In those cases, when animals remain as larvae, feeding can continue for up to 4 weeks, and the resulting larvae are substantially bigger than those shown in **Figure 3.6E** and **Figure 3.7**, which were collected ~3 days after controls had pupariated. In addition, two of the remaining three lines display normal body size (*CG11762* and *Mes2*) (**Figure 3.6F**), although pupal lethality was observed in both lines. The only line that gives a completely different category of phenotype is *curled/nocturnin*, resulting in a smaller body size when knocked down in the prothoracic gland. This reduction of body size can indicate a premature attempt to pupariate, which would shorten larval feeding times. This developmental acceleration represents a relatively rare phenotype, which was observed in only three other cases. These include the *DHR4^l* mutant (see Chapter 2), animals that express a constitutively active Ras in the PG (*phm22>Ras^{V12}*), and animals with a PG-specific knockdown of a Toll-like receptor encoded by the *tollo* gene (Wasserman, 2000) (Jie Zeng, personal communication). These data imply that *curled/nocturnin* may be necessary for properly repressing ecdysone synthesis in the prothoracic gland. Furthermore, PG-specific knockdown of *Hsp70Ba* results in another rare phenotype termed the L2 pupa phenotype, in which case animals pupariate directly from the L2 without molting into a third instar (**Figure 3.6C**). This particular phenotype was first observed in animals that are mutant for *E75A* (Chapter 1), which have severely reduced levels of ecdysone due to loss of *E75A* function. It should be noted that

the body size of L2 pupa was comparable to that of wild type L3 pupa (**Figure 3.6C**), implying that *phm22>Hsp70Ba*-RNAi animals continue feeding as second instars for prolonged times prior to pupariation.

The *phm22-Gal4* driver has some expression in the fat body, raising the possibility that some of the phenotypes observed in the PG RNAi screen may arise from silencing the gene function in the fat body. To rule out this possibility, I crossed all RNAi lines that exhibited mutant phenotypes with *phm22-Gal4* to a strong fat body-specific Gal4 driver, *Cg-Gal4*. None of these RNAi lines resulted in any obvious phenotypes when crossed to *Cg-Gal4* (data not shown), indicating that the observed defects result from specifically interfering with the gene function in the prothoracic gland (**Table 3.3**).

To further characterize these genes, I asked whether supplementing fly media with 20E, the biologically active metabolite of ecdysone, would alleviate at least some of the RNAi phenotypes observed in larvae and pupae. This idea is based on the fact that the main function of the prothoracic gland is to generate ecdysteroids during the larval stages. To address this question, I raised *phm22>RNAi* animals on 20E-supplemented media to examine whether they can progress further compared to their counterparts reared on standard media. This strategy worked for all but one RNAi cross, *phm22>Ugt37c1*-RNAi, which results in embryonic lethality. In this particular case, *Ugt37c1*-RNAi embryos were soaked in a buffer containing 20E to test for rescue. A complete rescue by 20E (defined as most animals reaching the adulthood) was observed in 7 of the 25 crosses (*CG30471*, *phantom*, *disembodied*, *shadow*, *shroud*, *spookier* and *spätzle5*) (**Figure 3.7**, **Table 3.3**). A partial rescue of RNAi phenotypes by 20E was observed in 14 other lines, which was defined operationally as either reaching later developmental stages or restoring a normal body size due to a rescue of developmental timing (**Figure 3.7**, **Table 3.3**). However, no rescue was seen in 4

of the genes (*curled*, *Mes2*, *MstProx*, and *Ugt37c1*).

It is worth noting that only 2 out of the 20 non-Halloween genes tested in this assay, *spätzle5* and *CG30471*, could be rescued all the way to adulthood, suggesting that most genes identified in the screen do not directly mediate a specific step in the ecdysone biosynthetic pathway like the Halloween genes. Rather they may have broader roles that include other aspects of PG function, not just ecdysteroidogenesis. In addition, a few reasons may exist that could explain why 20E failed to rescue four of the *phm22*>RNAi crosses. For instance, in the case of *curled/nocturnin*, I observed developmental acceleration, which might be due to higher levels or the premature release of ecdysone (see Chapter 2 for a detailed discussion of developmental acceleration). It is therefore in line with the observation that 20E was not able to reverse the *phm22*>*noc*-RNAi phenotype. Secondly, *phm22*>*MstProx*-RNAi and *phm22*>*Mes2*-RNAi both result in mid-pupal lethality, it therefore might prove ineffective to provide animals with sufficient levels of hormone to rescue relatively late pupal processes, for the simple reason that pupae do not feed.

3.3.4 High-throughput qPCR reveals gene expression profiles in third instar larvae

The microarray analysis appears to be robust in identifying tissue-specific transcripts, but only 4 time points during the L3 have been examined, which limits the understanding on how gene expression correlates with the occurrence of those low-titer ecdysone peaks (**Figure 3.1B**). I next wanted to examine the expression of 25 selected transcripts via a different approach by using high-throughput qPCR (Fluidigm BioMark). These include *PTTH*, *Torso*, cytochrome P450 genes, transcription factors, circadian clock genes, and an ABC transporter *Atet*. Total RNA was isolated from the brain-ring gland complex of larvae collected in 4-hr

intervals throughout the L3 stage, and used in the qPCR analysis of gene expression patterns. In addition, flies used in this experiment were entrained by a 12hr light/dark cycle in advance, and the same condition continued until sample collection. This strategy not only enables us to capture a wider picture of gene expression during the L3, but also gains us insight into whether any gene expression is related to the circadian rhythm.

First of all, my data showed that *PTTH* expression exhibits a cyclic pattern in L3 larvae (**Figure 3.8A**), which is based on the geometric mean of 80 measurements of *PTTH* mRNA levels per time point throughout the L3 (see Methods). This result is largely in line with the previous finding that the *PTTH* transcript levels oscillate (McBrayer et al., 2007). However, an inconsistency was observed for *PTTH* expression from 4 hours to 16 hours after the L2/L3 molt (**Figure 3.8A, solid and dotted line**). One possible reason could be because the original study was based on a single measurement of *PTTH* mRNA levels in whole larvae samples (compared to BRRGs in this study) per time point by semi-quantitative PCR, which may not be sensitive enough to precisely quantify gene expression changes when transcript levels are low. Overall, this observation indicates that my approach is able to detect changes in gene expression precisely.

Furthermore, *Torso*, the principle PTTH receptor (Rewitz et al., 2009), was demonstrated to be strongly upregulated at the end of the L3, more specifically, after the 36-hr L3 time point (**Figure 3.8A**). Prior to this time point, *Torso* expression exhibits a fairly “flat” pattern (**Figure 3.8A**), which is consistent with the microarray data. This observation suggests that higher levels of *Torso* are required for the appropriate PTTH signaling prior to metamorphosis. It was shown that *Torso* expression is severely reduced when Activin/TGF β signaling is inactive in the PG (Gibbens et al., 2011). However, it remains unclear whether the elevation of *Torso* transcript levels during the onset of metamorphosis is under the

control of this pathway.

Secondly, for the transcription factors being examined, I observed that *vv1*, *E75A*, *DHR4*, *mld*, *woc*, and *dre4* transcript levels are all elevated towards the end of the L3 (**Figure 3.8A**). In particular, the expression of *vv1*, a ring gland-enriched transcript (>10fold), was significantly upregulated after the 36-hr L3 time point (**Figure 3.8A**). It is in line with the microarray data showing that *vv1* expression exhibits a fairly “flat” pattern during the first 36 hours of the third instar (see Result 3.3.2). These data raise the possibility that this POU/homeodomain protein is required for ecdysone synthesis or other aspects of ring gland function right before metamorphosis. However, the early larval lethality produced by *phm22>vv1*-RNAi prevents us from looking into this aspect of *vv1* function (**Figure 3.7**). A conditional knockdown of *vv1* gene function in the ring gland will be one of the future directions, such as the use of a temperature-sensitive Gal80 protein (Gal80^{ts}) to transiently inactivate RNAi expression in early stages. Interestingly, the expression of *mld* goes up significantly all the way to the end of the third instar (**Figure 3.8A**), in contrast to a fairly “flat” expression profile observed in the microarray.

It is of great interest to determine the expression profiles of the cytochrome P450 genes in third instars, which allows one to correlate the transcriptional regulation of cytochrome P450s, including the known ecdysone biosynthetic genes, with the occurrence of the three low-titer ecdysone peaks and PTTH oscillations during the L3. Firstly, the expression of the Halloween genes, including *spookier*, *phantom*, *disembodied*, and *shadow*, was shown to increase dramatically after animals initiate wandering behavior (after 32 hours L3) (**Figure 3.8A**). This observation is consistent with the previous finding that PTTH signaling is required for the upregulation of the Halloween genes, mainly for *disembodied* and *spookier*, prior to pupariation in the *Drosophila* ring gland

(Gibbens et al., 2011). Secondly, I noticed that the *phantom* transcript levels suddenly drop after they reach the peak at the 40-hr L3 time point (**Figure 3.8A**), but it remains unclear why *phantom* expression is regulated in this particular way, and what this downregulation signifies. Intriguingly, a similar behavior was observed for the *shroud* gene (**Figure 3.8A**), which encodes a component in the “Black Box” that is right upstream of the step mediated by the Phantom enzyme. These findings demonstrate that *shroud* and *phantom* are regulated in a similar fashion. Thirdly, a discrepancy exists between the microarray data and the qPCR results concerning the expression of these classic ecdysone enzymatic genes at the end of L3. Specifically, I found that the microarray data did not resolve the upregulation of these abundantly expressed transcripts at the 36-hr L3 time point. This is possibly because their expression levels at this point already exceed the upper limit that the scanner could detect (**Figure 3.5E**, **Figure 3.8A**). Ultimately, I observed the downregulation of five cytochrome P450 genes (*Cyp28c1*, *Cyp18a1*, *Cyp303a1*, *Cyp4g1* and *Cyp6a14*) (**Figure 3.8B**) throughout the L3 and an interesting oscillatory expression pattern in three other CYP genes (*Cyp317a1*, *Cyp6a13*, and *Cyp12e1*) (**Figure 3.8A**). This unusual cyclic pattern raises the question as to whether they are regulated by any rhythmic signals, such as the PTTH signal or the circadian rhythm.

Components of the circadian clock have been successfully identified in *Drosophila*, which are conserved from insects to mammals. The circadian genes *period* and *timeless* encode transcription factors that regulate the expression of clock-controlled genes. *period* was previously shown to be rhythmically expressed in the prothoracic gland of fly pupae (Emery et al., 1997), suggesting the existence of a circadian clock in the gland at this stage. Plus, in my ring gland microarrays, *timeless* was identified as a ring gland-enriched transcript (**Figure 3.4A**). These findings raise the question as to whether an independent circadian

clock exists in the ring gland during larval stages. To test this, I determined the expression profiles of *period* and *timeless* in the third instar brain-ring gland complex. As shown in **Figure 3.8B**, *period* transcript levels exhibit oscillations during the first half of the L3, but it steadily goes up towards the end of larval development. On the other hand, *timeless* expression mainly exhibits a decreasing trend during the L3 (**Figure 3.8B**), which nicely matches the ring gland microarray result. Based on these observations, it is clear that *period* and *timeless* do not display circadian features on the transcriptional level in the third instar brain-ring gland. However, the possibility that the circadian rhythm is manifested on the protein level cannot yet be ruled out.

Another interesting observation is that the expression of *Atet*, which encodes an ATP-binding cassette transporter protein, increases dramatically towards the end of the third instar (**Figure 3.8B**), suggesting a potential role of *Atet* in the ring gland right prior to metamorphosis. This notion is corroborated by the observation that knocking down *Atet* specifically in the PG causes larval arrest in the third instar (**Figure 3.7**).

3.3.5 Microarrays reveal genes affected by PTTH signaling

(This project was funded by Dr. Michael O'Connor laboratory, U of Minnesota, USA. Qiuxiang Ou did all the work shown here.)

Targets of the PTTH signaling pathway are largely unknown. For this reason I wanted to identify genes with PTTH-dependent expression. To do this, I carried out microarrays on ring gland RNA isolated from controls, larvae expressing a constitutively active Ras (Ras^{V12}) and larvae expressing *Torso*-RNAi at two developmental times in the L3, a “blue gut”/feeding stage (-18 hr PPF) that is indicative of a low PTTH phase and a “partial blue”/late wandering stage (-8 hr PPF) that is indicative of a high PTTH phase, respectively (**Figure 3.3**). I

examined differential ring gland gene expression changes between these two time points in the control and larvae expressing *Torso*-RNAi. Using stringent filtering criteria (>2fold change in *Torso*-RNAi relative to the control), I have observed a set of 87 transcripts with their expression affected in *Torso*-RNAi ring glands (**Table 3.7**). Specifically, I have identified 42 transcripts with expression increased from -18 hr PPF to -8 hr PPF in the control and this upregulation is affected by >2fold when *Torso* is silenced (**Table 3.7**). For instance, *CG9541*, an adenylate cyclase encoding gene, *DHR4*, a nuclear receptor that has been demonstrated to be a key readout of the PTTH cascade (Chapter 2), *CG30438* and *CG17323* which both encode a UDP-glycosyltransferase, *Kif3C*, a kinesin encoding gene, and *smooth* which encodes an RNA-binding protein, are all significantly upregulated with >2fold at the later time point (-8 hr PPF), however, this upregulation is completely lost in *phm22>Torso*-RNAi ring glands (**Figure 3.9A-F**). This observation strongly suggests that PTTH signaling positively modulates the expression of these genes.

Furthermore, I noticed that the expression of *CG9541*, *DHR4*, *CG30438*, *CG17323*, and *Kif3C* are significantly elevated in the ring gland of larvae expressing *Ras^{V12}* where the PTTH pathway is constitutively active (**Figure 3.9A-F**), further suggesting that the PTTH signaling pathway positively regulates the transcription of these genes. However, it should be noted that *smooth*, which is upregulated in the control between the -18 hr and -8 hr PPF time points, exhibits downregulation in *phm22>Ras^{V12}* ring glands although *Torso*-RNAi blunts the gene upregulation observed in the control (**Figure 3.9F**). For this, one possibility is that *smooth* does not represent a direct target of the PTTH pathway.

On the other hand, I identified a subset of 45 transcripts with expression decreased from -18 hr PPF to -8 hr PPF in controls, but they were de-repressed in *Torso*-RNAi ring glands (**Table 3.7**). For instance, *NPC-2c* and *NPC-2h*, which

both encode putative cellular cholesterol transporters, *nocturnin*, and *snail* are all significantly downregulated at the -8 hr PPF time point in the control in comparison with -18 hr PPF (**Figure 3.9G-J**). However, loss of *Torso* results in the de-repression of their transcription, indicating that the PTTH pathway negatively regulates the expression of these transcripts (**Figure 3.9G-J**). Consistently, a constitutively active Ras (Ras^{V12}) was able to reduce the transcript levels of *NPC-1c*, *NPC-2h*, and *nocturnin* in the ring gland (**Figure 3.9G-I**), further indicating that PTTH signaling represses the transcription of these genes. However, an inconsistency was observed for *snail*, of which the expression failed to regress in the presence of Ras^{V12} (**Figure 3.9J**), suggesting the possibility that *snail* might not be a direct target of the PTTH pathway.

3.3.6 Analysis of cytochrome P450 genes in the ring gland by fluorescence *in situ* hybridization (FISH)

Using microarrays, I have identified a total of 16 transcripts which encode cytochrome P450 enzymes with >3fold enrichment in the ring gland at any of the four time points being examined, and this includes the classic Halloween genes such as *spookier*, *phantom*, *disembodied*, and *shadow*, *Cyp6t3*, *Cyp6g2*, *Cyp18a1*, and nine other cytochrome P450 genes with as yet uncharacterized functions in the ring gland (also see **Table 3.5**). To test whether they have an ecdysteroidogenic role by an independent strategy of gene function analysis from RNAi, I wanted to determine in which part of the ring gland these genes are expressed, the prothoracic gland, the *corpus allutum*, or the *corpora cardiac*, by fluorescence RNA *in situ* hybridization (FISH). I have noticed that 4 of the aforementioned nine transcripts with uncharacterized function in the ring gland, *Cyp303a1*, *Cyp28c1*, *Cyp6v1*, and *Cyp317a1*, are of relatively low abundance in the ring gland (>20fold lower than the Halloween transcripts) although with high

specificity (**Table 3.5**). This observation provides an explanation of why they were not detected in an earlier report, where the authors used alkaline phosphatase (AP)-based *in situ* hybridizations to examine the expression patterns of *Drosophila* cytochrome P450s (Chung et al., 2009; Tautz and Pfeifle, 1989). To overcome this problem, I carried out fluorescence *in situ* detection of these low-abundance transcripts coupled with a tyramide signal amplification (TSA) procedure, which is able to detect previously undetectable targets with up to 1000fold higher sensitivity than the conventional AP-based method, for instance (<http://www.perkinelmer.com>). As shown in **Figure 3.10**, I observed that transcripts of *Cyp6v1*, and *Cyp317a1* are predominantly present in the prothoracic gland, with some expression in the two neighboring tissues (**Figure 3.10A, B**). These findings are consistent with my previous observations that the PG-specific RNAi knockdown of *Cyp6v1* and *Cyp317a1* results in larval lethality and embryonic lethality, respectively. These data stress that *Cyp6v1* and *Cyp317a1* have important functions in the prothoracic gland possibly as components of the ecdysteroidogenic pathway. Transcripts of *Cyp28c1* and *Cyp303a1* appear to be uniformly distributed in the ring gland (**Figure 3.10C, D**). In addition, *Cyp18a1* appears to be ubiquitously expressed in the ring gland, imaginal discs, and the CNS (**Figure 3.10E**), which is in agreement with its role in the 20E inactivation process (Guittard et al., 2011; Rewitz et al., 2010). The validation of the above results by sense probes of respective genes is in progress. The distribution patterns of *Cyp6u1*, *Cyp6a13*, *Cyp6a14*, and *Cyp12e1* transcripts are still under investigation.

3.4 Discussion

Evaluating differential gene expression and identifying tissue-specific transcripts represents a valuable approach to determine genes with important

functions for the tissue in question. I applied this approach to analyze the endocrine functions of the *Drosophila* larval ring gland and identified a number of previously known transcripts that are specifically expressed in the ring gland, serving as proof that this strategy successfully identifies already known ring gland components with important functions in steroid hormone production. For instance, the classic Halloween genes that encode enzymes mediating the synthesis of ecdysone were all identified by my microarray approach except *shade*, which is specific to ecdysone target tissues. This indicates high specificity and validity of my method in identifying components of importance in the ring gland. In total, I found 233 transcripts with strong enrichment (>10fold) in the ring gland, including transcription factors, GPCRs, cell signaling molecules, kinases, oxidoreductases, and other categories (**Figure 3.4**). To examine the roles of these genes in ecdysteroidogenesis, I used PG-specific RNAi to interfere with these genes in a tissue-specific manner. My results identified 25 genes, 20 of which likely have novel roles in ecdysone synthesis, as manifested by a range of dramatic phenotypes that are consistent with a loss or reduction of ecdysone production (**Figure 3.7**). I have also shown that many of these phenotypes can be rescued by adding ecdysone to the diet, confirming key roles of these genes in the synthesis of ecdysone, which include cytochrome P450 genes, transcription factors, ABC transporters and signaling pathway components.

3.4.1 Cytochrome P450 enzymes with novel functions in the prothoracic gland

My data have revealed 3 previously uncharacterized cytochrome P450 genes with strong transcript enrichment (>10fold) in the ring gland, *Cyp303a1*, *Cyp28c1*, and *Cyp6a13*. I showed that *Cyp28c1* in particular has a high likelihood of playing a novel role in the ecdysteroidogenic pathway, because knocking down

Cyp28c1 specifically in the prothoracic gland results in developmental defects similar to what was observed in animals expressing RNAi of the Halloween gene (**Figure 2.18, 3.7**) (Ou et al., 2011). Interestingly, the expression of *Cyp28c1* in the ring gland declines towards the end of the third instar, implying a distinct mechanism underlying the regulation of *Cyp28c1* from that of the classic Halloween genes in steroid hormone synthesis (**Figure 3.5A&E, Figure 3.8**). Future directions have to determine at which step (if any) *Cyp28c1* acts during ecdysone synthesis, and what lies upstream of *Cyp28c1* to appropriately regulate this enzyme during ecdysteroidogenesis. Furthermore, animals with PG-specific *Cyp303a1*-RNAi and *Cyp6a13*-RNAi are fully viable, however, it remains to be seen whether this result is due to inefficient gene disruption of *Cyp303a1* and *Cyp6a13* by RNAi. In addition, my data have also shown that transcripts of *Cyp6v1*, *Cyp6u1*, *Cyp6a14*, *Cyp317a1*, and *Cyp12e1* are moderately enriched (2~4fold) in the third instar larval ring gland (**Table 3.5**). Functional analysis via PG-specific RNAi has suggested a role for *Cyp6v1* and *Cyp317a1* in the synthesis of ecdysone (**Table 3.3**). However, further experiments are needed to examine what reactions they mediate in the conversion of cholesterol into ecdysone.

Among all these CYP genes, *Cyp12e1* appears to be the only gene reported whose transcripts are enriched in the ring gland by both Niwa et al. (2011) and this study, except *Cyp6g2* and the Halloween genes, such as *phantom*, *disembodied* and *shadow* (Niwa et al., 2011). My data demonstrated that both transcript isoforms of *Cyp12e1*, *Cyp12e1-RA* and *Cyp12e1-RB*, are ~3fold enriched in the ring gland (**Table 3.5**). However, whether this gene is implicated in ecdysone biosynthesis has to be addressed in future experiments because the initial PG-specific RNAi analysis of *Cyp12e1* does not support that *Cyp12e1* has an essential role in prothoracic gland cells. It will be of interest to determine whether *Cyp12e1* is expressed in the PG or the other two organs of the ring gland

by *in situ* RNA hybridizations in the future. Furthermore, it should be noted that *Cyp4g1*, which was shown to be strongly expressed in a subset but not all of the PG cells in wandering L3 larvae (Niwa et al., 2011), fails to be detected as a ring gland-enriched transcript in this study. This is possibly caused by genetic background differences. Niwa et al. (2011) identified *Cyp4g1* as a ring gland-enriched transcript in the wild type laboratory strain Oregon-R rather than *w¹¹¹⁸* in this study. Another possible reason lies in the difference of the experimental setup of these two approaches. *Cyp4g1* is strongly expressed in the epidermis but not the CNS (Niwa et al., 2011), indicating that the ratio of its ring gland expression compared to the whole-larva level in this study may not be as prominent when compared to the CNS expression by Niwa et al. (2011). This discrepancy raises the possibility that a group of genes with potential roles in the ring gland fail to be detected by the current approach due to their relatively higher expression in other larval tissues. Thus, an improved *in situ* detection of the expression patterns of cytochrome P450s (see Result 3.4.6) represents a valuable means to test this possibility in the future.

3.4.2 Atet: an ABC transporter highly specific to the ring gland in L3 larvae

Atet belongs to the ATP-binding cassette (ABC) transporter superfamily, which represents one of the largest protein families that are conserved from archaea to humans. ABC transporter proteins are of fundamental importance to membrane transport for a wide spectrum of substrates, including amino acids, ions, lipids, peptides, and other compounds (Higgins, 1992). Atet is designated as ABC Transporter Expressed in Trachea because the transcript was localized to the respiratory system in *Drosophila* embryos by an RNA *in situ* hybridization analysis (Kuwana et al., 1996). Atet belongs to the G subfamily of ABC transporters that consists of half-transporters, and it was suggested to be involved

in transporting a small molecule after dimerization (Dean et al., 2001; Kuwana et al., 1996). Members of the ABCG subfamily were previously shown to mediate the ATP-dependent transport of steroids and lipids (Velamakanni et al., 2007). For instance, ABCG1 and ABCG4 (a very close homolog to ABCG1) prevent cholesterol accumulation in hepatocytes and in macrophages in various mice tissues by inducing cholesterol transfer to high-density lipoproteins (HDL) (Kennedy et al., 2005; Wang et al., 2004), raising the possibility that *Atet* may be responsible for importing or exporting similar substrates.

Currently, my data indicate that (1) *Atet* transcripts are highly enriched in the larval ring gland, suggesting a potential role for *Atet* in this tissue during larval development (**Figure 3.4A**); (2) PG-specific disruption of *Atet* function via RNAi results in larval L3 arrest. However, *phm22>Atet*-RNAi animals successfully attempted pupariation in the presence of 20E, indicating that loss of *Atet* impairs ecdysone production or release (**Figure 3.7, Table 3.3**); (3) the *Atet* expression profile during the L3 reveals that *Atet* transcripts increase dramatically at the end of the L3, during the major ecdysone pulse prior to metamorphosis (**Figure 3.8B**). Together, these observations suggest that *Atet* may have a critical role in exporting the steroid hormone ecdysone from the larval ring gland, which finds support in the previous finding that another member of the ABC transporter G subfamily, ABCG2, also called the breast cancer resistance protein (BCRP), mediates the efflux of sterols such as estrone sulfate and 17 β -estradiol sulfate in the epithelial cells of the porcine kidney (Imai et al., 2003). Furthermore, it was found that ABCG2 mediates the efflux of androgen in rat prostate stem cells (Huss et al., 2005; Pascal et al., 2007). In humans, initial stages of prostate cancer growth could be suppressed by reducing the availability of androgens to cancer cells via androgen deprivation therapy (ADT) that results in cell apoptosis. This ABCG2-mediated efflux of androgen serves as a mechanism for maintenance of

the prostate stem cell phenotype by avoiding androgen deprivation-induced apoptosis, thus leading to the failure of ADT and recurrent prostate cancer. Together, these findings further support the idea that *Atet* is involved in exporting the steroid hormone ecdysone from the ring gland. In the future, it will be interesting to determine whether the secretion of ecdysone fails to occur when *Atet* is depleted in the ring gland and whether ecdysone represents the specific substrate of *Atet*.

3.4.3 Methuselah-like receptors: a group of GPCRs enriched in the ring gland

The G protein-coupled receptors (GPCRs) constitute a large and ancient superfamily of integral cell membrane proteins that play a central role in signal transduction (Brody and Cravchik, 2000). My data revealed a number of GPCR-encoding genes with highly enriched expression in the ring gland (**Figure 3.4A**). The GPCRs encoded by these genes include *NepYr*, *Proc-R*, and *Star1*, which all belong to the rhodopsin-like GPCR family (Brody and Cravchik, 2000). In addition, I have noticed an enrichment of transcripts that encode the Methuselah-like receptors, including *Mthl6*, *Mthl7*, *Methl12*, and *Mthl13*, which belong to the Methuselah/Methuselah-like (Mth/Mthl) family of the secretin-like GPCR family (Brody and Cravchik, 2000). The founding member of the *mth/mthl* gene family, *methuselah*, functions in controlling aging. The *Drosophila* mutant for *methuselah* and its endogenous ligand, *stunted*, both have increased adult lifespan and enhanced resistance to various forms of stress (Cvejic et al., 2004; Lin et al., 1998), indicating that signaling pathways conducted by Stunted-Methuselah modulate stress response and adult lifespan. However, little is known regarding the developmental functions of Mth or any of its paralogs. Previous data showed that *mthl6*, *mthl7*, *mthl12*, and *mthl13* represent an

independent clade of the *methuselah* superclade (Patel et al., 2012), suggesting a possibility that these receptors may function redundantly in the ring gland. RNAi knockdown of these genes individually in the prothoracic gland did not result in any obvious defects, further implying compensatory buffering between family members. Analysis of dominant negative mutations of these genes may be a future direction in examining the functions of these receptors in the ring gland. Ultimately, Patel et al. (2012) also reported that the clade represented by *mthl6*, *mthl7*, *mthl12*, and *mthl13* is primarily found in *Drosophila melanogaster* and *Drosophila yakuba*, but not in other *Drosophila* species that were examined (Patel et al., 2012). This finding indicates that *mthl6*, *mthl7*, *mthl12*, and *mthl13* are relatively young members of the *methuselah* gene family, and also raises the question as to whether there are other *methuselah-like* paralogs carrying out similar functions in the ring gland of other *Drosophila* species.

3.5 Outlook

While the precise function of the components identified in this study remains to be addressed in full, my findings open up new avenues of research into the molecular details underlying the regulation of ecdysteroidogenesis and other aspects of PG biology during *Drosophila* larval development. A few directions will be of interest to pursue in the future: (1) the potential role of Atet in exporting the steroid hormone ecdysone; (2) the function of the circadian clock gene *timeless* in the PG, and whether there exists an independent clock in this tissue that modulates ecdysone production; (3) whether *nocturnin* and *DHR4* (see Chapter 2) function in the same pathway, since the rare small animal phenotype were observed for both PG-specific knockdown of *nocturnin* and *DHR4*.

3.6 Tables

GO term	P-value	Gene
Receptor activity	6.59E-07	<i>mthl6; Toll-4; mthl7; sev; CG8784; Glu-RIB; CG9935; star1; mthl12; CG33958; CG33492; MstProx; torso; CG7497; NepYr; Sr-CIII; CG12290; Hmu; CG6986</i>
Response to heat	1.49E-06	<i>Hsp70bc; Hsp70bb; Hsp70ab; hsp70ba; hsp70bbb</i>
Sterol metabolic process	1.36E-05	<i>mld; dib; Npc1a; phm; sad</i>
Hormone biosynthetic process	4.00E-05	<i>mld; dib; phm; sad; jhamt</i>
Signal transduction	1.47E-04	<i>mthl6; Toll-4; mthl7; sev; CG8784; Pvf2; IFa; Cng; Ext2; Traf4; star1; mthl12; CG33492; torso; MstProx; CG7497; NepYr; Hs6st; CG12290; Akh; CG6986</i>
Oxidoreductase activity	2.73E-04	<i>CG1319; dib; phm; CG40160; CG40050; CG40485; CG17691; Cyp6g2; sad; Cyp303a1; CG17374; CG9522; shroud; Cyp28c1; CG9747; Cyp6a13; CG4716; CG8630</i>
GPCR signaling pathway	2.73E-04	<i>mthl6; mthl7; CG8784; NepYr; CG7497; CG12290; IFa; Akh; CG6986; star1; mthl12</i>
Tube morphogenesis	3.11E-02	<i>Hs6st; esg; form3; torso; warts; snail; hand; vvl</i>

Table 3.1. Gostat results for 233 ring gland-specific transcripts

Gene	VDRC ID	Gene	VDRC ID
<i>Atet</i>	42750, 100404	<i>curled</i>	25176, 45441, 45442, 45443, 109759
<i>CG2893</i>	40987	<i>Cyp6a13</i>	4019, 104735
<i>CG3618</i>	100941	<i>Cyp6g2</i>	105333
<i>CG4678</i>	106490	<i>Cyp28c1</i>	51073
<i>CG4680</i>	107457	<i>Cyp303a1</i>	51493, 51495, 107902
<i>CG4681</i>	103752	<i>disembodied</i>	101117
<i>CG4688</i>	101884	<i>dro4</i>	103505
<i>CG4822</i>	105922	<i>Eip63E</i>	106824
<i>CG5225</i>	109851	<i>escargot</i>	9794
<i>CG5278</i>	107919	<i>Glu-RIB</i>	106269
<i>CG6232</i>	31020	<i>Hand</i>	23306
<i>CG7571</i>	37295	<i>Hs6st</i>	110424
<i>CG7730</i>	105256	<i>Hsp70Ba</i>	50381, 50382
<i>CG8105</i>	104510	<i>ImpE1</i>	104613
<i>CG8784</i>	103822	<i>Ir41a</i>	109772
<i>CG9184</i>	108474	<i>jhamt</i>	103958, 19172
<i>CG9522</i>	19861	<i>Kif3C</i>	43641
<i>CG9747</i>	1394	<i>Mes2</i>	37782, 109111
<i>CG9813</i>	45935	<i>mld</i>	102023
<i>CG11437</i>	9452	<i>MstProx</i>	108034
<i>CG11592</i>	104099	<i>mthl6</i>	47949, 108048
<i>CG11762</i>	108919	<i>mthl7</i>	102811
<i>CG12290</i>	100939	<i>mthl12</i>	48402, 105546
<i>CG13045</i>	102537	<i>mthl13</i>	3431
<i>CG13121</i>	105199	<i>mub</i>	28024
<i>CG13813</i>	104249	<i>NepYr</i>	1258, 1259, 103973
<i>CG14075</i>	102202	<i>Npc1a</i>	105405
<i>CG14107</i>	102232	<i>pdm3</i>	30537
<i>CG14110</i>	110053	<i>phantom</i>	100811
<i>CG14111</i>	100360	<i>Plc21C</i>	26557, 26558, 108395
<i>CG14153</i>	101041	<i>Proc-R</i>	7217
<i>CG15115</i>	102219	<i>Punch</i>	107296
<i>CG15550</i>	100063	<i>Rbp6</i>	29799, 29800
<i>CG15919</i>	109936	<i>Rgk1</i>	30103, 30104
<i>CG17626</i>	40795	<i>RYamide</i>	109264, 109267
<i>CG30054</i>	102887	<i>SCNF</i>	32091
<i>CG30471</i>	100166	<i>sevenless</i>	107048
<i>CG32027</i>	103512	<i>shadow</i>	106356
<i>CG33156</i>	103902	<i>shakB</i>	24578
<i>CG33347</i>	48565	<i>shroud</i>	50111
<i>CG33461</i>	105904	<i>snail</i>	6232, 50003, 50004
<i>CG33557</i>	23517, 23518, 109868	<i>spookier</i>	51081
<i>CG33958</i>	4978, 101861, 106547	<i>spz5</i>	41295, 102389
<i>CG33970</i>	101855	<i>Sr-CIII</i>	13031, 102716
<i>CG34263</i>	109380	<i>tinman</i>	12655, 12656, 32510, 101825
<i>CG40336</i>	109752	<i>timeless</i>	2885, 2886, 101100
<i>CG40818</i>	109264	<i>Toll-4</i>	47966, 47967, 102642
<i>CG40856</i>	109150	<i>Traf4</i>	21214
<i>CG41059</i>	109746	<i>TrpA1</i>	37249
<i>CG41336</i>	109093	<i>Ugt37c1</i>	46514
<i>CG41587</i>	109567	<i>vvl</i>	47182, 47185, 110723

Table 3.2. RNAi lines screened with the *phm22-Gal4* driver

Gene	VDRC ID	Phenotypes (strongest line)	20E rescue
Driver: <i>phm22-Gal4</i> (prothoracic gland)			
<i>Atet</i>	42750, 100404	Large permanent L3, no Pupae	attempt PF
<i>CG5278</i>	107919	Large L3/Pupae/Adults	normal timing/size*
<i>CG11762</i>	108919	Prepupal lethality	not tested
<i>CG30471**</i>	100166	Large L3/Pupae, no adults	form adults
<i>CG33557</i>	23517, 23518, 109868	Large permanent L3, no Pupae	attempt PF
<i>CG33958</i>	4978, 106547, 101861	Large L3/Pupae/Adults	normal timing/size
<i>curled</i>	25176, 45441, 45442, 45443, 109759	Small L3/P, form adults	no rescue
<i>Cyp28c1</i>	51073	Large L3, few Pupae	attempt PF
<i>disembodied</i>	101117	Large L3, larval lethality	form adults
<i>Hsp70Ba</i>	50381, 50382	L2 arrest, large L2, no L3 or Pupae	attempt PF
<i>Mes2</i>	109111, 37782	Pupal lethality	no rescue
<i>MstProx</i>	108034	~20% pupal lethality	no rescue
<i>Npc1a</i>	105405	L1 arrest	wandering L3
<i>phantom</i>	108359	L1 arrest	form adults
<i>Plc21C</i>	26558, 108395, 26557	Large L3/Pupae/Adults	normal timing/size [#]
<i>Rgk1</i>	30103, 30104	L2 arrest	form L3/P
<i>shadow</i>	106356	Large L3/Pupae	form adults
<i>shroud</i>	50111	L1 arrest	form adults
<i>snail</i>	50003, 50004, 6232	Small and large L3, no Pupae	wandering L3
<i>spz5</i>	41295, 102389	Large permanent L3, no Pupae	form adults
<i>spookier</i>	51081	Large L3/Pupae	form adults
<i>tinman</i>	12655, 12656, 32510, 101825	Large permanent L3, no Pupae	wandering L3
<i>timeless</i>	2885, 2886, 101100	Large permanent L3, no Pupae	attempt PF
<i>Ugt37c1</i>	46514	Embryonic lethality	no rescue
<i>vvl</i>	47182, 47185, 110723	L1 arrest	form L2/L3
Control cross: <i>Cg-Gal4</i> (fat body)			
None of the above lines resulted in phenotypes when RNAi was expressed in the fat body.			
* <i>CG5278</i> Large L3/Pupae, also adults with 20E size and timing normal.			
** <i>CG30471</i> (model withdrawn) Large L3/Pupae, no adults, with 20E form adults			
# <i>Plc21C</i> with 20E no adults			
Red type, lines did not give obvious RNAi phenotypes.			

Table 3.3. RNAi lines identified with the ring gland- and fat body-specific *Gal4* drivers

Gene Name	Roche probe#	Gene Name	Roche probe#
<i>Cyp6v1</i>	25	<i>Cyp18a1</i>	137
<i>Atet</i>	102	<i>Cyp6a13</i>	23
<i>ventral veinless</i>	75	<i>Shroud</i>	18
<i>Period</i>	61	<i>Torso</i>	51
<i>Cyp28c1</i>	10	<i>Timeless</i>	133
<i>Cyp303a1</i>	116	<i>E75A</i>	58
<i>Disembodied</i>	157	<i>Cyp317a1</i>	52
<i>Phantom</i>	79	<i>Cyp6a14</i>	25
<i>Shadow</i>	62	<i>Cyp12e1</i>	50
<i>Spookier</i>	54	<i>Without children</i>	137
<i>DHR4</i>	40	<i>Dre4</i>	50
<i>Cyp4g1</i>	86	<i>Molting defective</i>	56
<i>Tm1*</i>	10	<i>PTTH</i>	98
<i>Rpl140*</i>	63	<i>Rp49*</i>	105
<i>Rpl24*</i>	147	<i>αTubulin*</i>	3

* internal controls

Table 3.4. Primer/probe mix used in the high-throughput qPCR time-course experiment

Table 3.5. Cytochrome P450 genes with moderate to strong transcript enrichment in ring glands from third instar larvae.													
Sequence ID	Transcript	Gene	L3: 4 hours		L3: 8 hours		L3: 24 hours		L3: 36 hours		Tissue	<i>in situ</i> (Chung et al.)	<i>in situ</i> (this study)
			72	160	70	152	91	109	61	144			
FBr0088009	<i>Cyp6g2-RA</i>	<i>Cyp6g2</i>	11496	160	10511	152	91	109	8766	144	whole body ring gland	Corpus allatum	n/a
FBr0073205	<i>dib-RA</i>	<i>disembodied</i>	12595	131	11476	86	186	75	13856	45	whole body ring gland	Prothoracic glands	Corpus allatum (early L3) & Prothoracic gland
FBr0080828	<i>Cyp303a1-RA</i>	<i>Cyp303a1</i>	1698	74	1513	69	22	58	815	54	whole body ring gland	Not detected	ring gland (late L3)
FBr0114175	<i>spok-RA</i>	<i>spookier</i>	13189	48	15594	61	258	19	16489	13	whole body ring gland	Prothoracic glands	n/a
FBr0082475	<i>sad-RA</i>	<i>shadow</i>	22748	45	23661	34	690	14	24982	9	whole body ring gland	Prothoracic glands	n/a
FBr0073565	<i>Cyp28c1-RA</i>	<i>Cyp28c1</i>	575	25	313	14	23	6	78	5	whole body ring gland	Salivary glands Not detected in RGs	Corpus allatum (early L3) & Prothoracic gland
FBr0074603	<i>phm-RA</i>	<i>phantom</i>	33820	23	35414	25	2181	16	30703	11	whole body ring gland	Prothoracic glands	Prothoracic gland (late L3)
FBr0087993	<i>Cyp6t3-RA</i>	<i>Cyp6t3</i>	226	10	176	8	18	7	67	3	whole body ring gland	Not detected	Corpus allatum (early L3) & Prothoracic gland
FBr0088690	<i>Cyp6a13-RA</i>	<i>Cyp6a13</i>	3772	6	4980	10	477	7	4347	5	whole body ring gland	Midgut, Malpighi Not detected in RGs	n/a
FBr0074609	<i>Cyp18a1-RA</i>	<i>Cyp18a1</i>	4421	6	5084	6	504	4	961	5	whole body ring gland	Not detected	ring gland and eye discs (early L3)
FBr0077276	<i>Cyp6v1-RA</i>	<i>Cyp6v1</i>	630	1	715	1	606	2	1072	3	whole body ring gland	Gonads Not detected in RGs	ring gland (late L3)
FBr0086185	<i>Cyp6u1-RA</i>	<i>Cyp6u1</i>	2098	2	2176	2	1096	2	2473	3	whole body ring gland	Gonads Not detected in RGs	n/a
FBr0088734	<i>Cyp6a14-RA</i>	<i>Cyp6a14</i>	116	1	170	3	70	3	128	2	whole body ring gland	Midgut Not detected in RGs	n/a
FBr0087405	<i>Cyp317a1-RA</i>	<i>Cyp317a1</i>	765	1	899	1	626	4	1313	4	whole body ring gland	Not detected	Prothoracic gland (late L3)
FBr0082250	<i>Cyp12e1-RB</i>	<i>Cyp12e1</i>	7366	2	8543	3	4071	2	7417	2	whole body ring gland	Not detected	n/a
FBr0082249	<i>Cyp12e1-RA</i>	<i>Cyp12e1</i>	7272	2	8469	3	4807	2	7863	2	whole body ring gland	Not detected	n/a

Sequence ID: Nimblegen Identifier for specific probe set, based on Flybase transcript IDs. Numbers in light print indicate average expression value based on triplicate Nimblegen arrays, top row for whole body, lower row for ring glands. The higher the number, the higher the abundance of the transcript. Numbers in bold indicate relative enrichment in ring glands vs. whole body for four time points during development of third instar larvae (hours relative to the L2/L3 molt) Daborn *in situ*: Data published by Chung et al. in PNAS 106, 5731

Gene	Primer Sequence
<i>phantom</i>	Forward 5' atccaagccaggagcagagtgagg Reverse 5' cttcgccgggacacattcgatagc
<i>Cyp28c1</i>	Forward 5' aategctgtttgactgcgtcctgg Reverse 5' tegctgagatccagttccctctgc
<i>Cyp303a1</i>	Forward 5' cactctatggtgcatgctgagcgg Reverse 5' tetgaccgcctccaaggtgatagc
<i>Cyp6v1</i>	Forward 5' gaggaacacgcaatcggagatcgg Reverse 5' ccatgtcgagaaactccatgcggg
<i>Cyp18a1</i>	Forward 5' tggaccccaatctgtgggagaagc Reverse 5' ctagccggtatccggatgtgctcc
<i>Cyp317a1</i>	Forward 5' aattgcaagtacgtgtgcgggagg Reverse 5' ataccaatgcaactgcgagcacc

Table 3.6. Primer pairs for *in situ* probes

Genes	Fold change (Control -18hr vs -8hr	ttest	Fold change (Torso RNAi -18hr vs -8hr	ttest
Downregulated in the control ring gland -18hr vs -8hr				
CG18180	-7.66	0.0002	-2.32	0.0009
CG7201	-8.69	0.0170	-1.60	0.1050
CG32373	-2.85	0.0001	1.19	0.7220
CG8492	-4.29	0.0044	-1.43	0.0688
CG10433	-4.07	0.0038	-1.80	0.0573
CG13492	-4.64	0.0279	-2.01	0.2590
lethal (2) essential for life	-2.67	0.0259	1.45	0.3110
CG15211	-2.25	0.0075	-1.31	0.0380
Cyp311a1	-2.25	0.0314	1.28	0.4320
CG4318	-3.10	0.0492	-1.50	0.1970
CG9981	-10.30	0.0051	-3.42	0.0495
CG4998	-2.62	0.0134	1.43	0.0911
Cytochrome P450-4d8	-3.75	0.0476	1.15	0.8290
CG14275	-3.04	0.0232	-1.22	0.3010
CG7224	-2.15	0.0367	-1.01	0.9450
Pde1c	-2.48	0.0132	-1.33	0.6310
snail	-28.97	0.0058	-5.17	0.0174
alpha-Esterase-9	-2.62	0.0041	-1.11	0.6790
alpha-Esterase-9	-2.68	0.0085	-1.03	0.9210
Copper transporter 1B	-5.65	0.0002	-2.83	0.0097
Niemann-Pick type C-2c	-8.49	0.0052	-4.78	0.0737
UDP-glycosyltransferase 35a	-2.89	0.0030	-1.87	0.0091
CG8925	-10.04	0.0013	-1.61	0.0969
CG8927	-9.96	0.0052	-4.08	0.0057
CG31148	-15.68	0.0223	-1.07	0.9150
CG13632	-5.81	0.0219	-2.67	0.1550
CG6879	-12.48	0.0033	-6.38	0.0033
CG6296	-7.86	0.0101	-3.08	0.2010
Papilin	-2.70	0.0291	-1.98	0.0488
CG31051	-2.03	0.0175	-1.29	0.1230
Jonah 99Ci	-9.03	0.0013	-2.17	0.0382
CG15534	-42.36	0.0013	-1.93	0.0715
Niemann-Pick type C-2h	-5.82	0.0059	-1.84	0.1530
Amylase distal	-3.41	0.0014	1.48	0.5060
Cuticular protein 49Ah	-3.34	0.0454	-1.13	0.9040

Table 3.7, continued				
TwdlBeta	-8.61	0.0025	-2.60	0.0358
CG12897	-2.24	0.0073	1.50	0.4820
Larval visceral protein H	-4.25	0.0210	-1.02	0.9830
CG33965	-2.47	0.0205	-1.27	0.5640
CG8927	-9.43	0.0024	-4.30	0.0052
CG8795	-3.22	0.0000	-1.40	0.2620
CG34217	-3.89	0.0470	-1.00	0.9600
Nocturnin	-2.64	0.0004	-1.65	0.1880
CG8925	-10.87	0.0008	-1.62	0.0772
CG42249	-7.07	0.0198	-1.23	0.7630
Upregulated in the control ring gland -18hr vs -8hr				
Metallothionein B	3.89	0.0385	2.25	0.2430
CG5715	2.42	0.0126	1.19	0.5850
α PS4	2.42	0.0453	2.17	0.5470
CG30438	2.91	0.0003	1.62	0.1600
CG12680	3.45	0.0018	1.12	0.2380
CG13594	2.49	0.0124	1.66	0.3490
CG18258	2.53	0.0292	6.07	0.5580
CG13050	4.66	0.0024	2.99	0.5010
CG7841	2.45	0.0033	2.59	0.8830
CG32037	8.45	0.0002	5.60	0.3800
CG12446	5.24	0.0028	2.76	0.4910
CG7442	3.24	0.0040	4.24	0.5430
CG11034	17.34	0.0001	13.08	0.2020
CG9171	2.59	0.0057	2.24	0.3590
CG9541	2.03	0.0066	1.30	0.0637
CG17323	3.65	0.0005	2.04	0.1480
CG17321	2.62	0.0081	-4.60	0.0051
CG13284	6.60	0.0489	-1.38	0.8480
CG30438	3.16	0.0002	1.64	0.0931
smooth-RA	2.12	0.0018	-1.54	0.4900
smooth-RC	2.07	0.0026	-1.49	0.6390
smooth-RD	2.14	0.0003	-1.58	0.8310
smooth-RB	2.37	0.0010	-1.32	0.4880
CG5756	4.34	0.0234	1.46	0.1070
CG15615	2.21	0.0285	-1.05	0.0103
CG30008	2.63	0.0098	2.71	0.6030
CG1941	3.65	0.0079	4.70	0.3960
CG11260	2.25	0.0329	1.08	0.4520

Table 3.7, continued				
Kif3C	2.33	0.0214	1.08	0.0739
CG34235	2.02	0.0108	1.84	0.7160
Hr4	2.72	0.0417	3.25	0.9340
smooth-RG	2.45	0.0014	-1.60	0.6570
CG41482	4.44	0.0022	3.21	0.1560
CG41476	2.85	0.0041	1.79	0.5170
CG40500	3.48	0.0001	3.90	0.0876
CG41474	5.76	0.0001	2.44	0.1750
CG41473	3.34	0.0009	2.49	0.5100
CG34172	3.13	0.0011	3.60	0.1340
CG34252	2.98	0.0045	7.74	0.3360
CG10663	3.14	0.0028	1.87	0.3280
Sarcoplasmic calcium-binding protein 1	2.07	0.0062	1.31	0.9120
CG40625	5.32	0.0013	2.89	0.2890

Table 3.7. Genes affected by PTH signaling.

Listed genes are either down- or upregulated in the control ring gland from -18hr PPF to -8hr PPF. This response was affected >2fold in the ring gland with *Torso* function disrupted via RNAi specifically in the prothoracic gland. *P* values were also calculated based on Student's *t*-test. If $p > 0.05$, it was considered as no significant fold change between -18hr PPF and -8hr PPF. A total of 87 transcripts (45 downregulated and 42 upregulated) fulfill the filtering standard used here, 10 selected transcripts are shown in **Figure 3.9**. PPF, prior to the puparium formation.

3.7 Figures

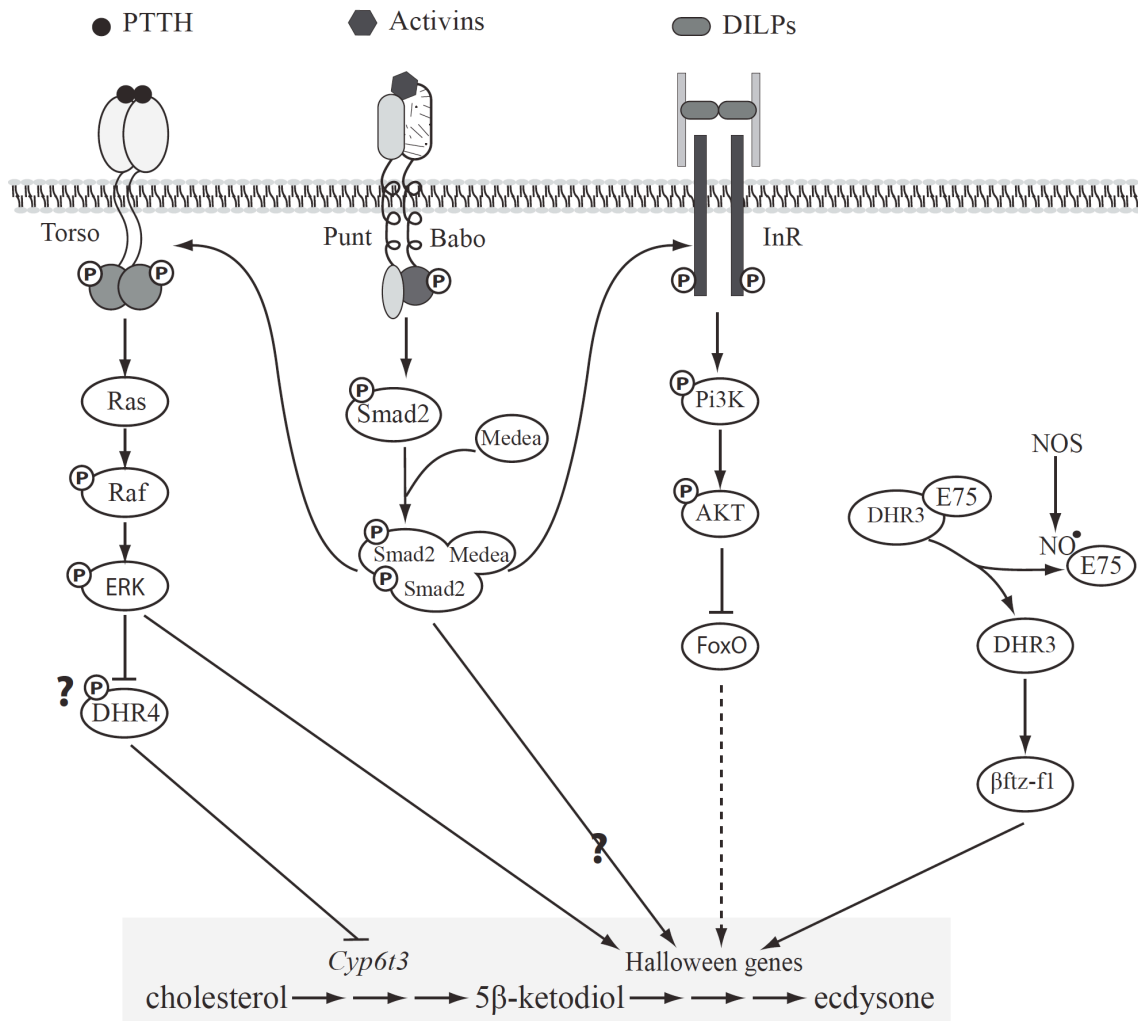


Figure 3.1. An overview of mechanisms underlying regulation of ecdysone biosynthesis in the *Drosophila* prothoracic gland. A schematic diagram of multiple signaling cascades that regulate ecdysone biosynthesis in the prothoracic gland. Inactivation of these pathways could compromise ecdysone production and result in developmental defects. Arrows represent positive regulations, and lines indicate inhibitory effects. P, phosphorylation; NO, nitric oxide radical.

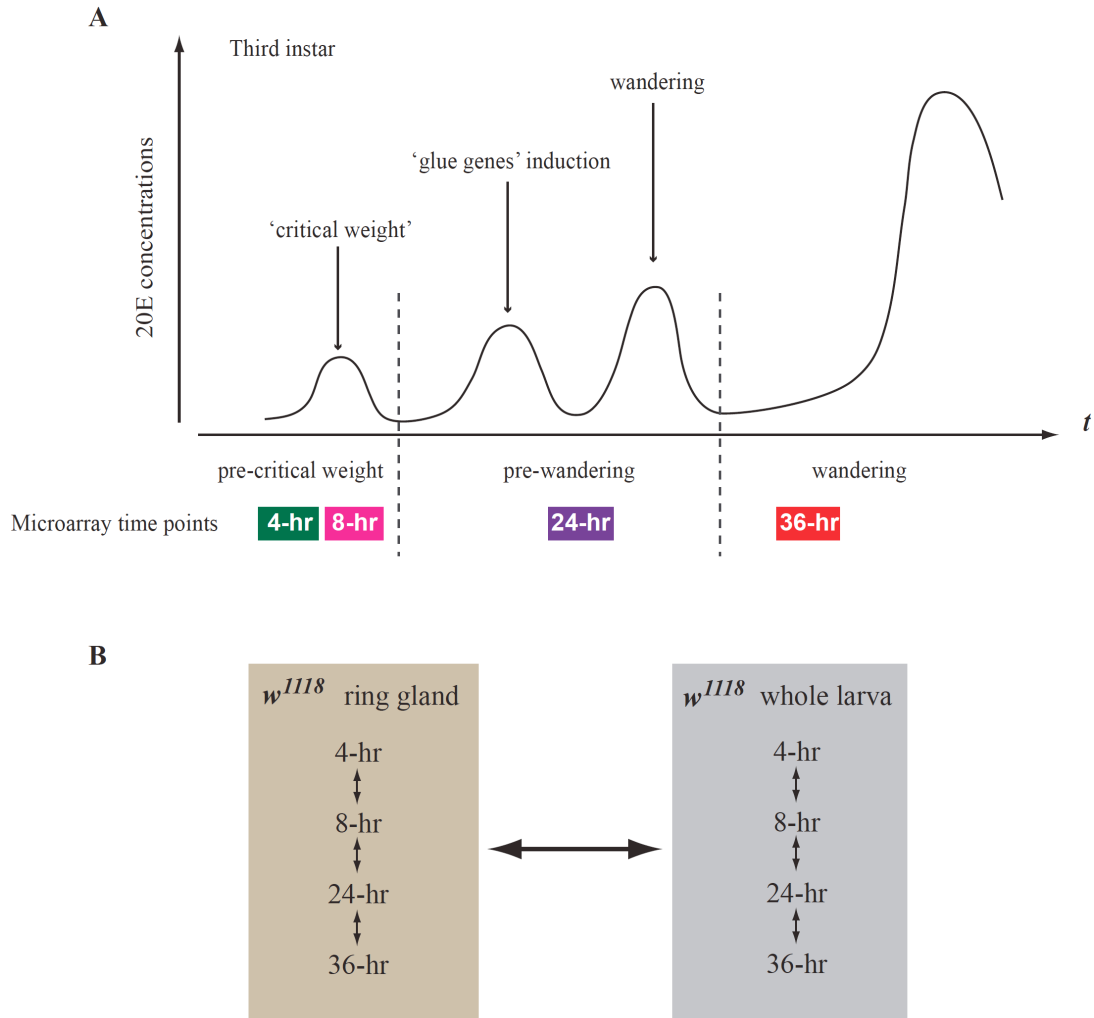


Figure 3.2. Experimental design and timeline of *Drosophila* larval ring gland microarrays.

(A) Three low-titer ecdysone pulses during the larval third instar (L3) are depicted. Ring glands of w^{1118} larvae were isolated for microarray analysis at four time points during the L3. The 4-hr and 8-hr time points are pre-critical weight, while the other two time points 24-hr and 36-hr are pre-wandering and a wandering stage, respectively. (B) Differential gene expression was analyzed between the ring gland and the whole larva at each time point. The array signal ratio of each transcript, or relative transcript enrichment, is determined by the ratio of the ring-gland array signal to the whole-larva array signal.

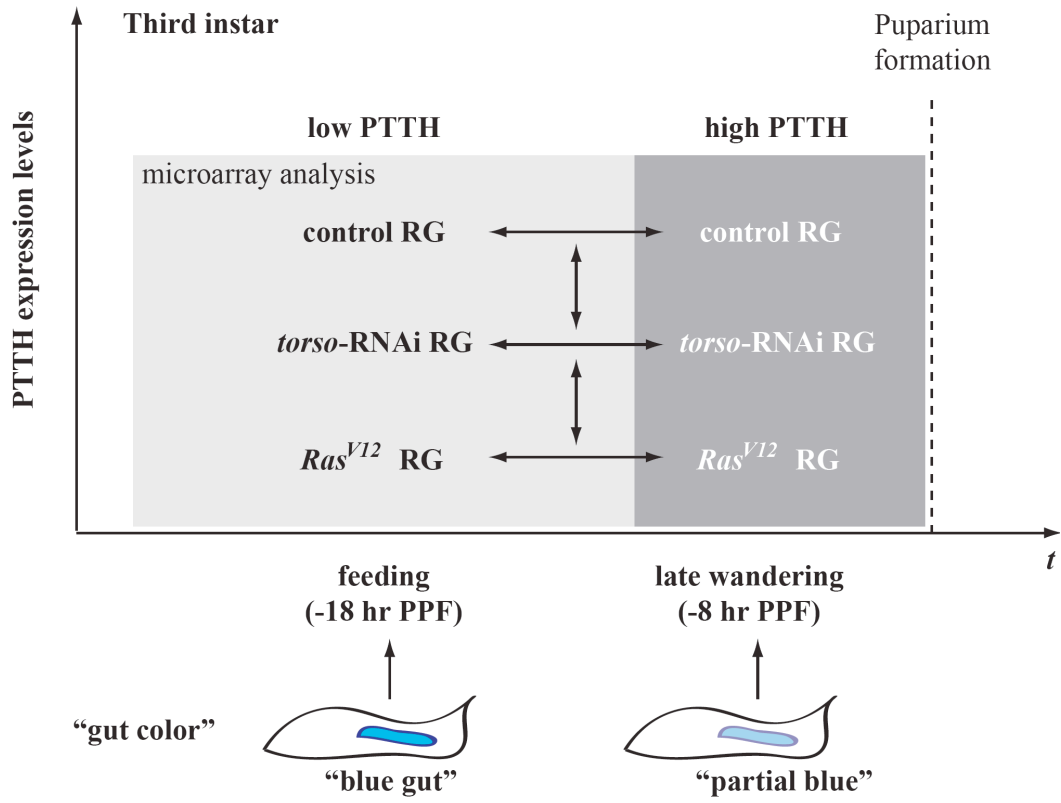


Figure 3.3. Experimental design and timeline of ring gland microarrays examining gene expression changes affected by altered PTTH signaling. Microarrays were carried out on the ring gland isolated from controls *UAS-Dicer phm22>w¹¹¹⁸*, *UAS-Dicer; phm22 >Torso-RNAi*, and *UAS-Dicer; phm22>Ras^{V12}* at two developmental times. “Blue-gut” is an indication of a feeding stage (-18 hr PPF) (Andres and Thummel, 1994; Maroni, 1983) that corresponds to a low-PTTH phase. “Partial blue” is indicative of a wandering stage (-8 hr PPF) (Andres and Thummel, 1994; Maroni, 1983) that corresponds to a high-PTTH phase. PPF, prior to puparium formation.

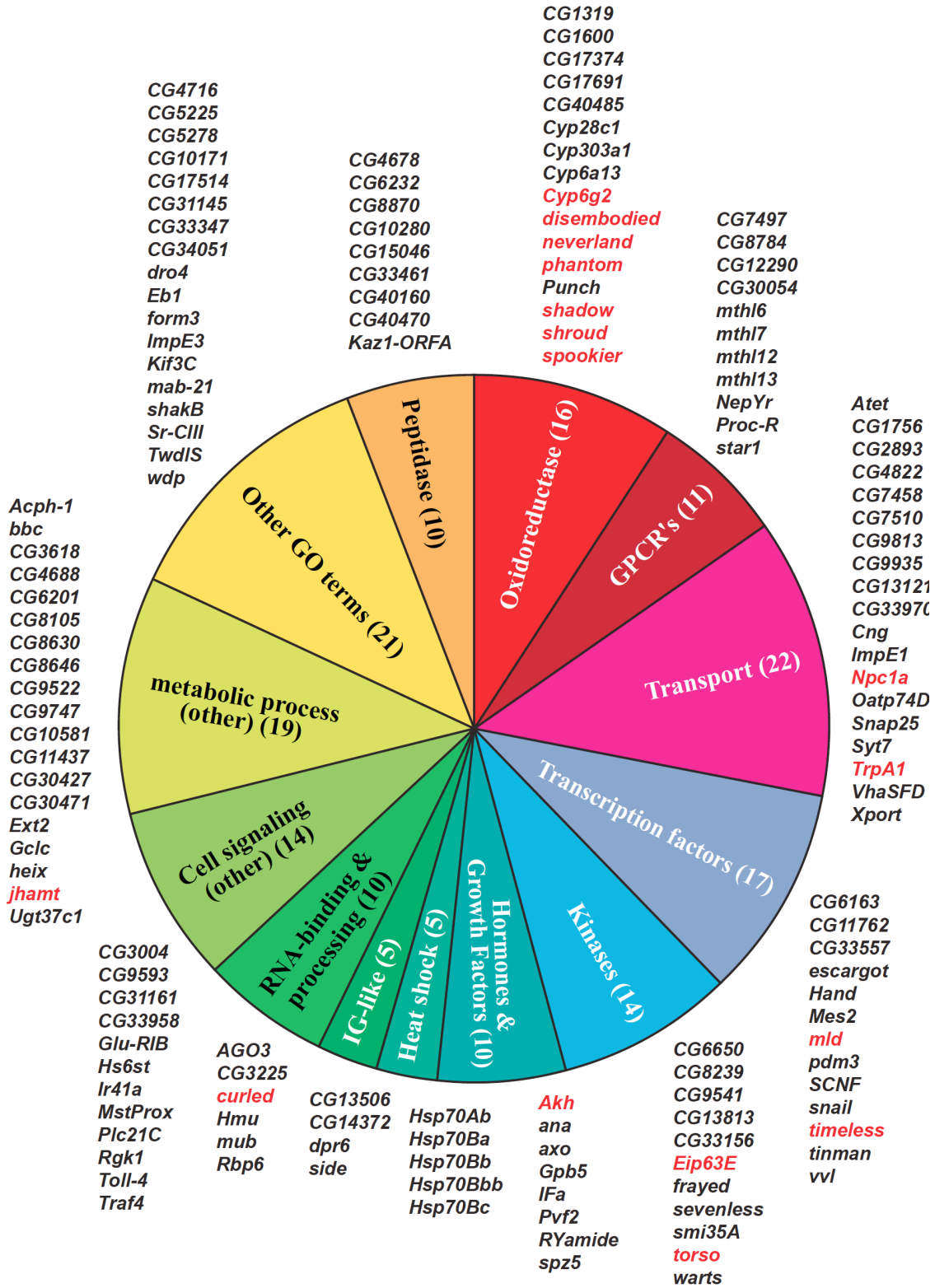


Figure 3.4A

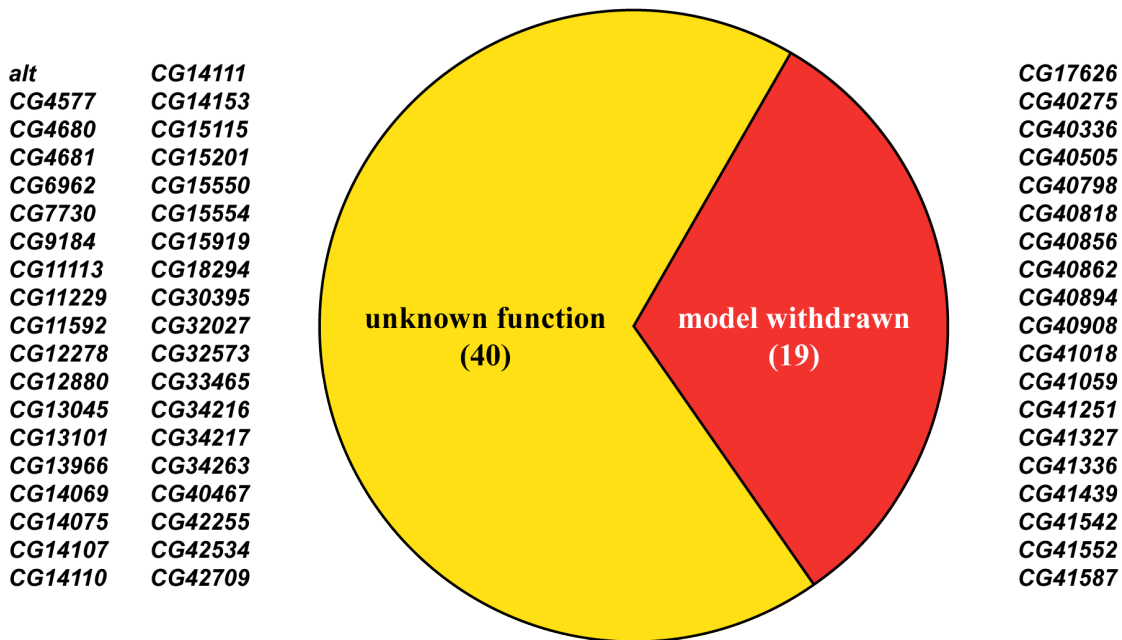


Figure 3.4B

Figure 3.4. Pie charts show the distribution of 233 ring gland-enriched transcripts representing 208 genes.

Transcripts exhibiting more than 10fold enrichment in the ring gland for at least one of the four time points are list here. Gene annotations were derived from FlyBase. Numbers of transcripts in each class are shown with genes listed. Genes that were previously described to have specific expression in the ring gland are highlighted in red.

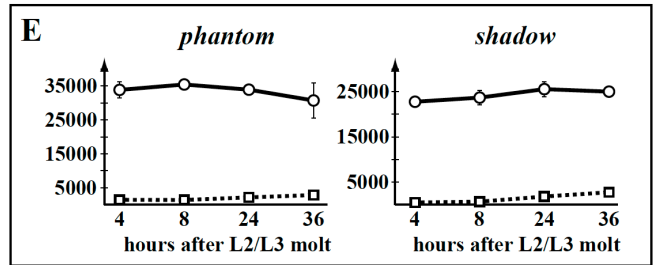
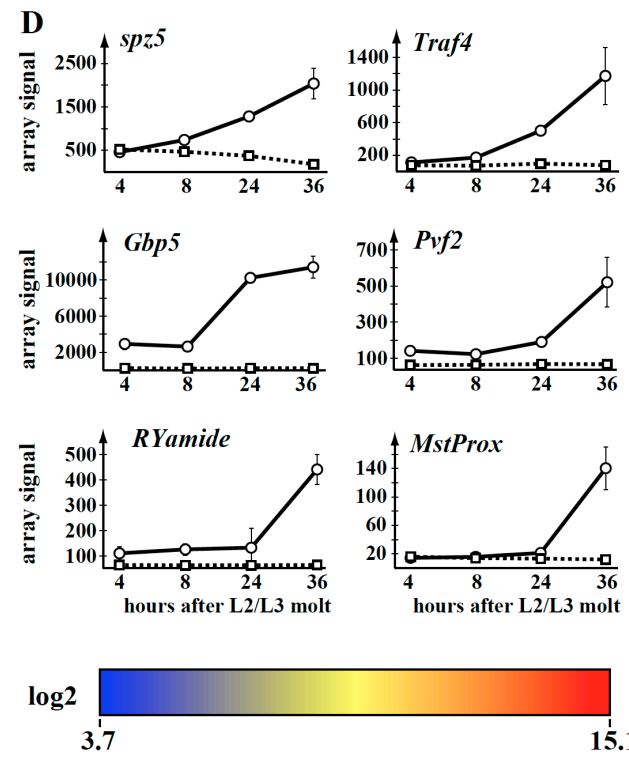
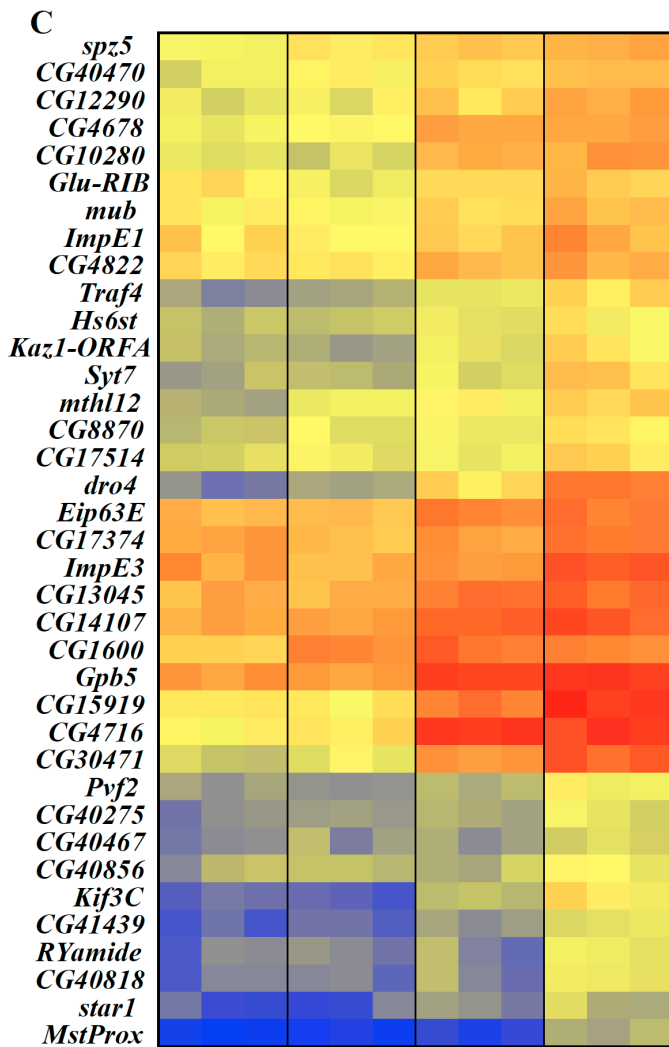
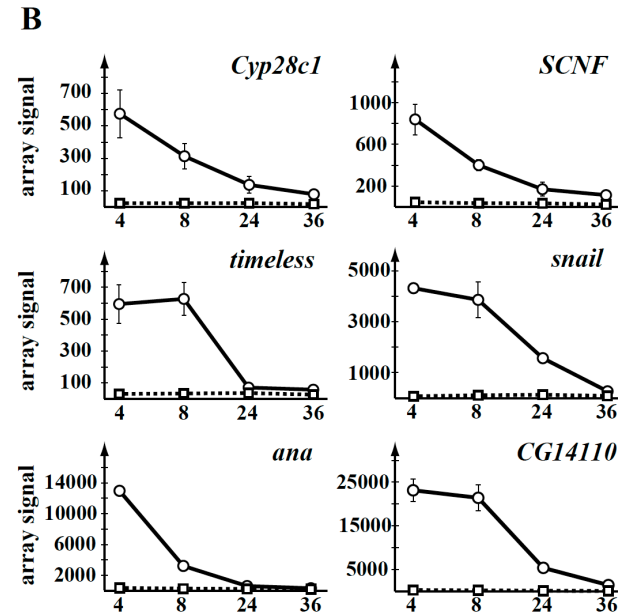
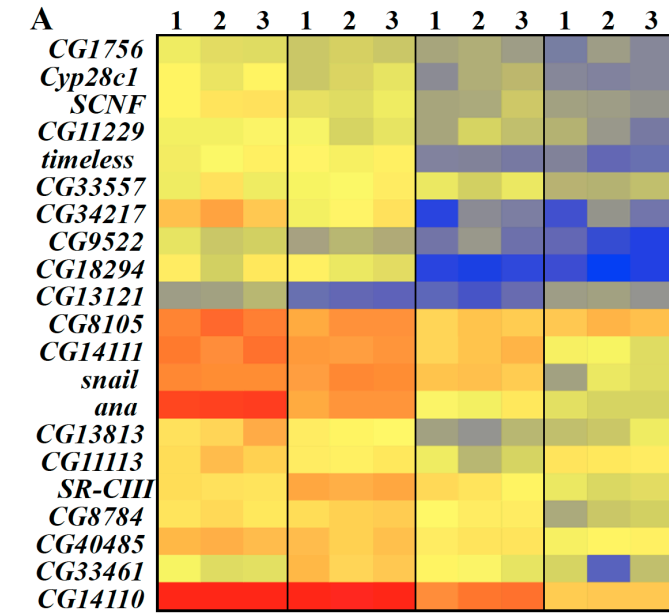
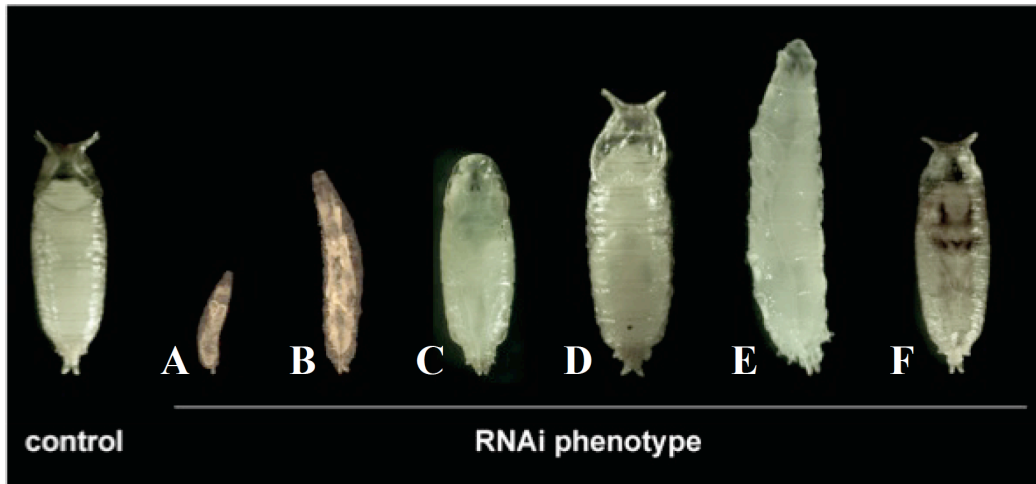


Figure 3.5. Microarray heat map of ring gland-specific transcripts that undergo dynamic changes from early L3 to late L3.

(A) Microarray heat map of 21 genes showing more than 3fold downregulation between early (either 4-hr L3 or 8-hr L3) and late (either 24-hr L3 or 36-hr L3) time points. Three biological replicates were tested per time point, represented by 1, 2, and 3 on the top of the map. (B) The expression profiles of six genes from (A). (C) Microarray heat map of 37 genes showing more than 3fold upregulation between early (either 4-hr L3 or 8-hr L3) and late (either 24-hr L3 or 36-hr L3) time points. (D) The expression profiles of six genes from (C). (E) The expression profiles of two Halloween genes, *phantom* and *shadow*. (A, C) The numbers used to generate these heat maps are the ring gland array signals (\log_2). (B, D, and E) Ring gland array signals are indicated by solid lines. Dotted lines depict whole larva array signals for each gene. Error bars represent standard deviation.



Category	RNAi phenotype
A	L1 arrest
B	L2 arrest
C	L2 pupa
D	Giant L3 pupa
E	Permanent L3 larva
F	Pupal lethality

Figure 3.6. Different categories of PG-specific RNAi phenotypes.

Examples of PG-specific RNAi knockdown phenotypes, including embryonic lethality (not shown here), early larval lethality (A and B), L2 pupae (C), giant L3 pupae (D), permanent L3 larvae (E), and pupal lethality (F).

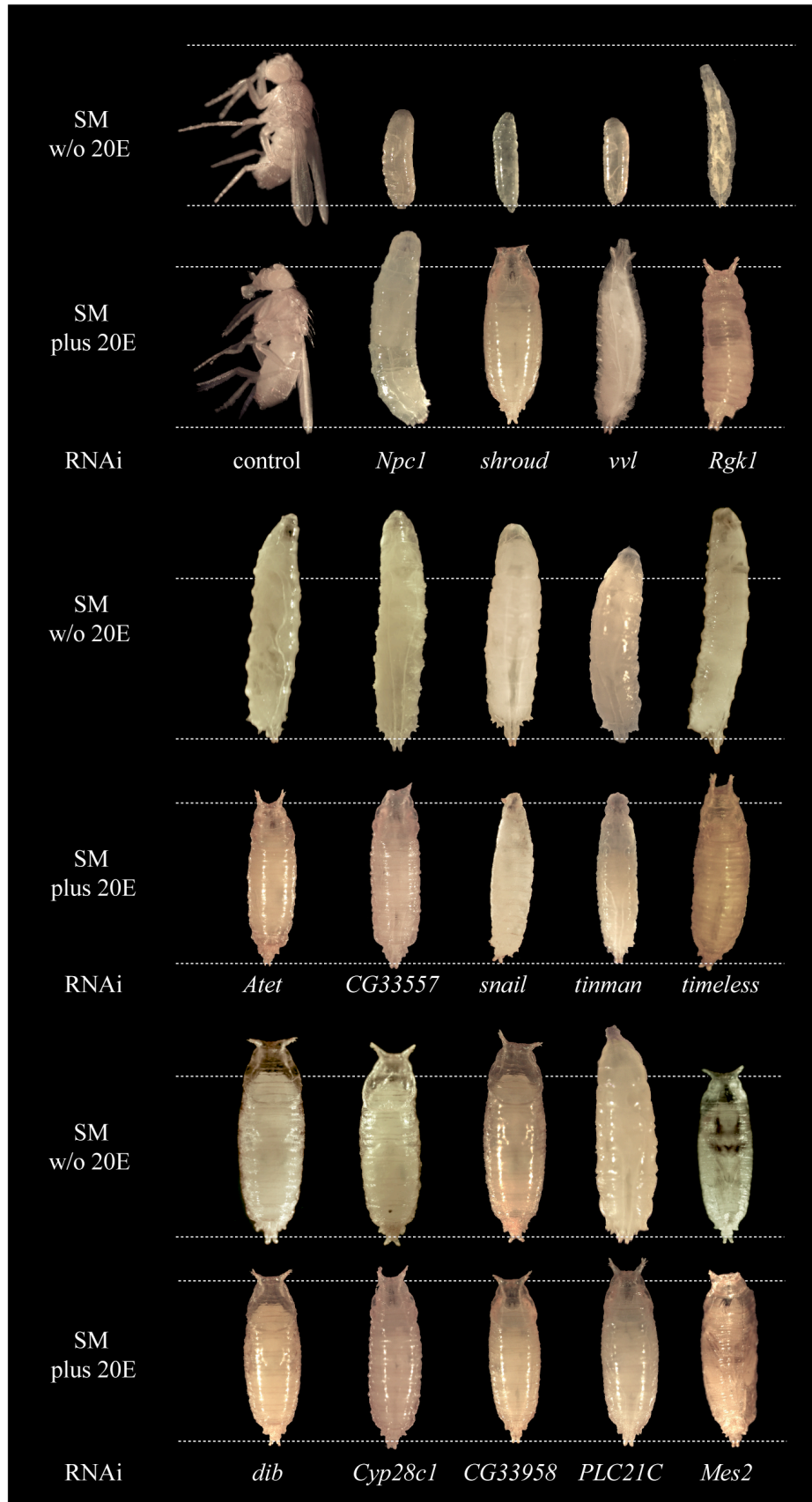


Figure 3.7. 20E rescue of PG-specific RNAi phenotypes.

Images shown indicate the furthest developmental stages that a given *phm22*>RNAi line is able to reach on standard medium (SM) or 20E-supplemented medium. Dotted lines indicate control body size. 20E, 20-hydroxyecdysone.

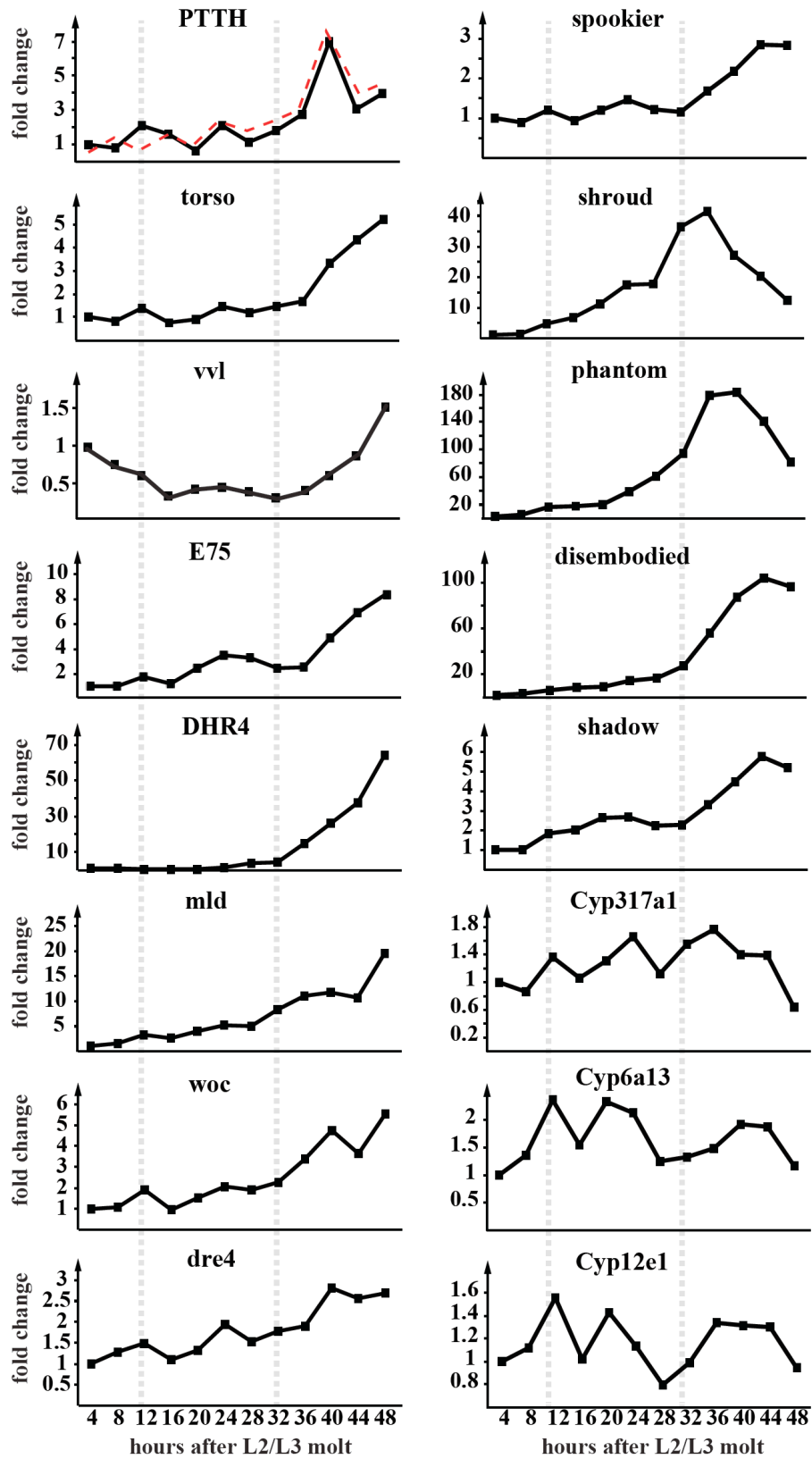


Figure 3.8A

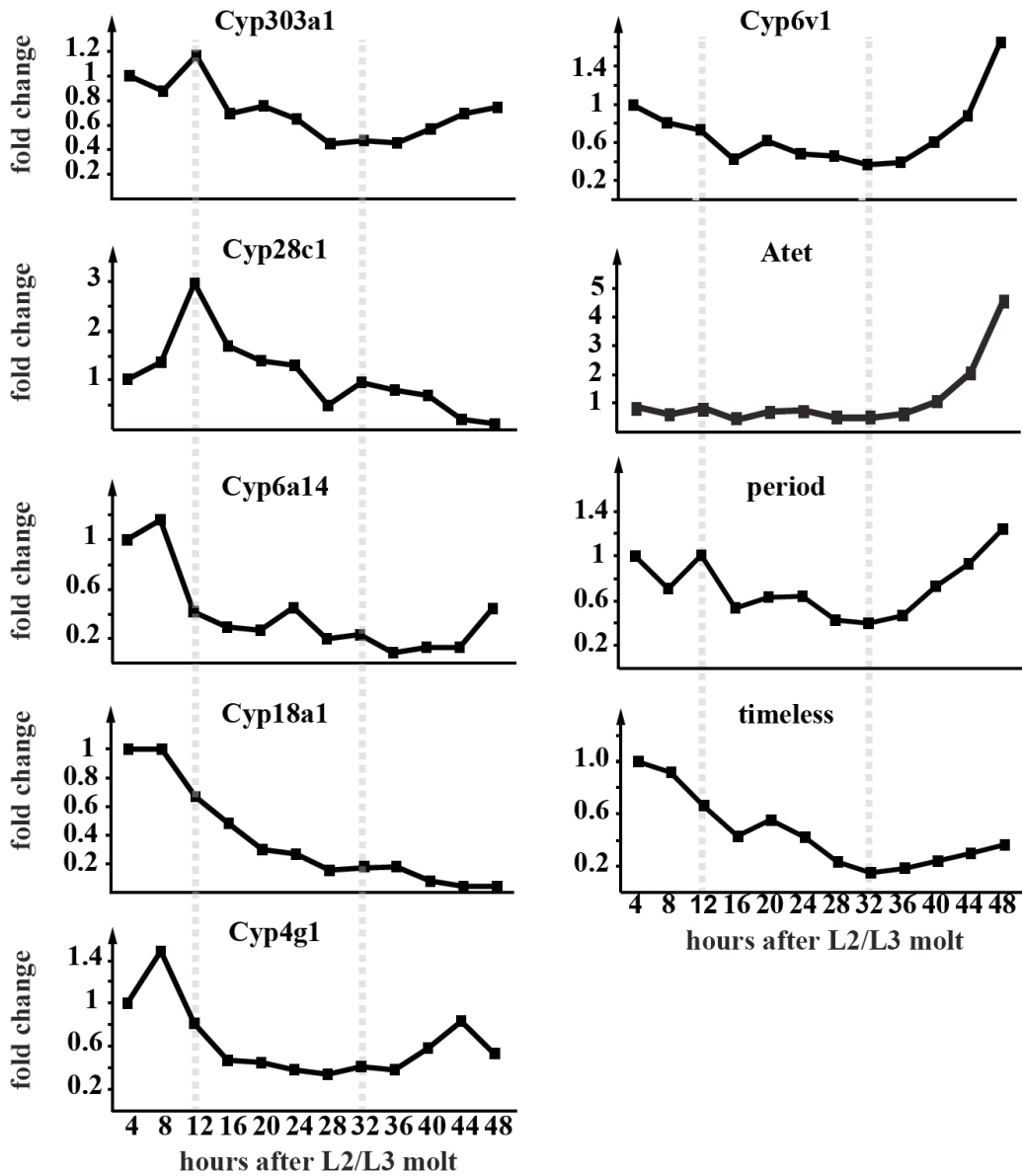
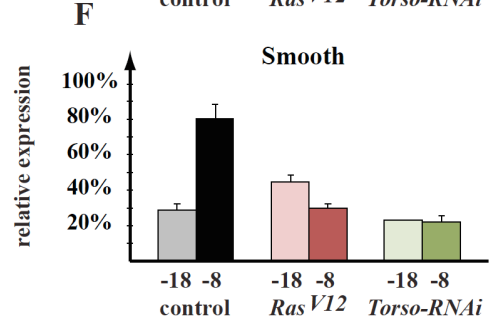
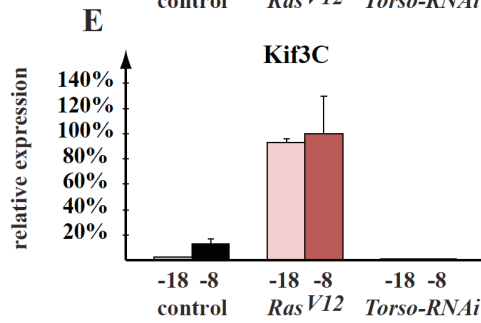
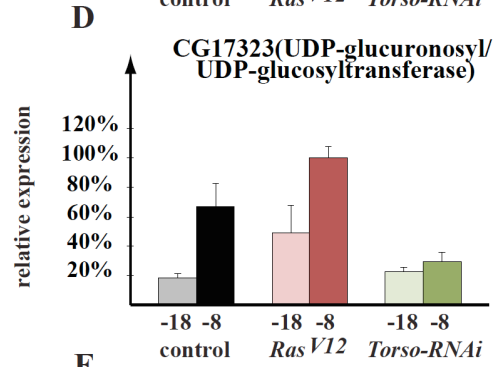
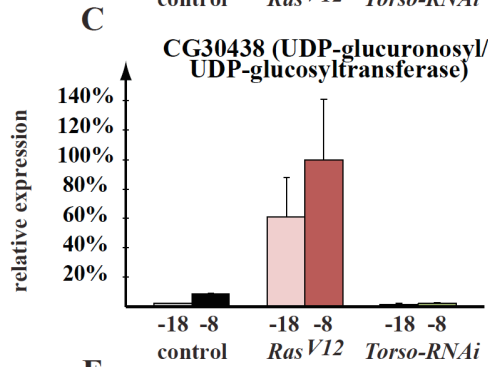
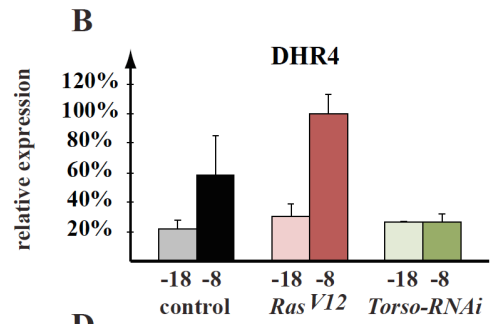
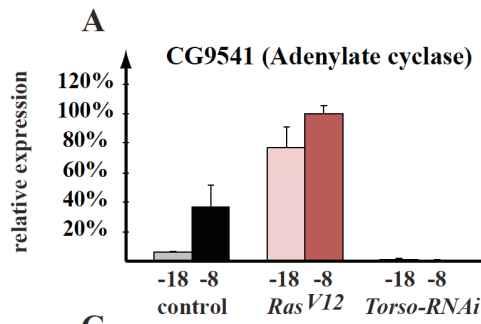


Figure 3.8B

Figure 3.8. qPCR analysis of gene expression in the brain-ring gland complex (BRRG) of L3 larvae. Data shown here represent the geometric mean of 80 measurements per time point. All fold changes were normalized to the 4-hr time point. Hours (prior to the 24-hr time point) are relative to the L2/L3 molt. Animals were resynchronized at 24 hours L3 using *Sgs*-GFP. The 48-hr L3 represents the formation of white prepupa. Grey dotted lines indicate the 12-hr L3 and the 32-hr L3 time points, which corresponds to the critical weight and the

initiation of wandering behavior, respectively. The red dashed line in (A) represents the semi-qPCR data of PTH expression in L3 larvae reported by McBrayer et al. (2007).

upregulated in controls



downregulated in controls

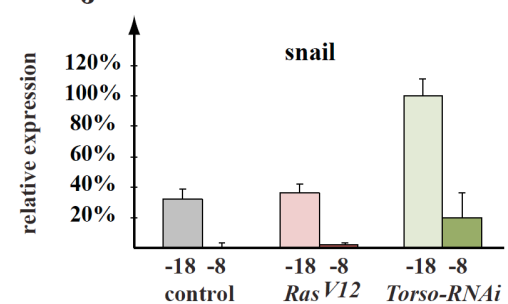
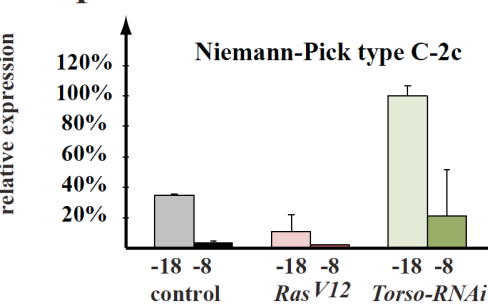
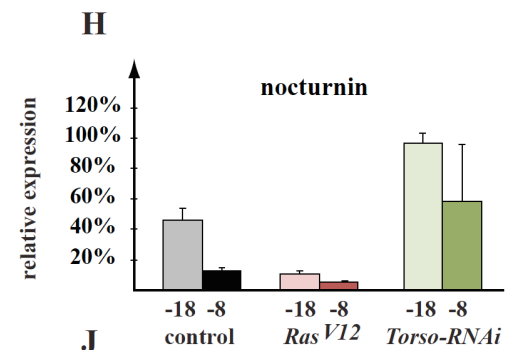
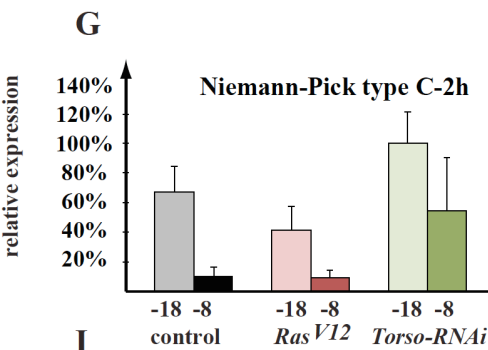


Figure 3.9. Genes affected by PTTH signaling.

Shown genes are either up- or downregulated in controls (grey and black columns), but this response is affected in *Torso*-RNAi animals (light and dark green columns). A total of 87 transcripts fulfill the filtering standard used (see **Table 3.7**), 10 genes are shown here. Results for *Ras^{V12}* transgenic animals are included as well (light and dark red columns). Transgenes are specifically expressed in the PG due to the *phm22-Gal4; UAS-Dicer* driver (see **Methods**). Numbers along the *x*-axis indicate hours before the puparium formation. Error bars represent standard deviation. Highest expression of a set was normalized to 100%.

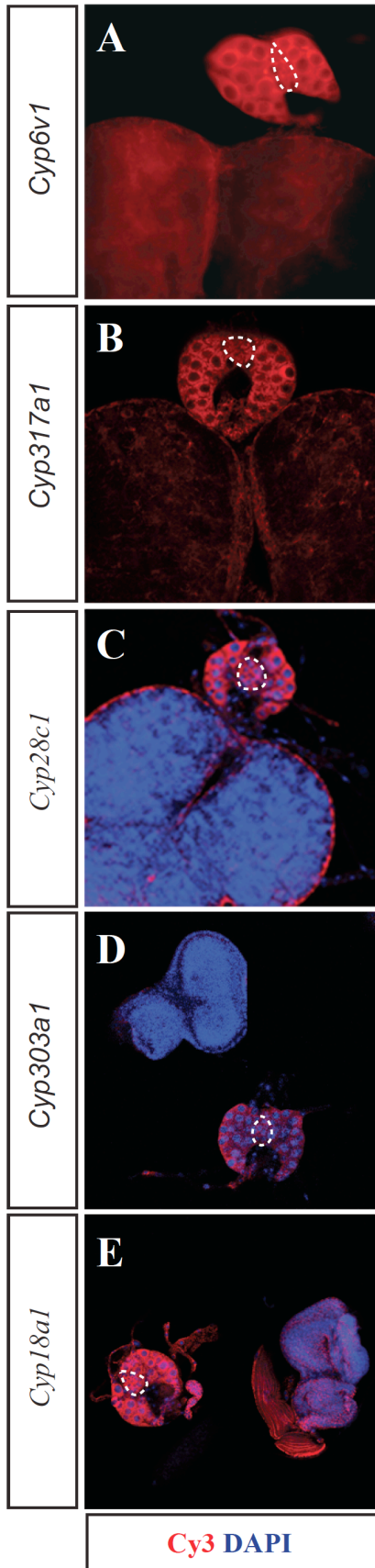


Figure 3.10. RNA *in situ* analysis of cytochrome P450 genes. Spatial patterns of the expression of five cytochrome P450 genes in the ring gland using fluorescence *in situ* hybridization (FISH). Ring glands of late wandering L3 were analyzed for *Cyp6v1* and *Cyp317a1* (A, B). Ring glands of early L3 were analyzed for *Cyp28c1*, *Cyp303a1* and *Cyp18a1* (C-E). 5 ring glands were tested per condition. A DAPI stain of nuclei is included in (C-E). The *corpus allatum* is highlighted by dotted lines.

3.8 Bibliography

- Adams, M.D., and Sekelsky, J.J. (2002). From sequence to phenotype: reverse genetics in *Drosophila melanogaster*. *Nature reviews* 3, 189-198.
- Andres, A.J., and Thummel, C.S. (1994). Methods for quantitative analysis of transcription in larvae and prepupae. *Methods Cell Biol* 44, 565-573.
- Beissbarth, T., and Speed, T.P. (2004). GOstat: find statistically overrepresented Gene Ontologies within a group of genes. *Bioinformatics* 20, 1464-1465.
- Bellen, H.J., O'Kane, C.J., Wilson, C., Grossniklaus, U., Pearson, R.K., and Gehring, W.J. (1989). P-element-mediated enhancer detection: a versatile method to study development in *Drosophila*. *Genes & development* 3, 1288-1300.
- Bellen, H.J., Vaessin, H., Bier, E., Kolodkin, A., D'Evelyn, D., Kooyer, S., and Jan, Y.N. (1992). The *Drosophila* couch potato gene: an essential gene required for normal adult behavior. *Genetics* 131, 365-375.
- Biyasheva, A., Do, T.V., Lu, Y., Vaskova, M., and Andres, A.J. (2001). Glue secretion in the *Drosophila* salivary gland: a model for steroid-regulated exocytosis. *Developmental biology* 231, 234-251.
- Boedigheimer, M., Bryant, P., and Laughon, A. (1993). Expanded, a negative regulator of cell proliferation in *Drosophila*, shows homology to the NF2 tumor suppressor. *Mechanisms of development* 44, 83-84.
- Boedigheimer, M., and Laughon, A. (1993). Expanded: a gene involved in the control of cell proliferation in imaginal discs. *Development (Cambridge, England)* 118, 1291-1301.
- Bolstad, B.M., Irizarry, R.A., Astrand, M., and Speed, T.P. (2003). A comparison of normalization methods for high density oligonucleotide array data based on variance and bias. *Bioinformatics* 19, 185-193.
- Brody, T., and Cravchik, A. (2000). *Drosophila melanogaster* G protein-coupled receptors. *The Journal of cell biology* 150, F83-88.
- Brummel, T., Abdollah, S., Haerry, T.E., Shimell, M.J., Merriam, J., Raftery, L., Wrana, J.L., and O'Connor, M.B. (1999). The *Drosophila* activin receptor baboon signals through dSmad2 and controls cell proliferation but not patterning during larval development. *Genes & development* 13, 98-111.
- Bunney, T.D., and Katan, M. (2011). PLC regulation: emerging pictures for molecular mechanisms. *Trends Biochem Sci* 36, 88-96.
- Caceres, L., Necakov, A.S., Schwartz, C., Kimber, S., Roberts, I.J., and Krause, H.M. (2011). Nitric oxide coordinates metabolism, growth, and development via the nuclear receptor E75. *Genes & development* 25, 1476-1485.
- Chavez, V.M., Marques, G., Delbecque, J.P., Kobayashi, K., Hollingsworth, M., Burr, J., Natzle, J.E., and O'Connor, M.B. (2000). The *Drosophila* disembodied gene controls late embryonic morphogenesis and codes for a cytochrome P450 enzyme that regulates embryonic ecdysone levels. *Development (Cambridge, England)* 127, 4115-4126.
- Chintapalli, V.R., Wang, J., and Dow, J.A. (2007). Using FlyAtlas to identify better *Drosophila melanogaster* models of human disease. *Nat Genet* 39, 715-720.

- Chung, H., Sztal, T., Pasricha, S., Sridhar, M., Batterham, P., and Daborn, P.J. (2009). Characterization of *Drosophila melanogaster* cytochrome P450 genes. *Proceedings of the National Academy of Sciences of the United States of America* *106*, 5731-5736.
- Chung, H.R., Schafer, U., Jackle, H., and Bohm, S. (2002). Genomic expansion and clustering of ZAD-containing C2H2 zinc-finger genes in *Drosophila*. *EMBO Rep* *3*, 1158-1162.
- Cirelli, C., LaVaute, T.M., and Tononi, G. (2005). Sleep and wakefulness modulate gene expression in *Drosophila*. *J Neurochem* *94*, 1411-1419.
- Colombani, J., Bianchini, L., Layalle, S., Pondeville, E., Dauphin-Villemant, C., Antoniewski, C., Carre, C., Noselli, S., and Leopold, P. (2005). Antagonistic actions of ecdysone and insulins determine final size in *Drosophila*. *Science (New York, NY)* *310*, 667-670.
- Correll, R.N., Pang, C., Niedowicz, D.M., Finlin, B.S., and Andres, D.A. (2008). The RGK family of GTP-binding proteins: regulators of voltage-dependent calcium channels and cytoskeleton remodeling. *Cell Signal* *20*, 292-300.
- Cvejic, S., Zhu, Z., Felice, S.J., Berman, Y., and Huang, X.Y. (2004). The endogenous ligand Stunted of the GPCR Methuselah extends lifespan in *Drosophila*. *Nature cell biology* *6*, 540-546.
- Davidowitz, G., D'Amico, L.J., and Nijhout, H.F. (2003). Critical weight in the development of insect body size. *Evolution & development* *5*, 188-197.
- Dean, M., Rzhetsky, A., and Allikmets, R. (2001). The human ATP-binding cassette (ABC) transporter superfamily, pp. 1156-1166.
- Ebens, A.J., Garren, H., Cheyette, B.N., and Zipursky, S.L. (1993). The *Drosophila* anachronism locus: a glycoprotein secreted by glia inhibits neuroblast proliferation. *Cell* *74*, 15-27.
- Emery, I.F., Noveral, J.M., Jamison, C.F., and Siwicki, K.K. (1997). Rhythms of *Drosophila* period gene expression in culture. *Proceedings of the National Academy of Sciences of the United States of America* *94*, 4092-4096.
- Freeman, M.R., Dobritsa, A., Gaines, P., Segraves, W.A., and Carlson, J.R. (1999). The dare gene: steroid hormone production, olfactory behavior, and neural degeneration in *Drosophila*. *Development (Cambridge, England)* *126*, 4591-4602.
- Fuse, N., Hirose, S., and Hayashi, S. (1996). Determination of wing cell fate by the escargot and snail genes in *Drosophila*. *Development (Cambridge, England)* *122*, 1059-1067.
- Garofalo, R.S. (2002). Genetic analysis of insulin signaling in *Drosophila*. *Trends in endocrinology and metabolism: TEM* *13*, 156-162.
- Gibbens, Y.Y., Warren, J.T., Gilbert, L.I., and O'Connor, M.B. (2011). Neuroendocrine regulation of *Drosophila* metamorphosis requires TGFbeta/Activin signaling. *Development (Cambridge, England)* *138*, 2693-2703.
- Giesen, K., Hummel, T., Stollewerk, A., Harrison, S., Travers, A., and Klambt, C. (1997). Glial development in the *Drosophila* CNS requires concomitant activation of glial and repression of neuronal differentiation genes. *Development (Cambridge, England)* *124*, 2307-2316.
- Gilbert, L.I. (2004). Halloween genes encode P450 enzymes that mediate steroid hormone biosynthesis in *Drosophila melanogaster*. *Molecular and cellular endocrinology* *215*,

1-10.

- Gilbert, L.I., Combest, W.L., Smith, W.A., Meller, V.H., and Rountree, D.B. (1988). Neuropeptides, second messengers and insect molting. *Bioessays* *8*, 153-157.
- Gilbert, L.I., Rybczynski, R., and Warren, J.T. (2002). Control and biochemical nature of the ecdysteroidogenic pathway. *Annual review of entomology* *47*, 883-916.
- Grossniklaus, U., Bellen, H.J., Wilson, C., and Gehring, W.J. (1989). P-element-mediated enhancer detection applied to the study of oogenesis in *Drosophila*. *Development (Cambridge, England)* *107*, 189-200.
- Guittard, E., Blais, C., Maria, A., Parvy, J.P., Pasricha, S., Lumb, C., Lafont, R., Daborn, P.J., and Dauphin-Villemant, C. (2011). CYP18A1, a key enzyme of *Drosophila* steroid hormone inactivation, is essential for metamorphosis. *Developmental biology* *349*, 35-45.
- Gutierrez, E., Wiggins, D., Fielding, B., and Gould, A.P. (2007). Specialized hepatocyte-like cells regulate *Drosophila* lipid metabolism. *Nature* *445*, 275-280.
- Han, Z., and Olson, E.N. (2005). Hand is a direct target of Tinman and GATA factors during *Drosophila* cardiogenesis and hematopoiesis. *Development (Cambridge, England)* *132*, 3525-3536.
- Harvie, P.D., Filippova, M., and Bryant, P.J. (1998). Genes expressed in the ring gland, the major endocrine organ of *Drosophila melanogaster*. *Genetics* *149*, 217-231.
- Henrich, V.C. (1995). Comparison of ecdysteroid production in *Drosophila* and *Manduca*: pharmacology and cross-species neural reactivity. *Archives of insect biochemistry and physiology* *30*, 239-254.
- Hietakangas, V., and Cohen, S.M. (2009). Regulation of tissue growth through nutrient sensing. *Annu Rev Genet* *43*, 389-410.
- Higgins, C.F. (1992). ABC transporters: from microorganisms to man. *Annu Rev Cell Biol* *8*, 67-113.
- Hovemann, B., Richter, S., Walldorf, U., and Cziepluch, C. (1988). Two genes encode related cytoplasmic elongation factors 1 alpha (EF-1 alpha) in *Drosophila melanogaster* with continuous and stage specific expression. *Nucleic acids research* *16*, 3175-3194.
- Hsu, W.H., Xiang, H.D., Rajan, A.S., Kunze, D.L., and Boyd, A.E., 3rd (1991). Somatostatin inhibits insulin secretion by a G-protein-mediated decrease in Ca²⁺ entry through voltage-dependent Ca²⁺ channels in the beta cell. *The Journal of biological chemistry* *266*, 837-843.
- Huang, X., Suyama, K., Buchanan, J., Zhu, A.J., and Scott, M.P. (2005). A *Drosophila* model of the Niemann-Pick type C lysosome storage disease: *dnpc1a* is required for molting and sterol homeostasis. *Development (Cambridge, England)* *132*, 5115-5124.
- Hunter, S., Jones, P., Mitchell, A., Apweiler, R., Attwood, T.K., Bateman, A., Bernard, T., Binns, D., Bork, P., Burge, S., *et al.* (2012). InterPro in 2011: new developments in the family and domain prediction database. *Nucleic acids research* *40*, D306-312.
- Huss, W.J., Gray, D.R., Greenberg, N.M., Mohler, J.L., and Smith, G.J. (2005). Breast cancer resistance protein-mediated efflux of androgen in putative benign and malignant prostate stem cells. *Cancer research* *65*, 6640-6650.

- Ida, T., Takahashi, T., Tominaga, H., Sato, T., Kume, K., Ozaki, M., Hiraguchi, T., Maeda, T., Shiotani, H., Terajima, S., *et al.* (2011). Identification of the novel bioactive peptides dRYamide-1 and dRYamide-2, ligands for a neuropeptide Y-like receptor in *Drosophila*. *Biochemical and biophysical research communications* *410*, 872-877.
- Ikonen, E. (2008). Cellular cholesterol trafficking and compartmentalization. *Nat Rev Mol Cell Biol* *9*, 125-138.
- Imai, Y., Asada, S., Tsukahara, S., Ishikawa, E., Tsuruo, T., and Sugimoto, Y. (2003). Breast cancer resistance protein exports sulfated estrogens but not free estrogens. *Mol Pharmacol* *64*, 610-618.
- Inbal, A., Levanon, D., and Salzberg, A. (2003). Multiple roles for u-turn/ventral veinless in the development of *Drosophila* PNS. *Development (Cambridge, England)* *130*, 2467-2478.
- Ishibashi, J., Kataoka, H., Isogai, A., Kawakami, A., Saegusa, H., Yagi, Y., Mizoguchi, A., Ishizaki, H., and Suzuki, A. (1994). Assignment of disulfide bond location in prothoracicotropic hormone of the silkworm, *Bombyx mori*: a homodimeric peptide. *Biochemistry* *33*, 5912-5919.
- Ishizaki, H., and Suzuki, A. (1994). The brain secretory peptides that control moulting and metamorphosis of the silkworm, *Bombyx mori*. *The International journal of developmental biology* *38*, 301-310.
- Janning, W. (1997). FlyView, a *Drosophila* image database, and other *Drosophila* databases. *Seminars in cell & developmental biology* *8*, 469-475.
- Jefcoate, C.R., McNamara, B.C., and DiBartolomeis, M.J. (1986). Control of steroid synthesis in adrenal fasciculata cells. *Endocr Res* *12*, 315-350.
- Kavanagh, K.L., Jornvall, H., Persson, B., and Oppermann, U. (2008). Medium- and short-chain dehydrogenase/reductase gene and protein families : the SDR superfamily: functional and structural diversity within a family of metabolic and regulatory enzymes. *Cell Mol Life Sci* *65*, 3895-3906.
- Kennedy, M.A., Barrera, G.C., Nakamura, K., Baldan, A., Tarr, P., Fishbein, M.C., Frank, J., Francone, O.L., and Edwards, P.A. (2005). ABCG1 has a critical role in mediating cholesterol efflux to HDL and preventing cellular lipid accumulation. *Cell metabolism* *1*, 121-131.
- Kim, S.E., Cho, J.Y., Kim, K.S., Lee, S.J., Lee, K.H., and Choi, K.Y. (2004). *Drosophila* PI3 kinase and Akt involved in insulin-stimulated proliferation and ERK pathway activation in Schneider cells. *Cell Signal* *16*, 1309-1317.
- King-Jones, K., and Thummel, C.S. (2005). Nuclear receptors--a perspective from *Drosophila*. *Nature reviews* *6*, 311-323.
- Kiriishi, S., Nagasawa, H., Kataoka, H., Suzuki, A., and Sakurai, S. (1992). Comparison of the in vivo and in vitro effects of bombyxin and prothoracicotropic hormone on prothoracic glands of the silkworm, *Bombyx mori*. *Zool Sci* *9*, 149-155.
- Koelle, M.R., Talbot, W.S., Segreaves, W.A., Bender, M.T., Cherbas, P., and Hogness, D.S. (1991). The *Drosophila* EcR gene encodes an ecdysone receptor, a new member of the steroid receptor superfamily. *Cell* *67*, 59-77.

- Kuwana, H., Shimizu-Nishikawa, K., Iwahana, H., and Yamamoto, D. (1996). Molecular cloning and characterization of the ABC transporter expressed in Trachea (ATET) gene from *Drosophila melanogaster*. *Biochimica et biophysica acta* *1309*, 47-52.
- Kwon, H.B., Kim, S.H., Kim, S.E., Jang, I.H., Ahn, Y., Lee, W.J., and Choi, K.Y. (2002). *Drosophila* extracellular signal-regulated kinase involves the insulin-mediated proliferation of Schneider cells. *The Journal of biological chemistry* *277*, 14853-14858.
- Lane, M.E., and Kalderon, D. (1993). Genetic investigation of cAMP-dependent protein kinase function in *Drosophila* development. *Genes & development* *7*, 1229-1243.
- Lee, G., and Park, J.H. (2004). Hemolymph sugar homeostasis and starvation-induced hyperactivity affected by genetic manipulations of the adipokinetic hormone-encoding gene in *Drosophila melanogaster*. *Genetics* *167*, 311-323.
- Leptin, M. (1991). twist and snail as positive and negative regulators during *Drosophila* mesoderm development. *Genes & development* *5*, 1568-1576.
- Lin, Y.J., Seroude, L., and Benzer, S. (1998). Extended life-span and stress resistance in the *Drosophila* mutant methuselah. *Science (New York, NY)* *282*, 943-946.
- Llimargas, M., and Casanova, J. (1997). ventral veinless, a POU domain transcription factor, regulates different transduction pathways required for tracheal branching in *Drosophila*. *Development (Cambridge, England)* *124*, 3273-3281.
- Lloyd, T.E., Verstreken, P., Ostrin, E.J., Phillippi, A., Lichtarge, O., and Bellen, H.J. (2000). A genome-wide search for synaptic vesicle cycle proteins in *Drosophila*. *Neuron* *26*, 45-50.
- Maroni, G.a.S., C (1983). Use of blue food to select synchronous late third instar larvae. *Drosophila Information Service* *59*, 142-143.
- McBrayer, Z., Ono, H., Shimell, M., Parvy, J.P., Beckstead, R.B., Warren, J.T., Thummel, C.S., Dauphin-Villemant, C., Gilbert, L.I., and O'Connor, M.B. (2007). Prothoracicotropic hormone regulates developmental timing and body size in *Drosophila*. *Developmental cell* *13*, 857-871.
- Meier, S., Sprecher, S.G., Reichert, H., and Hirth, F. (2006). ventral veins lacking is required for specification of the tritocerebrum in embryonic brain development of *Drosophila*. *Mechanisms of development* *123*, 76-83.
- Mirth, C., Truman, J.W., and Riddiford, L.M. (2005). The role of the prothoracic gland in determining critical weight for metamorphosis in *Drosophila melanogaster*. *Curr Biol* *15*, 1796-1807.
- Mlodzik, M., and Hiromi, Y. (1992). Enhancer trap method in *Drosophila*: its application to neurobiology. *Methods in Neurobiology 9: Gene Expression in Neural Tissues*, edited by P.M. Conn. Academic Press, New York, 397-414.
- Myers, E.M., Yu, J., and Sehgal, A. (2003). Circadian control of eclosion: interaction between a central and peripheral clock in *Drosophila melanogaster*. *Curr Biol* *13*, 526-533.
- Nagasawa, H., Kataoka, H., Isogai, A., Tamura, S., Suzuki, A., Mizoguchi, A., Fujiwara, Y., Takahashi, S.Y., and Ishizaki, H. (1986). Amino acid sequence of a prothoracicotropic hormone of the silkworm *Bombyx mori*. *Proceedings of the National Academy of Sciences of the United States of America* *83*, 5840-5843.

- Neubueser, D., Warren, J.T., Gilbert, L.I., and Cohen, S.M. (2005). molting defective is required for ecdysone biosynthesis. *Developmental biology* 280, 362-372.
- Niwa, R., Namiki, T., Ito, K., Shimada-Niwa, Y., Kiuchi, M., Kawaoka, S., Kayukawa, T., Banno, Y., Fujimoto, Y., Shigenobu, S., *et al.* (2010). Non-molting glossy/shroud encodes a short-chain dehydrogenase/reductase that functions in the 'Black Box' of the ecdysteroid biosynthesis pathway. *Development (Cambridge, England)* 137, 1991-1999.
- Niwa, R., Sakudoh, T., Matsuya, T., Namiki, T., Kasai, S., Tomita, T., and H., K. (2011). Expressions of the cytochrome P450 monooxygenase gene Cyp4g1 and its homolog in the prothoracic glands of the fruit fly *Drosophila melanogaster* (Diptera: Drosophilidae) and the silkworm *Bombyx mori* (Lepidoptera: Bombycidae). *Applied Entomology and Zoology* 46, 533-543.
- Niwa, R., Sakudoh, T., Namiki, T., Saida, K., Fujimoto, Y., and Kataoka, H. (2005). The ecdysteroidogenic P450 Cyp302a1/disembodied from the silkworm, *Bombyx mori*, is transcriptionally regulated by prothoracicotropic hormone. *Insect molecular biology* 14, 563-571.
- Nusslein-Volhard, C., and Wieschaus, E. (1980). Mutations affecting segment number and polarity in *Drosophila*. *Nature* 287, 795-801.
- O'Kane, C.J., and Gehring, W.J. (1987). Detection in situ of genomic regulatory elements in *Drosophila*. *Proceedings of the National Academy of Sciences of the United States of America* 84, 9123-9127.
- Oldham, S., and Hafen, E. (2003). Insulin/IGF and target of rapamycin signaling: a TOR de force in growth control. *Trends in cell biology* 13, 79-85.
- Ono, H., Rewitz, K.F., Shinoda, T., Itoyama, K., Petryk, A., Rybczynski, R., Jarcho, M., Warren, J.T., Marques, G., Shimell, M.J., *et al.* (2006). Spook and Spookier code for stage-specific components of the ecdysone biosynthetic pathway in Diptera. *Developmental biology* 298, 555-570.
- Ou, Q., Magico, A., and King-Jones, K. (2011). Nuclear receptor DHR4 controls the timing of steroid hormone pulses during *Drosophila* development. *PLoS biology* 9, e1001160.
- Park, S., Bustamante, E.L., Antonova, J., McLean, G.W., and Kim, S.K. (2011). Specification of *Drosophila corpora cardiaca* neuroendocrine cells from mesoderm is regulated by Notch signaling. *PLoS genetics* 7, e1002241.
- Parvy, J.P., Blais, C., Bernard, F., Warren, J.T., Petryk, A., Gilbert, L.I., O'Connor, M.B., and Dauphin-Villemant, C. (2005). A role for betaFTZ-F1 in regulating ecdysteroid titers during post-embryonic development in *Drosophila melanogaster*. *Developmental biology* 282, 84-94.
- Pascal, L.E., Oudes, A.J., Petersen, T.W., Goo, Y.A., Walashek, L.S., True, L.D., and Liu, A.Y. (2007). Molecular and cellular characterization of ABCG2 in the prostate. *BMC Urol* 7, 6.
- Patel, M.V., Hallal, D.A., Jones, J.W., Bronner, D.N., Zein, R., Caravas, J., Husain, Z., Friedrich, M., and Vanberkum, M.F. (2012). Dramatic expansion and developmental expression diversification of the methuselah gene family during recent *Drosophila* evolution. *J Exp*

- Zool B Mol Dev Evol 318, 368-387.
- Petryk, A., Warren, J.T., Marques, G., Jarcho, M.P., Gilbert, L.I., Kahler, J., Parvy, J.P., Li, Y., Dauphin-Villemant, C., and O'Connor, M.B. (2003). Shade is the *Drosophila* P450 enzyme that mediates the hydroxylation of ecdysone to the steroid insect molting hormone 20-hydroxyecdysone. *Proceedings of the National Academy of Sciences of the United States of America* 100, 13773-13778.
- Rewitz, K.F., Yamanaka, N., Gilbert, L.I., and O'Connor, M.B. (2009). The insect neuropeptide PTH activates receptor tyrosine kinase torso to initiate metamorphosis. *Science (New York, NY)* 326, 1403-1405.
- Rewitz, K.F., Yamanaka, N., and O'Connor, M.B. (2010). Steroid hormone inactivation is required during the juvenile-adult transition in *Drosophila*. *Developmental cell* 19, 895-902.
- Riddiford, L.M. (1993). Hormone receptors and the regulation of insect metamorphosis. *Receptor* 3, 203-209.
- Roth, G.E., Gierl, M.S., Vollborn, L., Meise, M., Lintermann, R., and Korge, G. (2004). The *Drosophila* gene *Start1*: a putative cholesterol transporter and key regulator of ecdysteroid synthesis. *Proceedings of the National Academy of Sciences of the United States of America* 101, 1601-1606.
- Schmierer, B., and Hill, C.S. (2007). TGFbeta-SMAD signal transduction: molecular specificity and functional flexibility. *Nat Rev Mol Cell Biol* 8, 970-982.
- Smibert, P., and Saint, R. (2003). Characterisation of the developmental and cellular roles of the *Drosophila melanogaster* RGK GTPase family. Program and Abstracts 44th Annual *Drosophila* Research Conference, Chicago, 2003, 226A.
- Suster, M.L., and Bate, M. (2002). Embryonic assembly of a central pattern generator without sensory input. *Nature* 416, 174-178.
- Tautz, D., and Pfeifle, C. (1989). A non-radioactive in situ hybridization method for the localization of specific RNAs in *Drosophila* embryos reveals translational control of the segmentation gene *hunchback*. *Chromosoma* 98, 81-85.
- Thomas, H.E., Stunnenberg, H.G., and Stewart, A.F. (1993). Heterodimerization of the *Drosophila* ecdysone receptor with retinoid X receptor and ultraspiracle. *Nature* 362, 471-475.
- van Hille, B., Vanek, M., Richener, H., Green, J.R., and Bilbe, G. (1993). Cloning and tissue distribution of subunits C, D, and E of the human vacuolar H(+)-ATPase. *Biochemical and biophysical research communications* 197, 15-21.
- Velamakanni, S., Wei, S.L., Janvilisri, T., and van Veen, H.W. (2007). ABCG transporters: structure, substrate specificities and physiological roles : a brief overview. *J Bioenerg Biomembr* 39, 465-471.
- Wang, N., Lan, D., Chen, W., Matsuura, F., and Tall, A.R. (2004). ATP-binding cassette transporters G1 and G4 mediate cellular cholesterol efflux to high-density lipoproteins. *Proceedings of the National Academy of Sciences of the United States of America* 101, 9774-9779.
- Warren, J.T., Petryk, A., Marques, G., Jarcho, M., Parvy, J.P., Dauphin-Villemant, C., O'Connor, M.B., and Gilbert, L.I. (2002). Molecular and biochemical characterization of two P450

- enzymes in the ecdysteroidogenic pathway of *Drosophila melanogaster*. *Proceedings of the National Academy of Sciences of the United States of America* *99*, 11043-11048.
- Warren, J.T., Petryk, A., Marques, G., Parvy, J.P., Shinoda, T., Itoyama, K., Kobayashi, J., Jarcho, M., Li, Y., O'Connor, M.B., *et al.* (2004). Phantom encodes the 25-hydroxylase of *Drosophila melanogaster* and *Bombyx mori*: a P450 enzyme critical in ecdysone biosynthesis. *Insect biochemistry and molecular biology* *34*, 991-1010.
- Warren, J.T., Yerushalmi, Y., Shimell, M.J., O'Connor, M.B., Restifo, L.L., and Gilbert, L.I. (2006). Discrete pulses of molting hormone, 20-hydroxyecdysone, during late larval development of *Drosophila melanogaster*: correlations with changes in gene activity. *Dev Dyn* *235*, 315-326.
- Wasserman, S.A. (2000). Toll signaling: the enigma variations, pp. 497-502.
- Wilson, C., Pearson, R.K., Bellen, H.J., O'Kane, C.J., Grossniklaus, U., and Gehring, W.J. (1989). P-element-mediated enhancer detection: an efficient method for isolating and characterizing developmentally regulated genes in *Drosophila*. *Genes & development* *3*, 1301-1313.
- Yao, T.P., Forman, B.M., Jiang, Z., Cherbas, L., Chen, J.D., McKeown, M., Cherbas, P., and Evans, R.M. (1993). Functional ecdysone receptor is the product of *EcR* and *Ultraspiracle* genes. *Nature* *366*, 476-479.
- Yoshiyama, T., Namiki, T., Mita, K., Kataoka, H., and Niwa, R. (2006). Neverland is an evolutionally conserved Rieske-domain protein that is essential for ecdysone synthesis and insect growth. *Development (Cambridge, England)* *133*, 2565-2574.
- Zhou, X., Zhou, B., Truman, J.W., and Riddiford, L.M. (2004). Overexpression of broad: a new insight into its role in the *Drosophila* prothoracic gland cells. *The Journal of experimental biology* *207*, 1151-1161.
- Zhu, B., Pennack, J.A., McQuilton, P., Forero, M.G., Mizuguchi, K., Sutcliffe, B., Gu, C.J., Fenton, J.C., and Hidalgo, A. (2008). *Drosophila* neurotrophins reveal a common mechanism for nervous system formation. *PLoS biology* *6*, e284.

Chapter 4

Examining the role of neurotrophin Spätzle5 and NO signaling in the regulation of heme synthesis during *Drosophila* larval development

4.1 Introduction

4.1.1 *Drosophila* neurotrophin Spätzle5 and larval development

Neurotrophins (NTs) are secreted signaling molecules that represent a major class of growth factors promoting neuronal survival in vertebrates (Chao, 2003). The NTs are of great importance to many aspects of central nervous system (CNS) functions, ranging from cell proliferation and neuronal differentiation to axonal and dendritic elaborations and synapse plasticity (Lu et al., 2005). Vertebrate neurotrophins consist of brain-derived neurotrophic factor (BDNF), nerve growth factor (NGF), NT3, and NT4/5 (plus NT6/7 in fish). Like other secreted proteins, neurotrophins mature from pro-NTs via proteolytical cleavage. Mature NTs and pro-NTs have distinct effects on cell survival or cell death, because they act through different mechanisms (Reichardt, 2006). Pro-NTs bind to an atypical tumor necrosis factor receptor (TNFR) superfamily member, p75, resulting in either cell death or cell survival via JNK and NF κ B signaling, respectively. However, mature NTs bind preferentially to the Receptor Tyrosine Kinase family proteins Trks to promote cell survival by activating the MAPK/ERK and AKT pathways (**Figure 4.1**).

Recently, a protein family of neurotrophin-like molecules was identified in *Drosophila*, comprised of DNT1 (*Drosophila* Neurotrophin 1, encoded by *spätzle2*, DNT2 (*Drosophila* Neurotrophin 2, encoded by *spätzle5*, and Spätzle (Zhu et al., 2008). The homologous nature of these fly proteins to vertebrate neurotrophins is based on a structural feature referred to as a cysteine knot that is found in both protein families. It has been demonstrated that *Drosophila* neurotrophic factors promote neuronal survival and targeting in the CNS during embryogenesis, representing a link between aspects of neuronal function in flies and vertebrates (Zhu et al., 2008). However, it remains unknown to which receptors *Drosophila* neurotrophins are able to bind. Spätzle was originally

identified as a component of a signaling pathway that controls dorsal-ventral patterning through activation of the trans-membrane receptor Toll in *Drosophila* embryos (Schneider et al., 1994). There are a total of nine Toll receptors in the *Drosophila* genome and therefore, DNTs may bind to any of these receptors (Parker et al., 2001; Valanne et al., 2011). It is also possible that DNT1 and DNT2 bind to *Drosophila* Trk and p75 homologs to stimulate neurotrophic responses (Beck et al., 2004). It was shown that *Wengen* encodes the only *Drosophila* homolog of the TNFR family, which binds to its ligand Eiger to induce cell death by activating JNK signaling in eyes and wings (Kauppila et al., 2003; Moreno et al., 2002). In addition, three *Drosophila* genes, *otk*, *Ror*, and *Nrk*, encode receptor tyrosine kinases that are highly related to the Trk family of the mammalian neurotrophin receptors (Oishi et al., 1997; Pulido et al., 1992; Wilson et al., 1993). However, it remains unknown whether any of these functions as receptors of DNTs. Ultimately, DNTs may be promiscuous ligands that bind to multiple receptor types, resulting in different cellular outcomes dependent on the cellular context.

Intriguingly, our ring gland-specific microarrays have revealed that transcripts of *spätzle5* are highly enriched in the *Drosophila* ring gland (as discussed in Chapter 3). Loss of *spätzle5* function specifically in the prothoracic gland via RNAi results in profound developmental defects and larval lethality (see Chapter 3, **Figure 3.7**), suggesting that the *Drosophila* neurotrophin, Spätzle5, has a critical function in the prothoracic gland. However, the mechanisms by which Spätzle5 modulates larval growth and development remain unknown.

4.1.2 Nitric oxide and ecdysteroidogenesis

Nitric oxide (NO), produced by nitric oxide synthase, is a short-lived molecule that acts as an intracellular and intercellular messenger mediating a

range of physiological functions in both vertebrates and invertebrates (Bredt and Snyder, 1994). The *Drosophila* genome contains only one nitric oxide synthase gene called *dNOS1* (*CG6713*, hereafter referred to as *NOS*). *NOS* is expressed throughout *Drosophila* development (Stasiv et al., 2001), and previous studies have shown that NO plays important roles in imaginal disc development, including synaptogenesis, the formation of a retinal projection pattern, hypoxia response, and behavioral responses (Suman et al., 2008). A report published in 2004 found that a null mutation in *NOS* results in early larval lethality (Regulski et al., 2004), suggesting that *NOS* is an essential gene for *Drosophila* development. However, this finding is not in line with the recent observation claiming that *NOS* is not required for *Drosophila* development (Yakubovich et al., 2010). Therefore, a closer examination on the functions of different protein isoforms encoded by *NOS* would clearly be necessary in future studies.

A recent report from the Krause lab has shown that the *NOS* knockdown specifically in the prothoracic glands via RNAi results in a failure to undergo metamorphosis likely due to a lack of ecdysone in the mutant, corroborating the idea that *NOS* is an essential gene (Caceres et al., 2011). How does NO modulate ecdysone biosynthesis, and what are the downstream events of NO signaling in prothoracic gland cells? The connection made between NO and DHR3/E75 regulation of *βftz-fl* originates from our knowledge on E75 as a heme-binding protein. Reinking et al. (2005) demonstrated that the *Drosophila* ecdysone inducible receptor E75 contains a heme prosthetic group in its ligand pocket and can respond to the diatomic molecule NO to control its ability of binding to DHR3 (Reinking et al., 2005), suggesting that NO serves as a ligand for this nuclear receptor. The expression of *βftz-fl* is controlled by DHR3/E75 heterodimer dependent on the disappearance of E75 at the beginning of metamorphosis (White et al., 1997). In addition to its role as a competence factor

responding to ecdysone in *Drosophila* prepupal development, *βftz-f1* was also shown to be an important player of ecdysone biosynthesis (Broadus et al., 1999; Parvy et al., 2005; Yamada et al., 2000). In a remarkable parallel to its vertebrate counterpart, steroidogenic factor 1 (SF-1), βFTZ-F1 also acts as a pivotal regulator of steroid hormone synthesis (Parker and Schimmer, 1997). In particular, the expression of at least two genes that encode ecdysone biosynthetic enzymes, *phantom* and *disembodied*, are under the control of βFTZ-F1 (Parvy et al., 2005). *SF-1* expression is found only in steroidogenic tissues in mice, and is at least partly responsible for the tissue-specific expression of genes involved in steroid hormone synthesis such as those encoding steroid hydroxylases (Parker and Schimmer, 1997). Although findings in Parvy et al. (2005) were based on the examination of these two ecdysteroidogenic enzymes on the protein levels in the *βftz-f1* mosaic clones, it is reasonable to speculate that βFTZ-F1 regulates the expression of these two enzymes on the transcriptional level, similar to what has been reported for SF-1. Taken together, Caceres et al. (2011) proposed that NO signaling employs the DHR3/E75-mediated regulation of *βftz-f1* expression, which in turn modulates ecdysone synthesis possibly through controlling the expression of ecdysone biosynthetic enzymes. However, it remains unknown what acts upstream of NO signaling in the *Drosophila* prothoracic gland (**Figure 4.2**).

Another intriguing phenotype of the PG-specific *NOS* RNAi animals is that they have overgrown red ring glands (Caceres et al., 2011), which was also observed in *phm22>spätzle5*-RNAi (hereafter referred to as *PG> spätzle5*-RNAi) mutants. NO is a well-known regulator of cell proliferation (Villalobo, 2006), which raises an interesting question as to whether the hypertrophy of *NOS* RNAi ring gland tissue is due to an increase in cell number or cell size. Since cells of the *Drosophila* ring gland undergo endoreplication (Shingleton, 2010), where the cell number determined during embryogenesis, it seems to be consistent with the idea

that NO acts as a negative effector of cell growth. The bright-red color of these enlarged ring glands has been one of the most puzzling observations. However, this is consistent with the possibility that E75 and its vertebrate homolog Rev-erbs act as heme sensors (Marvin et al., 2009; Raghuram et al., 2007).

4.1.3 Heme and ecdysteroidogenesis

As mentioned in the earlier chapters, a number of enzymes in the ecdysone biosynthetic pathway, such as the Halloween enzymes, belong to the cytochrome P450 superfamily (Feyereisen, 1999; Rewitz et al., 2006). Cytochrome P450 enzymes are a group of proteins containing a heme cofactor and, therefore, are hemoproteins (Werck-Reichhart and Feyereisen, 2000). Heme, also known as iron protoporphyrin IX, is a molecule of central importance to diverse biological processes, including electron transfer during respiration, signal transduction, enzyme catalysis, apoptosis and detoxification (Layer et al., 2010). Heme biosynthesis is a tightly controlled process since excessive intracellular heme is highly toxic to cells causing damage to DNA, proteins, membrane lipids, etc. and, hence, it has to be strictly maintained at low levels (Franken et al., 2011). Previous data showed that the expression of the Halloween genes is greatly upregulated preceding the major ecdysone pulse during the onset of metamorphosis (McBrayer et al., 2007). It is therefore plausible that heme production needs to be upregulated to meet the demand of newly formed cytochrome P450 enzymes that require heme as a cofactor (**Figure 4.3**), thus boosting ecdysone synthesis at the end of the third instar. However, it is unknown whether there is an actual upregulation of heme production prior to metamorphosis, and if so, what triggers this response. Furthermore, little is known about how heme biosynthesis is regulated in *Drosophila* prothoracic gland.

4.1.4 Heme biosynthesis in insects and vertebrates

Heme biosynthesis is comprised of a series of eight enzymatic reactions that occur in both mitochondria and the cytoplasm (**Figure 4.4**). The reaction starts with a condensation step between glycine and succinyl-CoA to form δ -aminolevulinic acid (ALA) by δ -aminolevulinic synthase (ALAS) in mitochondria, which is the rate-limiting step of the heme biosynthetic pathway. ALA is exported to the cytosol, where it is converted to coproporphyrinogen III in four consecutive steps. Coproporphyrinogen III is then oxidized by the CPOX enzyme in the mitochondrial intermembrane space, and is further oxidized to protoporphyrin IX (PPIX) by the PPOX enzyme in the mitochondrial matrix. The final step of heme biosynthesis is the incorporation of iron into protoporphyrin IX by ferrochelatase (FECH), an enzyme that harbors an iron-sulfur (Fe-S) cluster (Ajioka et al., 2006).

Among the components of the heme biosynthetic pathway, the heme biosynthetic enzymes are the most thoroughly studied. Deficiencies in these enzymes result in a group of human disorders collectively known as porphyrias and X-linked sideroblastic anemia (Puy et al., 2010) (**Figure 4.5**). Depending on the enzymatic step that is impaired in patients, various porphyrins and their precursors that are highly toxic accumulate in tissues and are excreted in urine and/or stool. For instance, a defect in the human *PPOX* gene, which encodes the penultimate enzyme in the heme biosynthetic pathway, results in variegate porphyria (VP), with clinical manifestations including neurological disorders, or cutaneous photosensitivity, or both (Sassa, 2006).

In vertebrates, regulation of heme biosynthesis is characterized in a tissue-specific fashion. Simply put, in erythroid cells, heme synthesis is under the control of erythroid-specific transcription factors and the availability of iron. In

non-erythroid cells, the pathway is regulated by heme-mediated feedback inhibition (Ajioka et al., 2006). In particular, the rate-limiting enzyme ALAS is encoded by two different genes (May et al., 1995; Riddle et al., 1989). *ALAS2* (also known as *ALAS-E*) is expressed exclusively in erythroid cells, where it is necessary for the synthesis of hemoglobins (Conboy et al., 1992; Schoenhaut and Curtis, 1989). The second *ALAS* gene, *ALAS1* (also known as *ALAS-N*) is expressed ubiquitously with the highest level detected in the liver, where it is necessary for the production of cytochrome P450 enzymes (Ferreira and Gong, 1995). This particular step of heme synthesis mediated by the ALAS enzyme is regulated in a significant tissue-specific manner. *ALAS1* expression in the liver is repressed by heme (Roberts and Elder, 2001), however, *ALAS2* expression in erythroid cells is not (Ponka, 1997).

The *Drosophila ALAS* gene is a single copy gene, which encodes the putative housekeeping isoform of *Drosophila ALAS* (Ruiz de Mena et al., 1999). It was shown that the regulatory region of the *Drosophila ALAS* gene contains DNA recognition sites for NPF-1 (nuclear respiratory factor-1) (Ruiz de Mena et al., 1999), a transcription factor that activates the expression of some crucial metabolic genes required for cellular growth and genes required for respiration (Tiranti et al., 1995). This highlights an important role of the ALAS enzyme in mitochondrial functions, and suggests a link between heme biosynthesis and mitochondrion biogenesis. In addition, heme was also able to inhibit the expression of the *ALAS* gene by blocking the interaction of putative regulatory proteins to its promoter region (Ruiz de Mena et al., 1999). However, it remains unknown whether *Drosophila ALAS* is a regulatory target for heme biosynthesis, be it in response to developmental cues or low cellular heme levels.

Another major aspect of the regulation of heme production is through controlling cellular iron availability. Iron is vital for almost all living organisms,

participating in a broad spectrum of biological processes, including heme biosynthesis, Fe-S cluster biogenesis, DNA synthesis, and electron transport (Lieu et al., 2001). However, cellular iron concentrations must be tightly regulated because excessive iron leads to tissue damage, as a consequence of generation of free radicals (Papanikolaou and Pantopoulos, 2005). Dysfunctions in iron metabolism result in a number of human diseases with diverse clinical manifestations that range from anemia to iron overload (Lieu et al., 2001). In vertebrates, iron is absorbed from the diet and transported by transferrin (Tsf) in blood. Many cells can get access to transferrin-bound iron through the transferrin receptor pathway (TfR). After being delivered into cells, iron is mainly sequestered by ferritins, the principle iron storage protein, in the cytosol and mitochondrion (Hentze et al., 2004).

In mammals, iron uptake can be modulated via the interaction between iron regulatory proteins (IRPs), which are capable of binding to RNA when iron levels are low, and mRNA target sequences called iron responsive elements (IREs) (Hentze and Kuhn, 1996). IRPs, IRP1 and IRP2, bind to IREs present in either 5'-UTR or 3'-UTR of mRNA encoding several proteins, thereby permitting iron-responsive translational control of protein synthesis (Hentze and Kuhn, 1996). In particular, if the IRE is located in the 5'-UTR, IRP/IRE interaction represses mRNA translation. In contrast, if the IRE is located in the 3'-UTR, the IRP/IRE interaction protects the mRNA from degradation. When cellular iron levels are high, the IRP1 protein incorporates an Fe-S cluster in its catalytic center, effectively converting the activity of the protein to a cytosolic aconitase, which catalyzes the reversible isomerization of citrate and isocitrate *via cis*-aconitate (Gruer et al., 1997). Thus, when cellular iron concentrations are high, the decreased interaction between IRP and IRE allows for de-repression of ferritin translation (thus increasing iron storage) but reduces transferrin receptor synthesis

(thus reducing cellular iron uptake) (Hentze and Kuhn, 1996). Hence, IRPs, in particular, IRP1, function as an iron sensor. Interestingly, other cellular factors, such as NO and H₂O₂, are also able to regulate IRP/IRE interaction by altering Fe-S cluster retention in IRP1 (Pantopoulos et al., 1996; Stys et al., 2011). Other mechanisms might also exist to regulate iron uptake. For instance, inhibition of heme biosynthesis due to loss of *ALAS2* results in aberrant mitochondrial iron accumulation in erythroid cells, suggesting that the end product, heme, somehow regulates entry of iron into mitochondria (Camaschella, 2009).

Insect genomes encode distinct forms of the serum iron transport protein, transferrin, and the iron storage protein, ferritin (Nichol et al., 2002). However, so far, no transferrin receptor has been identified in insects. The first insect IRP was identified in the early 1990s (Rothenberger et al., 1990), and it was then demonstrated that insect IRPs represent members of the IRP1 family, and not IRP2 homologs (Muckenthaler et al., 1998). The *D. melanogaster* genome contains two IRP1-like proteins, IRP-1A and IRP-1B, and only IRP-1A can bind to IREs (Lind et al., 2006). The IRE is also found among insects (Nichol et al., 2002). A 5'-UTR IRE is found in the gene encoding a heavy chain of *Drosophila* ferritin (Fer1HCH encoded by *CG2216*), as well as in the mRNA of succinate dehydrogenase subunit B (SDHB) of *Drosophila* (Georgieva et al., 2002; Gray et al., 1996; Lind et al., 1998). In insects, IRP/IRE interaction permits iron-responsive translational control of protein synthesis for both SDHB and Fer1HCH (**Figure 4.6**). In addition, it has been suggested that NO is able to target the Fe-S cluster of IRP1 and thereby modulate translation of these proteins in insects (Nichol et al., 2002).

4.1.5 Aims of Project

As alluded to above, *Drosophila* neurotrophin Spätzle5 and nitric oxide

(NO) have critical roles in the prothoracic glands. Knocking down *spätzle5* or ablating NO production specifically in the PG display similar mutant phenotypes, however, it remains unclear whether Spätzle5 and NO function in the same signaling pathway. Notably, several lines of evidence suggest that Spätzle5 and NO may both function in regulation of heme synthesis in the PG (see Results), a process that is poorly understood in this tissue. Thus, the major aims of this project are: (1) to investigate the function of Spätzle5 and NO in controlling heme synthesis, and thereby indirectly regulating ecdysone synthesis in the PG; (2) to examine whether the upregulation of heme production prior to metamorphosis is developmentally controlled, and what the developmental cue(s) are for this presumed induction, if it occurs; (3) to understand how heme synthesis is modulated in the prothoracic glands via identifying novel components of the heme biosynthetic pathway in fruit flies; and (4) to examine possible links between aspects of regulation of heme biosynthesis in flies and vertebrates.

4.2 Methods

Drosophila stocks

GAL4 drivers were obtained from labs indicated by the references. Ring gland: *phm22-Gal4* (referred to as *PG>*) (Rewitz et al., 2009). Fat body: *Cg-Gal4* (Asha et al., 2003). Larval oenocytes: *PromE800(4M)-Gal4* (hereafter referred to as *OE>*) (Billeter et al., 2009). Ubiquitous drivers: *tubulin-Gal4/TM3, Sb*; *actin5C-Gal4/CyO*, *act-GFP*. *w¹¹¹⁸* (#3605), *UAS-GFP.KDEL* (#9899), and *UAS-PI3K.Exel* (wild type PI3K) (#8286) were ordered from the Bloomington Stock Center. RNAi lines were ordered from Vienna *Drosophila* RNAi Center unless otherwise indicated (stock number of NIG, Japan). *ALAS* RNAi (NIG 3017R1), *spätzle5* RNAi (V102389 and V41295), *spätzle5* RNAi (NIG 9972R1), *PPOX* RNAi (V100577 and V40607), *FECH* RNAi (V101496 and V20804),

Pbgs RNAi (V107988), *NOS* RNAi (V108433, V27722, V27725), *DHR51* RNAi (V37617 and V37618). *NOS* RNAi (IR-X), *E75* RNAi, *UAS-NOS^{mac}*, and *hsNOS^{mac}* are kind gifts from Dr. Henry M Krause (University of Toronto, Canada). The *DHR51* miRNA stocks were obtained from Dr. Tsumin Lee (HHMI, Janelia Farm, USA). Larval oenocytes *Gal4* driver was obtained from Dr. Joel Levine (University of Toronto, Canada). RNAi lines used in the PG mini-screen of *spätzle* gene family and Toll receptors were obtained from the VDRC, including *spätzle* (#7571 and #105017), *spätzle3* (#18949 and #102871), *spätzle4* (#7679), *spätzle6* (#18823 and #100897), *Toll* (#100078), *Toll-2* (#963, #965, #966, #44386, and #44387), *Toll-3* (#31513, #108034), *Toll-4* (#47966, #47967, and #102642), *Toll-5* (#839, #17903, #44704, and #109705), *Toll-6* (#108907, #928, #27102, and #7995), *Toll-7* (#6541, #24473, and #39176), *Toll-8* (#9430, #9431, #13549, #27098, and #27099), and *Toll-9* (#923, #924, #925, and #36308). Flies were reared on standard agar-cornmeal medium at 25°C.

Transgenic constructs

Full-length *spätzle5* cDNA in the *pOT2* vector was ordered from the *Drosophila* Genomics Resource Center (Indiana University, Bloomington). The hairpin targeting region of *UAS-spätzle5*-RNAi (V102389) is modified by using alternative genetic codons (Akashi, 1994; Moriyama and Powell, 1997) (**Figure 4.9B**). A fragment of 596 bp oligos was synthesized by the Biomatik Corp. (Ontario, Canada), and constructed into wild type *pUAST-spätzle5* resulting in a modified *spätzle5* cDNA, which is designated as *pUAST-spätzle5(N747)*. Wild type *pUAST-spätzle5* and the modified construct *pUAST-spätzle5(N747)* were sent to the Bestgene Inc. (California, USA) for generation of transgenic flies.

Real-time quantitative PCR (qPCR)

Flies were allowed to lay eggs twice for 2 hr in order to reduce egg retention. After 2-hr egg collection intervals at 25°C, eggs were transferred to food plates and reared at 25°C. Larvae were resynchronized at the L2/L3 molt, and brain-ring gland complexes were collected at the developmental times indicated. RNA was isolated using the Ambion RNAqueous kit or the Qiagen RNeasy kit. RNA samples (0.5–2 µg/reaction) were reverse transcribed using ABI High Capacity cDNA Synthesis kit (Cat. No. 4368814). Unused RNA samples were aliquoted and stored at -80°C. The synthesized cDNA was used for qPCR (StepOnePlus, Applied Biosystems) using KAPA Green PCR master mix (Kapa Biosystems) with 5 ng of cDNA template with a primer concentration of 200 nM. Samples were normalized to *rp49* based on the $\Delta\Delta\text{Ct}$ method. All primer sequences used in this Chapter can be found in **Table 4.1**. The primer design (melting temperature [T_m]=60+/-1°C) was based on the Roche online assay design center.

Ecdysone measurements

The same protocol as described in the Methods of Chapter 2.

Sterol rescue experiments

The final concentrations for the precursors used in the sterol rescue experiments of *PG>spätzle5-RNAi* animals were: cholesterol: 20 µg/ml, 7-dehydrocholesterol: 100 µg/ml, E: 40 µg/ml, 20E: 200 µg/ml. The same protocol as described in the Methods of Chapter 2.

DAF2-DA staining

Tissues were quickly dissected in room temperature (RT) Ringer's

solution, and incubated in 10 μ M DAF2-DA (Cayman, Cat. No. 85165) staining solution at 28°C for 35 min to 1 hour in the dark with gentle agitation (Caceres et al., 2011). Tissues were then rinsed twice with fresh Ringer's solution, and briefly fixed in 4% paraformaldehyde at RT for 10 min. Before imaging, tissues were rinsed twice by fresh Ringer's solution, and carefully mounted in 50% glycerol/Ringer's solution. Samples were immediately analyzed by epifluorescence microscopy (Nikon AZ-C1 Microscope System).

MitoTracker Green staining

Tissues were quickly dissected in room temperature Ringer's solution, and incubated in 500 nM MitoTracker Green (Molecular Probes M-7514) staining solution at 37°C for 35 min in the dark with gentle agitation. Tissues were then briefly rinsed with fresh Ringer's solution, mounted in 50% glycerol/Ringer's solution, and immediately analyzed by confocal microscopy (Nikon AZ-C1 Confocal Microscope System).

Total heme measurements

Brain-ring gland complexes were isolated and thoroughly homogenized in PBS+1%Triton. Total heme content was quantified using a QuantiChrom heme assay kit purchase from BioAssay Systems, and changes in absorbance (OD_{405}) were measured in a BIOTEK microplate spectrophotometer. The protein content of samples was measured with a Pierce BCA protein assay kit, and tissue heme levels were calibrated as pmol/ug protein.

Determination of autofluorescence

Heme precursors, protoporphyrins, are highly fluorescent molecules. When excited with light in the regions of 405 nm or 540 nm, protoporphyrin IX

has an emission in the region of 635 nm (Lara et al., 2005; Woods and Miller, 1993). To determine increases in heme precursors, fluorescence of brain-ring gland complex (in 1% PBT) homogenates were measured from the top of the plate by a BIOTEK microplate reader using an excitation wavelength of 405 nm and emission of 620 nm \pm 20 nm. Data are shown in the arbitrary fluorescence units measured (AU) with background fluorescence subtracted. The protein content was measured with a Pierce BCA protein assay kit as well.

Epifluorescence microscopy

Brain-ring gland complexes were dissected in ice-cold PBS, briefly rinsed by fresh PBS, and immediately mounted in 30 to 50 μ l of 50% PBS/glycerol prior to imaging. The autofluorescent images reflect the emission collected in the region of 573 nm to 648 nm either under UV light (Leica) or excited by light in the region of 530 nm to 560 nm (Nikon). Images were processed with the Adobe Photoshop software.

4.3 Results

4.3.1 The neurotrophin Spätzle5 is developmentally required for *Drosophila* metamorphosis

spätzle5 is one of six *spätzle* genes in the fly (Parker et al., 2001), for which some evidence suggest that it acts as a neurotrophin in *Drosophila* embryos (Zhu et al., 2008). During the course of the third instar, *spätzle5* transcript levels rise dramatically in the prothoracic gland, but not in the whole body (**Figure 4.7A**), suggesting a possible role for *spätzle5* in the production of the late larval ecdysone peak that triggers metamorphosis. An initial PG-specific RNAi screen has revealed that disrupting *spätzle5* function specifically in the prothoracic gland (PG) causes developmental arrest. *PG>spätzle5*-RNAi animals (nearly 100%)

remain as third instar larvae for up to 30 days, resulting in giant permanent larvae (**Figure 4.7B**). However, when *PG>spätzle5*-RNAi larvae were reared on ecdysone-supplemented standard medium, around 20% of the population pupariated at normal timing similar to *PG>w¹¹¹⁸* controls and were able to eclose as viable adults (**Figure 4.7B, C**). However, the application of ecdysteroid precursors, such as cholesterol and 7-dehydrocholesterol, were not able to restore the viability of *PG>spätzle5*-RNAi larvae (**Figure 4.7D**). This suggests that the developmental arrest caused by PG-specific *spätzle5* loss-of-function might be because of low ecdysone levels. To test this, both whole-larva and tissue-specific ecdysone titers were determined by the standard EIA method as described earlier (see Chapter 2). Indeed, the ecdysone levels in the *PG>spätzle5*-RNAi whole larva or the brain-ring gland complex isolated from *PG>spätzle5* knockdowns were significantly lower than those in the control, reinforcing the finding that disrupting *spätzle5* in the PG impairs ecdysone biosynthesis (**Figure 4.8**). Taken together, my data suggest that *Drosophila* neurotrophin Spätzle5 plays a critical role in controlling ecdysone production in the PG. Importantly, it is worth noting that the expression of *spätzle5* is developmentally regulated in the PG, although via an uncharacterized mechanism.

4.3.2 Expression of RNAi-resistant *spätzle5* cDNA in the PG partially remedies *spätzle5* RNAi phenotype

While RNAi undoubtedly represents a useful tool to study gene function in an intact fly, a major drawback of any RNAi approach is the off-target effect, which occurs when unintended targets are knocked down rather than the anticipated gene (Jackson and Linsley, 2010). Proofs demonstrating the association of an RNAi phenotype with a particular gene include: (1) The RNAi phenotype is recapitulated by a classical mutant. (2) The RNAi phenotype can be

confirmed by a second siRNA construct that targets a completely independent region of the target gene. (3) The RNAi phenotype can be rescued with a transgene that is impervious to the RNAi, which can be achieved by introducing an orthologous gene from another closely related species or expressing a modified cDNA with alternative codons (Langer et al., 2010). In my hands, four different *spätzle5*-RNAi lines have been used in analyzing *spätzle5* function in the PG. As shown in **Figure 4.9A**, #102389 and #41295 (VDRC) overlap to a large degree with respect to the siRNA targeting regions, while #9972R1 and #9972R3 (NIG) are independent from the VDRC constructs. I observed that *PG>spätzle5i* (#102389) causes 100% L3 arrest, and *PG>spätzle5i* (#41295) results in a partial L3 arrest (~50%), however, no obvious phenotypes were observed with *spätzle5*-RNAi lines (#9972R1 and #9972R3). In addition, I also analyzed the only publicly available mutant allele for *spätzle5* (*spätzle5^{e03444}*). Zhu et al. (2008) have reported that *spätzle5^{e03444}* results in a moderate increase of apoptotic neurons as well as neuronal targeting defects in the muscle in embryos, implying that *spätzle5^{e03444}* may represent a weak allele of *spätzle5*. Developmental timing of *spätzle5^{e03444}* homozygotes and *spätzle5^{e03444}/Df(3L)exel6092*, a deficiency that covers the *spätzle5* gene region, is completely normal as well as its ring gland morphology. This result suggests that *spätzle5^{e03444}* may not be penetrant enough to elicit mutant phenotype in the ring gland, and tissue-specific disruption of gene function exhibits stronger phenotype than mutants for unknown reasons.

To clarify that the *PG>spätzle5*-RNAi phenotype (#102389 and #41295) does not result from silencing RNAi off-targets, I first examined whether an ortholog of *spätzle5* in *Drosophila pseudoobscura* is suitable for RNAi rescue in terms of hairpin sequence divergence (Langer et al., 2010). Using BLAST, I found that the sequence similarity between *D. melanogaster* and *D. pseudoobscura* for *spätzle5* targeted by the V102389 hairpin is **33%**. The largest

stretch of exact match is 20 nucleotides (**Figure 4.10**, grey box), suggesting that hairpins produced by V102389 may still affect the *D. pseudoobscura spätzle5* transgene. Alternatively, a modified *spätzle5* cDNA [*UAS-spätzle5-N747*] was generated using alternative genetic codons (**Figure 4.9B**), which is presumed to be impervious to the RNAi. Eight different lines of *UAS-spätzle5-N747* were ultimately established, and *UAS-spätzle5-N747(10M)* is currently under investigation. I found that *PG>spätzle5-N747(10M)* animals are fully viable. When *N747* is expressed in *PG>spätzle5-RNAi* ring glands, a partial rescue of the *spätzle5i*-mediated ring gland phenotype was observed (**Figure 4.9C**), although no viable adults were seen in *PG>spätzle5-RNAi; N747* population. This observation indicates that the overgrown fluorescent ring gland phenotype is specific to the knockdown of *spätzle5* in the PG. However, the observed partial rescue suggests that *N747* may not be efficient enough to completely overcome the lethality associated with *spätzle5-RNAi*.

4.3.3 *spätzle5* is required for nitric oxide (NO) production in the PG

Phenotypes very similar to the *spätzle5* RNAi line were recently reported by Henry Krause's lab (Caceres et al., 2011) when they knocked down the gene for the *Drosophila* nitric oxide synthase (NOS) specifically in the prothoracic gland. Both cases give rise to giant non-pupariating larvae (**Figure 4.11A**), and more interestingly, overgrown brown-reddish ring glands (see **Figure 4.14A, B**). These observations suggest that Spätzle5 and NO may function in the same pathway. A simple explanation would be that NOS transcript levels are dependent on *spätzle5* function. To test this idea, I first wanted to examine whether the NOS transcripts levels were reduced when *spätzle5* is silenced. For this, I carried out qPCR on RNA of brain-ring gland complexes isolated from two different *spätzle5* RNAi lines (VDRC #102389 and #41295). Interestingly, NOS transcripts were

not reduced in either of these PG-specific *spätzle5* knockdowns, but rather, transcript levels were increased (**Figure 4.11B**). To test whether NOS activity is attenuated, I performed a series of DAF2-DA staining, which detects the presence of nitric oxide. Firstly, I found that nitric oxide (NO) is present in the control ring gland during the late wandering stage (**Figure 4.11C**) but not in the ring gland from the early wandering stage (data not shown), suggesting that NO has a role in ecdysone production, which occurs also in late third instar larvae. However, in *PG>spätzle5* RNAi ring glands, NO production was completely abolished during the late wandering stage, indicating that *spätzle5* is required for NO production in the *Drosophila* ring gland at the end of larval development (**Figure 4.11C**). These data supported the notion that *spätzle5* regulates NOS activity in the prothoracic gland, while it remains to be seen whether this occurs in a direct or an indirect manner. These data also suggested that the increase of *NOS* transcripts might be a feedback that tends to compensate for the reduced NOS activity.

To corroborate that NOS acts downstream of Spätzle5, I wanted to test whether a known effector gene of the NO signaling, *βftz-f1*, and its presumed downstream target *disembodied* (*dib*) (Parvy et al., 2005), were downregulated when *spätzle5* is knocked down in the PG. Firstly, I examined transcript levels of *βftz-f1* and *dib* via qPCR in the brain-ring gland complex isolated from *PG>spätzle5*-RNAi animals. As shown in **Figure 4.12**, neither *βftz-f1* nor *dib* expression were decreased in the *PG>spätzle5*-RNAi brain-ring glands, rather, they were significantly upregulated. Initially, this observation did not support our hypothesis that Spätzle5 controls NOS activity, thereby regulating the expression of *βftz-f1* and *dib*. However, when I tried to recapitulate the data published by Caceres et al. (2011) that *βftz-f1* expression is reduced in *PG>NOS*-RNAi ring glands (**Figure 4.12A**), I observed that neither *βftz-f1* nor *dib* expression were detrimentally affected in *PG>NOS*-RNAi brain-ring glands via qPCR (**Figure**

4.12B). This finding is inconsistent with the observation made by Caceres et al. (2011), at least not for *βftz-fl* (**Figure 4.12A**). In the future, I will take other approaches, such as using the ring glands (RGs) alone instead of the brain-ring glands (BRRGs) for qPCR analysis, to further examine whether *βftz-fl* or *dib* expression is under the control of Spätzle5 or NO signaling.

4.3.4 A constitutively active form of NOS, NOS^{mac}, or ectopic expression of *βftz-fl* does not rescue *spätzle5* RNAi phenotypes

To further test the hypothesis that NOS is downstream of Spätzle5, I introduced a heat-inducible continuously active NOS (*NOS^{mac}*) into the *PG>spätzle5-RNAi* background. A single heat treatment was carried out during early wandering stage (roughly 30 to 35 hours after the L2/L3 molt), and newly formed puparia were scored two days later. Secondly, I overexpressed *βftz-fl* via a *hsp70* promoter during early wandering stage, and like before, newly formed puparia were scored after two days. As shown in **Figure 4.13A**, I found that a constitutively active form of NOS (*NOS^{mac}*) and the ectopic expression of *βftz-fl* were able to rescue ~10% of *PG>spätzle5i; hsNOS^{mac}* and *PG>spätzle5i; hsβftz-fl* populations to pupariation compared to less than ~1% in the populations without heat treatment. However, unexpectedly, I also observed that ~20% of the heat-shocked *PG>spätzle5i* populations, which served as a negative control, were also able to pupariate compared to ~1% in the populations without heat treatment. These data suggest that heat treatment alone is able to partially rescue *PG>spätzle5-RNAi* L3 arrest, although the overgrown red ring glands are still present. It is therefore difficult to determine whether *NOS^{mac}* or the ectopic expression of *βftz-fl* could rescue the *PG>spätzle5-RNAi* phenotype using this approach. This interesting observation raises the questions as to (1) whether heat-shock treatment interferes with the *spätzle5* function directly or indirectly

and (2) whether other stress, such as starvation, is able to rescue the *PG>spätzle5*-RNAi phenotype. Indeed, I observed that ~60% of the starved *PG>spätzle5*-RNAi animals were able to pupariate in two days after starvation started (**Figure 4.13B, C**), compared to ~1% in the populations without starvation. These observations suggest that stress, such as heat shock or starvation, is able to reverse *PG>spätzle5*-RNAi phenotype at least in part through a yet unknown mechanism(s).

4.3.5 Spätzle5 and NO are necessary for regulating heme synthesis

PG-specific knockdown of *spätzle5* or *NOS* results in L3 arrest (permanent third instar larvae) phenotype, which also causes severely overgrown red ring glands (**Figure 4.14A, B**). Specifically, the *PG>spätzle5*-RNAi ring gland cells are large with enlarged nuclei, indicating that the gland overgrowth is due to an increase of the cell size rather than the cell number (**Figure 4.15**). This overgrown ring gland is brown-reddish in color under the dissecting microscope, and more strikingly, when excited with UV light, it autofluoresces in a bright red, which has never been observed in wild type ring glands (**Figure 4.14**). This unique phenotype has also been observed in larvae mutant for the *Drosophila PPOX* gene (Arash Bashirullah, pers. communication), which encodes an enzyme that mediates the penultimate step of heme biosynthesis. Under UV light, *PPOX* mutants display autofluorescence in the larval ring gland, larval oenocytes, and the larval gut system (**Figure 4.16A, B**). This is possibly due to an accumulation of heme precursors that are highly fluorescent in these tissues under UV light. These findings suggest the idea that Spätzle5 and NO signaling both has a role in regulating heme production in the *Drosophila* prothoracic gland. When a ubiquitous GAL4 driver *tubulin-gal4* was used to knock down *spätzle5* or *NOS* via RNAi, *tub>spätzle5i* and *tub>NOSi* both result in animals arrested as third

instar larvae with only a few escapers that reach adulthood (less than 5%). Intriguingly, strong autofluorescence was observed from the larval ring gland and the larval oenocytes of both *tub>spätzle5* and *tub>NOS* knockdowns (**Figure 4.16B, C**). This observation suggests the notion that both, Spätzle5 and NO signaling, are required for the regulation of heme synthesis in at least two tissues, the ring gland and oenocytes, during *Drosophila* larval development.

4.3.6 Disrupting *spätzle5* or *NOS* in the PG causes upregulation of *ALAS*—the rate-limiting gene of heme biosynthesis

The enzyme encoded by *ALAS* mediates the rate-limiting step of heme biosynthesis in vertebrates. The de-repression of *ALAS* is a hallmark of the heme biosynthetic dysfunctions (Hift, 2012). For instance, *ALAS-1* transcript levels were enhanced by 3-5 fold during acute porphyric attacks in the rodent liver (Handschin et al., 2005). This phenomenon is indicative of a potential feedback mechanism through enhancing *ALAS* expression to compensate for heme deficiency. To test whether *ALAS* is affected when either *spätzle5* or *NOS* is disrupted in the PG, qPCR was carried out on *spätzle5*- and *NOS*-silenced brain-ring gland samples. Remarkably, I found that the *ALAS* transcript levels were more than 6fold increased in *PG>spätzle5i* and *PG>NOSi* samples during the early wandering stage (at 30 hours after the L2/L3 molt) when compared to controls. *ALAS* expression was even more drastically upregulated (>13fold relative to controls) 14 hours later (at 44 hours after L2/L3 molt) (**Figure 4.17A**). This finding strongly suggests the idea that heme biosynthesis is impaired when *spätzle5* or *NOS* is knocked down in the *Drosophila* prothoracic gland, which in turn upregulates the *ALAS* expression as an apparent compensatory attempt to increase heme production. In addition, to determine whether other components of the heme biosynthetic pathway are affected, I examined the expression of other

heme biosynthetic genes by qPCR. My data indicates that none of these components are significantly impaired when *spätzle5* or *NOS* is silenced, at least not on the transcriptional level (**Figure 4.17B**).

4.3.7 *ALAS* expression is required for the PG autofluorescence in *spätzle5* knockdowns

To test whether the autofluorescence of *spätzle5*-silenced ring glands is attributed to *ALAS* expression and/or upregulation, I knocked down *ALAS* via RNAi in *PG>spätzle5-RNAi* ring glands. I observed that the autofluorescence, which results from loss-of-*spätzle5* in the PG, was completely lost if *ALAS* is silenced (**Figure 4.18**), suggesting that *ALAS* expression is required for the autofluorescence of *spätzle5*-silenced ring glands. In order to rule out the possibility that a second UAS transgene could compromise the *spätzle5-RNAi* expressivity, I introduced a *UAS-GFP.KDEL* into *spätzle5-RNAi* ring gland as negative control. I observed that *PG>spätzle5i; UAS-GFP.KDEL* exhibits exactly the same phenotype as that is displayed by *PG>spätzle5-RNAi* alone, indicating that a second *UAS* transgene does not alleviate *spätzle5-RNAi* effect (included in later experiments as well). Additionally, it should be noted that the *ALAS* knockdown alone in the PG results in overgrown but nonfluorescent ring glands, presumably because heme production is abolished before the formation of fluorescent protoporphyrins. Why the loss of *ALAS* function, or loss of *spätzle5*, *NOS*, and *PPOX* function cause tissue hypertrophy remains unclear.

4.3.8 Loss of Spätzle5 or NO signaling results in accumulation of heme precursors in PG mitochondria

To further test whether *PG>spätzle5* or *PG>NOS* knockdowns have impaired heme biosynthesis, I examined the total heme concentrations in

brain-ring gland complexes isolated from *PG>spätzle5* or *NOS* RNAi animals using QuantiChrom heme kit (BioAssay System, US). I observed that *PG>spätzle5*-RNAi and *PG>NOS*-RNAi brain-ring glands both have higher total heme levels than those of controls at the end of L3 (day 2 L3) (**Figure 4.19A**). At first glance, this result appears to contradict my hypothesis that *spätzle5* RNAi and *NOS* RNAi disrupt heme biosynthesis, however, the fact that the kit does not distinguish between heme and its precursors may account for the apparent discrepancy. This observation suggests the possibility that the “higher total heme levels” is owing to higher levels of heme precursors in *spätzle5* RNAi and *NOS* RNAi ring gland caused by the upregulation of *ALAS*. According to our current knowledge, heme precursors that form a porphyrin ring structure are highly fluorescent, however, heme itself is not (Morrison, 1965). I therefore determined the autofluorescence of brain-ring glands of different genotypes using fluorescence spectrophotometer. Indeed, when excited at 360 nm, I observed higher emission signals from *PG>spätzle5i* and *PG>NOSi* BRRG homogenates at 635 nm than controls as 2-day old L3s. Intriguingly, the autofluorescence increased by >3fold in *PG>spätzle5*-RNAi and *PG>NOS*-RNAi glands on day 4 after the L2/L3 molt (**Figure 4.19B**). These results suggest that loss of *spätzle5* or *NOS* in the PG results in accumulation of heme precursors, but it still remains unclear whether heme levels are lower than controls in these knockdowns.

Heme biosynthesis takes place in mitochondria and the cytoplasm. Determining the location where heme precursors are stuck may provide clues for tracing the defective steps of heme synthesis. Using confocal microscopy, I observed that the highly fluorescent heme precursors are distributed in a punctate manner (**Figure 4.20A**). Based on this finding, I wondered whether these molecules accumulate in mitochondria, where the last three steps of heme biosynthesis take place. Using MitoTracker Green staining, I found that

mitochondria stains overlap with the autofluorescent signals of the *PG>spätzle5i* ring gland (**Figure 4.20B**). This observation indicates that (a) when *spätzle5* function is disrupted in the PG, heme precursors build up in mitochondria and (b) the heme synthetic steps up to and including re-entry into mitochondria are intact.

4.3.9 Disruption of nuclear receptor DHR51 suppresses *spätzle5*-RNAi phenotype

The finding that *ALAS* expression is upregulated when heme is limiting (presumed for prothoracic glands isolated from *PG>spätzle5*-RNAi and *PG>NOS*-RNAi larvae) raises the intriguing possibility that a heme sensor controls *ALAS* transcription in response to changes of cellular heme concentrations. A previous study has reported that two *Drosophila* nuclear receptors are able to bind heme, E75, the fly homologue of the vertebrate REV-ERB α/β , and DHR51 (the *Drosophila* Hormone Receptor 51), the fly homologue of the vertebrate photoreceptor-specific nuclear receptor (PNR) (de Rosny et al., 2008). This finding implies that heme may serve as a ligand of E75 or DHR51, which is able to respond to diatomic molecules, such as NO and CO in the heme-bound state. The same report also demonstrated that apoDHR51-LBD binds heme with a K_d of 0.43 μ M. A similar K_d value has been reported for the nuclear receptor REV-ERB α , which acts as a heme sensor in coordinating cellular circadian clock, glucose homeostasis, and energy metabolism (Yin et al., 2007). These findings suggest that DHR51 may function as a heme sensor rather than a gas sensor. While E75 binds heme with a K_d possibly in the nanomolar region (de Rosny et al., 2008), suggesting that E75 is more likely to act as a gas sensor due to its high affinity to heme.

To determine whether DHR51 or E75 functions as a heme sensor in prothoracic gland cells, I carried out *DHR51*-RNAi and *E75*-RNAi specifically in

the PG in a *spätzle5*-RNAi background. The PG-specific knockdown of *spätzle5* and *DHR51* (VDRC#37618) both result in an L3 arrest phenotype (permanent larvae). However, remarkably, I observed that around 60% of *PG>spätzle5; DHR51* double knockdowns were able to pupariate with a slight developmental delay (**Figure 4.21A, B**). These animals were also able to eclose as viable adults, as shown in **Figure 4.21B**. To test that the ability of suppressing *spätzle5*-RNAi is specific to *DHR51* loss-of-function caused by RNAi (VDRC#37618) rather than RNAi off-target effects, a second *DHR51* RNAi line (*UAS-DHR51-miRNAi*) was used (Lin et al., 2009), which is completely independent from the former line by targeting a different region of the *DHR51* transcript. *PG>DHR51-miRNAi* causes prolonged third instar (3- to 4-day compared to a 2-day in the control) resulting in big animals that are fully viable to adults. When *DHR51* miRNAi was induced together with *spätzle5*-RNA in the PG, ~30% of the double knockdowns were able to pupariate and eclose as viable adults. Together, these data have demonstrated that the suppression of the *PG>spätzle5*-RNAi phenotypes is specific to loss-of-*DHR51* function. In contrast, loss-of-*E75* function was not able to reverse *PG>spätzle5*-RNAi L3 arrest phenotype. *PG>spätzle5; E75* double knockdowns were arrested as second or third instar larvae, possibly because *PG>E75*-RNAi alone causes early larval lethality, suggesting that loss of *E75* does not ameliorate *spätzle5*-RNAi phenotype (as illustrated in **Table 4.2**).

4.3.10 *DHR51* is required for *ALAS* upregulation in *spätzle5*-RNAi knockdowns

I have demonstrated that silencing *DHR51* specifically in the PG reverses the *PG>spätzle5*-RNAi L3 arrest phenotype. The next question I asked was whether the overgrown fluorescent ring gland phenotype caused by *spätzle5*-RNAi could also be suppressed by *DHR51* loss-of-function. Indeed, I

observed that ring glands of *PG>spätzle5; DHR51* double knockdowns (via both siRNAi and miRNAi) are neither overgrown nor fluorescent under UV light, strongly indicating that disrupting *DHR51* in the PG suppresses gland overgrowth and autofluorescence inflicted by loss-of-*spätzle5* (**Figure 4.22A**). Furthermore, in *PG>spätzle5; DHR51* double knockdowns (via siRNAi), *ALAS* transcript levels drop back to control levels (**Figure 4.22B**), indicating that *DHR51* is required for *ALAS* upregulation in *spätzle5*-silenced ring glands, consistent with the observation that the autofluorescence was completely lost in double knockdowns. In addition, it is worth noting that *PG>DHR51*-RNAi animals have small ring glands compared to controls, which was also observed in the double RNAi larvae (**Figure 4.22A, upper panel**). This suggests that *DHR51* carries out a potential role in regulation of tissue growth. Together, I have demonstrated that *DHR51* is required for *ALAS* upregulation in ring glands isolated from *PG>spätzle5*-RNAi larvae. In contrast, ring glands of *PG>spätzle5*-RNAi; *E75*-RNAi third instar larvae are still overgrown and fluorescent (**Table 4.2**), suggesting that *E75* does not function as a heme sensor under these conditions.

4.3.11 Loss of *DHR51* rescues *NOS*-RNAi ring gland phenotype

To test whether loss of *DHR51* could also rescue *PG>NOS*-RNAi phenotypes, I carried out *DHR51* RNAi in *PG>NOS*-RNAi ring glands. As expected, I observed that disrupting *DHR51* function in the PG was able to reverse the *PG>NOS*-RNAi ring gland phenotype, namely, ring glands of *PG>NOS; DHR51* double knockdowns are neither overgrown nor fluorescent under UV light (**Figure 4.23**). However, *PG>NOS; DHR51* double mutants are still third instar larval lethal. Together, I have shown that loss of *DHR51* suppresses the *PG>NOS*-RNAi overgrown fluorescent ring gland phenotype, and presumably restores *ALAS* expression to control levels. However, larval lethality

caused by *NOS* RNAi in the PG was not rescued, suggesting that NO may serve other essential biological functions in this tissue.

4.3.12 Loss of *DHR51* rescues *PPOX*-RNAi ring gland phenotype

So far, I have demonstrated that interfering with *DHR51* function in the PG suppresses the ring gland phenotype caused by PG-specific *spätzle5*-RNAi and *NOS*-RNAi, both have indirectly been shown to result in heme deficiency. I have also observed that the *ALAS* upregulation caused by PG-specific *spätzle5*-RNAi and *PG>NOS*-RNAi is completely abrogated when *DHR51* function is disrupted in the PG. However, *PG>DHR51*-RNAi alone does not affect *ALAS* expression (**Figure 4.22B**). These findings suggest the idea that *DHR51* functions as a heme sensor in the PG, specifically, when heme is limiting, apo*DHR51* (the heme-unbound state) induces the upregulation of *ALAS* as a mechanism to enhance heme synthesis (**Figure 4.24**).

To further test this idea, I introduced *DHR51*-RNAi into a *PG>PPOX*-RNAi (VDRC#100577) background, which is known to disrupt heme production. I then examined whether loss of *DHR51* was able to rescue the overgrown fluorescent ring gland phenotype inflicted by the *PPOX* silencing. *PG>PPOX*-RNAi animals are mainly arrested in the third instar (<5% escapers to adults). They develop overgrown fluorescent ring glands (**Figure 4.23**), consistent with the role of the *PPOX* enzyme being a key component of the heme biosynthetic pathway. As expected, when *DHR51* is silenced, the ring gland phenotype caused by *PPOX*-RNAi is completely abolished (**Figure 4.23**). This result further supports that *DHR51* serves as a heme sensor in the *Drosophila* PG. In addition, I also observed a partial rescue of the larval lethality mediated by *PPOX*-RNAi in the double knockdowns, suggesting that the non-pupariating phenotype caused by loss-of-*PPOX* function is at least partly contributed by the

toxicity owing to the accumulation of heme precursors.

4.3.13 Loss of *DHR51* partially rescues protoporphyrin accumulation in oenocytes of *spätzle5*-RNAi larvae

So far, several lines of evidence have strongly suggested that DHR51 acts as a heme sensor in the PG, which is why I wanted to test whether DHR51 has a similar role in other tissues, such as the larval oenocytes, which represent the other major tissue that emits autofluorescence when *spätzle5* is muted. To test this idea, I carried out a double knockdown of *spätzle5* and *DHR51* in larval oenocytes using the oenocyte-specific *Gal4* driver *PromE-Gal4* (hereafter refer to as *OE for oenocyte-Gal4*). As shown in **Figure 4.25A**, *OE>spätzle5* knockdowns are mainly viable, although eclosion defects were observed in ~20% of the population that were unable to extricate from the pupal case. This eclosion defect was previously observed in animals lacking larval oenocytes (Gutierrez et al., 2007), suggesting that *spätzle5* has an important function in these cells. *OE>spätzle5*-RNAi results in fluorescent oenocytes under UV light (**Figure 4.25B**), however, it is unclear whether these cells are enlarged like prothoracic gland cells from *PG>spätzle5*-RNAi larvae. *OE>DHR51*-RNAi results in a higher rate of eclosion defects (~40%), however, no fluorescent oenocytes were detected (**Figure 4.25A, B**). Finally, in the double knockdowns, I observed a rate of eclosion defects (~40%) comparable to *OE>DHR51*-RNAi alone (**Figure 4.25A**), along with a partial rescue of protoporphyrin accumulation in oenocytes of *OE>spätzle5*-RNAi larvae (**Figure 4.25B**, arrow). Further experiments will be carried out to examine whether *ALAS* transcript levels are reduced in oenocytes of *OE>spätzle5i; DHR51i* larvae compared to that of *spätzle5*-silenced oenocytes.

4.3.14 Genetic interactions between Spätzle5/NO signaling and Ras signaling

As demonstrated earlier, larvae expressing *PG>spätzle5-RNAi* or *PG>NOS-RNAi* exhibit overgrown fluorescent ring glands, and the gland overgrowth is due to an increase in cell size instead of cell number. I therefore wanted to examine whether Spätzle5 or NO signaling plays a role in regulating tissue growth. The Ras/MAPK signaling pathway is tightly coupled with tissue proliferation and viability (Prober and Edgar, 2002). Since the *Drosophila* ring gland is an endoreplicative organ, I tested whether the tissue hypertrophy caused by *PG>spätzle5i* or *PG>NOSi* is due to Ras hyperactivation. To test this idea, I first knocked down *Ras* via RNAi in *spätzle5-RNAi* ring glands, which showed that *PG>spätzle5-RNAi; Ras-RNAi* results in ring glands with a significant reduction in size, indicating that Ras activity contributes to the observed gland overgrowth of *PG>spätzle5-RNAi* animals (**Figure 4.26**). In addition, I observed that fluorescence of glands from *PG>spätzle5; Ras* double knockdowns was also reduced, suggesting that the observed accumulation of heme precursors is at least in part dependent on Ras activity (**Figure 4.26**). Secondly, I wanted to test whether a constitutively active form of NOS (*UAS-NOS^{mac}*) could suppress the Ras hyperactivation phenotype. As described earlier, *PG>Ras^{V12}* results in accelerated development forming small pupae with overgrown ring glands. However, when *NOS^{mac}* and *Ras^{V12}* were co-expressed, the gland overgrowth phenotype caused by the *Ras^{V12}* hyperactivation was completely abolished (**Figure 4.27**), suggesting that NOS is epistatic to Ras. Taken together, these findings suggest that Spätzle5 and NO signaling are epistatic to Ras signaling, which has critical impacts on tissue growth and the accumulation of heme precursors (**Figure 4.28**).

4.3.15 Genetic interactions between Spätzle5/NO signaling and PI3K signaling

In addition to the Ras/MAPK pathway, DILP/PI3K signaling also carries out key functions in the regulation of tissue growth. To determine whether PI3K signaling interacts with Spätzle5 and NO signaling, I expressed a wild type PI3K (*UAS-PI3K^{Exel}*) in *PG>spätzle5-RNAi* ring glands. I found that ring glands from *PG>spätzle5-RNAi; PI3K^{Exel}* larvae are still overgrown, however, compared to ring glands of *PG>spätzle5-RNAi* alone, the autofluorescence intensity was reduced (**Figure 4.29**). This result indicates that active PI3K signaling is able to alleviate the toxic accumulation of heme precursors in *spätzle5*-silenced PG, which is consistent with the observation that ~10% of *PG>spätzle5-RNAi; PI3K^{Exel}* population was able to pupariate and eclose as viable adults. Together, my data suggest that increased PI3K signaling can lower the accumulation of heme precursors and improve viability of larvae with reduced *spätzle5* function in their prothoracic glands.

4.3.16 Ubiquitous expression of *spätzle5* results in pupariation defects

The earlier observation that lack of *spätzle5* induces PG overgrowth suggests a role of Spätzle5 in suppressing tissue growth under normal circumstances. To further examine this idea, I overexpressed wild type *spätzle5* cDNA specifically in the PG to test whether this could impair PG growth, thereby affecting larval development. Nine independent *UAS-spätzle5* lines were tested. What I observed was that PG-specific expression of *spätzle5* does not affect PG growth. *PG>spätzle5* animals are fully viable without any significant developmental delay. However, when *spätzle5* is ubiquitously expressed, *actin>spätzle5* results in 100% pupariation defects and prepupal lethality in all lines that were examined (**Figure 4.30**). In addition, it should be noted that a

portion of *actin>spätzle5* animals were of smaller body size relative to controls, demonstrating that the expression of *spätzle5* in larval tissues other than the PG disturbs larval growth and development.

4.3.17 PG-specific RNAi screen of *Drosophila spätzle* family genes and Toll-like receptors

Spätzle5 belongs to the *Drosophila spätzle* family, which is comprised of *spätzle* and *spätzle2-6*. To test whether other members of this family have a similar role as *Spätzle5* in the PG, Brittany Antoniuk (Undergraduate research project student) and I decided to knock down these genes via RNAi specifically in the PG. Antoniuk found that *PG>spätzle3-RNAi* (VDRC#18949 and #102871) results in a range of developmental defects, such as delays into metamorphosis and partial L3 arrest, suggesting that *spätzle3* has an important role in the PG. However, no obvious phenotype was observed when *spätzle*, *spätzle4*, or *spätzle6* is silenced in this tissue. To clarify whether *spätzle3* has a similar function as *spätzle5* in manipulating heme synthesis, I examined the ring gland phenotype of *PG>spätzle3-RNAi* knockdowns. I found that loss of *spätzle3* function does not give rise to overgrown fluorescent ring glands, suggesting that *spätzle3* has a distinct role in the PG.

Given that the *spätzle* gene encodes the activating ligand for the Toll receptor, I wondered whether *Spätzle5* represents the activating ligand for any of *Drosophila* Toll-like receptors. Interestingly, my ring gland microarrays (Chapter 3, Figure 3.4A) have shown that transcripts of two Toll-receptors, Toll-4 and MstProx, exhibit >10fold enrichment in the ring gland, raising the possibility that *spätzle5* acts as a ligand for one of them. To test this idea, Brittany and I carried out PG-specific RNAi of genes encoding *Drosophila* Toll-like receptors, including *Toll*, *18-wheeler*, *mstProx* (*Toll-3*), *Toll-4*, *Tehao* (*Toll-5*), *Toll-6*, *Toll-7*,

Tollo (*Toll-8*), and *Toll-9*, to screen for mutant phenotypes similar to that in *PG>spätzle5* knockdowns. What was found is that *PG>MstProx*-RNAi (VDRC#108034) results in minor delays in pupariation and partial pupal lethality, *PG>Tehao*-RNAi (VDRC#44704) causes major delays into metamorphosis, *PG>Tollo*-RNAi (VDRC#9430), interestingly, accelerates developmental timing and results in small animals, while other lines did not give any obvious mutant phenotypes. Ring glands of *MstProx*-RNAi (VDRC#108034), *Tehao*-RNAi (VDRC#44704), and *Tollo*-RNAi (VDRC#9430) were also examined, however, unfortunately, none of them are fluorescent and/or overgrown, suggesting that Spätzle5 may either not bind to any of the Toll-like receptors or does not represent the activating ligand.

4.3.18 Genome-wide RNAi screen for novel players in regulation of heme biosynthesis in the *Drosophila* PG

(This work represents a secondary screen following the collaborative project with Dr. Michael O'Connor laboratory at the University of Minnesota, USA, and Dr. Kim F. Rewitz laboratory at the University of Copenhagen, Denmark. Note: Qiuxiang Ou did all the work for the secondary screen.)

Initially, a genome-wide RNAi screen was carried out in three labs to systemically analyze the endocrine function of the PG by identifying novel components of the ecdysteroidogenic pathway. Taking advantage of the existing screen data, I performed a secondary screen on the hits identified with developmental defects during the L3, either showing delays into metamorphosis or being arrested as L3 larvae, to further search for ring gland phenotypes similar to that in *PG>spätzle5* knockdowns, namely, the overgrown fluorescent ring gland phenotype. So far, a total of eleven independent RNAi lines representing 11 genes have been revealed to display this particular ring gland phenotype when

UAS-RNAi is driven in a PG-specific manner. These genes include transcription factors with uncharacterized functions in the PG, components of vital importance to the functions of mitochondria, molecules with possible roles in signaling cascades, and a G-protein coupled receptor (GPCR). In the near future, I will complete screening the rest of the hits (~450 lines). It will be of great interest to further characterize the roles of these novel players in modulating heme synthesis, and ultimately aim to build up a functional network underlying the regulation of heme production in the prothoracic gland towards a better understanding of ecdysone biosynthesis and thereby insect metamorphosis.

4.4 Discussion

4.4.1 Spätzle5: an autocrine factor governing heme homeostasis

So far, my work has uncovered that *Drosophila* neurotrophin Spätzle5 plays a critical role in the synthesis of heme. Specifically, disrupting *spätzle5* function via RNAi results in L3 larval arrest, along with an aberrant accumulation of protoporphyrins in the ring gland and oenocytes that is characteristic of heme biosynthetic dysfunctions. This observation is indicative of that *spätzle5* RNAi impairs heme production, which in turn results in larval lethality via blocking ecdysone synthesis, because heme is required as cofactor in ecdysteroidogenic enzymes. Since the *spätzle5* RNAi phenotype could not be recapitulated by the only available *spätzle5* mutant (*spätzle5*^{e03334}) or confirmed by a second independent RNAi line, a third approach of rescuing with an RNAi-immune transgene was carried out to examine whether the observed RNAi phenotype is not caused by silencing off-targets. The PG-specific expression of a modified *spätzle5* cDNA *N747*, which is presumed to be RNAi-impervious, was able to alleviate the ring gland phenotype caused by loss of *spätzle5*, demonstrating that the overgrown fluorescent ring gland phenotype is specific to the PG knockdown

of *spätzle5*. Together, these findings demonstrate a novel role of Spätzle5 in addition to its canonical function as a neurotrophin in promoting neuronal survival and differentiation (Zhu et al., 2008).

Furthermore, my microarrays (see Chapter 3) have revealed that *spätzle5* is strongly expressed in the ring gland, suggesting that it functions as an autocrine factor to modulate heme production in the PG (**Figure 4.31**). Notably, the *spätzle5* expression profile implies that it is developmentally regulated, with higher expression detected at later times of the larval third instar (at 24 hours and 36 hours L3) (**Figure 4.7A**). This observation is in line with the idea that increased expression of *spätzle5* in the ring gland prior to pupariation is required for generating the major ecdysone peak at the end of the third instar, thereby satisfying increased demands for heme production that are necessary for generating functional ecdysteroidogenic cytochrome P450 enzymes. However, at this point, it remains unclear whether there is an increase of heme synthesis prior to the major ecdysone peak in the ring gland. Future experiments will first examine heme levels in the ring gland at different developmental times, this including early L3 that corresponds to a low-ecdysone time and late L3 that corresponds to a high-ecdysone time. Secondly, it will be of interest to investigate the mechanism underlying *spätzle5* upregulation at the end of larval development. Identifying novel components with potential roles in heme biosynthesis in the PG will provide more clues about the pathways involved, thereby possibly shedding new light on the mechanistic details of the control of *spätzle5* expression. Ultimately, my work has suggested that Spätzle5 may not, at least, act as an activating ligand for any of *Drosophila* Toll receptors. Future experiments will first test whether *spätzle5* encodes the ligand for any of the identified *Drosophila* Trk-related receptors, including ROR, NSR, and OTR, via RNA interference of gene function specifically in the PG.

4.4.2 Nitric oxide (NO): a key molecule in regulation of heme biosynthesis

In addition to Caceras et al. (2011), who demonstrated that NOS/NO is necessary for *Drosophila* metamorphosis through controlling *βftz-fl* expression, I have revealed a novel role of NO in regulating heme production in the *Drosophila* prothoracic gland. Nitric oxide is a well-known effector molecule that regulates multiple cellular functions in both vertebrates and invertebrates. Therefore, what lies upstream of NO signaling? How is NOS activity modulated? The NO synthases exist as homodimers, and each monomer consists of two major domains: an N-terminal oxygenase domain containing a heme prosthetic group, and a C-terminal reductase domain homologous to cytochrome P450 reductase. In mammals, three NOS isoforms have been identified, nNOS (Neuronal Nitric oxide synthase), iNOS (Inducible Nitric oxide synthase), and eNOS (Endothelial Nitric oxide Synthase) (Suman et al., 2008). However, only one NOS gene has been identified in insects, which is most similar to the mammalian nNOS (Stasiv et al., 2001). The mammalian nNOS is constitutively expressed in neurons, and its activity is Ca²⁺/calmodulin dependent (Suman et al., 2008), raising the possibility that the activity of insect NOS might be modulated in a similar fashion. In addition, the catalytic activity of NOS can also be regulated through feedback inhibition of the end product, NO, likely by NO binding to the NOS cofactor heme and thereby blocking electron transfer (Wang et al., 1994).

My data shows that PG-specific knockdown of *spätzle5* completely abolishes NO production without reducing NOS transcripts, indicating that Spätzle5 controls NO generation likely through modulating NOS activity. So is Spätzle5 upstream of NOS signaling? I currently propose two possible mechanisms, which are consistent with the idea that NOS activity is downstream of Spätzle5 (**Figure 4.32**). An indirect mechanism would be through a reduction of heme levels, since heme is a required NOS cofactor. My data have

demonstrated that heme production is impaired when *spätzle5* is muted in the PG. Thus, a lack of heme could in turn detrimentally affect NOS activity and its ability to generate NO.

Alternatively, Spätzle5 and NO may function in the same pathway, where Spätzle5 signaling might directly modulate NOS activity. This hypothesis finds support in the finding that two vertebrate neurotrophins, BDNF and NT3, acutely and substantially increase NO production in a concentration-dependent manner in human pulmonary endothelium (Meuchel et al., 2011). This NO elevation is likely achieved by activating NOS through NT-induced increase in Ca^{2+} levels and phosphorylation of Akt, which represents the first demonstration of NT-induced NO generation. Therefore, it is possible that Spätzle5 stimulates NOS signaling in the PG in a similar fashion, and NO signaling in turn regulates iron availability. Previous data showed that in mammalian bone marrow macrophages, the presence of NO results in increased iron uptake through IRP1-dependent stabilization of *TfR* mRNA (Stys et al., 2011). This finding encourages two possible mechanisms by which NO regulates iron availability in the PG (**Figure 4.33**). Firstly, the putative Spätzle5/NO axis may enhance iron uptake into the PG during the onset of metamorphosis for increased heme synthesis. In line with this proposal, a lack of NO in the PG due to *NOS*-RNAi causes defects in iron influx, thereby in turn disturbing heme biosynthesis (**Figure 4.33A**). To test this hypothesis, future experiments will first examine whether there is increased iron uptake in the PG prior to the onset of metamorphosis and whether this process is affected by NOS signaling. However, attention should be given to the fact that the insect genome do not encode any TfR homologs (Lambert, 2012), suggesting a difference in iron transport and regulation between insects and mammals. The other interesting possibility is through regulating the levels of ferritin (**Figure 4.33B**), which sequesters iron from the intracellular labile iron pool to lock it up in a chemically

less reactive form. As described, an IRE site was identified in the 5'-UTR of the transcript encoding *Drosophila* Fer1HCH (Lind et al., 1998), thus allowing the IRP/IRE interaction to reduce ferritin levels through translational depression when iron is limiting. The presence of NO mimics an iron-depleted state, freeing iron from ferritin for cellular utilization, such as heme biosynthesis and Fe-S biogenesis (Nichol et al., 2002). In line with this proposal, in PG cells of *PG>spätzle5-RNAi* and *PG>NOS-RNAi* larvae, a lack of NO prevents the release of iron from ferritin, resulting in iron shortage for cellular functions, thereby ultimately affecting heme biosynthesis.

In summary, I surmise that NO may help maintain iron homeostasis in the *Drosophila* PG in addition to its function in controlling *βftz-fl* expression, as well I hypothesize that NO signaling could be regulated by the *Drosophila* neurotrophin Spätzle5 in a direct or an indirect fashion (**Figure 4.32**).

4.4.3 Nitric oxide: a negative regulator of ring gland growth

The data presented here show that loss of *spätzle5* or *NOS* results in ring gland overgrowth accompanied with a reduction in ecdysone production (**Table 4.3**). This hypertrophic ring gland phenotype has also been observed in animals that are mutant for *without children (woc)* and *molting defective (mld)* (Neubueser et al., 2005; Wismar et al., 2000). *woc* and *mld* are both transcription factors that have critical functions in regulating components of the ecdysone biosynthetic pathway. Loss of both *woc* and *mld* impairs ecdysone production, and the ring gland overgrowth was speculated to be a common strategy to compensate for the inability of the tissue to synthesize ecdysone. However, it remains unclear how this potential feedback mechanism works.

I have further shown here that dysfunctions in the heme biosynthetic enzymes also cause tissue hypertrophy. This is indicating that reduced heme

levels cause misregulation of tissue growth. Genetic analysis has revealed that the *spätzle5* RNAi-induced hypertrophic phenotype is partially attributed by Ras activation, suggesting that heme somehow suppresses Ras activity. This is possibly through ablating NOS activity, which requires heme as cofactor to generate NO. NO has been proposed to be a physiological modulator of cell proliferation, and in most cases able to promote cell cycle arrest (Villalobo, 2006). Therefore, I hypothesize that *spätzle5*, *NOS*, *ALAS*, and *PPOX* loss-of-function results in the shortage of heme, which disables NOS to produce NO, thereby in turn allows tissue overgrowth due to Ras activation. This notion is in line with the observation that a constitutively active NOS (*NOS^{mac}*) inhibits Ras^{V12}-induced gland hypertrophy. Taken together, I conclude that NO serves as a crucial regulator in negatively regulating ring gland growth through suppressing Ras activity.

4.4.4. Transcriptional regulation of *Drosophila ALAS* gene

The *Drosophila* genome contains only one *ALAS* gene, which encodes the housekeeping form of the *ALAS* enzyme. In contrast, in vertebrates, two isoforms of ALAS are encoded by two different genes, *ALAS1* (housekeeping) and *ALAS2* (erythroid-specific). The expression of *ALAS1* is inhibited by heme, however, *ALAS2* is not affected by heme at the transcriptional level (May et al., 1995). Previous data demonstrated that the activity of the *Drosophila ALAS* promoter is decreased in Schneider cells when treated with 30 μ M hemin (ferric heme) (Ruiz de Mena et al., 1999), although it remains unclear whether 30 μ M hemin represents a normal physiological condition. This study represents the first report in drawing the similarity underlying regulation of *Drosophila ALAS* and the vertebrate *ALAS1*. Handschin et al. (2005) showed that the *ALAS1* upregulation due to the blocking of heme biosynthesis by porphyrinogenic drugs is blunted by

knocking out the peroxisome proliferator-activated receptor- γ coactivator 1 α (PGC-1 α) (Liang and Ward, 2006), demonstrating that the expression of *ALAS1* is regulated by PGC-1 α in the vertebrate liver. One aspect of the PGC-1 α -mediated upregulation of *ALAS1* is through a transcription factor called nuclear respiratory factor 1 (NRF-1), which increases expression of nuclear-encoded mitochondrial genes (Virbasius and Scarpulla, 1994). NRF-1 directly binds to the NRF-1 binding sites within the *ALAS1* promoter when activated by PGC-1 α during acute porphyric attacks, thereby enhancing *ALAS1* expression (Handschin et al., 2005). Interestingly, a motif that is potentially recognized by factors of the NRF-1 family was also detected in the *Drosophila ALAS* promoter (Ruiz de Mena et al., 1999), raising the possibility that NRF-1 carries out a similar function downstream of a yet unknown regulator in modulating *Drosophila ALAS* expression when heme synthesis is impaired.

My work have shown that *ALAS* transcripts are dramatically increased when *spätzle5* or *NOS* is disrupted specifically in the PG. Currently, I propose two possible mechanisms underlying *ALAS* upregulation in the PG. Firstly, this may reflect a feedback mechanism likely involving factors of the NRF-1 family in augmenting *ALAS* expression when heme is limiting. This possibility finds support in the evidence that an increased *ALAS* expression was observed in PG-specific *PPOX* knockdowns, where the synthesis of heme is disrupted by abolishing the *PPOX* enzyme. The build-up of heme intermediates in mitochondria of PG cells from *PG>spätzle5-RNAi* and *PG>NOS-RNAi* larvae reflects a defective heme synthetic process, which is possibly due to the lack of iron when *spätzle5* or *NOS* is silenced, thus in turn upregulating the *ALAS* transcripts level. However, an alternative possibility is that *spätzle5* and *NOS* may participate in the repression of the *ALAS* gene through an unknown mechanism. Essentially, *ALAS* is repressed by the downstream effectors of *spätzle5* or *NOS*

under the normal condition, the removal of *spätzle5* or *NOS* leads to the de-repression of *ALAS* expression, however, without compromising the ability to make heme. Consequently, enhanced *ALAS* expression results in the accumulation of excessive protoporphyrins in PG mitochondria. Future experiments will first examine whether PG-specific knockdowns of *spätzle5* and *NOS* have lower heme levels than controls. Secondly, I will perform RNA-Seq on *PG>spätzle5-RNAi* and *PG>NOS-RNAi* ring glands to examine gene expression changes associated with *spätzle5* and *NOS* silencing in addition to the augmented expression of *ALAS* (Wang et al., 2009).

4.4.5 DHR51: a PG-specific heme sensor?

The arguably most striking observation I have made was the suppression of ring gland phenotypes of *spätzle5* RNAi and *NOS* RNAi by introducing *DHR51* RNAi into each of these backgrounds. This aspect of *DHR51* function is reinforced by either *DHR51-RNAi* or *DHR51-miRNAi*, which generates siRNA or miRNA that targets to different regions of *DHR51* transcripts, remedying the ring gland phenotype caused by PG-specific knockdown of *spätzle5* and *NOS*. Future experiments will test whether upregulation of *ALAS* under low-heme conditions is also abolished in *DHR51* mutants (Sung et al., 2009). Given that *DHR51* has been demonstrated to bind to heme in a reversible manner (de Rosny et al., 2008), I hypothesize that *DHR51* functions as a heme sensor, which upregulates the *ALAS* transcript level when heme concentrations drop (**Figure 4.31**). It remains unclear whether *DHR51* directly binds the *ALAS* promoter or through interacting with other proteins. My preliminary data showed that the expression of a fusion protein (Palanker et al., 2006), GAL4-DBD.*DHR51-LBD*, by the *hsp70* promoter did not significantly induce the expression of the reporter gene *UAS-EGFP* in wild type L3 larvae. This observation implies that *DHR51*

may require other protein(s) that is limiting, and/or only when heme levels are low, to stimulate *ALAS* expression. This possibility finds support in the evidence that PNR, the vertebrate homolog of DHR51, interacts with Crx (cone-rod homeobox protein) in regulating several cone and rod genes in rod photoreceptors of mice retina, and importantly, the promoter/enhancer occupancy of PNR is Crx-dependent (Peng et al., 2005). Future experiments will evaluate the transcriptional activity of wild type DHR51 (*UAS-DHR51*cDNA) in inducing the expression of *ALAS*, in both wild type and *DHR51* mutant background under either normal conditions or low-iron/heme conditions (**Figure 4.34**).

In addition, it remains poorly understood whether DHR51 acts as a heme sensor in other *Drosophila* tissues. I have found that both Spätzle5 and NOS are critical for heme synthesis in the larval oenocytes, another major tissue where heme is required for lipid metabolism to make cuticular hydrocarbons by cytochrome P450 enzymes (Qiu et al., 2012), for instance. However, loss of *DHR51* function did not completely rescue the accumulation of protoporphyrins in oenocytes isolated from *OE>spätzle5*-RNAi and *OE>NOS*-RNAi larvae, suggesting two possibilities that (1) the role of DHR51 as a heme sensor is specific to the prothoracic gland and (2) oenocytes have their own sensor in detecting heme levels. The latter possibility finds support in Handschin et al. (2005) demonstrating that in mice liver, *ALAS1* expression is induced by the peroxisome proliferator-activated receptor- γ coactivator 1 α (PGC-1 α) during fasting and under porphyric attacks. Since some lipid-processing functions of the mammalian liver are performed in insects by oenocytes (Gutierrez et al., 2007), this finding encourages the idea that the *Drosophila* orthologue of vertebrate PGC-1 α may as well govern heme homeostasis by inducing *ALAS* expression in oenocytes.

4.5 Tables

Gene	Primer sequence	
<i>ALAS</i>	Forward 5'	accaacggaacgtctcctac
	Reverse 5'	cttcgacggggaaacctt
<i>Pbgs</i>	Forward 5'	gaatcgctgaaggagcac
	Reverse 5'	aagagcagcaccgacgac
<i>l(3)02640</i>	Forward 5'	atagcctcgcttccaaagg
	Reverse 5'	acaccgtcaaatggggatac
<i>CG1885</i>	Forward 5'	ccgatacgtgctatccaag
	Reverse 5'	cagcgcgtctcgtacactt
<i>Updo</i>	Forward 5'	ggaccgttcacaaagaagg
	Reverse 5'	agtctgctctgctcctcag
<i>Coprox</i>	Forward 5'	gccttcaactttgtgtcaagc
	Reverse 5'	gtaccagcggcacgtagg
<i>PPOX</i>	Forward 5'	ttcacagcaagcaagaaagc
	Reverse 5'	ccgctcagcgaactgtag
<i>ferrochelataase</i>	Forward 5'	ctggccgagatcgaaaag
	Reverse 5'	tgagtaaataatggagttaaagctgga
<i>heme oxygenase</i>	Forward 5'	gaatgcaaagatcgcaacttg
	Reverse 5'	tgggtctcaaagaattgtacagt
<i>spätzle5</i>	Forward 5'	tctacaagccgcacactagg
	Reverse 5'	gggaggacgtttaatactttt
<i>nitric oxide synthase</i>	Forward 5'	gcatgtgtaccagaccatcag
	Reverse 5'	aactccgcctcgctttt
<i>βftz-f1</i>	Forward 5'	ccagaatttgttctcgcaagt
	Reverse 5'	gcagcttcatttggtcgtc

Table 4.1. Primer pairs for qPCR analysis

<i>PG-Gal4 X</i>		Phenotypes	
<i>UAS</i> -transgene 1	<i>UAS</i> -transgene 2	larvae	ring glands
<i>w¹¹¹⁸</i>	none	normal	
<i>spätzle5</i> -RNAi	<i>GFP.KDEL</i>	giant L3	
<i>E75</i> -RNAi	none	small L2	
<i>spätzle5</i> -RNAi	<i>E75</i> -RNAi	giant L2 and L3	
<i>DHR51</i> -RNAi	none	giant L3	
<i>spätzle5</i> -RNAi	<i>DHR51</i> -RNAi	normal	
<i>Ras</i> -RNAi	none	giant L3 and pupa	
<i>spätzle5</i> -RNAi	<i>Ras</i> -RNAi	giant L3	
<i>Ras^{V12}</i>	none	small L3 pupa	
<i>spätzle5</i> -RNAi	<i>Ras^{V12}</i>	5% small pupa	
<i>PI3K^{Exel}</i>	none	small L3 pupa	
<i>spätzle5</i> -RNAi	<i>PI3K^{Exel}</i>	10% small pupa	

Table 4.2. Genetic interactions

A summary of genetic interactions between *spätzle5* and *DHR51*, *E75*, *Ras* and *PI3K*. *GFP.KDEL* is included as negative control to clarify that a second transgene does not attenuate *spätzle5* RNAi effects. *Ras^{V12}*, a constitutively active form of *Ras*. *PI3K^{Exel}*, wild type *PI3K*. The color of the ring gland is an indication of the levels of protoporphyrin accumulation.

Category	Gene	Mutants with overgrown ring gland	Ecdysone biosynthesis
Signaling component	<i>spätzle5</i>	<i>PG>spätzle5-RNAi</i>	↓
	<i>NOS</i>	<i>PG>NOS-RNAi</i>	↓
Transcription factor	<i>woc</i>	<i>woc^{rgl}</i> mutant	↓
	<i>mld</i>	<i>mld⁴⁷</i> mutant	↓
Heme biosynthetic enzyme	<i>ALAS</i>	<i>PG>ALAS-RNAi</i>	n/d
	<i>PPOX</i>	<i>PG>PPOX-RNAi</i>	n/d

Table 4.3. Ring gland hypertrophy

A brief summary of mutants that display an overgrown ring gland phenotype. NOS, nitric oxide synthase. *woc*, without children. *mld*, molting defective. ALAS, 5'-aminolevulinic acid synthase. PPOX, protoporphyrinogen IX oxidase. n/d, not determined.

4.6 Figures

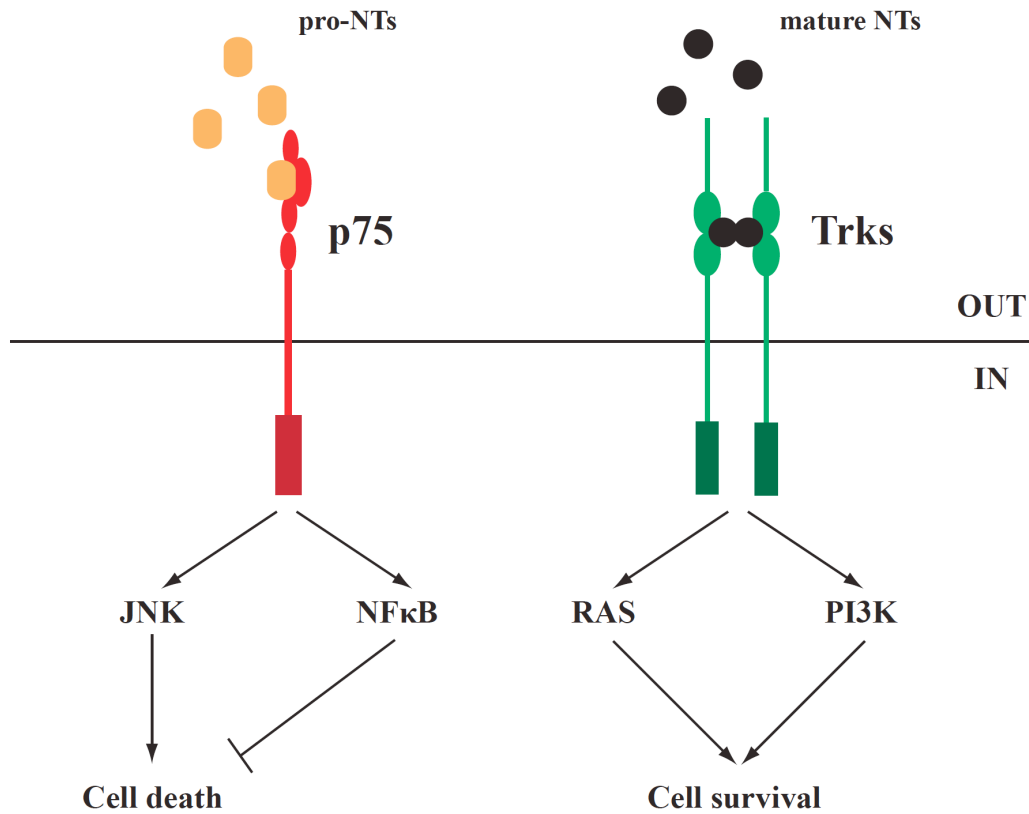


Figure 4.1. Neurotrophin signaling pathways.

Neurotrophins are secreted proteins that mature from pro-NTs via proteolytic cleavage. In vertebrates, pro-NTs bind to the atypical TNFR superfamily member, p75, resulting in either cell death or cell survival through JNK and NFκB, respectively. However, mature NTs have high affinity to the Receptor Tyrosine Kinase family proteins Trks. They preferentially bind to Trks and promote cell survival by activating the MAPK and AKT pathways. NT, neurotrophin. JNK, c-Jun N-terminal kinase. TNFR, tumor necrosis factor receptor. Trks, tropomyosin-receptor-kinases.

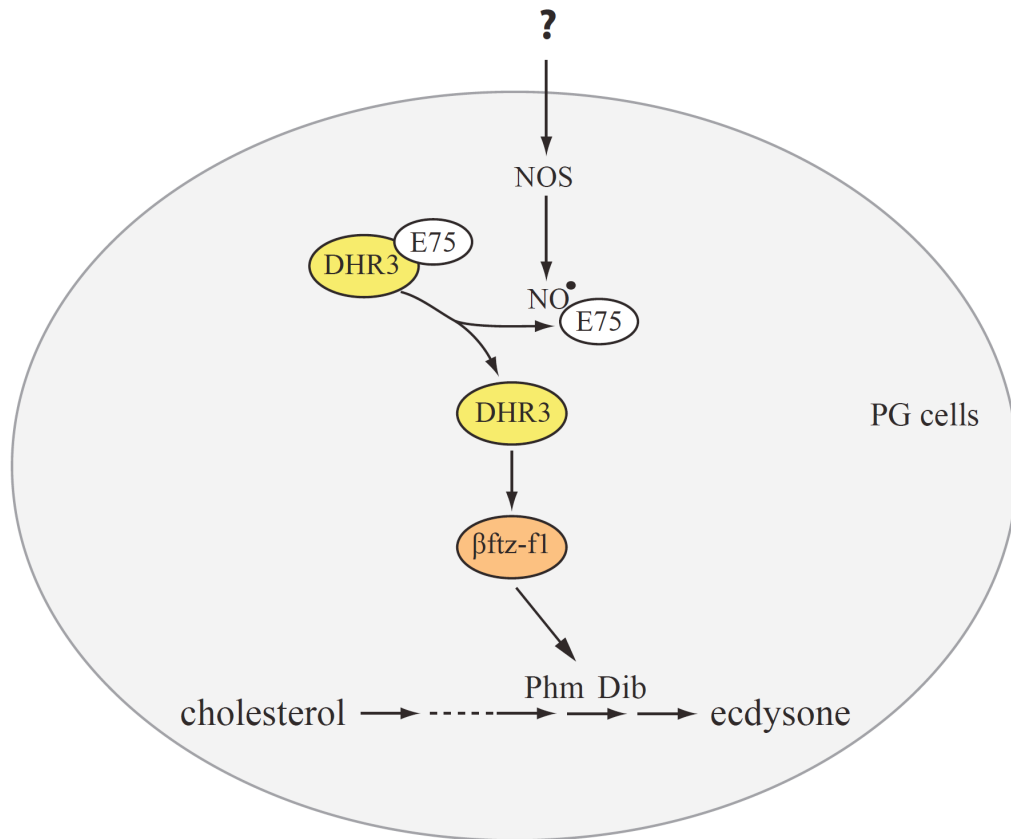


Figure 4.2. NO signaling regulates ecdysteroidogenesis in the *Drosophila* prothoracic gland.

NO is a short-lived gaseous molecule that is produced in cells by the nitric oxide synthase (NOS). It serves a critical function in the regulation of ecdysone production in the *Drosophila* PG. NO signaling is mediated by an interplay between two ecdysone hierarchy components, DHR3 and E75, in regulating another ecdysone hierarchy gene *betaftz-f1*. β FTZ-F1 was shown to regulate the expression of two classic Halloween enzymes, Phantom (Phm) and Disembodied (Dib). NO, nitric oxide. PG, the prothoracic gland.

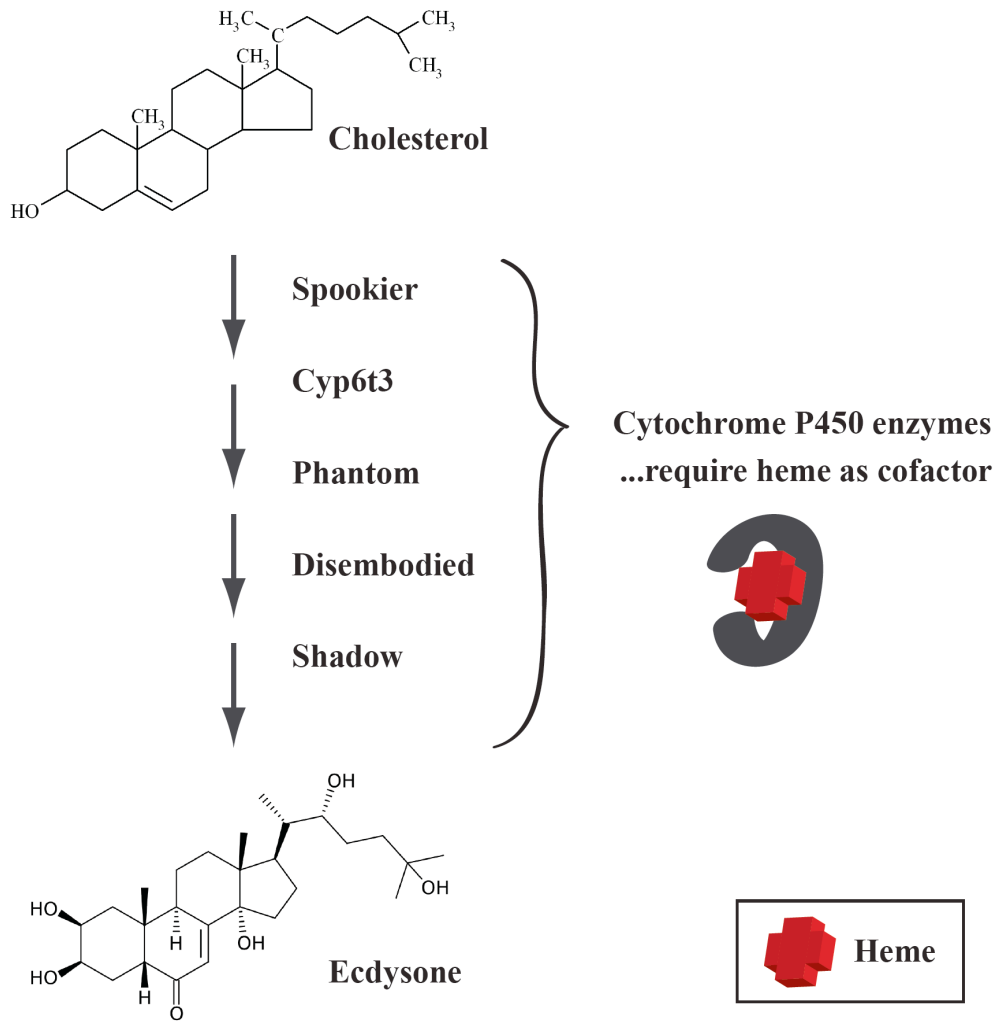


Figure 4.3. Role of heme in ecdysone biosynthesis.

Ecdysone is converted from dietary cholesterol through a series of enzymatic reactions. A majority of known ecdysteroidogenic enzymes belong to the cytochrome P450 enzyme superfamily that use heme as cofactor, this including Spookier, Cyp6t3, Phantom, Disembodied, and Shadow in the PG.

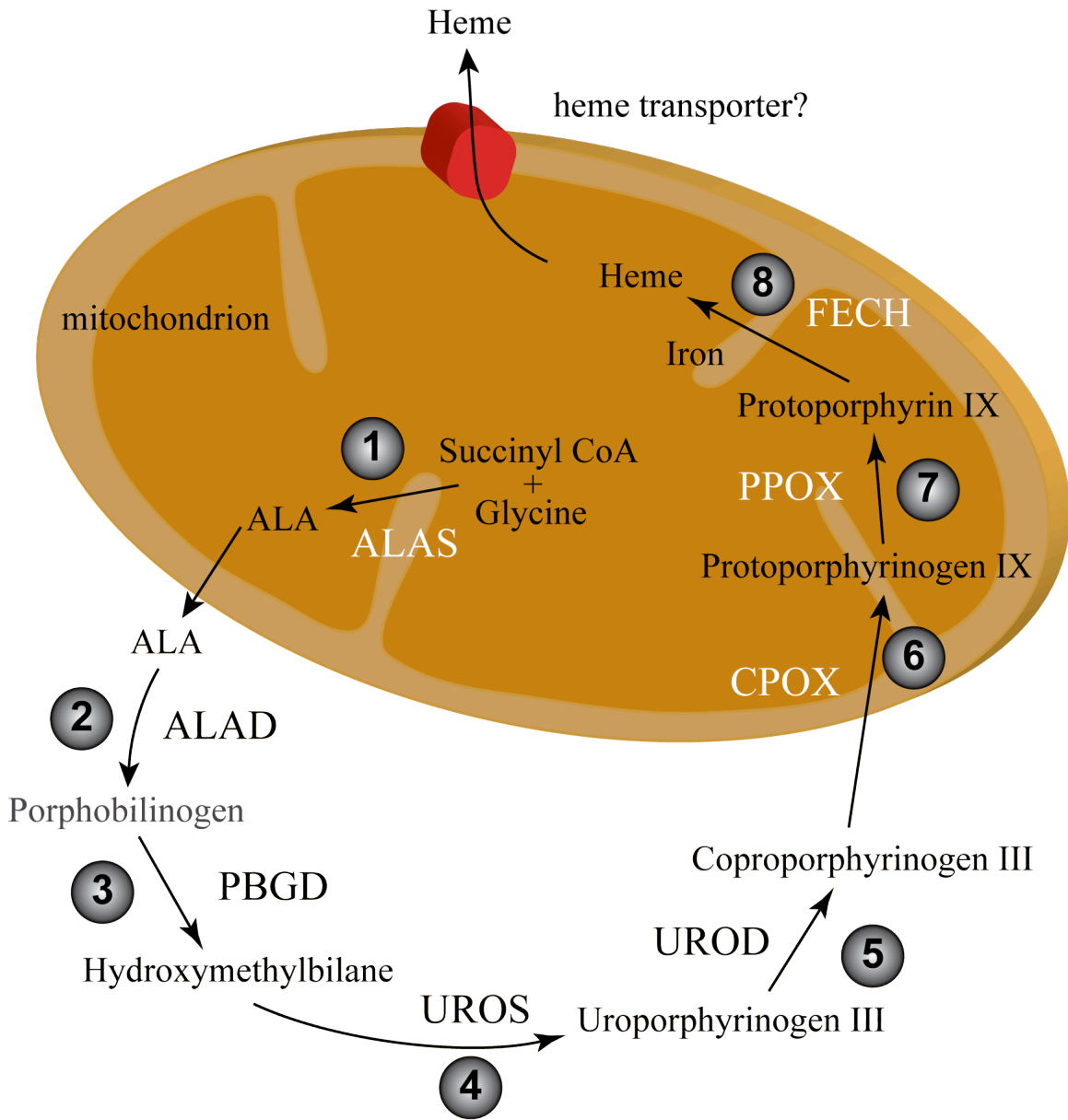


Figure 4.4. Heme biosynthesis in animals

Heme biosynthesis is initiated in mitochondria, continues in the cytosol before returning to mitochondria. It starts with a condensation of glycine and succinyl-CoA to 5'-aminolevulinic acid (ALA) by 5'-aminolevulinic acid synthase (ALAS). ALA is subsequently exported to the cytosol, where it is converted to coproporphyrinogen III that is re-directed to mitochondria.

Coproporphyrinogen III is then oxidized to protoporphyrinogen IX by the CPOX enzyme in the mitochondrial intermembrane space, and is further oxidized to protoporphyrin IX in the mitochondrial matrix by the PPOX enzyme. The heme biosynthesis is completed with the insertion of iron into protoporphyrin IX by FECH, an enzyme containing an iron-sulfur (Fe-S) cluster. Heme is then exported to the cytosol by as yet uncharacterized heme transporters. ALAS, 5'-aminolevulinic acid synthase. ALAD, 5'-aminolevulinic acid dehydratase. PBGD, porphobilinogen deaminase. UROS, uroporphyrinogen III synthase. UROD, uroporphyrinogen III decarboxylase. CPOX, coproporphyrinogen III oxidase. PPOX, protoporphyrinogen IX oxidase. FECH, ferrochelatase.

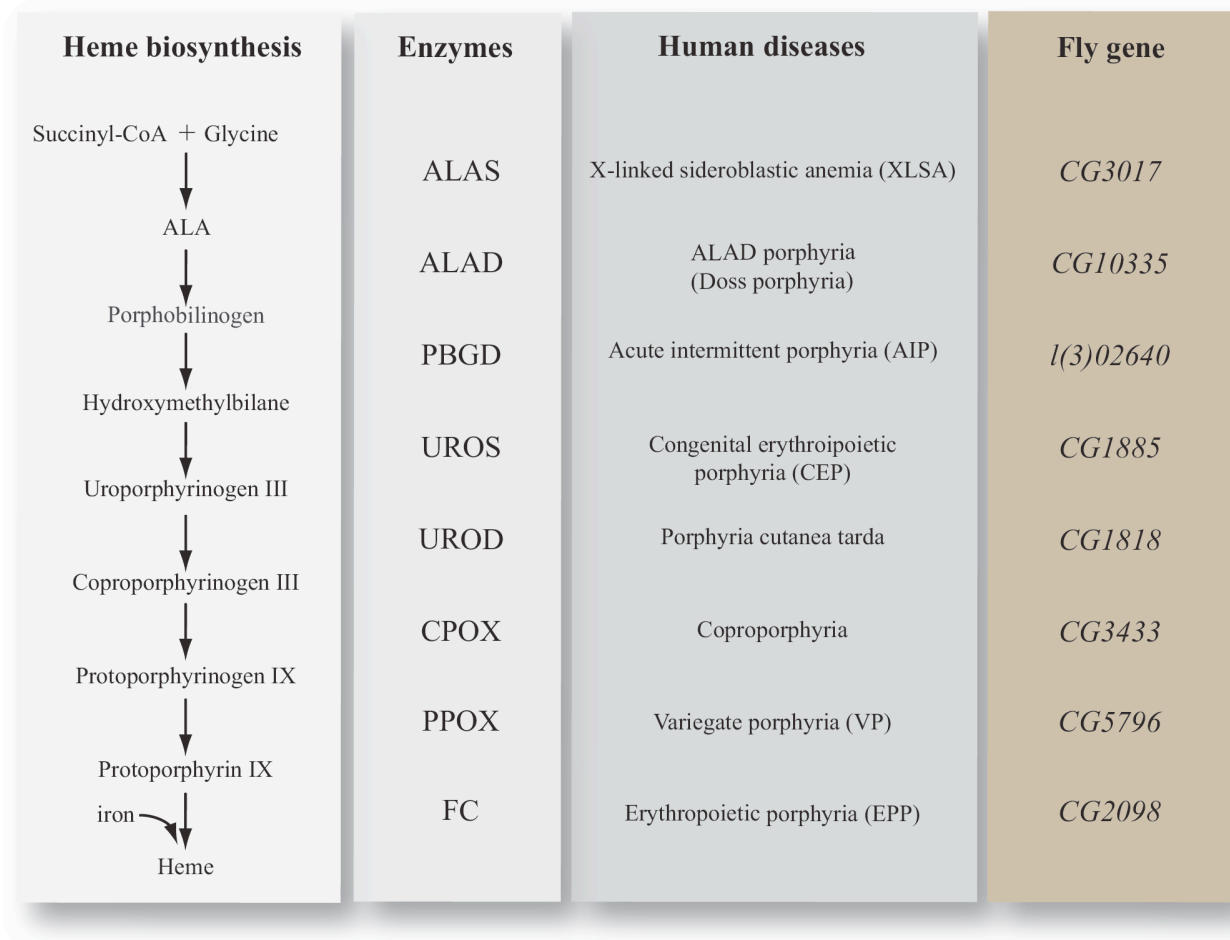


Figure 4.5. Deficiencies of heme biosynthetic enzymes result in a group of human disorders designated the porphyrias and X-linked sideroblastic anemia. *D. melanogaster* genes encoding enzymes required for heme synthesis are included. ALAS, 5'-aminolevulinic acid synthase. ALAD, 5'-aminolevulinic acid dehydratase. PBGD, porphobilinogen deaminase. UROS, uroporphyrinogen III synthase. UROD, uroporphyrinogen III decarboxylase. CPOX, coproporphyrinogen III oxidase. PPOX, protoporphyrinogen IX oxidase. FECH, ferrochelatase.

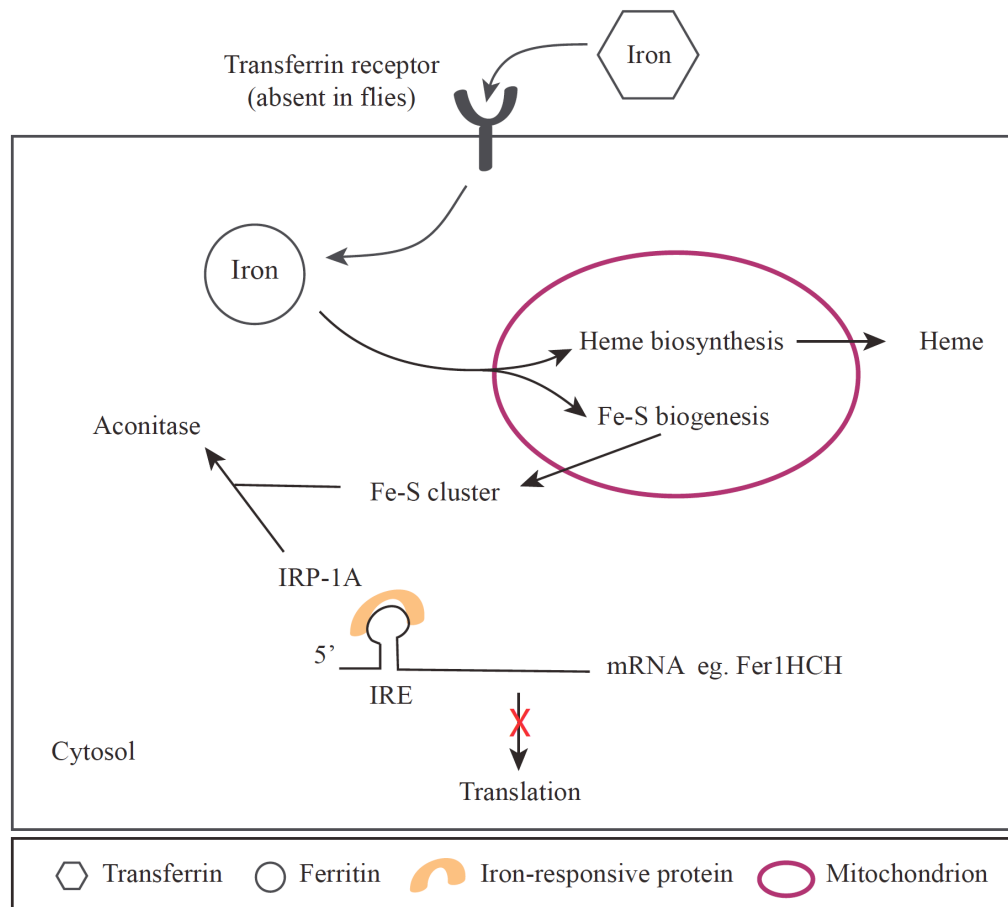
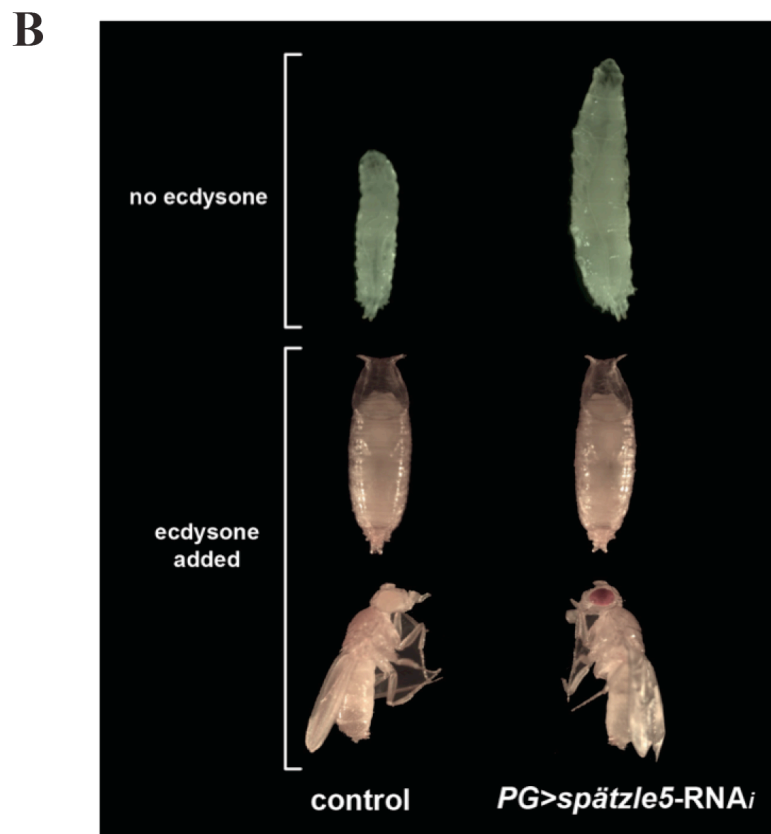
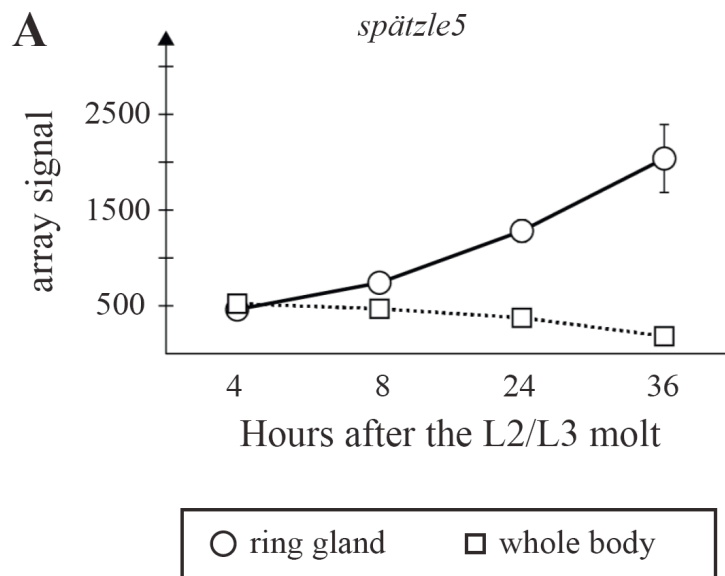


Figure 4.6. Iron metabolism in *Drosophila*

Iron is transported by the iron transport protein, transferrin, in the hemolymph. Upon it is delivered into cells, iron is sequestered by the iron storage protein, ferritin. Iron is mainly used for heme biosynthesis and iron-sulfur (Fe-S) biogenesis in mitochondria. IRP-1A functions as iron biosensor via IRP/IRE interaction. When cellular iron levels are high, IRP-1A is converted into aconitase. Loss of the IRP-1A-mediated RNA binding de-represses protein translation. For example, an IRE site is present in the 5'-UTR of the transcript that encodes a heavy chain of ferritin (Fer1HCH encoded by *CG2216*). Loss of IRP-1A binding increases cellular ferritin levels which promotes iron storage. IRP, iron regulatory protein. IRE, iron responsive element. UTR, untranslated region. Fer1HCH, ferritin 1 heavy chain.



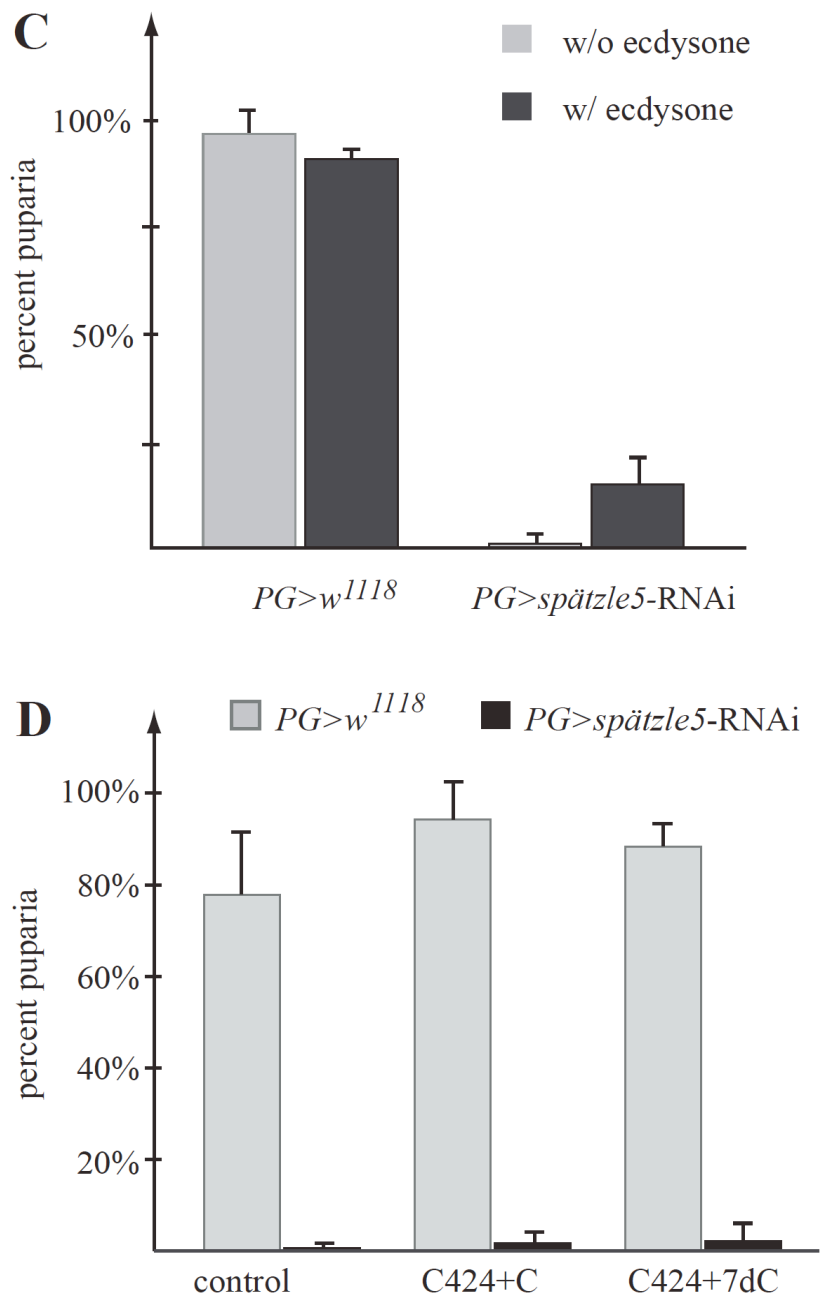


Figure 4.7. Neurotrophin Spätzle5 is developmentally required for *Drosophila* metamorphosis.

(A) *spätzle5* expression profile in the ring gland compared to whole larva during the third instar. The y-axis represents microarray signals. The x-axis represents

hours after the L2/L3 molt. (B) Phenotypes of PG-specific *spätzle5* RNAi on standard medium and 20E-supplemented medium. (C) The percentages of embryos that reached puparia on medium with and without 20E. *PG>w¹¹¹⁸* (control), N=48 (w/o 20E), N=120 (w/ 20E). *PG>spätzle5-RNAi*, N=109 (w/o 20E), N=95 (w/ 20E). (D) The percentages of embryos that reached puparia on C424 medium with ethanol (carrier), cholesterol (C), and 7-dehydrocholesterol (7dC). *PG>w¹¹¹⁸*, N=120-180. *PG>spätzle5-RNAi*, N=120-180. Error bars represent standard deviation.

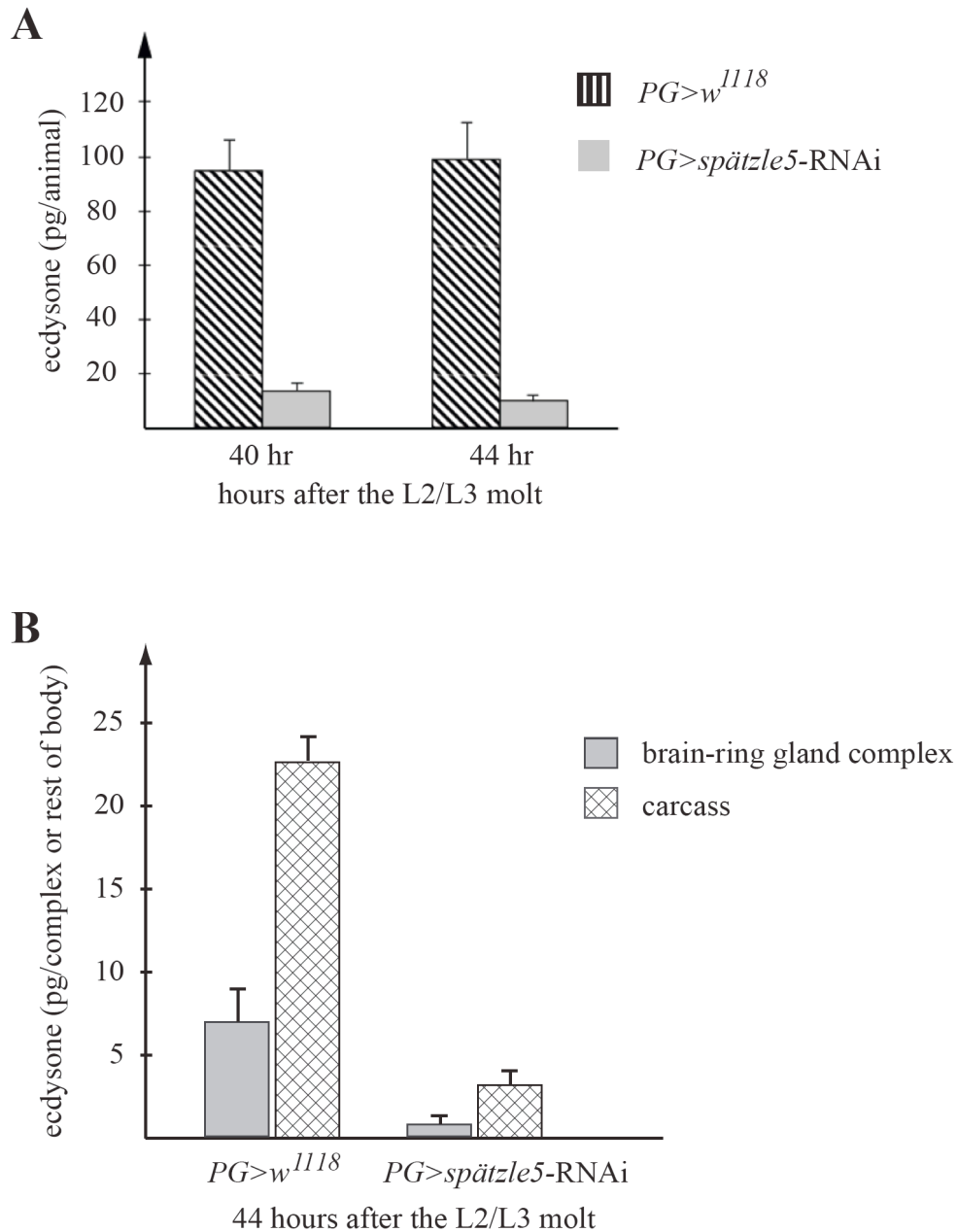


Figure 4.8. Loss of *spätzle5* specifically in the PG impairs ecdysone production. (A) The whole-body ecdysteroids titers of *PG>w¹¹¹⁸* controls (striped) and *PG>spätzle5-RNAi* animals (grey) at 40 hours and 44 hours after the L2/L3 molt. Three samples (8 larvae/sample) were tested per condition. Each sample was tested in triplicate. Error bars represent standard error. (B) Ecdysteroids measurements of the brain-ring gland complex (grey) and carcass (striped)

collected from $PG>w^{1118}$ controls and $PG>spätzle5$ -RNAi animals at 44 hours after the L2/L3 molt. Three samples (8 larvae/sample) were tested per genotype. Each sample was tested in triplicate. Error bars represent standard error.

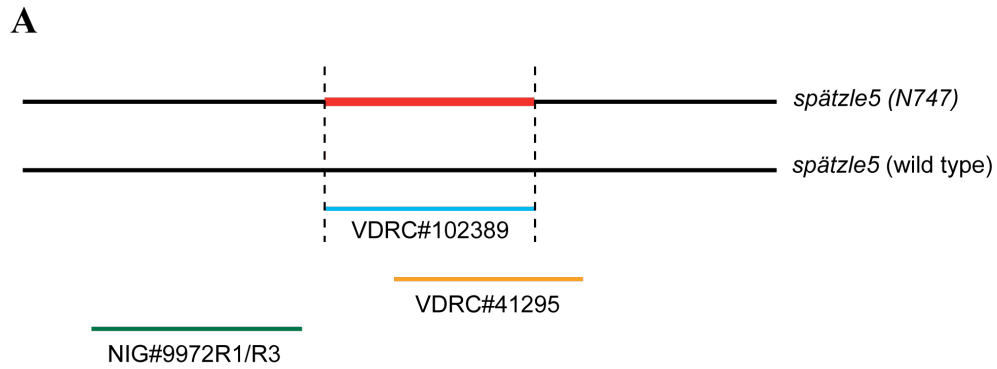
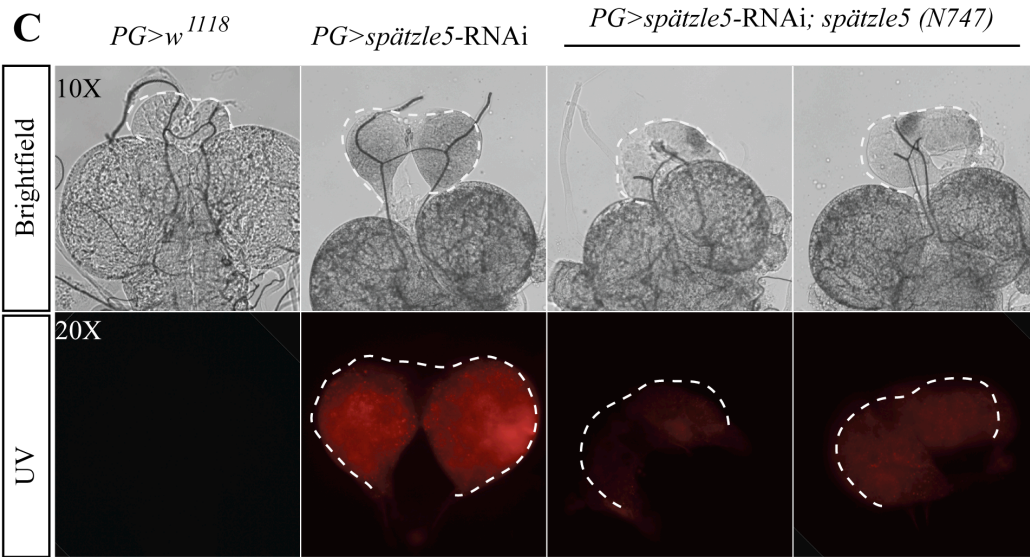


Figure 4.9. The expression of a modified *spätzle5* cDNA partially rescues the *PG>spätzle5*-RNAi ring gland phenotype.

(A) *spätzle5* RNAi lines. The hairpin targeting regions of VDR#102389 and VDR#41295 overlap to a large degree. NIG#9972R1 and R3 target to a different region from the VDR lines. (B) The hairpin region of VDR#102389 (between the dashed lines in [A]) is modified using alternative genetic codons (red type). A fragment of 596 bp oligos was synthesized and constructed into wild type *spätzle5* cDNA by restriction digestion, resulting in a modified *spätzle5* cDNA designated *spätzle5*-N747. (C) The ring gland phenotype under brightfield (upper panel, 10X) and under UV light (bottom panel, 20X). Ring glands of controls were isolated and examined at 44 hours after the L2/L3 molt. Ring glands of *PG>spätzle5*-RNAi and *PG>spätzle5*-RNAi; *spätzle5*-N747 larvae were isolated on day 3 after the L2/L3 molt and examined by epifluorescence using the same parameters. At least 20 ring glands were tested per condition.

B

wild type cDNA	tcg	ggt	cac	cgg	tat	aac	tcc	cag	ggc	gga	ggc	acc	tca
amino acid sequence	Ser	Gly	His	Arg	Tyr	Asn	Ser	Gln	Gly	Gly	Gly	Thr	Ser
N747	tc c	gg a	cac	cg c	ta c	aac	tc g	cag	ggc	gg c	ggc	acc	tc t
	tct	tct	ggc	ggt	cac	ttg	tac	atc	aat	cag	agt	gac	aag
	Ser	Ser	Gly	Gly	His	Leu	Tyr	Ile	Asn	Gln	Ser	Asp	Lys
	tc g	tc g	ggc	gg a	cac	tt a	tac	atc	aa c	cag	ag c	gac	aag
	tcg	act	ccc	tac	aat	gcc	acg	ctc	tgg	ctg	aag	cgc	ttg
	Ser	Thr	Pro	Tyr	Asn	Ala	Thr	Leu	Trp	Leu	Lys	Arg	Leu
	tc c	ac g	ccc	tac	aa c	gcc	ac c	ct g	tgg	ct c	aag	cg t	ct a
	gtc	agg	gat	ctc	agt	cgg	aag	cag	agg	caa	ccc	gac	gag
	Val	Arg	Asp	Leu	Ser	Arg	Lys	Gln	Arg	Gln	Pro	Asp	Glu
	gt g	agg	gat	ct g	tc t	cg t	aag	cag	ag a	ca g	cc g	gac	gag
	gtt	caa	gcg	gag	gtg	gtg	gag	ccg	gtg	aac	gag	cag	aca
	Val	Gln	Ala	Glu	Val	Val	Glu	Pro	Val	Asn	Glu	Gln	Thr
	gt c	caa	gc c	gag	gt c	gtg	gag	cc c	gt c	aac	gag	ca a	ac t
	gag	gag	gcc	gag	gaa	cag	gac	aac	ccg	gca	gag	gat	cac
	Glu	Glu	Ala	Glu	Glu	Gln	Asp	Asn	Pro	Ala	Glu	Asp	His
	gag	ga a	gcc	ga a	ga g	cag	ga t	aa c	cc c	gct	gag	ga c	cac
	cca	caa	agc	aag	cgc	gat	gtc	tcg	ctc	aac	atg	gat	ctc
	Pro	Gln	Ser	Lys	Arg	Asp	Val	Ser	Leu	Asn	Met	Asp	Leu
	cc g	caa	tc c	aag	cg g	ga c	gt g	tc c	ct g	aac	atg	ga c	ct g
	ttg	gat	atc	gtg	ggc	gtg	gaa	gcc	ccc	aat	ccg	ctg	aag
	Leu	Asp	Ile	Val	Gly	Val	Glu	Ala	Pro	Asn	Pro	Leu	Lys
	ct a	ga c	atc	gt c	ggc	gtg	ga g	gct	ccc	aa c	cc c	ct c	aag
	aag	cgt	tcg	agg	aca	aag	cgc	caa	agt	ccg	ggg	cgc	tcc
	Lys	Arg	Ser	Arg	Thr	Lys	Arg	Gln	Ser	Pro	Gly	Arg	Ser
	aag	cg c	ag c	ag a	ac t	aag	cgc	ca g	tc a	ccg	gg t	cgc	tc g
	acc	ctc	tgc	cag	acg	aca	tcg	cag	ttc	atc	acc	ccg	cag
	Thr	Leu	Cyc	Gln	Thr	Thr	Ser	Gln	Phe	Ile	Thr	Pro	Gln
	acc	ct g	tgc	cag	ac c	ac c	ag c	ca a	ttc	atc	ac g	cc c	cag
	gcg	gca	ctg	aat	agc	cgc	gga	aac	tgg	atg	ttt	gtg	gtc
	Ala	Ala	Leu	Asn	Ser	Arg	Gly	Asn	Trp	Met	Phe	Val	Val
	gc t	gc c	ctg	aa c	tc c	cg t	gg c	aa t	tgg	atg	tt c	gt c	gt g
	aac	g											
	Asn												
	aac	g											



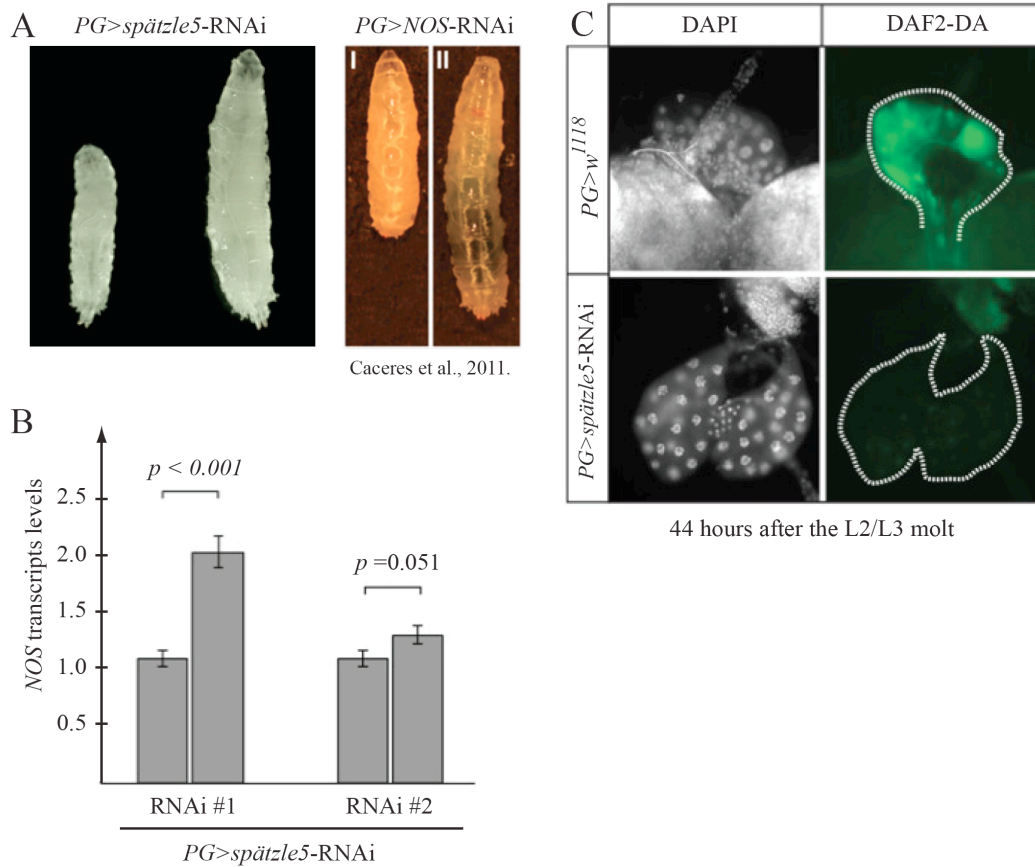


Figure 4.11. *Spätzle5* is required for NO production in the PG.

(A) The L3 arrest phenotype caused by PG-specific RNAi of *spätzle5* and *NOS*. Controls are on the left in both panels. (B) qPCR analysis of NOS transcripts levels in the brain-ring gland complex of *PG>spätzle5-RNAi* lines. RNAi#1 represents the *spätzle5* RNAi line VDRC#102389. RNAi#2 represents the *spätzle5* RNAi line VDRC#41295. Control is represented by the left column of each set. Error bars represent 95% confidence intervals. P values are based on Student's *t*-test. (C) DAF-2 DA stains. Ring glands of the control and *PG>spätzle5-RNAi* (VDRC#102389) larvae were isolated at 44 hours after the L2/L3 molt and stained with DAF2-DA to examine the presence of NO. 5-10 ring glands were tested per condition. NO, nitric oxide.

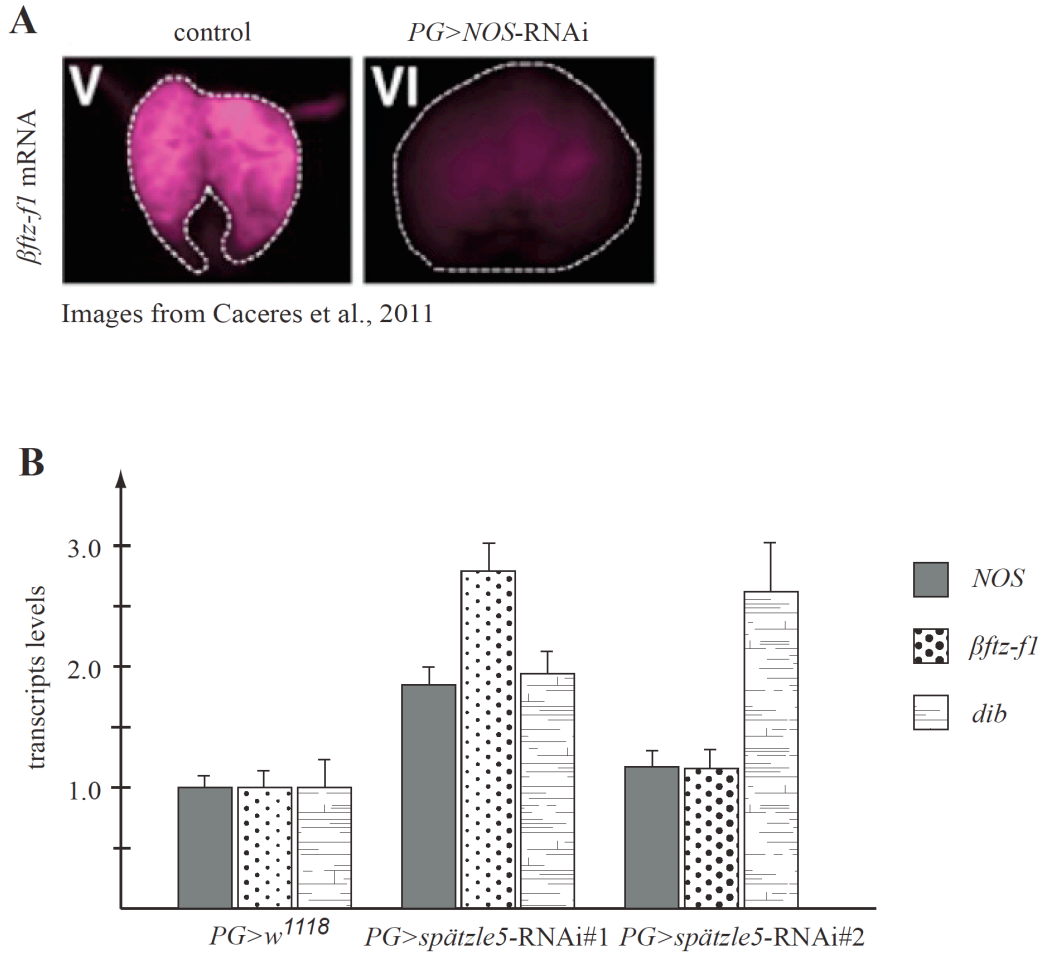


Figure 4.12. The expression of *betaftz-f1* and *dib* in the brain-ring gland complex of *PG>spatzle5-RNAi* larvae.

(A) *In situ* analysis of *betaftz-f1* expression levels in the ring gland of *PG>NOS-RNAi* late L3 wandering larvae. Images are from Caceres et al., 2011.

(B) qPCR analysis of *betaftz-f1* and *dib* transcripts levels in the brain-ring gland complex of controls (grey) and *PG>spatzle5-RNAi* larvae at 44 hours after the L2/L3 molt. RNAi#1 represents the *spatzle5* RNAi line VDRC#102389. RNAi#2 represents the *spatzle5* RNAi line VDRC#41295. Error bars represent 95% confidence intervals.

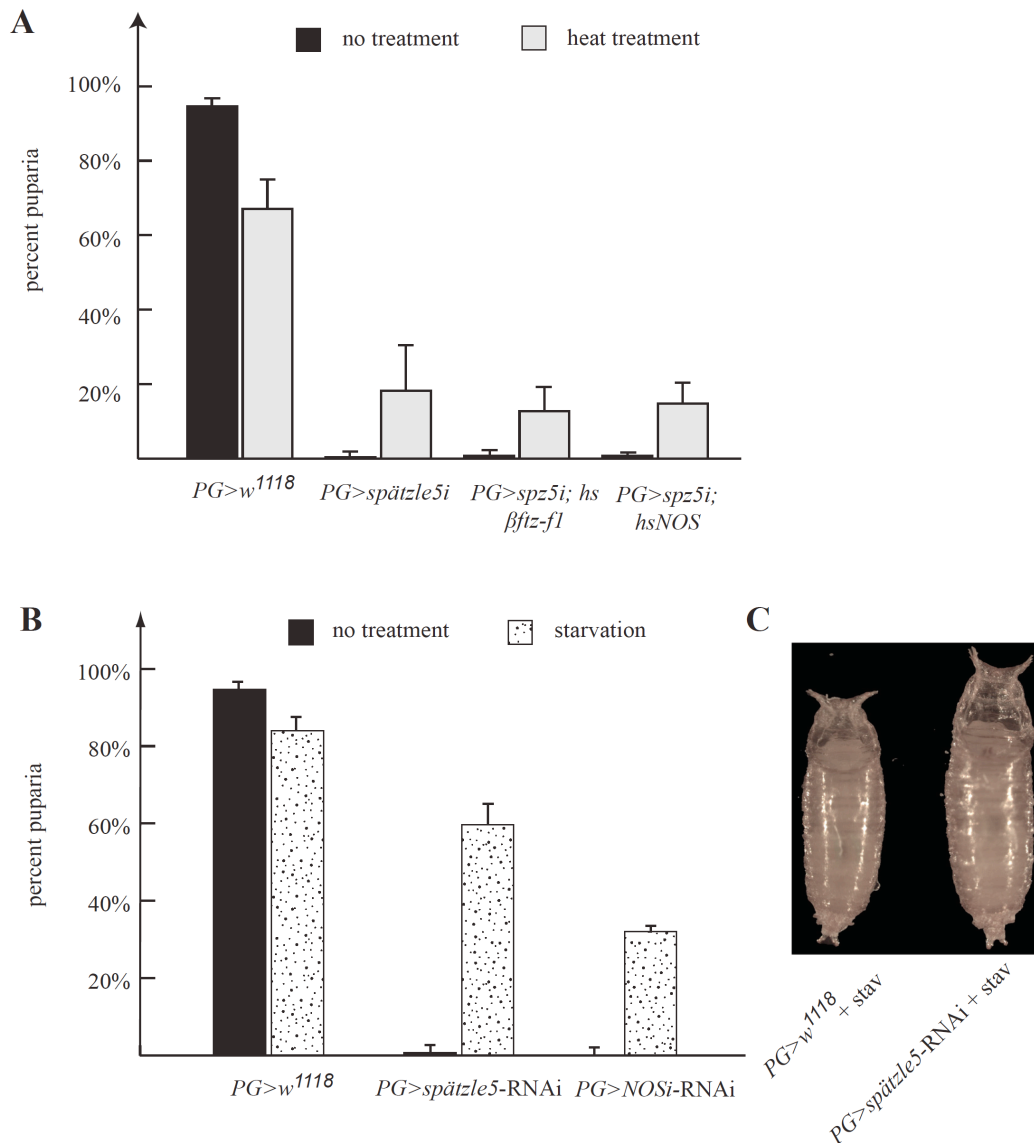


Figure 4.13. A constitutively active form of NOS (NOS^{mac}) or the ectopic expression of $\beta ftz-fl$ did not rescue $PG>spätzle5-RNAi$ phenotype.

(A) The percentages of embryos that reached puparia. A single heat shock was carried out in the control, $PG>spätzle5-RNAi$, $PG>spätzle5-RNAi; hsNOS^{mac}$, and $PG>spätzle5-RNAi; hs\beta ftz-fl$ populations during an early wandering stage (30~35 hours after the L2/L3 molt). $PG>w^{1118}$ (control), N=240 (no treatment), N=480 (heat treatment). $PG>spätzle5-RNAi$, N=480 (no treatment), N=800 (heat treatment). $PG>spätzle5-RNAi; hsNOS^{mac}$, N=480 (no treatment), N=600 (heat

treatment). *PG>spätzle5-RNAi; hsβftz-fl*, N=600 (no and heat treatment). Error bars represent standard deviation. (B) The percentages of L3 larvae that initiated metamorphosis. Starvation began in an early wandering stage (30~35 hour after the L2/L3 molt). *PG>w¹¹¹⁸*, N=240 (fed), N=130 (starved). *PG>spätzle5-RNAi*, N=480 (fed), N=66 (starved). *PG>NOS-RNAi*, N=50 (fed), N=47 (starved). Error bars represent standard deviation. (C) Starvation rescued *PG>spätzle5-RNAi* animals to puparia. *PG>spätzle5-RNAi* larvae that were under starvation from an early wandering stage started to pupariate in two days, in comparison to 0% puparia of the unstarved population at that time point. Stav, starvation.

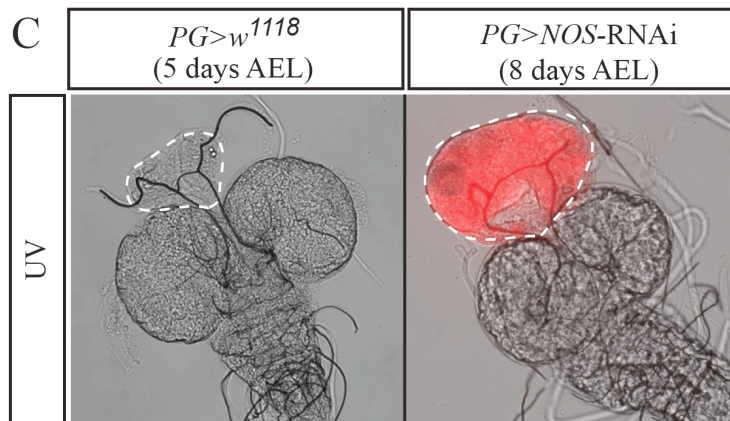
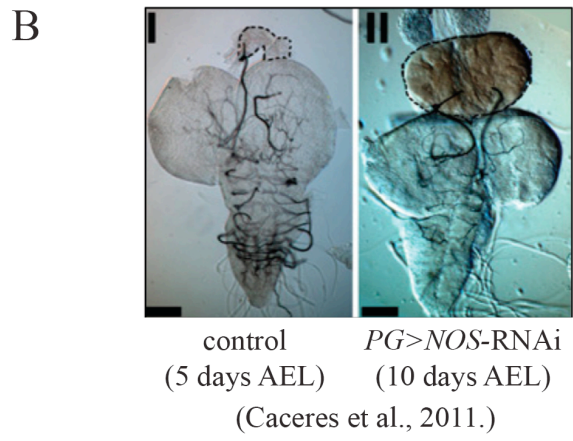
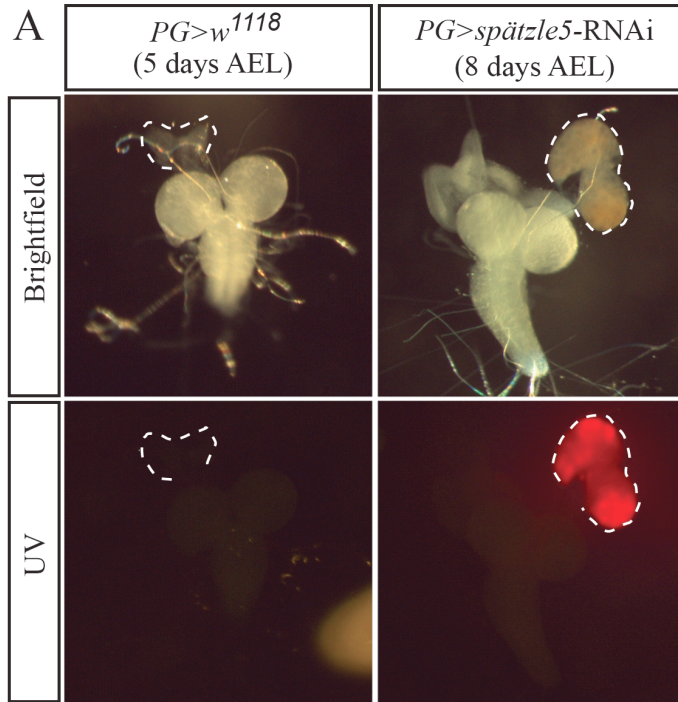


Figure 4.14. The ring gland phenotype of PG-specific disruption of *spätzle5* and *NOS* function.

(A) Loss of *spätzle5* specifically in the PG results in overgrown brown-reddish ring glands under brightfield microscopy (upper panel). Upon UV exposure, *PG>spätzle5-RNAi* ring glands display autofluorescence (bottom panel). At least 15 ring glands were examined. (B) Knocking down *NOS* specifically in the PG results in overgrown brown-reddish ring glands. Images are from Caceres et al., 2011. (C) *PG>NOS-RNAi* ring glands exhibit fluorescence under UV light. At least 15 ring glands were examined.

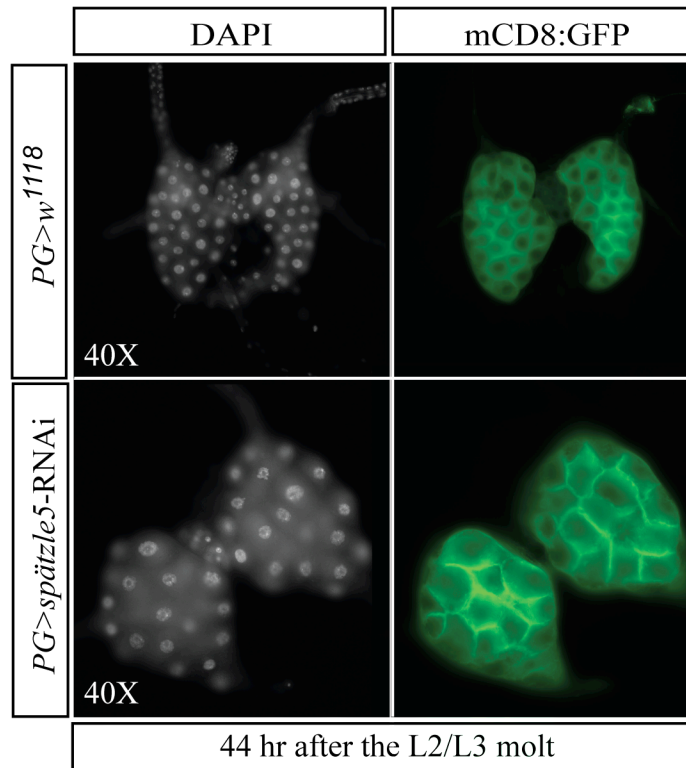


Figure 4.15. PG-specific knockdown of *spätzle5* results in the overgrowth of ring gland. Ring glands were isolated from *PG>w¹¹¹⁸* (control) and *PG>spätzle5-RNAi* larvae at 44 hours after the L2/L3 molt. A DAPI stain of the nuclei is included. mCD8:GFP highlights PG cell membrane. Images are at 40X magnification. 10~15 ring glands were examined per condition.

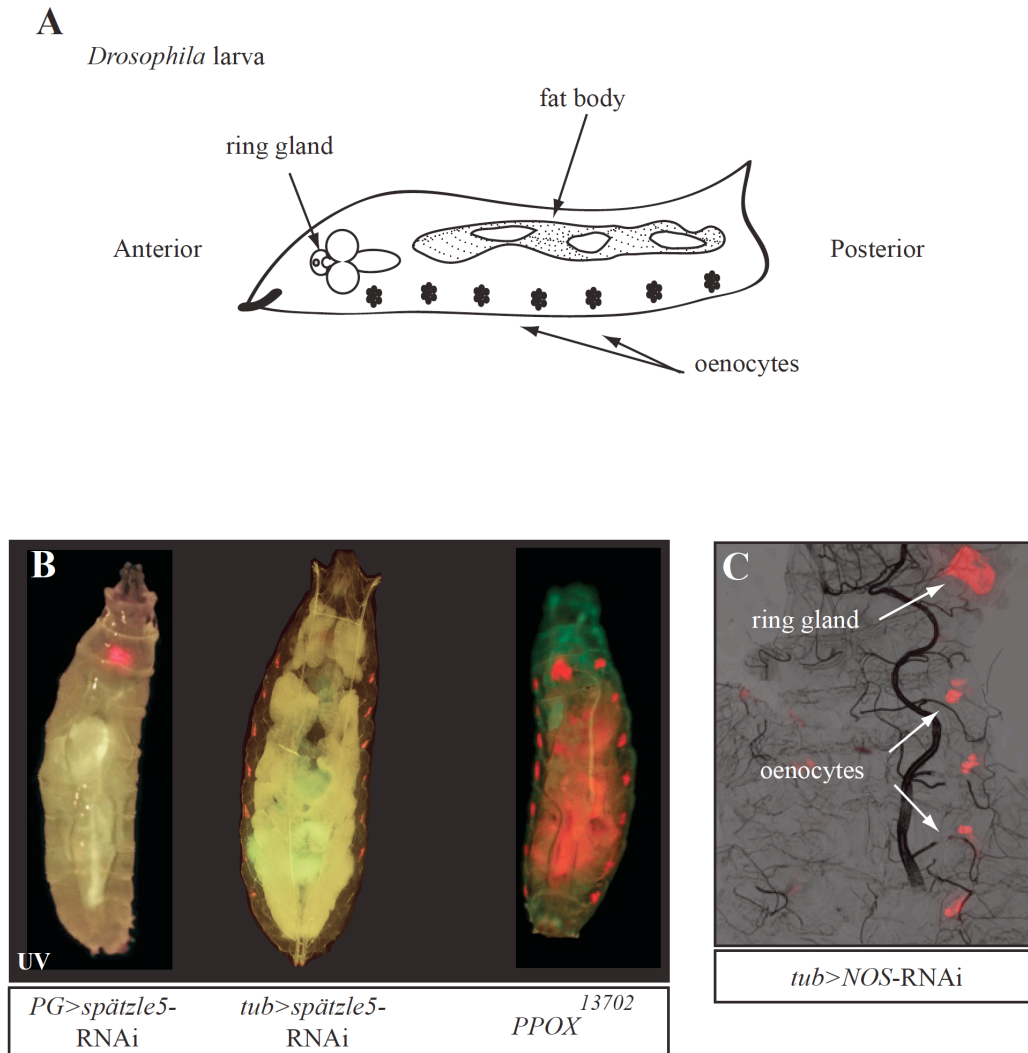


Figure 4.16. Ubiquitous knockdown of *spätzle5* or *NOS* gives a phenotype similar to that observed in the *PPOX*¹³⁷⁰² mutant.

(A) Schematic representation of the ring gland, larval oenocytes, and fat body in *Drosophila* larva. (B) Phenotypes of *PG>spätzle5-RNAi*, *tub>spätzle5-RNAi*, and the *PPOX*¹³⁷⁰² mutant under UV light. PG-specific RNAi of *spätzle5* causes fluorescent ring glands (left). A ubiquitous knockdown of *spätzle5* (*tub>spätzle5-RNAi*) results in fluorescent ring glands and oenocytes (middle). *PPOX*¹³⁷⁰² mutants display fluorescence in the ring gland, oenocytes, and the gut (right). (C) The phenotype of *tub>NOS-RNAi* upon UV exposure. Fluorescence is observed in the ring gland and oenocytes. *tub*, *tubulin-Gal4*.

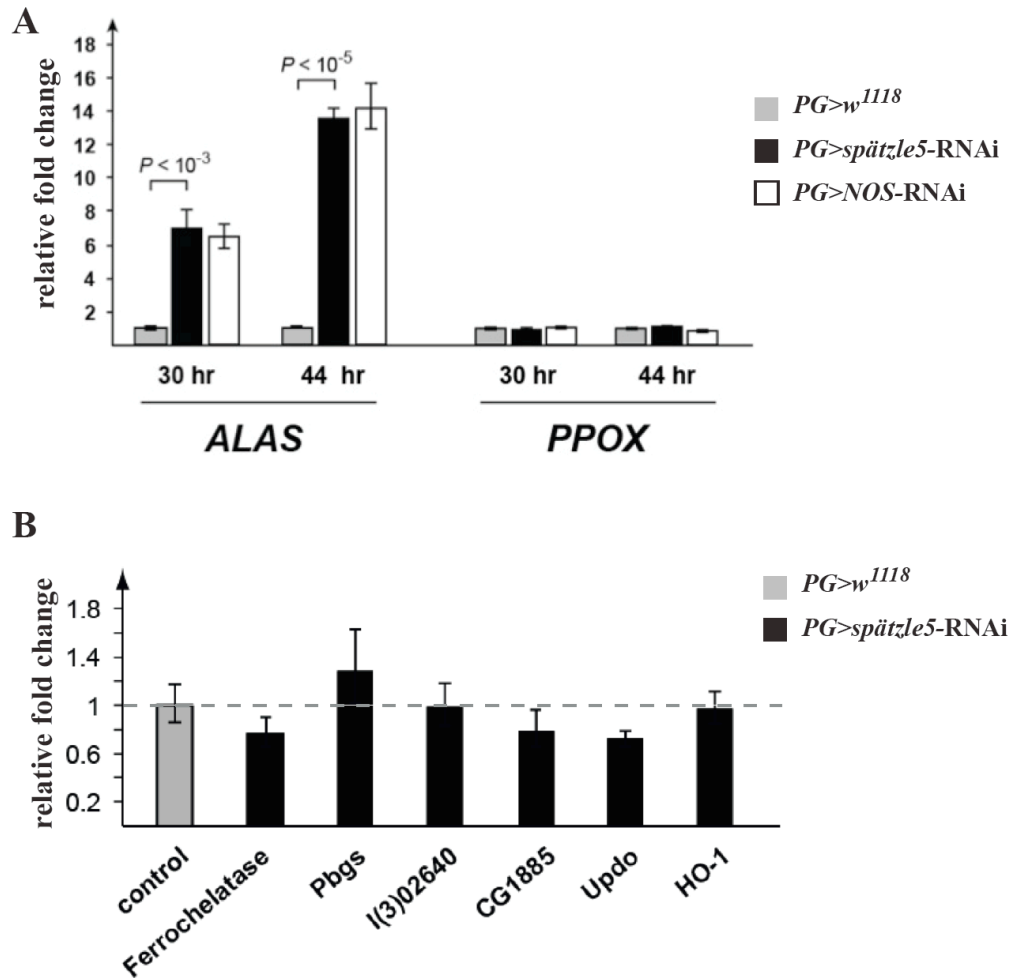


Figure 4.17. The expression of heme biosynthetic genes in PG-specific *spätzle5* and *NOS* knockdowns.

(A) qPCR analysis of *ALAS* and *PPOX* transcripts levels in the brain-ring gland complex of *PG>spätzle5-RNAi* and *PG>NOS-RNAi* larvae at two developmental times, 30 hours and 44 hours after the L2/L3 molt, respectively. (B) qPCR analysis of the expression of other heme biosynthetic genes, including *Pbgs*, *l(3)02640*, *CG1885*, *Updo*, and *Ferrochelatase*, in the brain-ring gland complex of the control and *PG>spätzle5-RNAi* animals at 44 hours after the L2/L3 molt. Transcripts levels of *HO-1* were also examined. Error bars represent 95% confidence intervals. P values in (A) are based on Student's *t*-test. Data are insignificant if P values are not shown. *ALAS*, 5'-aminolevulinic acid synthase.

Pbgs, also called *ALAD*, 5'-aminolevulinic acid dehydratase. *l(3)02640*, also called *PBGD*, porphobilinogen deaminase. *CG1885*, uroporphyrinogen III synthase. *Updo* (*CG1818*), uroporphyrinogen III decarboxylase. *PPOX*, protoporphyrinogen oxidase. HO-1, heme oxygenase-1.

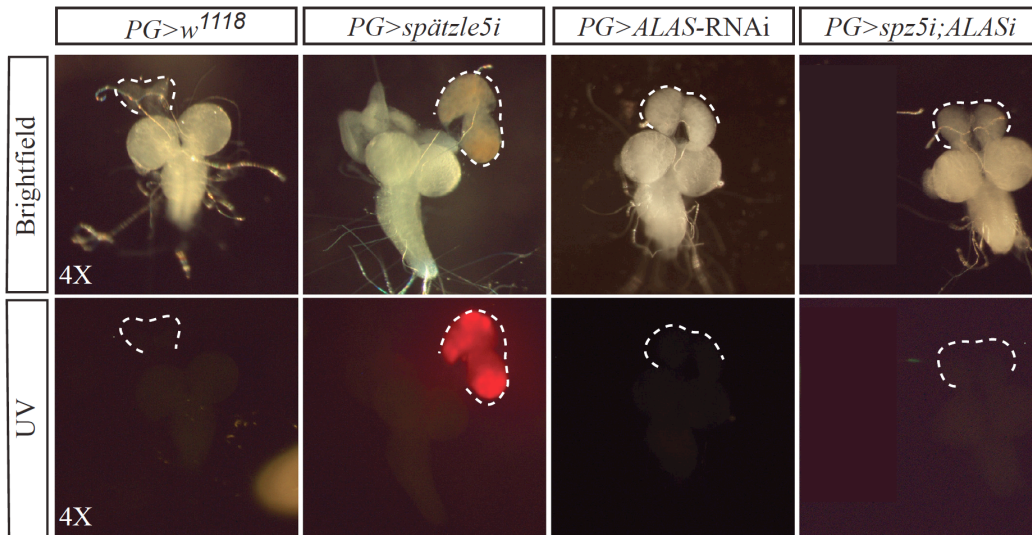


Figure 4.18. Loss of *ALAS* abolishes the autofluorescence displayed by the ring gland of *PG>spätzle5-RNAi* larvae. Ring glands of the control *PG>w¹¹¹⁸* were examined on day 2 after the L2/L3 molt. Ring glands of *PG>spätzle5-RNAi*, *PG>ALAS-RNAi*, and *PG>spätzle5-RNAi; ALAS-RNAi* were isolated on day 5 after the L2/L3. 15~20 ring glands were examined per condition.

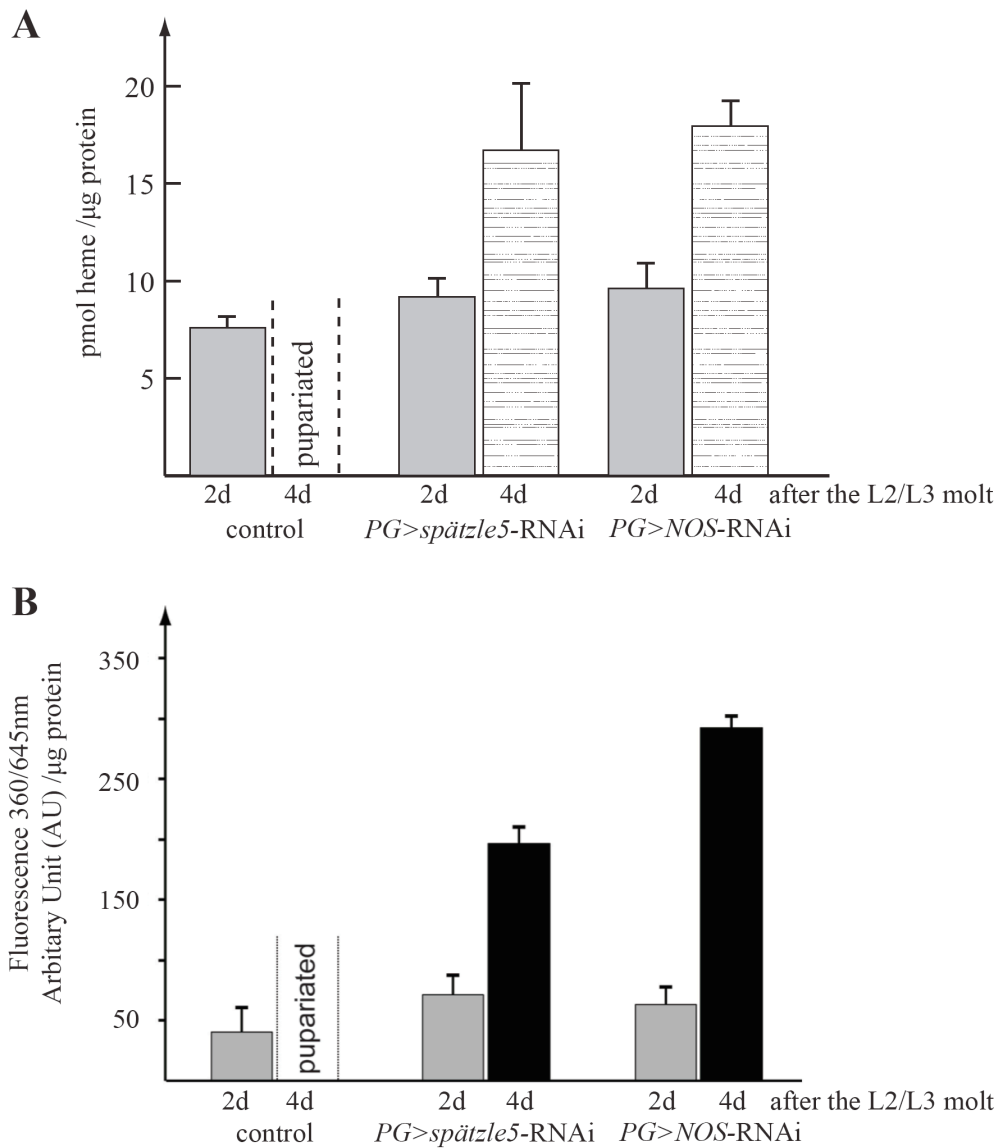


Figure 4.19. Loss of *spätzle5* and *NOS* result in an accumulation of heme precursors in the ring gland.

(A) Total heme measurements. Brain-ring gland complexes of the control, *PG>spätzle5-RNAi*, and *PG>NOS-RNAi* animals were isolated on day 2 L3 (at 44 hours after the L2/L3 molt) and day 4 L3 (at 92 hours after the L2/L3 molt), respectively. Total heme levels were calibrated as pmol/μg protein. Three samples were tested per condition. Each sample was tested in duplicate. Error bars represent standard error. (B) Measurements of the autofluorescence of BRRG

homogenates used in (A) under UV light. Total fluorescence levels were calibrated as AU/ μg protein. Three samples were tested per condition. Each sample was tested in duplicate. Error bars represent standard error. AU, arbitrary unit. BRRG, brain-ring gland complex.

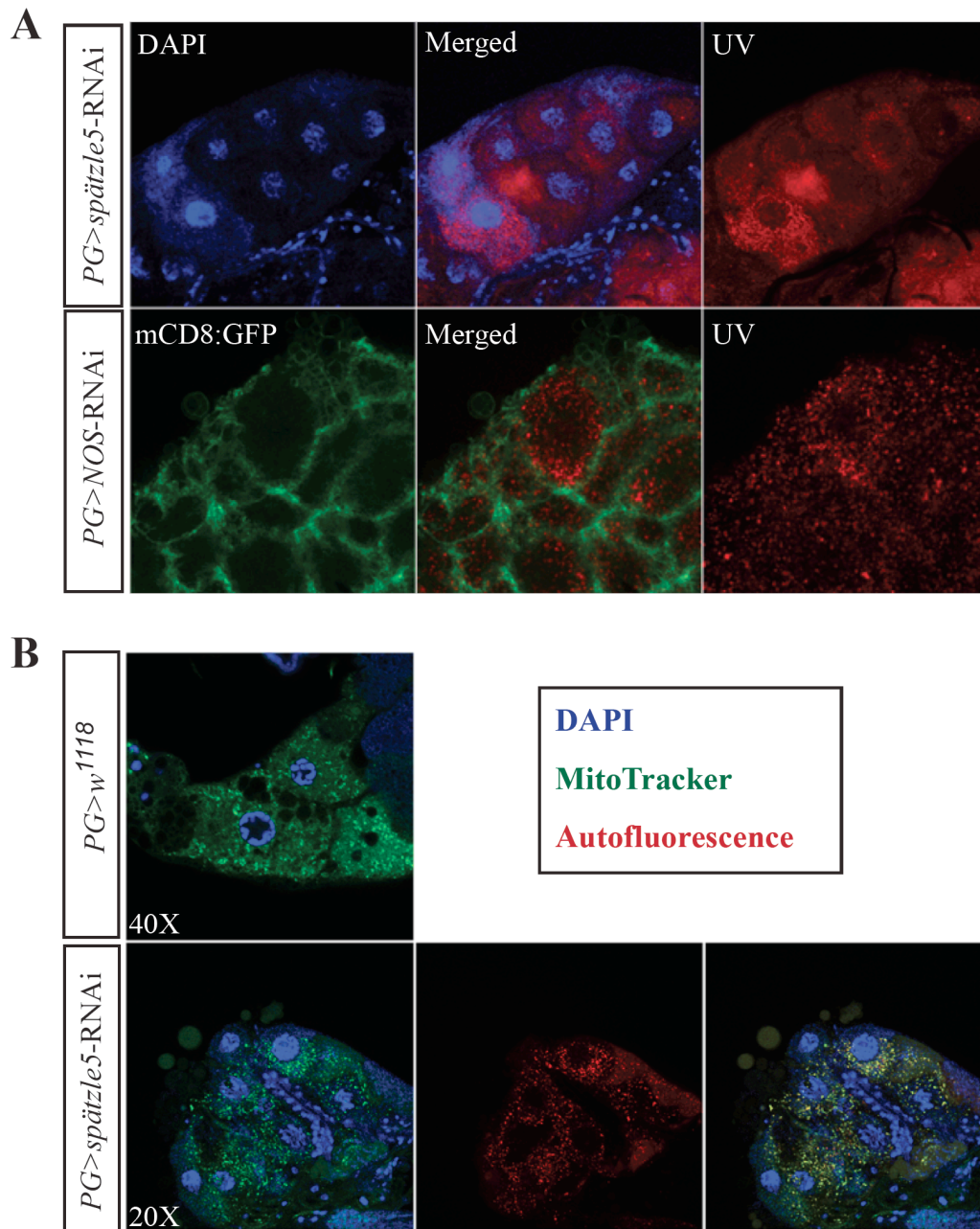


Figure 4.20. Disrupting *spätzle5* and *NOS* results in punctate fluorescence signals in the PG under UV.

(A) Loss of *spätzle5* and *NOS* in the PG gives punctate fluorescence signals under UV. Ring glands were isolated from *PG>spätzle5-RNAi* and *PG>NOS-RNAi* larvae on day 4 after the L2/L3 molt. Samples were examined at 20X magnification. (B) MitoTracker Green stains. Ring glands of the control and

PG>spätzle5-RNAi animals were isolated at 44 hours after the L2/L3 molt and immediately stained with MitoTracker Green. A DAPI stain of nuclei is included. The control ring gland was imaged at 40X magnification for a better resolution. The *PG>spätzle5*-RNAi ring gland was examined at 20X magnification.

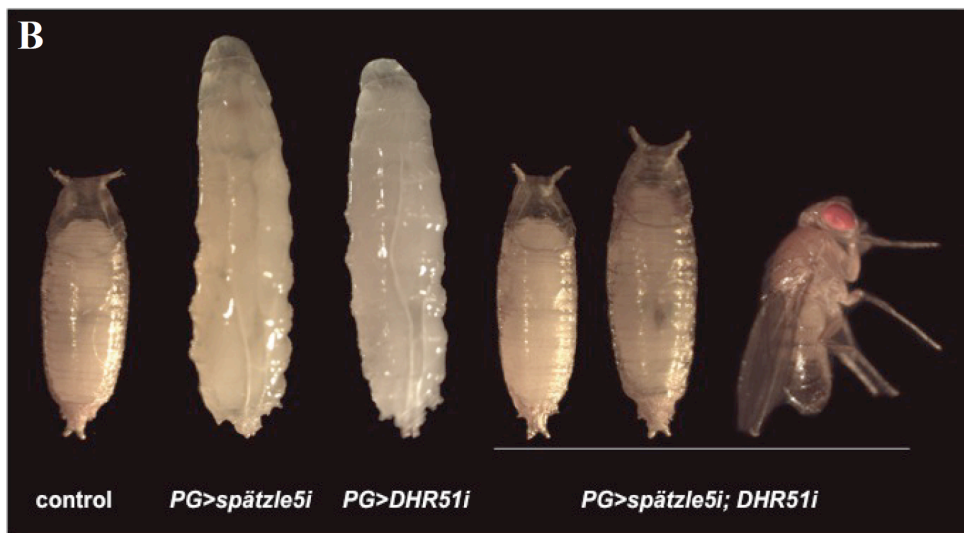
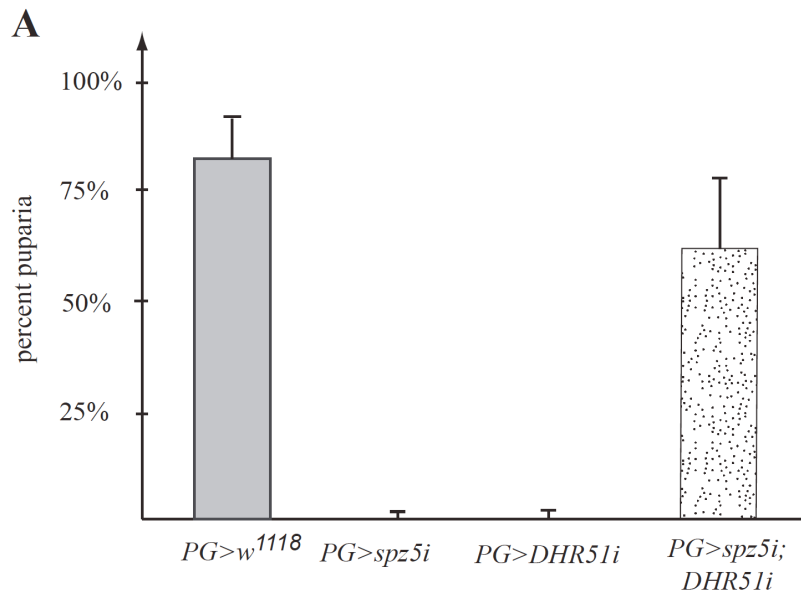


Figure 4.21. Loss of *DHR51* rescues the larval lethality caused by PG-specific knockdown of *spätzle5*.

(A) The percentages of embryos that reached puparia. Error bars indicate standard deviation. $PG>w^{1118}$, N=240. $PG>spätzle5$ -RNAi, N=140. $PG>DHR51$ -RNAi, N=140. $PG>spätzle5$ -RNAi; *DHR51*-RNAi, N=240. Error bars represent standard deviations. (B) RNAi phenotypes, from left to right: $PG>w^{1118}$ (control), $PG>spätzle5$ -RNAi (L3 arrest), $PG>DHR51$ -RNAi (L3 arrest), and $PG>spätzle5$ -RNAi; *DHR51*-RNAi (~60% puparia and viable adults).

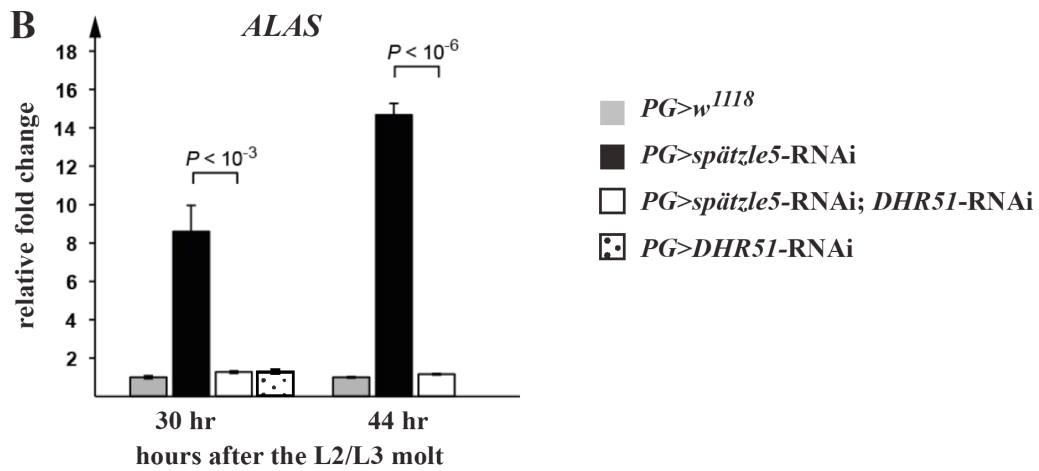
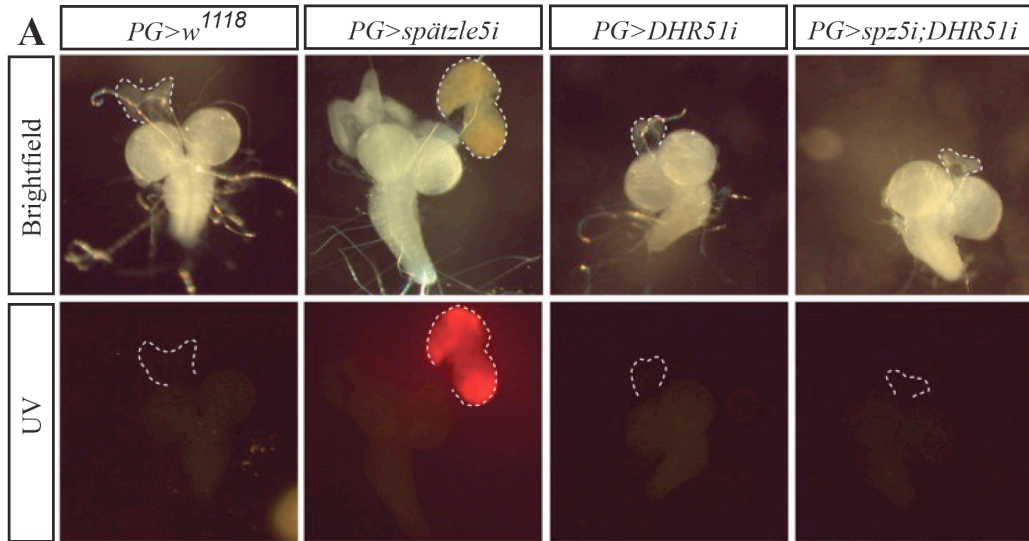


Figure 4.22. DHR51 is required for *ALAS* upregulation caused by PG-specific knockdown of *spätzle5*.

(A) Ring gland phenotypes. Ring glands were isolated from controls at 44 hours after the L2/L3 molt, and from other genotypes on day 5 after the L2/L3 molt. 15~20 ring glands were tested per condition. (B) qPCR analysis of *ALAS* transcripts levels in the brain-ring gland complex of the control, *PG>spätzle5-RNAi*, and *spätzle5; DHR51* double knockdowns at two developmental times, 30 hours and 44 hours after the L2/L3 molt. *ALAS* transcripts levels were also examined in the brain ring gland complex of

PG>DHR51-RNAi larvae 30 hours after the L2/L3 molt. Error bars represent 95% confidence intervals. P values were calculated with Student's *t* test.

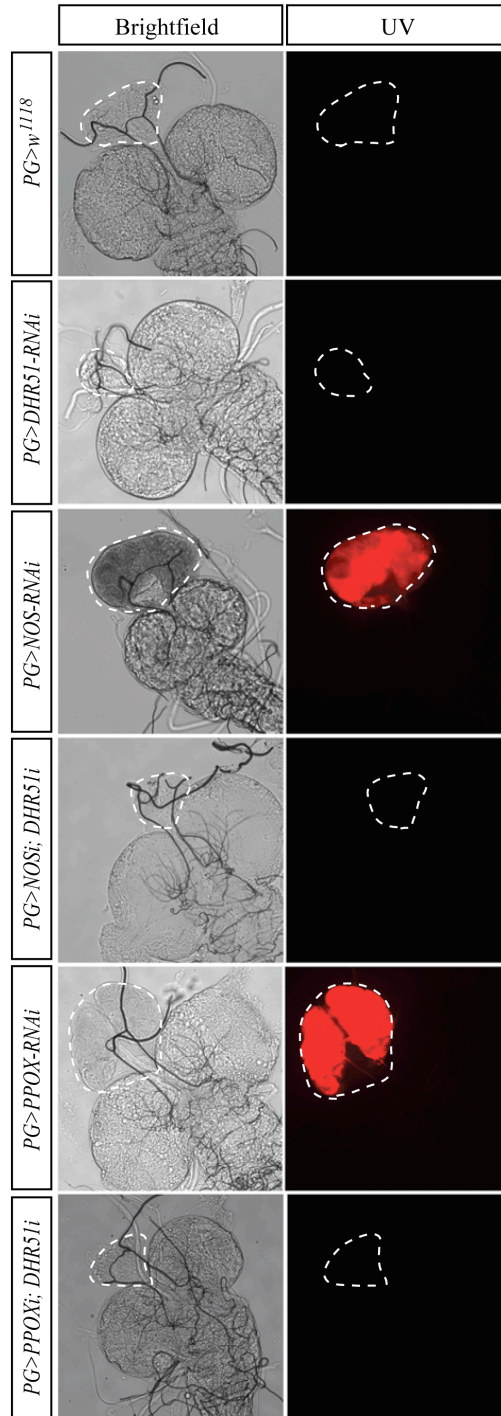


Figure 4.23. Knocking down *DHR51* rescues *NOS*-RNAi and *PPOX*-RNAi ring gland phenotypes. Ring glands were isolated from the control at 44 hours after the L2/L3 molt, and from other genotypes on day 5 L3 after the L2/L3 molt. 15~20 ring glands were tested in each condition.

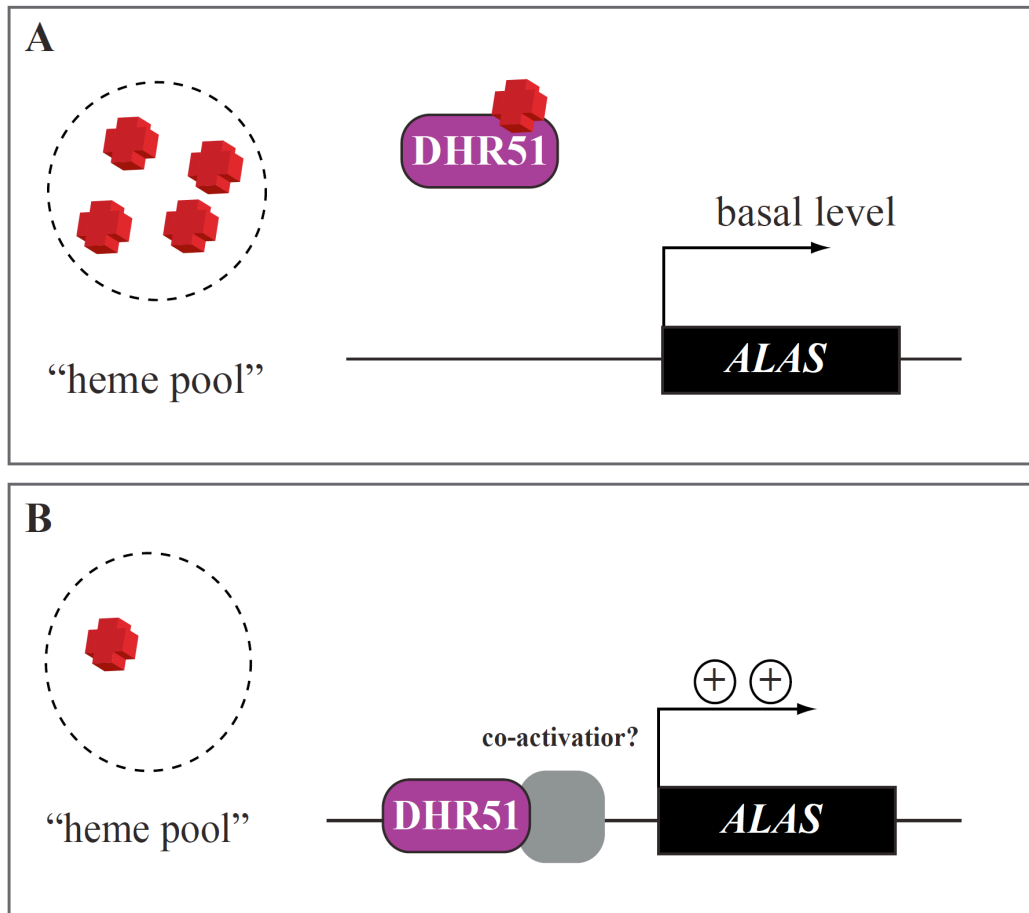


Figure 4.24. A model of nuclear receptor DHR51 acting as a heme sensor in the *Drosophila* PG.

(A) When heme is ample, DHR51 is heme-bound. ALAS, the first and rate-limiting enzyme of the heme biosynthetic pathway is expressed at basal levels. (B) When heme is limiting, apoDHR51 (the heme-unbound state) augments the expression of *ALAS* as a mechanism to enhance heme synthesis, possibly through recruiting other uncharacterized co-activator(s). ALAS, 5'-aminolevulinic acid synthase.

A

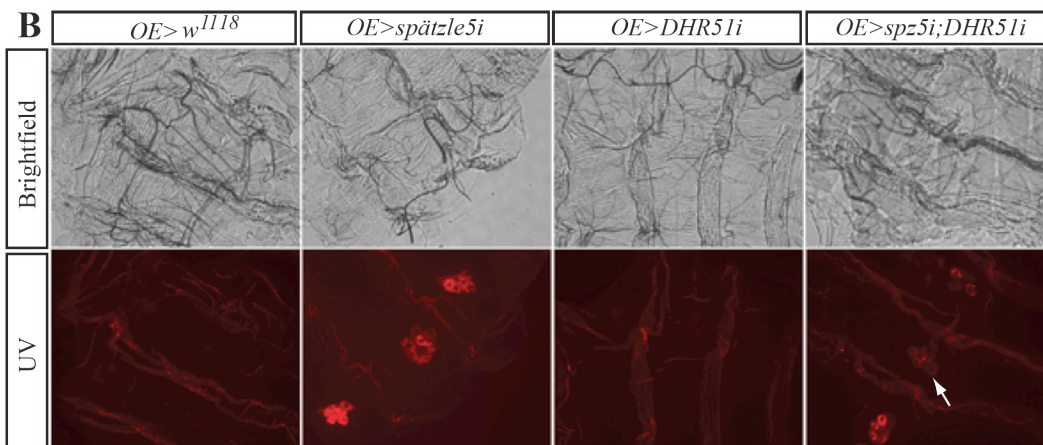


Figure 4.25. Loss of *DHR51* partially rescues protoporphyrin accumulation in *OE>spätzle5*-RNAi oenocytes.

(A) Oenocyte-specific knockdown of *spätzle5*, *DHR51*, or both results in eclosion defects during late pupal development. A control pupa is shown on the left. RNAi animals failed to eclose from the pupal case. (B) Oenocyte phenotypes under UV light. Larval oenocytes were examined at 44 hours after the L2/L3 molt. 15 or more larvae were tested per condition. The arrow indicates a cluster of oenocytes where the accumulation of protoporphyrins was suppressed by *DHR51*-RNAi.

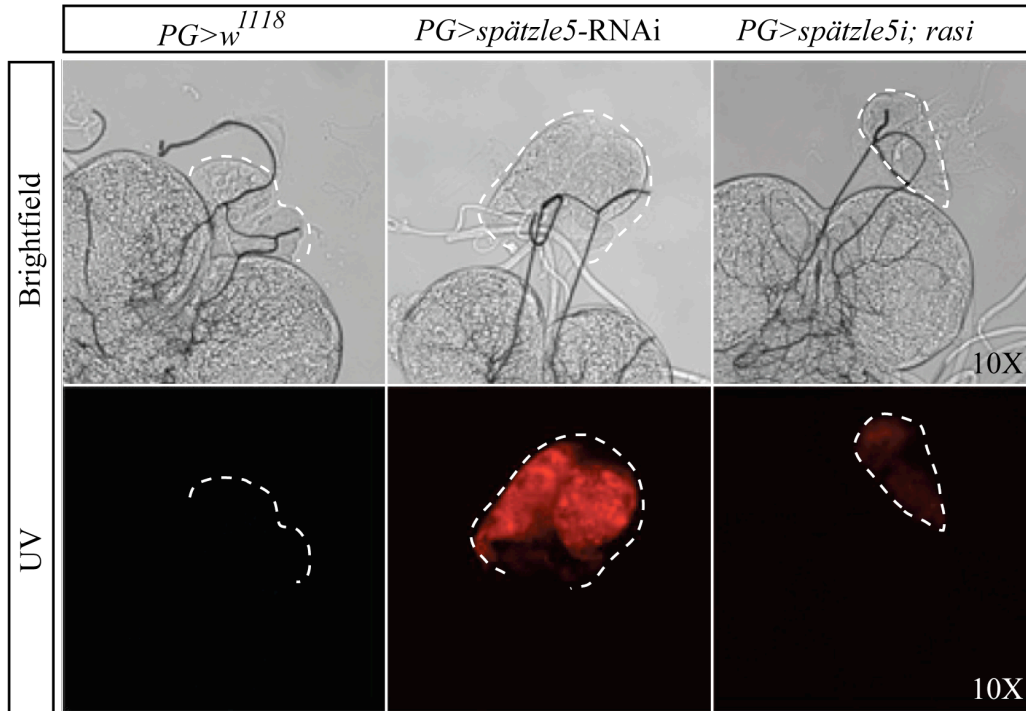


Figure 4.26. Ras contributes to the ring gland phenotype of *PG>spätzle5-RNAi* larvae. Ring glands were isolated from the control, *PG>spätzle5-RNAi* and *PG>spätzle5-RNAi; Ras-RNAi* on day 4 after the L2/L3 molt. 10 ring glands were tested per condition.

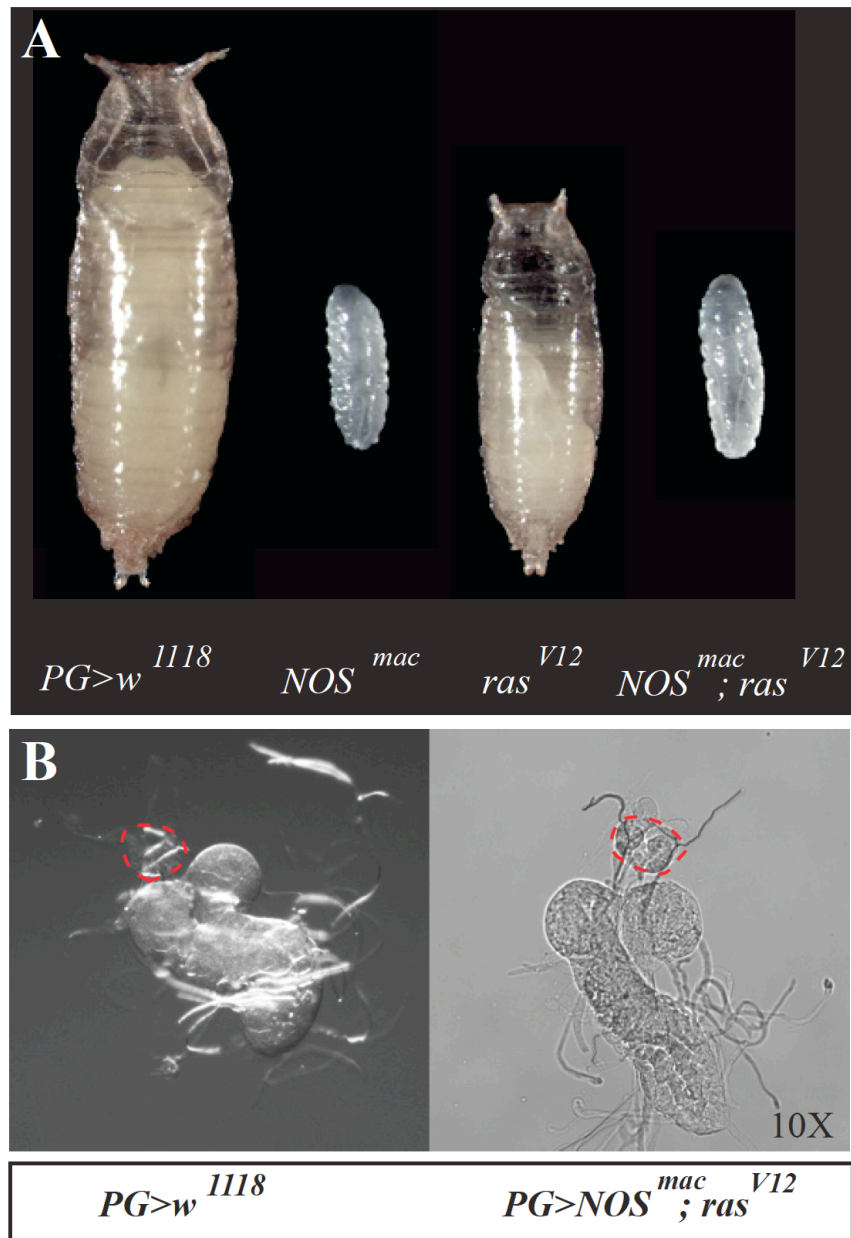


Figure 4.27. NO signaling is epistatic to Ras signaling.

(A) Phenotypes of animals expressing a constitutively active form of NOS (NOS^{mac}), a constitutively active form of Ras (Ras^{V12}), and both. (B) Ring gland phenotypes of animals expressing both NOS^{mac} and Ras^{V12} . Ring glands were isolated from the control and $PG>NOS^{mac}; Ras^{V12}$ larvae on day 2 AED, and imaged under brightfield microscopy at 10X magnification.

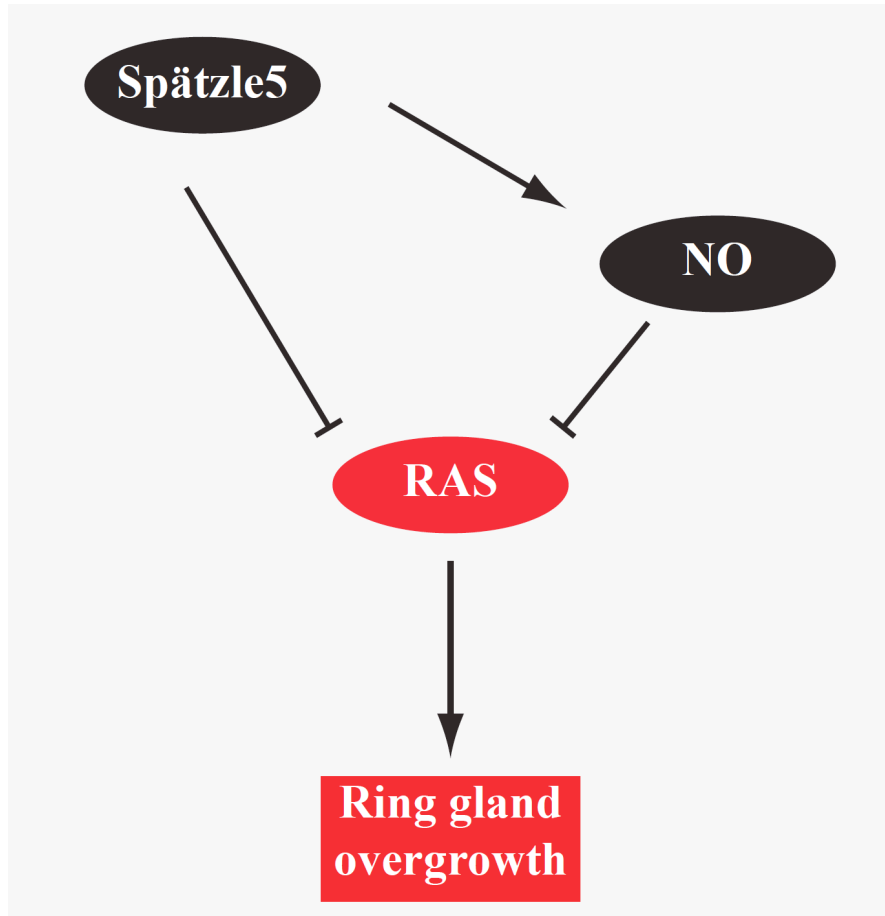


Figure 4.28. The epistasis of Spätzle5 and NO to Ras signaling.

Expressing a constitutively active form of Ras (Ras^{V12}) in the PG results in the overgrowth of ring gland. Ras signaling is required for the ring gland overgrowth caused by loss of *spätzle5* (**Figure 4.26**). A constitutively active form of NOS, NOS^{mac}, suppresses the ring gland overgrowth induced by the expression of Ras^{V12} (**Figure 4.27**).

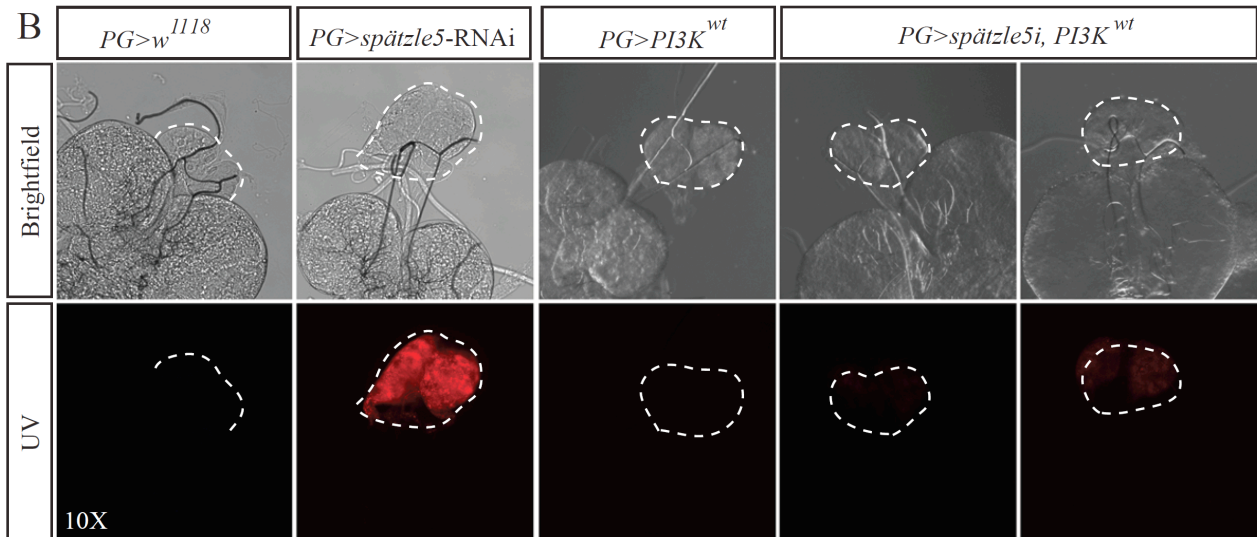
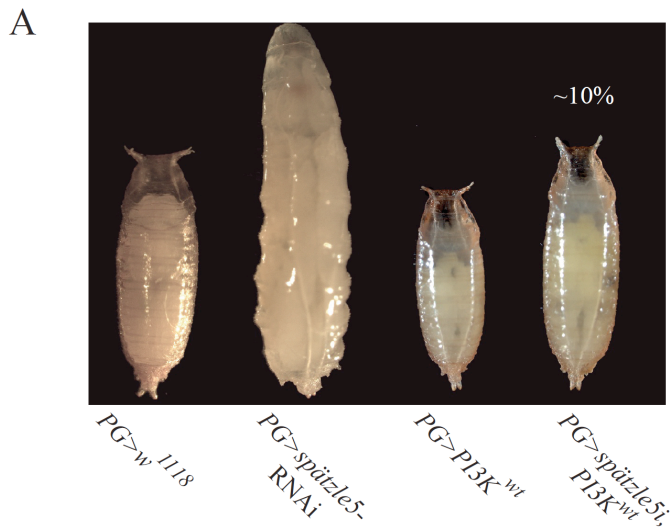


Figure 4.29. PI3K signaling ameliorates the accumulation of protoporphyrins in the PG caused by *spätzle5* RNAi.

(A) The expression of wild type PI3K in the PG partially rescues the larval lethality caused by PG-specific knockdown of *spätzle5*. (B) The expression of wild type PI3K in the PG ameliorates the accumulation of protoporphyrins caused by the silence of *spätzle5*. Ring glands were isolated from the control and *PG>PI3K*^{wt} at 44 hours after the L2/L3 molt. For *PG>spätzle5*-RNAi and *PG>spätzle5*-RNAi, *PI3K*^{wt} larvae, ring glands were examined on day 4 after the L2/L3 molt. 10 ring glands were tested per condition.



Figure 4.30. Ectopic expression of wild type *spätzle5* results in pupariation and growth defects.

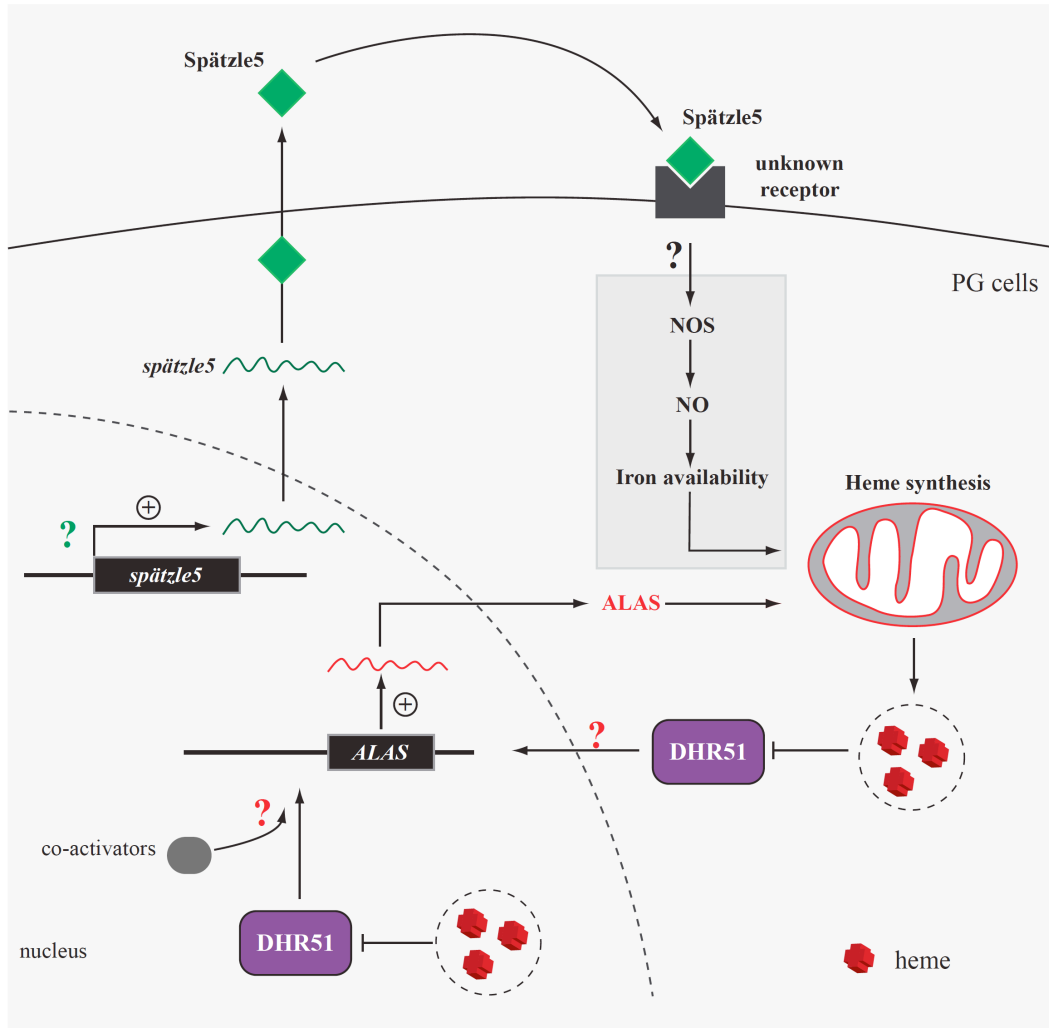


Figure 4.31. A model for the role of Spätzle5 and NO signaling in the regulation of heme synthesis in the *Drosophila* PG. The expression of *spätzle5* is developmentally regulated with increasing transcripts levels towards the end of larval development in the PG. Spätzle5 governs heme production in an autocrine fashion by binding to an unknown receptor on PG cells. NO signaling may serve as a downstream effector of Spätzle5 in regulating heme synthesis, possibly by affecting iron availability to the cell (? , black type). Loss of *spätzle5* and NO signaling adversely affects heme production, which leads to the activation of DHR51 to augment the expression of ALAS, the rate-limiting enzyme of heme synthesis, as a mechanism to restore normal heme levels. The upregulation of ALAS results in an accumulation of heme precursors in PG mitochondria. It

remains unknown what cue(s) is responsible for the upregulation of *spätzle5* in the PG prior to metamorphosis (? , green type). Little is known about the mechanism by which DHR51 stimulates *ALAS* expression (? , red type). DHR51 may undergo nuclear translocation to enhance *ALAS* transcription under low heme conditions, while it stays outside the nucleus when heme is ample. ApoDHR51 (the heme-unbound state) may also require the recruitment of uncharacterized co-activators to induce *ALAS* upregulation. NO, nitric oxide. NOS, nitric oxide synthase. ALAS, 5'-aminolevulinic acid synthase.

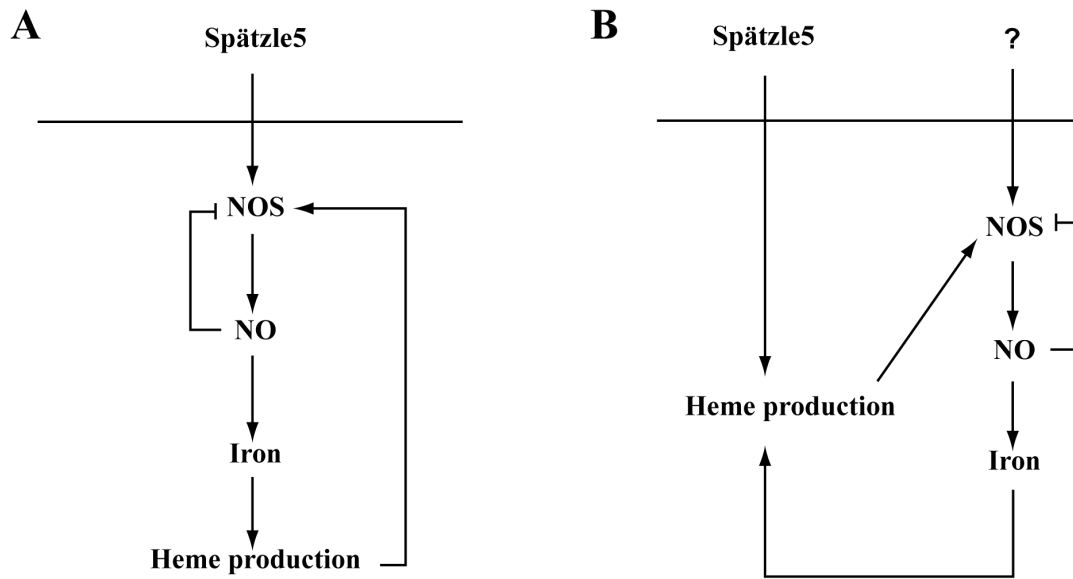


Figure 4.32. Two possible mechanisms underlying Spätzle5 and NO signaling in the regulation of heme synthesis in the *Drosophila* PG.

(A) A model illustrates that *Drosophila* neurotrophin Spätzle5 modulates heme production in the PG by directly controlling the activity of NOS, which in turn affects heme synthesis possibly through modulating iron availability. (B) An alternative model illustrates that Spätzle5 and NO signaling could independently affect heme biosynthesis in the PG. Loss of *spätzle5* disturbs heme production, which in turn impairs the activity of NOS that use heme as cofactor.

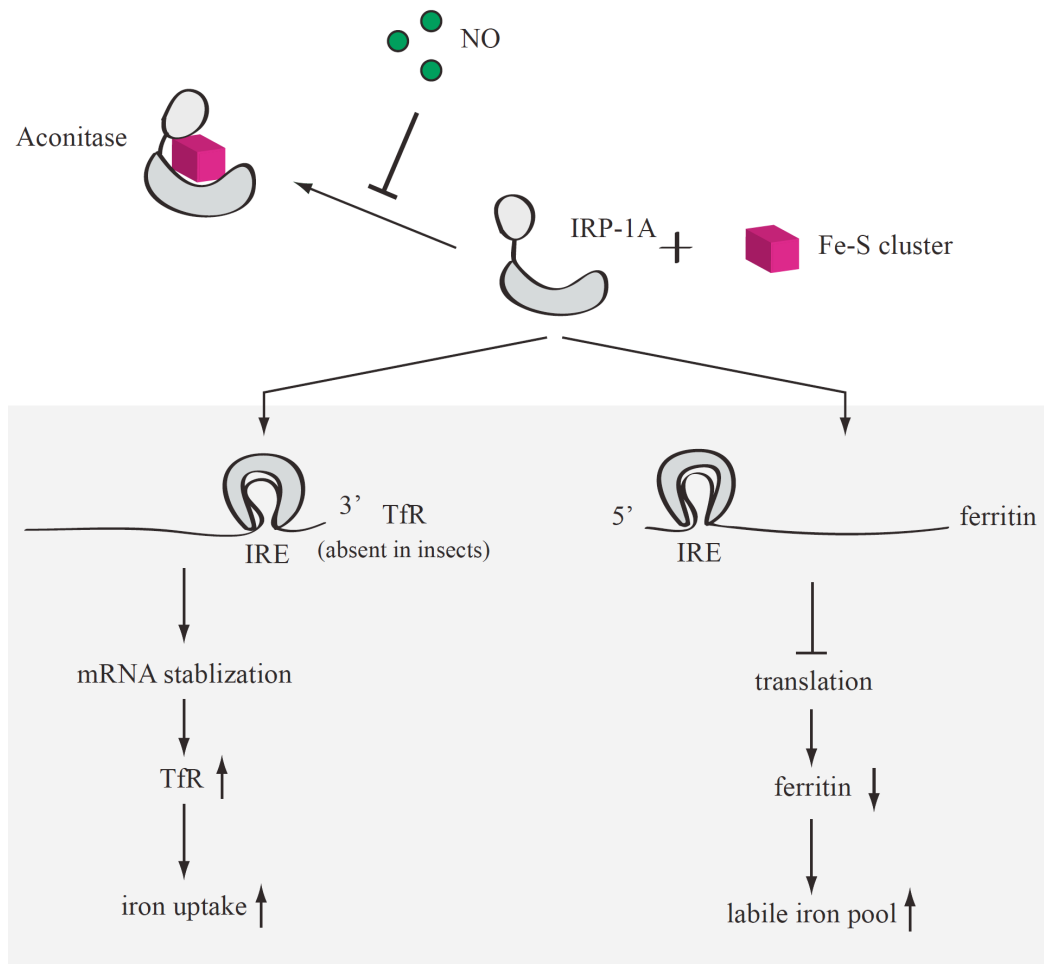


Figure 4.33. Possible roles of NO signaling in modulating cellular iron availability in the PG.

When cellular iron levels are low, IRP-1A becomes an RNA binding protein, which binds to IREs present in the 3'-UTR of TfR mRNA (absent in insects) and 5'-UTR of ferritin mRNA, permitting iron-responsive elevation of TfR levels (thus increasing iron uptake) and decrease of ferritin levels (thus reducing iron storage), respectively. When iron is ample, IRP1 incorporates a Fe-S cluster in its catalytic center, effectively converting the activity of the protein to an aconitase. This allows the de-repression of ferritin translation but reduces TfR synthesis. NO is able to regulate IRP/IRE interaction by altering Fe-S cluster retention in IRP1. In the presence of NO, the conversion of IRP1 into an aconitase when iron is

ample is blocked. This allows an increase of iron uptake and release from ferritins for cellular utilization, such as heme synthesis and Fe-S biogenesis.

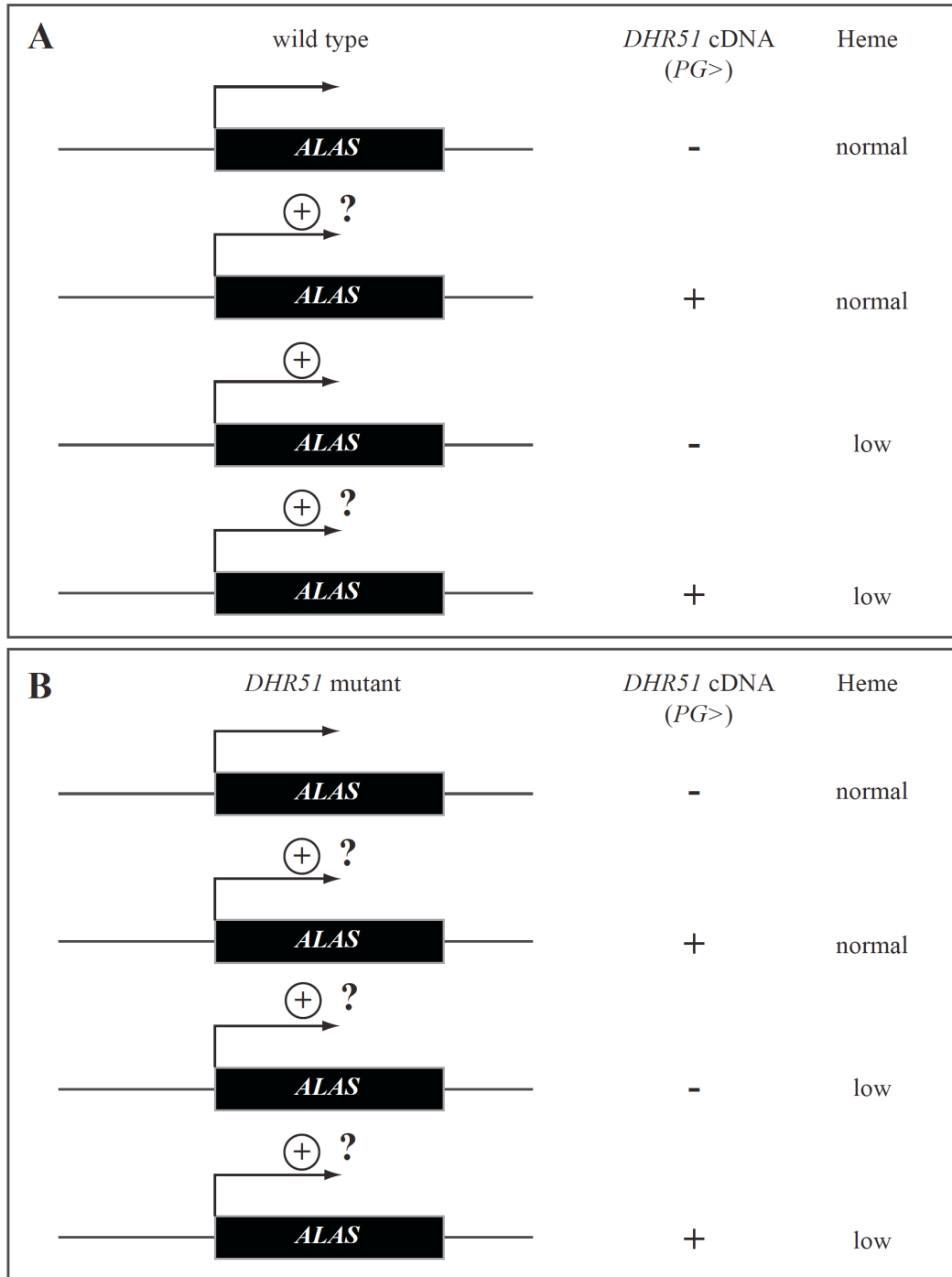


Figure 4.34. A proposed experiment of testing the transcriptional activity of *DHR51* under normal and low heme conditions.

Wild type *DHR51* cDNA will be expressed specifically in the PG in the control (A) and the *DHR51* mutant background (B), under normal and low heme conditions. The expression levels of *ALAS* will be examined in each condition.

4.7 Bibliography

- Ajioka, R.S., Phillips, J.D., and Kushner, J.P. (2006). Biosynthesis of heme in mammals. *Biochimica et biophysica acta* 1763, 723-736.
- Akashi, H. (1994). Synonymous codon usage in *Drosophila melanogaster*: natural selection and translational accuracy. *Genetics* 136, 927-935.
- Asha, H., Nagy, I., Kovacs, G., Stetson, D., Ando, I., and Dearolf, C.R. (2003). Analysis of Ras-induced overproliferation in *Drosophila* hemocytes. *Genetics* 163, 203-215.
- Beck, G., Munno, D.W., Levy, Z., Dissel, H.M., van-Minnen, J., Syed, N.I., and Fainzilber, M. (2004). Neurotrophic activities of trk receptors conserved over 600 million years of evolution. *Journal of Neurobiology* 60, 12-20.
- Billeter, J.C., Atallah, J., Krupp, J.J., Millar, J.G., and Levine, J.D. (2009). Specialized cells tag sexual and species identity in *Drosophila melanogaster*. *Nature* 461, 987-991.
- Bredt, D.S., and Snyder, S.H. (1994). Nitric oxide: a physiologic messenger molecule. *Annual review of biochemistry* 63, 175-195.
- Broadus, J., McCabe, J.R., Endrizzi, B., Thummel, C.S., and Woodard, C.T. (1999). The *Drosophila* beta FTZ-F1 orphan nuclear receptor provides competence for stage-specific responses to the steroid hormone ecdysone. *Molecular cell* 3, 143-149.
- Caceres, L., Necakov, A.S., Schwartz, C., Kimber, S., Roberts, I.J., and Krause, H.M. (2011). Nitric oxide coordinates metabolism, growth, and development via the nuclear receptor E75. *Genes & development* 25, 1476-1485.
- Camaschella, C. (2009). Hereditary sideroblastic anemias: pathophysiology, diagnosis, and treatment. *Semin Hematol* 46, 371-377.
- Chao, M.V. (2003). Neurotrophins and their receptors: a convergence point for many signalling pathways. *Nat Rev Neurosci* 4, 299-309.
- Conboy, J.G., Cox, T.C., Bottomley, S.S., Bawden, M.J., and May, B.K. (1992). Human erythroid 5-aminolevulinic synthase. Gene structure and species-specific differences in alternative RNA splicing. *The Journal of biological chemistry* 267, 18753-18758.
- de Rosny, E., de Groot, A., Jullian-Binard, C., Borel, F., Suarez, C., Le Pape, L., Fontecilla-Camps, J.C., and Jouve, H.M. (2008). DHR51, the *Drosophila melanogaster* homologue of the human photoreceptor cell-specific nuclear receptor, is a thiolate heme-binding protein. *Biochemistry* 47, 13252-13260.
- Ferreira, G.C., and Gong, J. (1995). 5-Aminolevulinic synthase and the first step of heme biosynthesis. *J Bioenerg Biomembr* 27, 151-159.
- Feyereisen, R. (1999). Insect P450 enzymes. *Annu Rev Entomol* 44, 507-533.
- Franken, A.C., Lokman, B.C., Ram, A.F., Punt, P.J., van den Hondel, C.A., and de Weert, S. (2011). Heme biosynthesis and its regulation: towards understanding and improvement of heme biosynthesis in filamentous fungi. *Applied microbiology and biotechnology* 91, 447-460.
- Georgieva, T., Dunkov, B.C., Dimov, S., Ralchev, K., and Law, J.H. (2002). *Drosophila melanogaster* ferritin: cDNA encoding a light chain homologue, temporal and tissue specific expression of both subunit types. *Insect Biochem Mol Biol* 32, 295-302.

- Gray, N.K., Pantopoulos, K., Dandekar, T., Ackrell, B.A., and Hentze, M.W. (1996). Translational regulation of mammalian and *Drosophila* citric acid cycle enzymes via iron-responsive elements. *Proceedings of the National Academy of Sciences of the United States of America* *93*, 4925-4930.
- Gruer, M.J., Artymiuk, P.J., and Guest, J.R. (1997). The aconitase family: three structural variations on a common theme. *Trends Biochem Sci* *22*, 3-6.
- Gutierrez, E., Wiggins, D., Fielding, B., and Gould, A.P. (2007). Specialized hepatocyte-like cells regulate *Drosophila* lipid metabolism. *Nature* *445*, 275-280.
- Handschin, C., Lin, J., Rhee, J., Peyer, A.K., Chin, S., Wu, P.H., Meyer, U.A., and Spiegelman, B.M. (2005). Nutritional regulation of hepatic heme biosynthesis and porphyria through PGC-1alpha. *Cell* *122*, 505-515.
- Hentze, M.W., and Kuhn, L.C. (1996). Molecular control of vertebrate iron metabolism: mRNA-based regulatory circuits operated by iron, nitric oxide, and oxidative stress. *Proceedings of the National Academy of Sciences of the United States of America* *93*, 8175-8182.
- Hentze, M.W., Muckenthaler, M.U., and Andrews, N.C. (2004). Balancing acts: molecular control of mammalian iron metabolism. *Cell* *117*, 285-297.
- Hift, R. (2012). The acute porphyrias. *European Gastroenterology & Hepatology Review* *8*, 14-21.
- Jackson, A.L., and Linsley, P.S. (2010). Recognizing and avoiding siRNA off-target effects for target identification and therapeutic application. *Nat Rev Drug Discov* *9*, 57-67.
- Kauppila, S., Maaty, W.S., Chen, P., Tomar, R.S., Eby, M.T., Chappo, J., Chew, S., Rathore, N., Zachariah, S., Sinha, S.K., *et al.* (2003). Eiger and its receptor, Wengen, comprise a TNF-like system in *Drosophila*. *Oncogene* *22*, 4860-4867.
- Lambert, L.A. (2012). Molecular evolution of the transferrin family and associated receptors. *Biochimica et biophysica acta* *1820*, 244-255.
- Langer, C.C., Ejsmont, R.K., Schonbauer, C., Schnorrer, F., and Tomancak, P. (2010). In vivo RNAi rescue in *Drosophila melanogaster* with genomic transgenes from *Drosophila pseudoobscura*. *PLoS One* *5*, e8928.
- Lara, F.A., Lins, U., Bechara, G.H., and Oliveira, P.L. (2005). Tracing heme in a living cell: hemoglobin degradation and heme traffic in digest cells of the cattle tick *Boophilus microplus*. *J Exp Biol* *208*, 3093-3101.
- Layer, G., Reichelt, J., Jahn, D., and Heinz, D.W. (2010). Structure and function of enzymes in heme biosynthesis. *Protein science : a publication of the Protein Society* *19*, 1137-1161.
- Liang, H., and Ward, W.F. (2006). PGC-1alpha: a key regulator of energy metabolism. *Adv Physiol Educ* *30*, 145-151.
- Lieu, P.T., Heiskala, M., Peterson, P.A., and Yang, Y. (2001). The roles of iron in health and disease. *Mol Aspects Med* *22*, 1-87.
- Lin, S., Huang, Y., and Lee, T. (2009). Nuclear receptor unfulfilled regulates axonal guidance and cell identity of *Drosophila* mushroom body neurons. *PLoS One* *4*, e8392.
- Lind, M.I., Ekengren, S., Melefors, O., and Soderhall, K. (1998). *Drosophila* ferritin mRNA:

- alternative RNA splicing regulates the presence of the iron-responsive element. *FEBS Lett* *436*, 476-482.
- Lind, M.I., Missirlis, F., Melefors, O., Uhrigshardt, H., Kirby, K., Phillips, J.P., Soderhall, K., and Rouault, T.A. (2006). Of two cytosolic aconitases expressed in *Drosophila*, only one functions as an iron-regulatory protein. *The Journal of biological chemistry* *281*, 18707-18714.
- Lu, B., Pang, P.T., and Woo, N.H. (2005). The yin and yang of neurotrophin action. *Nat Rev Neurosci* *6*, 603-614.
- Marvin, K.A., Reinking, J.L., Lee, A.J., Pardee, K., Krause, H.M., and Burstyn, J.N. (2009). Nuclear receptors homo sapiens Rev-erbbeta and *Drosophila melanogaster* E75 are thiolate-ligated heme proteins which undergo redox-mediated ligand switching and bind CO and NO. *Biochemistry* *48*, 7056-7071.
- May, B.K., Dogra, S.C., Sadlon, T.J., Bhasker, C.R., Cox, T.C., and Bottomley, S.S. (1995). Molecular regulation of heme biosynthesis in higher vertebrates. *Prog Nucleic Acid Res Mol Biol* *51*, 1-51.
- McBrayer, Z., Ono, H., Shimell, M., Parvy, J.P., Beckstead, R.B., Warren, J.T., Thummel, C.S., Dauphin-Villemant, C., Gilbert, L.I., and O'Connor, M.B. (2007). Prothoracicotrophic hormone regulates developmental timing and body size in *Drosophila*. *Developmental cell* *13*, 857-871.
- Meuchel, L.W., Thompson, M.A., Cassivi, S.D., Pabelick, C.M., and Prakash, Y.S. (2011). Neurotrophins induce nitric oxide generation in human pulmonary artery endothelial cells. *Cardiovasc Res* *91*, 668-676.
- Moreno, E., Yan, M., and Basler, K. (2002). Evolution of TNF signaling mechanisms: JNK-dependent apoptosis triggered by Eiger, the *Drosophila* homolog of the TNF superfamily. *Curr Biol* *12*, 1263-1268.
- Moriyama, E.N., and Powell, J.R. (1997). Codon usage bias and tRNA abundance in *Drosophila*. *J Mol Evol* *45*, 514-523.
- Morrison, G.R. (1965). Fluorometric Microdetermination of Heme Protein. *Analytical chemistry* *37*, 1124-1126.
- Muckenthaler, M., Gunkel, N., Frishman, D., Cyrklaff, A., Tomancak, P., and Hentze, M.W. (1998). Iron-regulatory protein-1 (IRP-1) is highly conserved in two invertebrate species--characterization of IRP-1 homologues in *Drosophila melanogaster* and *Caenorhabditis elegans*. *Eur J Biochem* *254*, 230-237.
- Neubueser, D., Warren, J.T., Gilbert, L.I., and Cohen, S.M. (2005). molting defective is required for ecdysone biosynthesis. *Developmental biology* *280*, 362-372.
- Nichol, H., Law, J.H., and Winzerling, J.J. (2002). Iron metabolism in insects. *Annu Rev Entomol* *47*, 535-559.
- Oishi, I., Sugiyama, S., Liu, Z.J., Yamamura, H., Nishida, Y., and Minami, Y. (1997). A novel *Drosophila* receptor tyrosine kinase expressed specifically in the nervous system. Unique structural features and implication in developmental signaling. *The Journal of biological chemistry* *272*, 11916-11923.

- Palanker, L., Necakov, A.S., Sampson, H.M., Ni, R., Hu, C., Thummel, C.S., and Krause, H.M. (2006). Dynamic regulation of *Drosophila* nuclear receptor activity in vivo. *Development* *133*, 3549-3562.
- Pantopoulos, K., Weiss, G., and Hentze, M.W. (1996). Nitric oxide and oxidative stress (H₂O₂) control mammalian iron metabolism by different pathways. *Mol Cell Biol* *16*, 3781-3788.
- Papanikolaou, G., and Pantopoulos, K. (2005). Iron metabolism and toxicity. *Toxicology and applied pharmacology* *202*, 199-211.
- Parker, J.S., Mizuguchi, K., and Gay, N.J. (2001). A family of proteins related to Spatzle, the toll receptor ligand, are encoded in the *Drosophila* genome. *Proteins* *45*, 71-80.
- Parker, K.L., and Schimmer, B.P. (1997). Steroidogenic factor 1: a key determinant of endocrine development and function. *Endocrine reviews* *18*, 361-377.
- Parvy, J.P., Blais, C., Bernard, F., Warren, J.T., Petryk, A., Gilbert, L.I., O'Connor, M.B., and Dauphin-Villemant, C. (2005). A role for betaFTZ-F1 in regulating ecdysteroid titers during post-embryonic development in *Drosophila melanogaster*. *Developmental biology* *282*, 84-94.
- Peng, G.H., Ahmad, O., Ahmad, F., Liu, J., and Chen, S. (2005). The photoreceptor-specific nuclear receptor Nr2e3 interacts with Crx and exerts opposing effects on the transcription of rod versus cone genes. *Hum Mol Genet* *14*, 747-764.
- Ponka, P. (1997). Tissue-specific regulation of iron metabolism and heme synthesis: distinct control mechanisms in erythroid cells. *Blood* *89*, 1-25.
- Prober, D.A., and Edgar, B.A. (2002). Interactions between Ras1, dMyc, and dPI3K signaling in the developing *Drosophila* wing. *Genes & development* *16*, 2286-2299.
- Pulido, D., Campuzano, S., Koda, T., Modolell, J., and Barbacid, M. (1992). Dtrk, a *Drosophila* gene related to the trk family of neurotrophin receptors, encodes a novel class of neural cell adhesion molecule. *EMBO J* *11*, 391-404.
- Puy, H., Gouya, L., and Deybach, J.C. (2010). Porphyrias. *Lancet* *375*, 924-937.
- Qiu, Y., Tittiger, C., Wicker-Thomas, C., Le Goff, G., Young, S., Wajnberg, E., Fricaux, T., Taquet, N., Blomquist, G.J., and Feyereisen, R. (2012). An insect-specific P450 oxidative decarbonylase for cuticular hydrocarbon biosynthesis. *Proceedings of the National Academy of Sciences of the United States of America* *109*, 14858-14863.
- Raghuram, S., Stayrook, K.R., Huang, P., Rogers, P.M., Nosie, A.K., McClure, D.B., Burris, L.L., Khorasanizadeh, S., Burris, T.P., and Rastinejad, F. (2007). Identification of heme as the ligand for the orphan nuclear receptors REV-ERBalpha and REV-ERBbeta. *Nature structural & molecular biology* *14*, 1207-1213.
- Regulski, M., Stasiv, Y., Tully, T., and Enikolopov, G. (2004). Essential function of nitric oxide synthase in *Drosophila*. *Curr Biol* *14*, R881-882.
- Reichardt, L.F. (2006). Neurotrophin-regulated signalling pathways. *Philosophical Transactions of the Royal Society B: Biological Sciences* *361*, 1545-1564.
- Reinking, J., Lam, M.M., Pardee, K., Sampson, H.M., Liu, S., Yang, P., Williams, S., White, W., Lajoie, G., Edwards, A., *et al.* (2005). The *Drosophila* nuclear receptor e75 contains heme and is gas responsive. *Cell* *122*, 195-207.

- Rewitz, K.F., Rybczynski, R., Warren, J.T., and Gilbert, L.I. (2006). The Halloween genes code for cytochrome P450 enzymes mediating synthesis of the insect moulting hormone. *Biochem Soc Trans* 34, 1256-1260.
- Rewitz, K.F., Yamanaka, N., Gilbert, L.I., and O'Connor, M.B. (2009). The insect neuropeptide PTH activates receptor tyrosine kinase torso to initiate metamorphosis. *Science* 326, 1403-1405.
- Riddle, R.D., Yamamoto, M., and Engel, J.D. (1989). Expression of delta-aminolevulinate synthase in avian cells: separate genes encode erythroid-specific and nonspecific isozymes. *Proceedings of the National Academy of Sciences of the United States of America* 86, 792-796.
- Roberts, A.G., and Elder, G.H. (2001). Alternative splicing and tissue-specific transcription of human and rodent ubiquitous 5-aminolevulinate synthase (ALAS1) genes. *Biochimica et biophysica acta* 1518, 95-105.
- Rothenberger, S., Mullner, E.W., and Kuhn, L.C. (1990). The mRNA-binding protein which controls ferritin and transferrin receptor expression is conserved during evolution. *Nucleic Acids Res* 18, 1175-1179.
- Ruiz de Mena, I., Fernandez-Moreno, M.A., Bornstein, B., Kaguni, L.S., and Garesse, R. (1999). Structure and regulated expression of the delta-aminolevulinate synthase gene from *Drosophila melanogaster*. *The Journal of biological chemistry* 274, 37321-37328.
- Sassa, S. (2006). Modern diagnosis and management of the porphyrias. *Br J Haematol* 135, 281-292.
- Schneider, D.S., Jin, Y., Morisato, D., and Anderson, K.V. (1994). A processed form of the Spatzle protein defines dorsal-ventral polarity in the *Drosophila* embryo. *Development* 120, 1243-1250.
- Schoenhaut, D.S., and Curtis, P.J. (1989). Structure of a mouse erythroid 5-aminolevulinate synthase gene and mapping of erythroid-specific DNase I hypersensitive sites. *Nucleic Acids Res* 17, 7013-7028.
- Shingleton, A.W. (2010). The regulation of organ size in *Drosophila*: physiology, plasticity, patterning and physical force. *Organogenesis* 6, 76-87.
- Stasiv, Y., Regulski, M., Kuzin, B., Tully, T., and Enikolopov, G. (2001). The *Drosophila* nitric-oxide synthase gene (dNOS) encodes a family of proteins that can modulate NOS activity by acting as dominant negative regulators. *The Journal of biological chemistry* 276, 42241-42251.
- Stys, A., Galy, B., Starzynski, R.R., Smuda, E., Drapier, J.C., Lipinski, P., and Bouton, C. (2011). Iron regulatory protein 1 outcompetes iron regulatory protein 2 in regulating cellular iron homeostasis in response to nitric oxide. *The Journal of biological chemistry* 286, 22846-22854.
- Suman, S., Seth, R.K., and Chandna, S. (2008). Role of nitric oxide synthase in insect cell radioresistance: an in-silico analysis. *Bioinformatics* 3, 8-13.
- Sung, C., Wong, L.E., Chang Sen, L.Q., Nguyen, E., Lazaga, N., Ganzer, G., McNabb, S.L., and Robinow, S. (2009). The unfulfilled/DHR51 gene of *Drosophila melanogaster* modulates

- wing expansion and fertility. *Dev Dyn* 238, 171-182.
- Tiranti, V., Rossi, E., Rocchi, M., DiDonato, S., Zuffardi, O., and Zeviani, M. (1995). The gene (NFE2L1) for human NRF-1, an activator involved in nuclear-mitochondrial interactions, maps to 7q32. *Genomics* 27, 555-557.
- Valanne, S., Wang, J.H., and Ramet, M. (2011). The *Drosophila* Toll signaling pathway. *J Immunol* 186, 649-656.
- Villalobo, A. (2006). Nitric oxide and cell proliferation. *The FEBS journal* 273, 2329-2344.
- Virbasius, J.V., and Scarpulla, R.C. (1994). Activation of the human mitochondrial transcription factor A gene by nuclear respiratory factors: a potential regulatory link between nuclear and mitochondrial gene expression in organelle biogenesis. *Proceedings of the National Academy of Sciences of the United States of America* 91, 1309-1313.
- Wang, J., Rousseau, D.L., Abu-Soud, H.M., and Stuehr, D.J. (1994). Heme coordination of NO in NO synthase. *Proceedings of the National Academy of Sciences of the United States of America* 91, 10512-10516.
- Wang, Z., Gerstein, M., and Snyder, M. (2009). RNA-Seq: a revolutionary tool for transcriptomics. *Nature reviews Genetics* 10, 57-63.
- Werck-Reichhart, D., and Feyereisen, R. (2000). Cytochromes P450: a success story. *Genome Biol* 1, REVIEWS3003.
- White, K.P., Hurban, P., Watanabe, T., and Hogness, D.S. (1997). Coordination of *Drosophila* metamorphosis by two ecdysone-induced nuclear receptors. *Science* 276, 114-117.
- Wilson, C., Goberdhan, D.C., and Steller, H. (1993). Dror, a potential neurotrophic receptor gene, encodes a *Drosophila* homolog of the vertebrate Ror family of Trk-related receptor tyrosine kinases. *Proceedings of the National Academy of Sciences of the United States of America* 90, 7109-7113.
- Wismar, J., Habtemichael, N., Warren, J.T., Dai, J.D., Gilbert, L.I., and Gateff, E. (2000). The mutation without children (rgl) causes ecdysteroid deficiency in third-instar larvae of *Drosophila melanogaster*. *Developmental biology* 226, 1-17.
- Woods, J.S., and Miller, H.D. (1993). Quantitative measurement of porphyrins in biological tissues and evaluation of tissue porphyrins during toxicant exposures. *Fundam Appl Toxicol* 21, 291-297.
- Yakubovich, N., Silva, E.A., and O'Farrell, P.H. (2010). Nitric oxide synthase is not essential for *Drosophila* development. *Curr Biol* 20, R141-142.
- Yamada, M., Murata, T., Hirose, S., Lavorgna, G., Suzuki, E., and Ueda, H. (2000). Temporally restricted expression of transcription factor betaFTZ-F1: significance for embryogenesis, molting and metamorphosis in *Drosophila melanogaster*. *Development (Cambridge, England)* 127, 5083-5092.
- Yin, L., Wu, N., Curtin, J.C., Qatanani, M., Szwegold, N.R., Reid, R.A., Waitt, G.M., Parks, D.J., Pearce, K.H., Wisely, G.B., *et al.* (2007). Rev-erbalpha, a heme sensor that coordinates metabolic and circadian pathways. *Science* 318, 1786-1789.
- Zhu, B., Pennack, J.A., McQuilton, P., Forero, M.G., Mizuguchi, K., Sutcliffe, B., Gu, C.J., Fenton, J.C., and Hidalgo, A. (2008). *Drosophila* neurotrophins reveal a common

mechanism for nervous system formation. PLoS biology 6, e284.

Chapter 5

Summary and future directions

5.1 The role of nuclear receptor DHR4 in the proper timing of ecdysone pulses during *Drosophila* development

In insects, maturation is under the control of a steroid hormone, 20-hydroxyecdysone (20E), the biologically active form of the insect molting hormone ecdysone (Thummel, 1996). Periodic pulses of ecdysone are released from the prothoracic gland (PG), thus directing major developmental transitions such as molts and metamorphosis. In *Drosophila*, major ecdysone pulses are responsible for stimulating hatching, molting and metamorphosis (**Figure 2.1B**). While the three low-titer ecdysone pulses that occur in the third instar (L3) are believed to be critical for the physiological changes such as the switch from feeding to wandering in mid-L3 (Warren et al., 2006) (**Figure 2.1B**), the molecular mechanisms underlying the regulation of ecdysone pulses remain poorly understood. PTTH, a brain-derived neuropeptide, stimulates ecdysone synthesis by activating the Ras/Raf/MAPK pathway through its receptor Torso in PG cells (Rewitz et al., 2009). However, little is known about the direct downstream targets of this pathway. Some biochemical studies have shown that the phosphorylation of the ribosomal protein S6 and a yet uncharacterized 120-kDa protein were induced rapidly by PTTH in the *Manduca* and *Bombyx* PG (Lin and Gu, 2011; Song and Gilbert, 1995), respectively. However, genetic evidence of their serving as direct targets of PTTH signaling is lacking. *Drosophila* PTTH mRNA levels oscillate with an 8-hour periodicity during the third instar (McBrayer et al., 2007), but how these oscillations are related to the timing of ecdysone pulses was unclear. In my subsequent analysis of *DHR4* function, I provided strong evidence showing that DHR4 is a direct target of the PTTH pathway.

DHR4 represents a component of the ecdysone hierarchy (**Figure 1.2**). DHR4 mutants display two major phenotypes: the premature onset of wandering

behavior and prepupal lethality (King-Jones et al., 2005). DHR4 is expressed in three major tissues, the prothoracic gland, the salivary glands, and the fat body. But it was unclear in which tissue the expression of DHR4 is associated with different phenotypes. Using tissue-specific RNAi, I showed that the expression of *DHR4* in the ring gland is linked to the premature onset of wandering behavior, and the function of DHR4 in the fat body is important for early prepupal development (**Figure 5.1A**). I found that DHR4 protein oscillates with 8-16 hour ultradian cycle times between cytoplasm and nucleus of PG cells (**Figure 2.10**), which closely matched the oscillations that were reported for *Drosophila* PTTH mRNA levels (McBrayer et al., 2007). This suggested a causal link between the cyclic behaviors of *PTTH* expression and DHR4 localization. I further provided strong evidence demonstrating that the oscillatory behavior of DHR4 is dependent on PTTH signaling: When PTTH neurons were ablated, DHR4 remained primarily in the nucleus, but when the PTTH pathway was hyperactivated, the protein was predominantly cytoplasmic (**Figure 2.12**). Consistently, hyperactivating the PTTH pathway also results in accelerated entry into metamorphosis (**Figure 2.11**), suggesting that this is achieved precisely by preventing DHR4 from entering the nucleus.

DHR4 mutants and larvae expressing ring gland-specific *DHR4*-RNAi display shortened feeding times and accelerated entry into metamorphosis, implying that this may arise from a premature occurrence of ecdysone pulses. Indeed, depleting *DHR4* in the ring gland via RNAi causes a faster rise of ecdysone levels that fail to regress when hormone levels normally drop (**Figure 2.8**). It is possible that the animal interprets these higher ecdysone levels as an early ecdysone pulse, resulting in developmental acceleration. Therefore, my model proposes that DHR4 acts as a repressor of ecdysone pulses by counteracting the PTTH-stimulated rises of ecdysone levels (**Figure 5.1B**). If

DHR4 serves as a target of the PTTH pathway, then one would expect that ERK phosphorylates DHR4 to trigger its removal from the nucleus when the PTTH signaling is active. While this has not been demonstrated directly, it appears that there is an inverse correlation between the subcellular localization of ERK and DHR4 (**Figure 2.15**), suggesting that there is a functional link. Indeed, DHR4 is predicted to have several clusters of ERK target sites (**Figure 2.24**), and future studies such as mutational analysis of putative ERK phosphorylation sites of DHR4 will have to be carried out in order to determine whether these sites affect the subcellular localization of the protein.

5.2 Cyp6t3: a novel player of ecdysone synthesis downstream of DHR4

The insect Halloween genes encode the cytochrome P450 hydroxylases that mediate the last four steps in the formation of 20E from dietary cholesterol (Chavez et al., 2000; Nusslein-Volhard and Wieschaus, 1980; Petryk et al., 2003; Warren et al., 2002; Warren et al., 2004). PTTH is necessary for the upregulation of the three Halloween genes, *phantom*, *disembodied*, and *shadow*, to generate the major ecdysone pulse prior to metamorphosis (Parvy et al., 2005). However, it was unclear whether the occurrence of low-titer ecdysone pulses is associated with the transcriptional regulation of these genes. I showed that their expression levels are relatively constant and fairly high in the ring gland of third instars long before the major PTTH pulses (**Figure 3.5E**), suggesting that the three minor ecdysone pulses are not simply a consequence of modulating mRNA levels of the Halloween genes. In line with this, none of the Halloween genes appeared to be affected in the ring gland of *DHR4* mutants or *DHR4* RNAi animals (**Figure 2.16D, E**).

So what are the downstream targets of DHR4? Using ring gland-specific microarrays, an uncharacterized cytochrome P450 gene, *Cyp6t3*, was identified as

a candidate DHR4 target. Firstly, I showed that *Cyp6t3* expression is highly specific to the ring gland, and that *Cyp6t3* mRNA levels oscillate, where lower levels correlate with times when DHR4 is nuclear. Secondly, I assigned a role for *Cyp6t3* as a novel player of the ecdysone biosynthetic pathway, because loss of *Cyp6t3* impairs ecdysone production. In addition, I showed that *Cyp6t3* is negatively regulated by DHR4, because high levels of *Cyp6t3* expression were observed in *DHR4* mutants and *DHR4* RNAi animals. However, it is still unclear whether *Cyp6t3* is a direct transcriptional target of *DHR4* due to a lack of direct evidence such as DHR4 DNA recognition sites. Nuclear receptor (subfamily 1, 2, 4-6) dimers bind to DNA sequences composed of two half-sites that are separated by variable spacing and can occur in different orientations (King-Jones and Thummel, 2005; Mangelsdorf et al., 1995; Rastinejad et al., 1995). By using NHR Scan (Sandelin and Wasserman, 2005), a DNA sequence termed DR0 half-sites element (repeats of the sequence AGGTCA without spacing) (Rastinejad et al., 1995) has been detected in the regulatory region of *Cyp6t3*. It is unclear whether the predicted DR0 site represents DHR4 binding site, but it finds support in previous studies demonstrating that GCNF, the vertebrate homolog of DHR4, binds to DNA sequences with half-sites of the DR0 model (Chen et al., 1994; Hentschke et al., 2006; Yan et al., 1997).

5.3 Transcriptome and functional analysis of *Drosophila* ring gland in controlling ecdysone synthesis

While we have a relatively good understanding of the enzymatic steps regarding the synthesis of steroid hormones in vertebrates and insects, our understanding of the regulatory processes underlying their production is not nearly as detailed. The *Drosophila* ring gland is a good model to study the steroidogenic regulation because of the lower-complexity of the insect endocrine

system in comparison to higher organisms. A systemic gene expression analysis of the ring gland represents a valuable means to increase our knowledge of the signaling pathways that regulate steroid hormone synthesis by identifying genes with specific expression in this particular tissue. However, this approach remained not attempted because it is technically challenging to dissect this small organ and the low RNA yields from it pose a problem for microarrays and RNA-Seq.

Aiming to systemically identify novel players of the ecdysteroidogenic pathway, I conducted the first comprehensive genomic and genetic analysis of the *Drosophila* ring gland by employing whole-genome microarray analysis as well as the study of gene function via RNAi. I have identified a total of 233 transcripts with strong enrichment (>10fold) in the ring gland of third instars. This list includes most previously known genes with specific expression in the ring gland, demonstrating that this experimental approach is successful in identifying known players in the ring gland. I have also identified 20 genes that have likely novel roles in ecdysone synthesis via RNAi analysis, and this includes cytochrome P450 genes, transcription factors, ABC transporters, and signaling pathway components. PG-specific RNAi knockdown of these genes results in a range of dramatic phenotypes that are consistent with a loss or reduction of ecdysone production. In addition, I showed that most of these phenotypes could be rescued by feeding larvae with 20E, confirming that these genes play important roles in ecdysone synthesis. Ultimately, I examined the temporal expression of 25 transcripts to correlate their profiles to the occurrence of ecdysone pulses during the L3. These data establish the ring gland as a prime model for examining signaling pathways that control the regulation of steroid hormone synthesis and release.

5.4 Microarrays reveal genes with PTTH-dependent expression

PTTH signaling represents a key regulator of ecdysone synthesis and

release, but its downstream targets are largely unknown. To increase our knowledge of this aspect, I examined for differential gene expression in the ring gland with altered PTTH signaling by microarray analysis, as a means to identify genes with PTTH-dependent expression. Using stringent filtering criteria (see Chapter 3, Result 3.3.5), I identified a total of 87 transcripts exhibiting PTTH-dependent expression profiles, suggesting that these genes act as downstream targets of PTTH signaling. These data broaden our current perspective of the ecdysteroidogenic regulation mediated by PTTH in the *Drosophila* ring gland. For instance, I observed that the PTTH pathway positively regulates the expression of *CG9541* (**Figure 3.9A**), which encodes a protein of adenylate cyclase activity. In line with this, in the PGs of *Manduca*, PTTH signaling increases the intracellular levels of free Ca^{2+} and cyclic AMP (cAMP), which in turn activates the cAMP-dependent signaling pathway leading to the phosphorylation of ribosomal protein S6, and ultimately a stimulation of ecdysone synthesis (Rountree et al., 1987; Song and Gilbert, 1995, 1997). These data suggest the possibility that *CG9541* serves as an important target of PTTH signaling in the *Drosophila* PG to enhance cAMP levels during the onset of metamorphosis. In addition, the expression of *snail* is negatively regulated by PTTH signaling (**Figure 3.9J**), which encodes a transcriptional repressor that is necessary for mesoderm formation in *Drosophila* embryos (Hemavathy et al., 2000). However, the function of *snail* in the PG remains unexplored. I showed that *snail* transcript levels were decreased in the ring gland towards the end of the L3 (**Figure 3.5B**). Larvae expressing PG-specific *snail*-RNAi are L3 lethal (**Figure 3.7**). These observations suggest the idea that Snail represses the expression of some unknown target genes that are necessary for the initiation of pupariation, and that this repression is relieved when PTTH signaling downregulates *snail* expression prior to metamorphosis. Future studies can look

into whether Snail represents another transcription factor employed by PTH signaling in controlling ecdysone production, and it will be of necessity to identify the downstream targets of *snail* to gain more insight into how Snail regulates metamorphosis.

5.5 The role of Spätzle5 and NO signaling in governing heme synthesis: A new layer of ecdysteroidogenic regulation

Ecdysteroidogenic enzymes belong to the cytochrome P450 superfamily, which recruit heme as a cofactor (Feyereisen, 1999; Rewitz et al., 2006). However, little is known about the mechanisms by which heme synthesis is governed and coordinated to boost ecdysone production in PG cells. My work represents the first insight into this aspect of ecdysteroidogenic regulation.

spätzle5 is one of the 233 ring gland-specific transcripts (**Figure 3.4**). I have shown that Spätzle5 is required for NO production possibly through controlling the activity of NOS (**Figure 4.11B, C**). RNAi knockdown of *spätzle5* or *NOS* specifically in the PG causes larval arrest (**Figure 4.11A**) and a dramatic upregulation of *ALAS* expression (**Figure 4.17**), which is the rate-limiting enzyme of heme synthesis. The de-repression of *ALAS* represents a hallmark of heme biosynthetic dysfunctions, which is indicative of a potential feedback mechanism through enhancing *ALAS* expression to compensate for heme deficiency. Thus, firstly, the upregulation of *ALAS* in *spätzle5* and *NOS* knockdowns suggested that heme synthesis is impaired when *spätzle5* or *NOS* function is lost. Elevated *ALAS* levels result in an accumulation of heme precursors in PG cells (**Figure 4.19, 4.20**), which makes *spätzle5*- or *NOS*-RNAi ring glands shine in a bright red under UV light (**Figure 4.14**). Secondly, it raised the possibility that an unknown heme sensor upregulates *ALAS* expression when heme concentrations fall below a critical threshold. In the vertebrate liver, the peroxisome proliferator-activated

receptor- γ coactivator 1 α (PGC-1 α) increases *ALAS* expression when heme synthesis is blocked during porphyrogenic attacks (Handschin et al., 2005). However, it remained unknown what the positive regulator of *Drosophila ALAS* is. Using a candidate gene approach, I showed that DHR51 is required for the upregulation of *ALAS* in *spätzle5* and *NOS* knockdowns (**Figure 4.22**). Knocking down *DHR51* in the *spätzle5*- or *NOS*-RNAi background restored *ALAS* expression back to normal, and suppresses the accumulation of fluorescent heme intermediates in PG cells (**Figure 4.23**). These data strongly support the idea that DHR51 acts as a heme sensor to upregulate *ALAS* expression when heme levels are below a critical threshold. Together, this study broadens our current perspective of ecdysteroidogenic regulation, and sheds light on a novel pathway signaled by Spätzle5 in controlling heme synthesis thereby regulating metamorphosis.

5.6 Future directions

Currently, several major questions are under investigation. Firstly, it is unclear whether there is an actual increase of heme production at the onset of metamorphosis. To answer this question, I will examine total heme levels of the wild type ring gland over a time course during the L3 by using QuantiHeme assay (BioAssay, CA). An unfortunate drawback of QuantiHeme assay is that it can not distinguish heme from its precursors. Therefore, to test whether loss of *spätzle5* or *NOS* results in low heme levels in the first place, I will take advantage of the fact that protoporphyrins are highly fluorescent molecules. Heme concentrations will be determined by the change of the fluorescence emitted by gland homogenates before and after being boiled in saturated oxalic acid (OA) solution, a procedure that converts heme into fluorescent protoporphyrins by releasing iron from it (Morrison, 1965).

Secondly, how do Spätzle5 and NO signaling control heme synthesis in PG cells? To answer this question, I propose two major approaches. First, RNA-Seq appears to be an attractive strategy to search for downstream targets of Spätzle5 and NO signaling via examining for differential gene expression in a *spätzle5*- or *NOS*-RNAi background. This will possibly reveal key players of the heme synthetic pathway that are under the control of Spätzle5 or NO signaling. Furthermore, it also helps to clarify whether Spätzle5 and NOS act in the same pathway by examining whether they share a same panel of downstream targets. Second, I hypothesize that Spätzle5 and NO signaling govern heme synthesis by regulating iron availability in PG cells prior to metamorphosis. In mammals, the presence of NO triggers a decrease of ferritin (iron storage protein) and an increase of TfR (transferrin receptor) via IRP/IRE interaction, resulting in elevated cellular iron concentrations (Hentze and Kuhn, 1996; Stys et al., 2011). In *Drosophila*, an IRE site was identified in the 5'-UTR of the transcript encoding a heavy chain of ferritin Fer1HCH (Lind et al., 1998), thus allowing IRP/IRE-mediated reduction of ferritin levels through translational repression (**Figure 4.33**). However, attention should be given to the fact that insect genomes do not encode any TfR homologs (Lambert, 2012), suggesting a difference in iron regulation between insects and mammals. To test my hypothesis, I will firstly examine the protein levels of ferritin in the ring gland during the early and late L3 by immunostaining and western blot. The polyclonal antibody for *Drosophila* Fer1HCH was obtained from Dr. Fanis Missirlis (Cinvestav, Mexico City). I expect to see lower levels of ferritin in the ring gland in the late L3 due to the presence of NO at this point. Reduced ferritin levels consequently free iron from storage and increase labile iron pool for cellular utilization. Secondly, I will examine whether ferritin levels fails to be diminished in *spätzle5*- and *NOS*-RNAi ring glands. If so, this would explain that the heme biosynthetic dysfunction

caused by *spätzle5*- and *NOS*-RNAi is due to a lack of NO, which prevents the release of iron from ferritin thereby resulting in iron shortage for cellular functions. Thirdly, I want to express IRP1A cDNA in a *spätzle5*- and *NOS*-RNAi background. The transgenic fly (*UAS-IRP1AcDNA*) was obtained from Dr. Maria I. Lind (Uppsala University, Sweden). Increased IRP1A levels inhibit ferritin translation, thus mimicking the presence of NO. I expect to see that increased *IRP1A* levels rescue the larval lethality and suppress the buildup of heme precursors caused by loss of *spätzle5* and *NOS* in PG cells.

Last but not least, to corroborate that DHR51 functions as a heme sensor, future experiments should address whether loss of *DHR51* suppresses the accumulation of heme precursors in a *PPOX* mutant background. The *PPOX*¹³⁷⁰² mutant was obtained from Dr. Arash Bashirullah (University of Wisconsin-Madison, US). *PPOX*¹³⁷⁰² mutants display autofluorescence in prothoracic glands, oenocytes, and the midgut. I will induce *DHR51*-RNAi or *DHR51*-miRNAi in the *PPOX*¹³⁷⁰² mutant using tissue-specific *Gal4* drivers. This approach enables me to examine the role of DHR51 as a heme sensor in these larval tissues from a low heme background. In addition, I am also interested in identifying the downstream targets of DHR51 in the PG in addition to *ALAS*. To do this, I will utilize RNA-Seq to search for putative DHR51 targets through examining for differential gene expression in the ring gland expressing *spätzle5*-RNAi; *DHR51*-RNAi, *spätzle5*-RNAi alone and *DHR51*-RNAi alone. I expect to identify genes acting downstream of DHR51 as components of a putative feedback mechanism to enhance heme synthesis when heme levels are below a critical threshold.

5.6 Figures

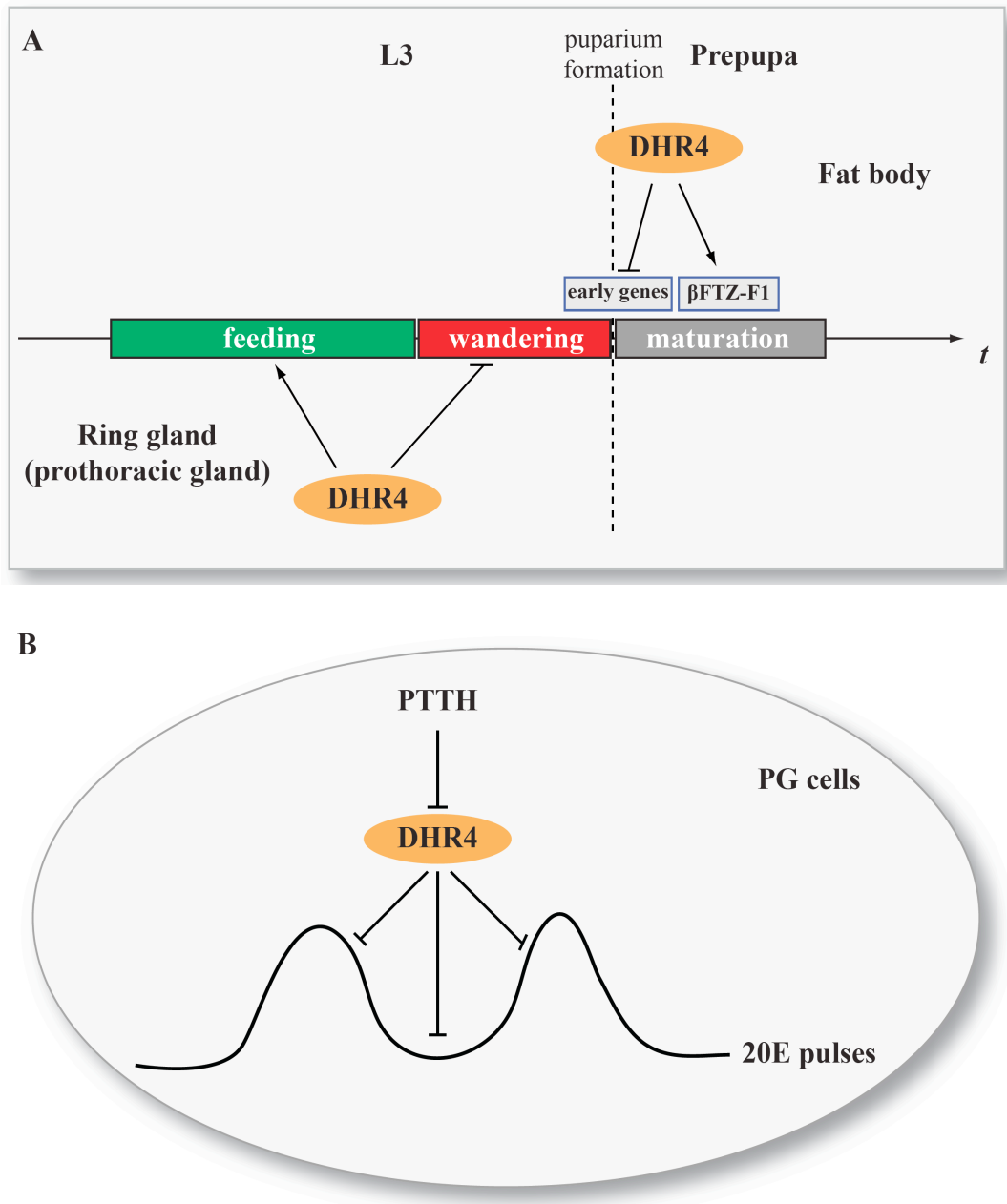


Figure 5.1. Dual function of DHR4 during *Drosophila* development

(A) DHR4 is expressed in three major larval tissues, the prothoracic gland, the salivary glands, and the fat body (Figure 2.4). *DHR4^l* mutant display two distinct phenotypes, the premature onset of wandering behavior and prepupal lethality. The expression of *DHR4* in the ring gland (or prothoracic gland) is linked to the

precocious wandering behavior, and the function of DHR4 in the fat body as a component of the ecdysone hierarchy is important for prepupal development (**Figure 1.2**). (B) In PG cells, DHR4 represses the occurrence of ecdysone peaks by counteracting the PTTH-stimulated rise of ecdysone levels (also see **Figure 2.23**).

5.7 Bibliography

- Chavez, V.M., Marques, G., Delbecque, J.P., Kobayashi, K., Hollingsworth, M., Burr, J., Natzle, J.E., and O'Connor, M.B. (2000). The *Drosophila* disembodied gene controls late embryonic morphogenesis and codes for a cytochrome P450 enzyme that regulates embryonic ecdysone levels. *Development (Cambridge, England)* *127*, 4115-4126.
- Chen, F., Cooney, A.J., Wang, Y., Law, S.W., and O'Malley, B.W. (1994). Cloning of a novel orphan receptor (GCNF) expressed during germ cell development. *Molecular endocrinology (Baltimore, Md)* *8*, 1434-1444.
- Feyereisen, R. (1999). Insect P450 enzymes. *Annu Rev Entomol* *44*, 507-533.
- Handschin, C., Lin, J., Rhee, J., Peyer, A.K., Chin, S., Wu, P.H., Meyer, U.A., and Spiegelman, B.M. (2005). Nutritional regulation of hepatic heme biosynthesis and porphyria through PGC-1alpha. *Cell* *122*, 505-515.
- Hemavathy, K., Ashraf, S.I., and Ip, Y.T. (2000). Snail/slug family of repressors: slowly going into the fast lane of development and cancer. *Gene* *257*, 1-12.
- Hentschke, M., Kurth, I., Borgmeyer, U., and Hubner, C.A. (2006). Germ cell nuclear factor is a repressor of CRIPTO-1 and CRIPTO-3. *The Journal of biological chemistry* *281*, 33497-33504.
- Hentze, M.W., and Kuhn, L.C. (1996). Molecular control of vertebrate iron metabolism: mRNA-based regulatory circuits operated by iron, nitric oxide, and oxidative stress. *Proceedings of the National Academy of Sciences of the United States of America* *93*, 8175-8182.
- King-Jones, K., Charles, J.P., Lam, G., and Thummel, C.S. (2005). The ecdysone-induced DHR4 orphan nuclear receptor coordinates growth and maturation in *Drosophila*. *Cell* *121*, 773-784.
- King-Jones, K., and Thummel, C.S. (2005). Nuclear receptors--a perspective from *Drosophila*. *Nature reviews Genetics* *6*, 311-323.
- Lambert, L.A. (2012). Molecular evolution of the transferrin family and associated receptors. *Biochimica et biophysica acta* *1820*, 244-255.
- Lin, J.L., and Gu, S.H. (2011). Prothoracicotropic hormone induces tyrosine phosphorylation in prothoracic glands of the silkworm, *Bombyx mori*. *Archives of insect biochemistry and physiology* *76*, 144-155.
- Lind, M.I., Ekengren, S., Melefors, O., and Soderhall, K. (1998). *Drosophila* ferritin mRNA: alternative RNA splicing regulates the presence of the iron-responsive element. *FEBS Lett* *436*, 476-482.
- Mangelsdorf, D.J., Thummel, C., Beato, M., Herrlich, P., Schutz, G., Umesono, K., Blumberg, B., Kastner, P., Mark, M., Chambon, P., *et al.* (1995). The nuclear receptor superfamily: the second decade. *Cell* *83*, 835-839.
- McBrayer, Z., Ono, H., Shimell, M., Parvy, J.P., Beckstead, R.B., Warren, J.T., Thummel, C.S., Dauphin-Villemant, C., Gilbert, L.I., and O'Connor, M.B. (2007). Prothoracicotropic hormone regulates developmental timing and body size in *Drosophila*. *Developmental cell* *13*, 857-871.

- Morrison, G.R. (1965). Fluorometric Microdetermination of Heme Protein. *Analytical chemistry* 37, 1124-1126.
- Nusslein-Volhard, C., and Wieschaus, E. (1980). Mutations affecting segment number and polarity in *Drosophila*. *Nature* 287, 795-801.
- Parvy, J.P., Blais, C., Bernard, F., Warren, J.T., Petryk, A., Gilbert, L.I., O'Connor, M.B., and Dauphin-Villemant, C. (2005). A role for betaFTZ-F1 in regulating ecdysteroid titers during post-embryonic development in *Drosophila melanogaster*. *Developmental biology* 282, 84-94.
- Petryk, A., Warren, J.T., Marques, G., Jarcho, M.P., Gilbert, L.I., Kahler, J., Parvy, J.P., Li, Y., Dauphin-Villemant, C., and O'Connor, M.B. (2003). Shade is the *Drosophila* P450 enzyme that mediates the hydroxylation of ecdysone to the steroid insect molting hormone 20-hydroxyecdysone. *Proceedings of the National Academy of Sciences of the United States of America* 100, 13773-13778.
- Rastinejad, F., Perlmann, T., Evans, R.M., and Sigler, P.B. (1995). Structural determinants of nuclear receptor assembly on DNA direct repeats. *Nature* 375, 203-211.
- Rewitz, K.F., Rybczynski, R., Warren, J.T., and Gilbert, L.I. (2006). The Halloween genes code for cytochrome P450 enzymes mediating synthesis of the insect moulting hormone. *Biochem Soc Trans* 34, 1256-1260.
- Rewitz, K.F., Yamanaka, N., Gilbert, L.I., and O'Connor, M.B. (2009). The insect neuropeptide PTH activates receptor tyrosine kinase torso to initiate metamorphosis. *Science* 326, 1403-1405.
- Rountree, D.B., Combust, W.L., and Gilbert, L.I. (1987). Protein phosphorylation in the prothoracic glands as a cellular model for juvenile hormone-prothoracicotropic hormone interactions. *Insect Biochemistry* 17, 943-948.
- Sandelin, A., and Wasserman, W.W. (2005). Prediction of nuclear hormone receptor response elements. *Molecular endocrinology (Baltimore, Md)* 19, 595-606.
- Song, Q., and Gilbert, L.I. (1995). Multiple phosphorylation of ribosomal protein S6 and specific protein synthesis are required for prothoracicotropic hormone-stimulated ecdysteroid biosynthesis in the prothoracic glands of *Manduca sexta*. *Insect biochemistry and molecular biology* 25, 591-602.
- Song, Q., and Gilbert, L.I. (1997). Molecular cloning, developmental expression, and phosphorylation of ribosomal protein S6 in the endocrine gland responsible for insect molting. *The Journal of biological chemistry* 272, 4429-4435.
- Stys, A., Galy, B., Starzynski, R.R., Smuda, E., Drapier, J.C., Lipinski, P., and Bouton, C. (2011). Iron regulatory protein 1 outcompetes iron regulatory protein 2 in regulating cellular iron homeostasis in response to nitric oxide. *The Journal of biological chemistry* 286, 22846-22854.
- Thummel, C.S. (1996). Files on steroids--*Drosophila* metamorphosis and the mechanisms of steroid hormone action. *Trends Genet* 12, 306-310.
- Warren, J.T., Petryk, A., Marques, G., Jarcho, M., Parvy, J.P., Dauphin-Villemant, C., O'Connor, M.B., and Gilbert, L.I. (2002). Molecular and biochemical characterization of two P450

- enzymes in the ecdysteroidogenic pathway of *Drosophila melanogaster*. Proceedings of the National Academy of Sciences of the United States of America *99*, 11043-11048.
- Warren, J.T., Petryk, A., Marques, G., Parvy, J.P., Shinoda, T., Itoyama, K., Kobayashi, J., Jarcho, M., Li, Y., O'Connor, M.B., *et al.* (2004). Phantom encodes the 25-hydroxylase of *Drosophila melanogaster* and *Bombyx mori*: a P450 enzyme critical in ecdysone biosynthesis. *Insect biochemistry and molecular biology* *34*, 991-1010.
- Warren, J.T., Yerushalmi, Y., Shimell, M.J., O'Connor, M.B., Restifo, L.L., and Gilbert, L.I. (2006). Discrete pulses of molting hormone, 20-hydroxyecdysone, during late larval development of *Drosophila melanogaster*: correlations with changes in gene activity. *Dev Dyn* *235*, 315-326.
- Yan, Z.H., Medvedev, A., Hirose, T., Gotoh, H., and Jetten, A.M. (1997). Characterization of the response element and DNA binding properties of the nuclear orphan receptor germ cell nuclear factor/retinoid receptor-related testis-associated receptor. *The Journal of biological chemistry* *272*, 10565-10572.